DOCTOR OF SCIENCES

Deciphering the senescent phenotype induced by radiotherapy, protontherapy and PARP inhibitors in cancer cell lines

Huart, Camille

Award date:
2022

Awarding institution:
University of Namur

Université de Namur
Faculté des Sciences – Département de Biologie
Namur Research Institute For Life Science (NARILIS)
Unité de recherche en Biologie Cellulaire (URBC)
Rue de Bruxelles, 61, B-5000 Namur, Belgique

Deciphering the senescent phenotype induced by radiotherapy, protontherapy and PARP inhibitors in cancer cell lines

Dissertation originale présentée par
Camille Huart
En vue de l'obtention du grade de
Docteur en Sciences

Composition du jury :

Prof. Carine Michiels (Promoteur)
NARILIS – URBC
UNamur, Namur, Belgique

Prof. Olivier Feron
IREC – FATH
UCLouvain, Woluwé-Saint-Lambert, Belgique

Prof. Sophie Lucas
Institut de Duve
UCLouvain, Woluwé-Saint-Lambert, Belgique

Dr. Anne-Catherine Wéra
CHU UCL Namur
UCLouvain, Saint-Elisabeth, Belgique

Dr. Florence Debacq-Chainiaux
NARILIS – URBC
UNamur, Namur, Belgique

Dr. Nicolas Malaquin
Institut du Cancer – CRCHUM
UdeM, Montréal, Canada

Prof. Stéphane Lucas (Président)
NARILIS – LARN
UNamur, Namur, Belgique

Octobre 2022

Table of Contents

Remerciements

Je souhaite remercier ma promotrice: Prof. Carine Michiels pour m'avoir fait confiance pendant cette période de 5 ans. Même si le début de thèse a été extrêmement laborieux, vous avez toujours réussi à garder une attitude positive à mon égard. De plus, vous avez toujours impliqué les différents membres de votre équipe dans les divers projets, cette démarche nous a permis d'être uni et solidaire dans les différentes épreuves liées à la thèse. Je voulais également vous remercier pour votre disponibilité (malgré un emploi du temps très chargé). Grâce à vous, j'ai pu concrétiser la volonté que j'avais de faire une thèse (et surtout, de mener un projet) ! Encore un tout grand merci !

Je souhaite remercier ma « co-promotrice » non officielle : Dr. AnK. La liste des choses pour lesquelles je dois te remercier est longue. Un tout grand merci pour ta positive attitude ! C'était vraiment très agréable de pouvoir travailler avec toi malgré le travail qui parfois était un peu moins agréable, par exemple: coller les chambres, laver les chambres, les clono… Un grand merci d'avoir toujours pris le temps de trouver une réponse à mes nombreuses questions (et celles de nos étudiants), même après ton départ! Un énorme merci pour l'ensemble des moments qu'on a passé ensemble à Manchester, pendant le temps de midi, les soupers/diners de Noël (je n'oublie pas le: « tu as des frères?!? »), … Et bien sûr, merci de m'avoir confié le reviewing de ton papier, ça m'a clairement permis de me remettre en selle pour terminer (ou plutôt, commencer) cette thèse. A très bientôt (au restaurant ?) !

Un tout grand merci aux membres de mon jury de thèse : Dr. Nicolas Malaquin, Prof. Stéphane Lucas, Prof. Sophie Lucas, Prof. Olivier Feron et Dr. Florence Chainiaux. Merci d'avoir pris le temps de lire mon manuscrit. Merci également pour la discussion très intéressante lors de la défense privée.

Un tout grand merci également à Dr. Benjamin pour tes conseils précieux ! Merci d'avoir trouvé le temps pour me challenger ! Merci pour ton implication dans mon projet de thèse mais également, pour tes conseils pour l'après thèse.

Merci aux membres de l'équipe TumHyp. Merci à Christoph pour ton attitude « Deutsch Qualiteit ». Merci à Karim pour nos petites discussions sénescence et Canada ! Merci à Jia-Wei pour nos discussions sur les plantes, les restaurants, Top Chef mais aussi pour tes bons conseils en pièce lentivirus! Merci également à François C. et Maude pour les nombreuses soirées « Game Night » ! Merci également à Dr. Victor pour les soirées badminton – j'espère un jour pouvoir gagner un match ! Merci également à Andrea, Dr. François B., Dr. Eleonore, Dr. Géraldine & Dr. Sophie.

Merci aux deux étudiants qui ont travaillé dans l'équipe TumHyp pendant l'année 2022: Arthur & Manon. Ca a été un plaisir de vous encadrer ainsi que de suivre votre évolution dans le groupe. On a clairement été gâté avec vous deux ! Je vous souhaite beaucoup de courage pour

la fin de votre mémoire et surtout, beaucoup de chance pour la suite ! Bon amusement en Italie & au Canada !

Merci également aux membres de l'URBC. Merci à Jérémy pour ta bonne humeur & toutes nos discussions autour d'un bon bocadillo ! Je te souhaite le meilleur pour la suite, et j'espère qu'on sera à nouveau collègue ! Merci également à Dr au carré. Lola pour ta joie de vivre et nos petites séances au spa ! Merci à Aude pour les découvertes culinaires, Louise pour les karaokés & Dr. Natacha pour les discussions resto' !

Merci à l'équipe du 4127 : Dr. Damien (DéDé) & Alexis (Khelfifi). Ca a été un plaisir de partager le bureau avec vous deux ! Merci pour ce magnifique roadtrip au Canada/USA. J'espère qu'on aura l'occaz' de refaire cela (surtout quand Alexis aura le permis, et qu'il pourra passer au rang de chauffeur). Merci Damien pour le « train-trip » au Japon, juste pendant le lockdown de la Belgique – heureusement que ta « chance » habituelle était avec nous pour nous permettre de monter dans le dernier avion. Vive le Kobe ! Merci Alexis d'avoir réussi à me supporter pendant 7 ans environ, mais aussi d'avoir été dépensé ton salaire avec moi au Coffee & More pour discuter de nos nombreux soucis de thèse !

Merci à Pauline de m'avoir supporté pendant une partie de cette thèse ! Merci de m'avoir encouragé pour que je puisse arriver au bout.

Un tout grand merci à toute ma famille pour leur aide précieuse dans la réalisation de cette thèse ! Merci d'avoir toujours été présent pour moi !

Et enfin, merci au F.R.S.-FNRS pour le soutien financier qui m'a permis de réaliser cette thèse.

Abstract

Radiotherapy is one of the most common forms of anti-cancer treatment. Interestingly, most of these therapies are known to trigger cellular senescence which corresponds to a state of permanent proliferation arrest. In the context of cancer, senescence can have a dual influence. Indeed, senescence has been described to have pro-tumoral and anti-tumoral effects. In the first part of this work, we showed that treatment with irradiation with either photons or protons combined or not to PARP inhibitors induced senescence. Indeed, an increase in the percentage of senescent cells treated with photons or protons was demonstrated. The percentage of senescent cells further increased when cancer cells were treated with photons or protons combined to PARP inhibitors. Moreover, we showed that the senescent cells could be targeted by Navitoclax (ABT-263), a senolytic, in order to increase the percentage of cell death. In the second part of this work, we determined how PARP inhibitors led to senescent cancer cells. We tested several PARP inhibitors: Veliparib, Rucaparib, Olaparib, Niraparib and Talazoparib onto different cancer cells. The results of our work demonstrated that Talazoparib induced the strongest phenotype of senescence in several cancer cell lines. Since all the inhibitors completely abrogated the catalytic activity of PARP, we are currently trying to understand if the differential induction of senescence by inhibitors of PARP is linked to the trapping of PARP1 onto the DNA by the inhibitors. In conclusion, this PhD thesis demonstrated that irradiation with photons or protons significantly increased the percentage of senescent cells, and that combination with PARP inhibitors further increased the percentage of senescent cells. Moreover, the senescent cells could be specifically targeted by senolytic to increase cell death. These preliminary results described a new therapeutic venue for cancer patients treated with conventional radiotherapy, protontherapy or inhibitors of PARP.

Résumé

La radiothérapie est l'une des formes les plus courantes de traitements anticancéreux. La plupart de ces thérapies sont connues pour déclencher un phénomène de sénescence cellulaire qui correspond à un état d'arrêt permanent de la prolifération. Dans le cadre du cancer, la sénescence peut avoir une double influence. En effet, la sénescence a été décrite comme ayant des effets pro-tumoraux et anti-tumoraux. Dans la première partie de ce travail, nous avons montré que le traitement par irradiation, soit avec des photons soit avec des protons, combiné ou non aux inhibiteurs de PARP induisait la sénescence. En effet, une augmentation du pourcentage de cellules sénescentes a été mise en évidence après irradiation avec des photons ou des protons. Le pourcentage de cellules sénescentes est encore augmenté lorsque les cellules cancéreuses sont irradiées avec des photons ou des protons et exposées à des inhibiteurs de PARP. De plus, nous avons montré que les cellules sénescentes pouvaient être ciblées par Navitoclax (ABT-263), un sénolytique, afin d'augmenter le pourcentage de mort cellulaire. Dans la deuxième partie de ce travail, nous avons déterminé comment les inhibiteurs de PARP conduisaient à la sénescence des cellules cancéreuses. Nous avons utilisé plusieurs inhibiteurs de PARP : Veliparib, Rucaparib, Olaparib, Niraparib et Talazoparib sur différentes cellules cancéreuses. Les résultats de nos travaux ont démontré que le Talazoparib induisait le phénotype de sénescence le plus fort dans plusieurs lignées cellulaires cancéreuses. Puisque tous les inhibiteurs ont complètement abrogé l'activité catalytique de PARP, nous cherchons actuellement à comprendre si l'induction différentielle de la sénescence par les différents inhibiteurs de PARP est liée au piégeage de PARP1 sur l'ADN par ces molécules. En conclusion, cette thèse de doctorat a démontré que l'irradiation avec des photons ou des protons augmentait significativement le pourcentage de cellules sénescentes, et que la combinaison avec des inhibiteurs de PARP augmentait encore le pourcentage de cellules sénescentes. De plus, les cellules sénescentes pourraient être spécifiquement ciblées par ABT-263 pour augmenter la mort cellulaire. Ces résultats préliminaires décrivent une nouvelle voie thérapeutique pour les patients cancéreux traités par radiothérapie conventionnelle, protonthérapie ou inhibiteurs de PARP.

List of abbreviations

AIF	Apoptosis inducing factor
ALTAIS	Accélérateur Linéaire Tandétron pour l'Analyse et l'Implantation des Solides
ATM	Ataxia Telangiectasia mutated
ATP	Adenosine triphosphate
ATR	AT-related kinase
BB	Broad beam
BER	Base excision repair
BRCA	Breast cancer antigen
BrdU	Bromodeoxyuridine
CDK	Cyclin-dependent kinases
CDKi	CDK inhibitors
CHD1L	Chromodomain helicase DNA binding protein 1 like
cNHEJ	Conventional non-homologous end joining
Co-60	Cobalt-60
CRT	Calreticulin
CtIP	CtBP-interacting protein
CTLA-4	Cytotoxic T lymphocyte protein 4
D	Dasatinib
DC	Dendritic cell
DDR	DNA damage response
DNA-PKcs	DNA-dependent protein kinase
DNA-SCARS	DNA segments with chromatin alterations reinforcing senescence
DR	Death receptor
DSBs	Double-strand breaks
dsDNA	Double-stranded DNA
EdU	5-ethynyl-2'-deoxyuridine
EGFR	Epidermal growth factor receptor
ER	Endoplasmic reticulum
F	Fisetin
FDA	Food and Drug Administration
GBM	Glioblastoma multiforme
Gy	Gray
HKII	Hexokinase II
HMGB-1	High mobility group box 1
HPV	Human papillomavirus
HR	Homologous recombination
ICD	Immunogenic cell death
IFN	Interferon
IMRT	Intensity-modulated radiotherapy
KD	Kinase dead
LET	Linear energy transfer
LI	Labeling index
L-Q	Linear-quadratic

MDSC	Myeloid-derived suppressor cells
MHC II	Major histocompability complex II
MIF	Migration inhibitory factor
MRT	Microbeam radiation therapy
NHEJ	Non-homologous end joining
NK	Natural killer
NSCLC	Non-small cell lung cancer
NTR	N-terminal region
OER	Oxygen enhancement ratio
OS	Overall survival
PARP	Poly(ADP-ribose) polymerase
PD-1	Programmed cell death protein 1
PD-L1	Programmed cell death ligand 1
PFS	Progression free survival
PPL	Piperlongumine
PPP	Pentose phosphate pathway
PROTAC	Proteolysis targeting chimera
PRRs	Pattern recognition receptors
Q	Quercetin
RB	Retinoblastoma protein
RBE	Relative biological effectiveness
ROS	Reactive oxygen species
RPA	Replication protein A
RT	Radiotherapy
SAHF	Senescence-associated heterochromatin foci
SASE	Senescent-associated super enhancers
SASP	Senescence-associated secretory phenotype
SA-β-Gal	Senescent-associated beta-galactosidase
SF	Survival fraction
SI	System of Units
SOBP	Spread out Bragg Peak
SRT	Stereotactic radiotherapy
SSBR	Single strand break repair
TCR	T cell receptor
TIS	Therapy-induced senescence
TK	Tyrosine kinase
UPR	Unfolded protein response
VMAT	Volumetric modulated arc therapy
WHO	World Health Organization
YAP	Yes-associated protein

Foreword

Cancer is a leading cause of death worldwide. The most common cancers are breast, lung, colon and prostate cancers. Several treatments exist such as surgery, chemotherapies, radiotherapies, immunotherapies and targeted therapies. These treatments are rarely curative, despite significant improvement in the recent decades. For this reason, new approaches are needed. Cellular senescence in cancer is of great interest. Cellular senescence is defined as a state of permanent cell cycle arrest. Several research teams demonstrated that cancer cells could become senescent following treatment with several anti-cancer therapies. These senescent cancer cells can have a pro-tumoral or an anti-tumoral effects. Interestingly, several researchers demonstrated that specifically targeting senescent cells could improve cancer outcomes. In this PhD thesis, we wanted to decipher the induction of senescence following irradiation with photons or with protons or following treatment with inhibitors of PARP. The purpose of this PhD thesis was thus to better understand the impact of anti-cancer therapies on cancer cells as these anti-cancer therapies can lead to cell death, but also to a senescent phenotype. To better understand the research work performed, the introduction is divided into five parts. The first chapter is a brief reminder on cancer and cancer treatments. The second chapter is decidated to the comparison between conventional radiotherapy and particle therapy. The third chapter is devoted to cellular senescence in the context of cancer. The fourth chapter tackled PARP inhibitors and the mechanism of action of these inhibitors. Finally, the last chapter is a summary of the current research regarding the induction of senescence by irradiation with photons, particle therapy or by treatment with inhibitors of PARP.

A. Introduction

1. Cancer

1.1. Introduction

Cancer has been observed in hominid fossils and human mummies. It was first described in Egypt, and the term “cancer” from the Greek word karkinos, was later given to the disease by the Greek physician, Hippocrates in reference to the shape of a crab [1]. Briefly, cancer is caused by abnormal cells which divide without control. These abnormal cells can also spread to other parts of the body. More than 100 types of cancer have been described. Cancers are often named after the tissue or the organ from where they arise [2].

The majority of cancers starts in epithelial tissues and these cancers are referred as carcinomas. These cancers include many of the most common cancers such as cancers arising from the epithelial cell layers of the gastrointestinal tract, skin, mammary gland, pancreas, lung, liver, ovary, uterus, prostate, gallbladder and urinary bladder. Carcinomas can be further divided into squamous cell carcinomas or adenocarcinomas. Adenocarcinomas originate from an organ or gland whereas squamous cell carcinomas arise from the squamous epithelium [2].

Although less frequent, cancers can also arise from non-epithelial tissues. These cancers can be sub-divided into sarcoma, leukemias, lymphomas, myelomas and neuro-ectodermal tumors. Sarcoma describes cancers which begin in connective tissues such as the bone, cartilage, fat, muscles and blood vessels [3]. Non-epithelial cancers can also develop from blood-forming cells. These types of cancers are referred to as leukemias, myelomas and lymphoma. Leukemia starts in the bone marrow and leads to an overproduction of abnormal white blood cells. Myeloma also originates in the bone marrow, but affects the plasma cells leading to an overproduction of abnormal plasma cells. Lymphoma starts in the lymphatic system and affects the lymph nodes and the lymph tissues. Finally, cells forming various components of the central and peripheral nervous systems can also be affected. These malignancies are termed neuro-ectodermal tumors [4].

Some cancers do not fit into this classification such as melanomas [5].

1.2. From normal cells to cancer cells

Transformation of a healthy cell into a cancer cell is a multi-step process, which is caused primarily by genetic mutations. Single mutated cell starts to proliferate abnormally due to mutations occurring in genes called cancer driver genes (or mutated driver genes). The consequence of these mutations is to confer a growth advantage to the mutated cells.

The first driver gene mutation usually allows the formation of a small clonal expansion, leading to the formation of a clinically undetectable benign lesion. The second driver gene mutation results in a second wave of local clonal expansion resulting into a clinically detectable benign lesion. The third mutation often confers significant growth advantage to the cancer cells, often resulting in the development of cancer (Figure 1) [6]. Interestingly, most cancer driver genes are acting as drivers in one or two cancer types, while only a group of approximately 10 genes are seen as cancer driver genes in more than 20 malignancies [7]. These genes are: KRAS, TP53, LRP1B, PTEN, PIK3CA, KMT2D, RB, KMT2C, NRAS, ARID1A [7].

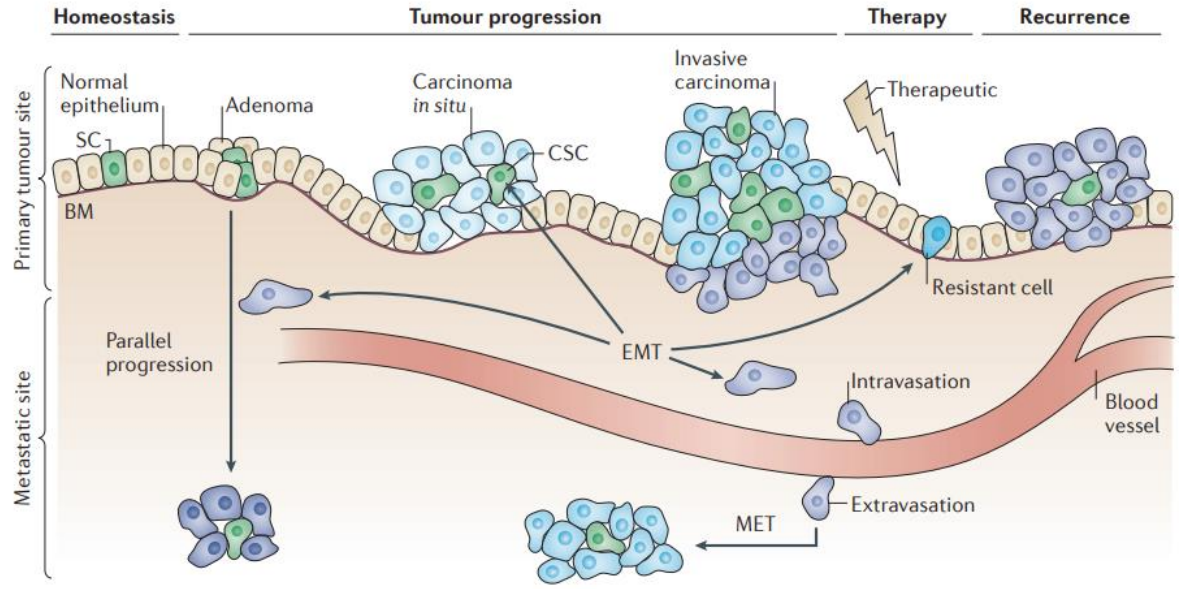

Figure 1 – Schematic representation of cancer progression. During the tumor progression phase, adenoma can occur referring to a benign tumor of the epithelial tissue. It can further progress to a carcinoma in situ if the cells acquire mutations in genes whose alterations bring growth advantage as well as receive appropriate signals from the environment [8].

In order to explain how cells make their way from normal cells to cancer cells, the Hallmarks of Cancer were suggested by Douglas Hanahan and Robert A. Weinberg in 2000. These hallmarks include: sustaining proliferation signaling, evading growth suppressors, resisting cell death, enabling replication immortality, inducing angiogenesis and activating invasion and metastasis [9]. In 2011, Douglas Hanahan and Robert A. Weinberg suggested that the acquisition of these hallmarks is possible because of genome instability and inflammation which were classified as enabling characteristics. Furthermore, two emerging hallmarks were added to the list : reprogramming of energy metabolism and evading immune destruction [10]. More recently, in 2022, Douglas Hanahan proposed to add phenotypic plasticity and disrupted differentiation has a discrete hallmark capability. The hallmarks were also adapted to include senescent cells, as these cells have recently been described to either promote anti- or pro-tumoral effects. Furthermore, non-mutational epigenetic reprogramming and polymorphic microbiomes were also added as two enabling characteristics which facilitate the acquisition of the cancer hallmarks mentioned above (Figure 2) [11].

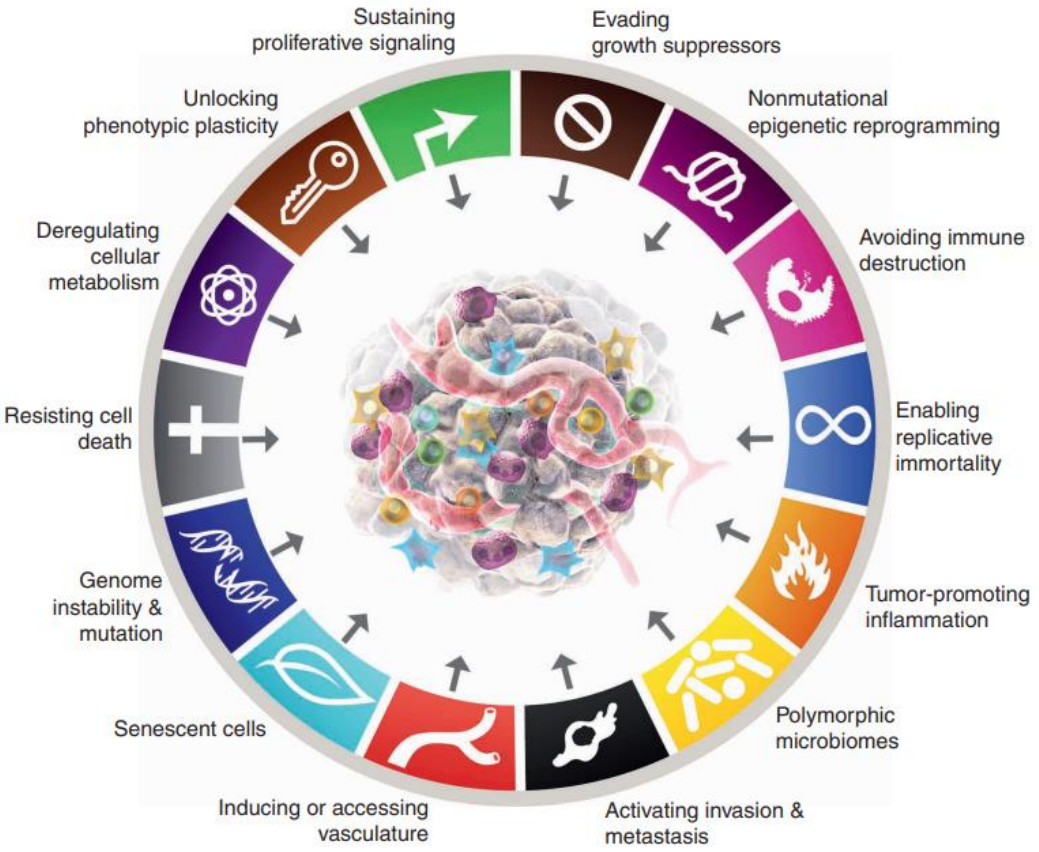

Figure 2 – Hallmarks of Cancer according to Douglas Hanahan and Robert A. Weinberg [11].

1.3. Epidemiology

According to the World Health Organization (WHO), cancer is the second leading cause of death globally, behind cardiovascular diseases. Moreover, WHO estimated that cancer accounted for nearly 10 million deaths worldwide in 2020 [12]. The most frequent cancers are breast, lung, prostate and colon cancers. Fortunately, these cancers are associated with high survival rates as most cancers are surgically resectable (Figure 3) [6]. However, the number of cancer patients with poor survival rate such as pancreatic cancers is projected to increase by 2030 [13]. To this day, the progress made by research to improve the survival of these types of cancers remained poor.

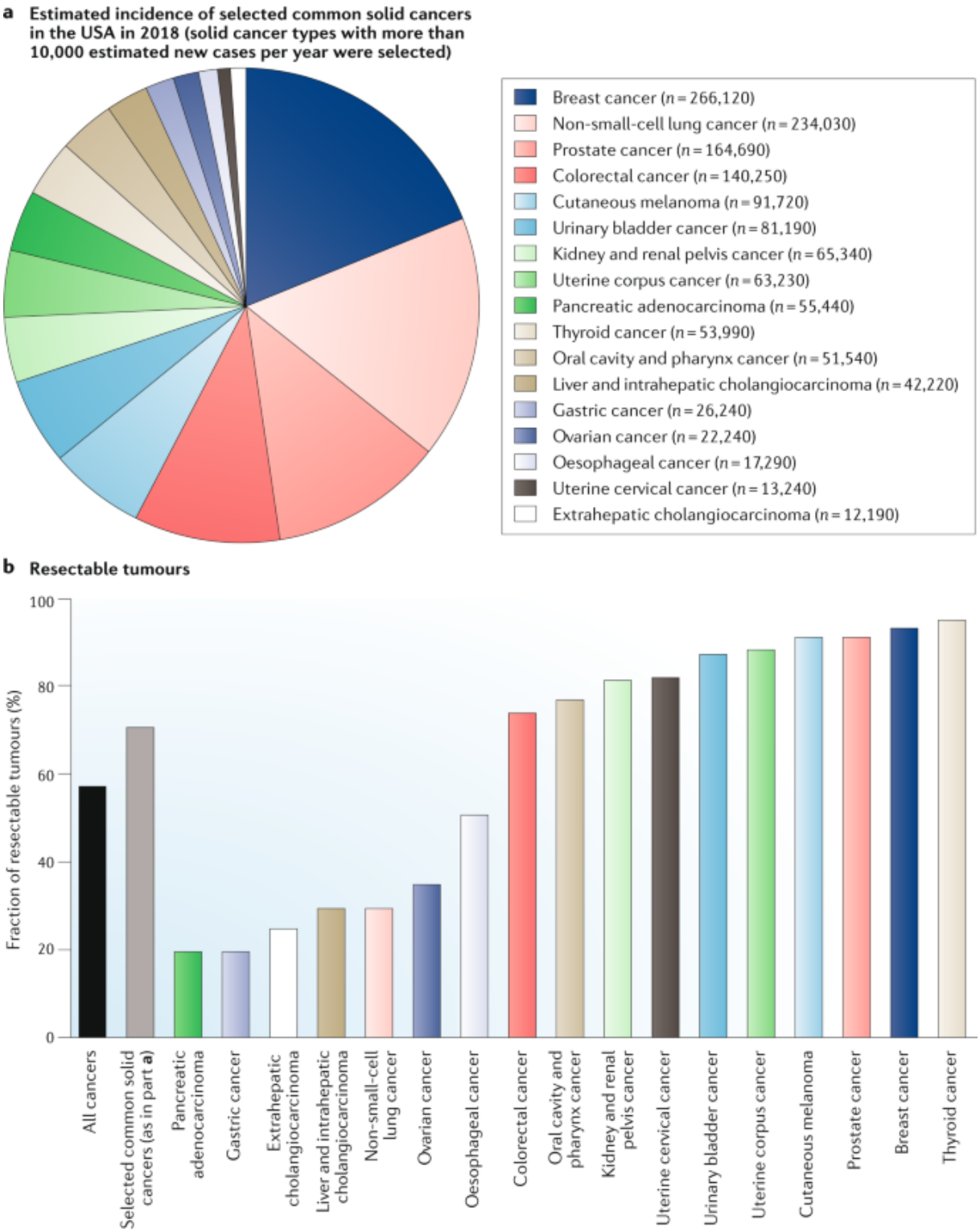

Figure 3 – (A) Estimated incidence of several solid cancer types in the United States of America (USA) in 2018. The cancer types selected presented more than 80% of all new cases in the USA. (B) Percentage of resectable tumors [6].

1.4. Risk factors

Finding risk factors associated with cancer has been instrumental in the pursuit of cancer prevention. Risk factors are often separated in two categories: intrinsic or non-intrinsic risk

factors. Intrinsic risk factors are unmodifiable risks, while non-intrinsic risk factors can be further sub-divided into exogenous and endogenous factors which are respectively, modifiable and partially modifiable factors [14].

As mentioned above, intrinsic factors refer to unmodifiable factors arising from spontaneous mutations which are the results of errors during DNA replication. In 2014, the 'bad luck' hypothesis was proposed by Tomasetti and Vogelstein after demonstrating that two-thirds of cancers are due to random mutations [15]. However, the hypothesis was disproven by Wu et al. Indeed, the authors showed that non-intrinsic factors play an important part in the development of most cancers [16].

Non-intrinsic factors are modifiable factors. These risk factors are divided into endogenous and exogenous factors. Exogenous risk factors are modifiable risk factors as these risk factors include lifestyle factors such as physical activity and diet. Moreover, several epidemiological studies have identified the following exogenous risk factors: tobacco smoke for lung cancer, UV radiation for skin cancer and viruses such as human papillomavirus (HPV) for cervical cancer [14]. Endogenous risk factors are partially modifiable factors. The two most well-known endogenous risk factors are inflammation and aging [14]. However, endogenous risk factors are complex to study as they are influenced by exogenous components as well as genetic components.

1.5. Treatments

Treatments used against cancer can be divided into two categories: systemic and local. Systemic treatments correspond to medications that travel through the bloodstream. The most common types of systemic treatments are chemotherapy and immunotherapy while local treatments such as surgery and radiotherapy only affect the targeted cells.

1.5.1. Systemic treatments

1.5.1.1. Chemotherapies

The use of chemotherapy for cancer treatment started in 1942 when a patient with non-Hodgkin's lymphoma was treated with nitrogen mustard [17,18]. Chemotherapy uses chemical substances which possess the ability to induce DNA damages or to prevent cancer cells from dividing (Figure 4). Due to the inability of chemotherapies to distinguish between normal cells and cancer cells, chemotherapies often lead to severe side effects such as alopecia, infections and anemia.

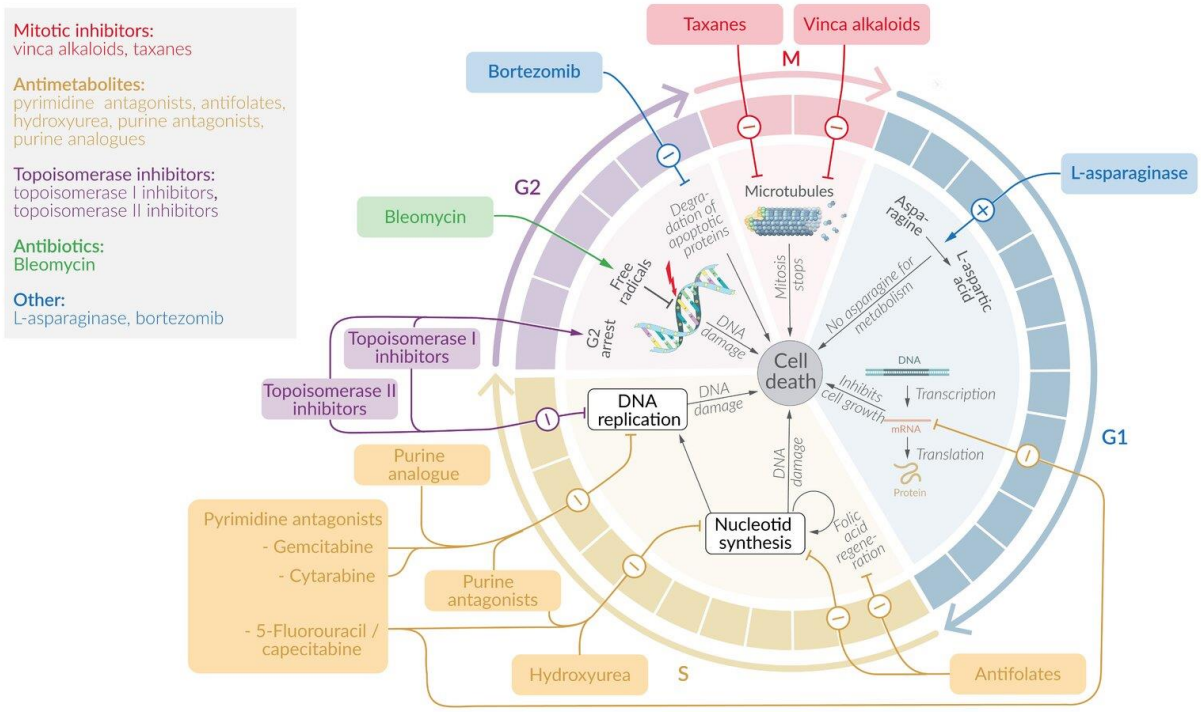

Figure 4 – Common chemotherapy agents with molecular mechanisms of action (from AMBOSS).

1.5.1.2. Targeted therapies

Chemotherapies do not possess the ability to distinguish between normal cells and cancer cells unlike targeted therapies. To do so, targeted therapies take advantage of genetic alterations which differentiate cancer cells from normal cells.

These therapies can for example, inhibit the CDK4/6 implicated in the cell cycle. These therapies can also target mitogenic signals such as Raf, Erk, mTOR and PI3K. In the context of this PhD thesis, inhibitors of poly(ADP-ribose) polymerase (PARP) were used. These inhibitors are known to target PARP which is required for DNA damage repair, thus, the inhibition of PARP triggered cell death [19]. Several side effects are associated with targeted therapies such as high blood pressure, fatigue, … The side effects associated with targeted therapies are often less severe than side effects associated with chemotherapies.

1.5.1.3. Immunotherapies

Immunotherapy appeared quite recently with the goal of re-purposing the immune system of the patient to fight cancer cells. The most famous type of immunotherapies are the ones targeting the adaptive immune system, namely T lymphocytes, such as the inhibitors targeting cytotoxic T lymphocyte protein 4 (CTLA-4), programmed cell death protein 1 (PD-1) and programmed cell death ligand 1 (PD-L1) [20]. For their discovery of cancer therapy by inhibition of negative immune regulation, James P. Allison and Tasuku Honjo were awarded the 2018 Nobel Prize in Physiology or Medicine. This therapeutic strategy is currently approved by the

Food and Drug Administration (FDA) for the treatment of several cancers either alone or in combination [21,22]. These inhibitors have significantly changed the treatment of several cancer types. Briefly, CTLA-4 and PD-1 are two inhibitory receptors present at the surface of T lymphocytes. CTLA-4 inhibits the activity of CD28, a major activating co-receptor also expressed at the surface of T lymphocytes. Indeed, CTLA-4 can bind B7.1 or B7.2 (CD80 or CD86) with a much higher affinity than CD28. The amount of CD28:B7 binding versus CTLA-4:B7 binding thus determines if a T lymphocyte is activated or not. PD-1 is a member of the B7/CD28 family of co-stimulatory receptors. PD-1 binding to PD-L1 inhibits T-cell proliferation, interferon-gamma, tumor necrosis factor-alpha production. The expression of PD-1 by T lymphocytes is often described as a marker of "exhausted" T cells. Thus, binding of PD-1 or PD-L1 restores effector functions of T lymphocytes (Figure 5) [23].

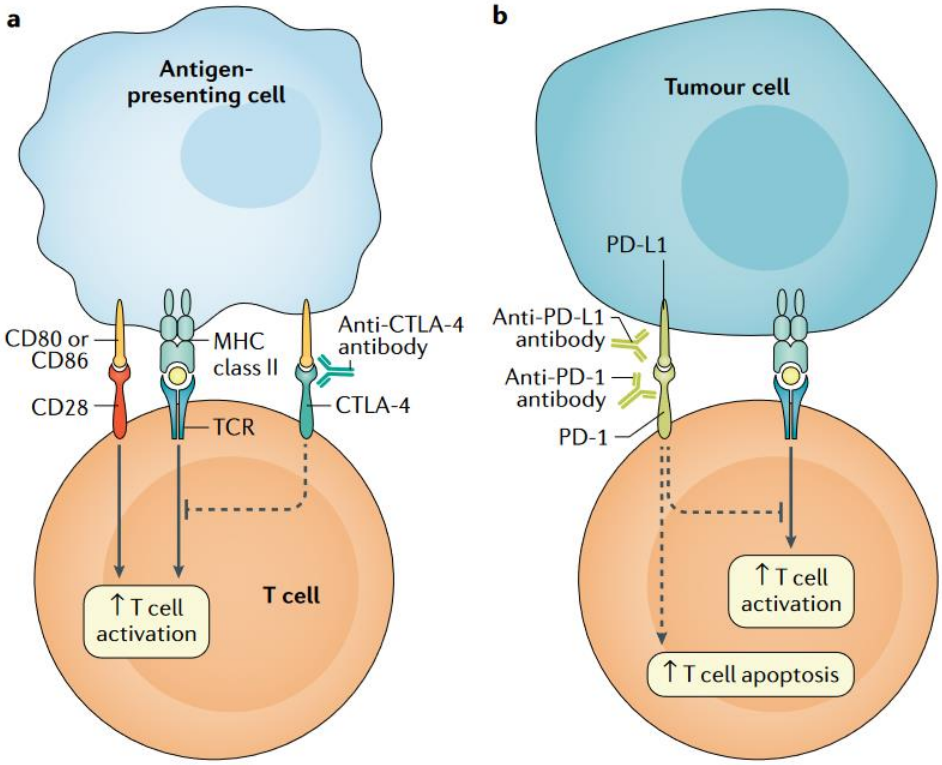

Figure 5 – The mechanism of immune checkpoint and immune checkpoint blockers. (A) The activation of T cells requires two signals: (i) the T cell receptor (TCR) from the T cell recognizes the antigen presented by the major histocompability complex II (MHC II) present at the surface of an antigen-presenting cell and (ii) CD80 or CD86 present at the surface of the antigen-presenting cell recognizes CD28 present at the surface of the T cell to give co-stimulatory signals necessary for T cell activation. CTLA-4 competes with CD28 to bind to CD80 or CD86 at the surface of the antigen-presenting cell, thus blocking T cell activation. (B) PD-L1 is a ligand expressed at the surface of tumor cell and myeloid cells whereas, its receptor (PD-1) is expressed at the surface of T cells. When interaction between PD-1 and PD-L1 occurs, T cell activation is inhibited and T cell apoptosis is promoted. Thus, the presence of anti-PD-L1 and anti-PD-1 antibodies favors T cell activation by blocking the interaction between PD-1 and PD-L1 [24].

Even if most successes in the field of immunotherapy occur while targeting T cells, several immunotherapies targeting the innate immune cells such as macrophages, natural killer (NK) cells, myeloid-derived suppressor cells (MDSC) are currently under investigation [25].

1.5.2. Local treatments

Local treatments only affect the targeted cells and the cells located in the near proximity of the targeted cells. The most common types of local treatments are surgery and radiotherapy. Since the focus of this PhD thesis is to determine the impact of conventional radiotherapy and proton therapy on cancer cells, the following chapter will be dedicated to conventional radiotherapy and particle therapy.

2. Conventional radiotherapy and particle therapy

Radiotherapy (RT) is a clinical modality dealing with the use of ionizing radiation in the treatment of cancer patients. The goal of RT is to precisely deliver a measured dose of ionizing radiation to the tumor while minimizing the damages to the surrounding tissues. It is estimated that 50% of all cancer patients will receive RT at some point of their treatment [26,27]. Indeed, RT is the treatment of choice in several cancers such as breast, cervix, colorectal, hematological, head and neck, lung, esophagus and prostate cancers [27]. Conventional RT involving photons (X-rays or gamma-rays) has recently improved with the use of new technologies such as intensity-modulated RT (IMRT). Furthermore, due to their interesting physical properties, charged particles such as protons and carbons have recently gained momentum in the treatment of several cancers [26,28–30]. In the following sections, conventional radiotherapy and particle therapy will be compared with a specific attention given to proton therapy.

2.1. The origins

X-rays were discovered by Wilhelm Conrad Rontgen in 1895. The German physicist was awarded the Nobel Prize in Physics in 1901 for his discovery. X-rays are photons which are emitted from processes outside the nucleus of an atom. In parallel, Antoine Henri Becquerel discovered natural radioactivity while he was studying phosphorescent materials (uranium salts). He showed that the penetrating radiation came from uranium itself. Later, Maria Sklodowska-Curie and her husband, Pierre Curie, discovered two radioactive elements: polonium and radium [31]. Marie Sklodowska-Curie, Pierre Curie and Antoine Henri Becquerel were awarded the Nobel Prize in Physics in 1903 for their work on radioactivity.

However, it is only in 1900 that it was demonstrated that these radioactive elements emit ionizing radiation as their atoms undergo radioactive decay, which corresponds to the emission of energy in the form of ionizing radiation. The emitted ionizing radiation can include alpha, beta and gamma rays. The alpha particle is composed of two protons and two neutrons. Due to the charge and mass of the alpha particle, they are unable to travel beyond a few centimeters in the air. Beta rays can take the form of an electron or a positron. Most of the electrons and the positrons are able to travel up to a few meters in the air. Finally, gamma rays are photons similarly to X-rays. The difference between gamma rays and X-rays resides in the way they are produced. Gamma rays originate from the excited nucleus itself while X-rays are produced by electronic transition or bremsstrahlung (“braking radiation” in german). This last process characterizes the X-rays emission arising when an electron trajectory bends when passing close to the positively charged nucleus. These photons can easily penetrate barriers capable of stopping alpha and beta rays. As gamma rays pass through the human body, they cause ionizations similarly to X-rays [32].

At that time, numerous studies used X-rays and radium in medicine. Radiations can be delivered either externally or internally. If radiations are delivered externally: the beam of radiation is delivered by a source of radiations which is external to the body. While if radiation is delivered internally, the radioactive source is placed inside the lesions. However, due to a lack of knowledge, the benefits of RT were poor. Furthermore, initial RT relied on low energy ionizing radiation with low penetration power. It is only in the 1950s that different machines for megavoltage therapy became available. These machines offered the advantage of higher depth doses [33]. The development of RT improved further with the emergence of IMRT, volumetric modulated arc therapy (VMAT), stereotactic radiotherapy (SRT), the CyberKnife technique and the GammaKnife technique [33].

Particle therapy was first reported in 1976. Particle therapy can use neutrons, protons, pions and ions. At the moment, protons, carbon ions and alpha particles are approved to treat cancer patients [28].

2.2. Concepts in radiotherapy

2.2.1. Production of photons

X-rays are produced using an X-ray machine. The latest contains a cathode which is made up by a tungsten filament. Firstly, a current passes through the tungsten filament to heat it, leading to the emission of electrons (in a process referred as the thermionic emission). Then, the electrons are accelerated towards the anode (i.e. the target) using a high voltage applied between the cathode and the anode. When the electrons strike the anode, two main processes lead to the production of X-rays (Figure 6). Firstly, if electrons collide with an inner shell electron (also, refers to as K-shell electron), characteristic X-ray photon is emitted. Those X-rays are emitted at given energies characteristic of the target. Secondly, if free electrons interact with the nucleus, bremsstrahlung radiation is generated. The energy spectrum obtained for this process is continuous and ranges from the very low energies to initial energy of the electrons (corresponding the high voltage applied between the cathode and the anode). The lowest energies correspond to electrons that were slightly deviated by the nucleus while the highest energies correspond to largest deviations. The X-ray spectrum can be modified by changing the X-ray tube current or voltage settings, or by adding filters in order to select the high energy X-rays.

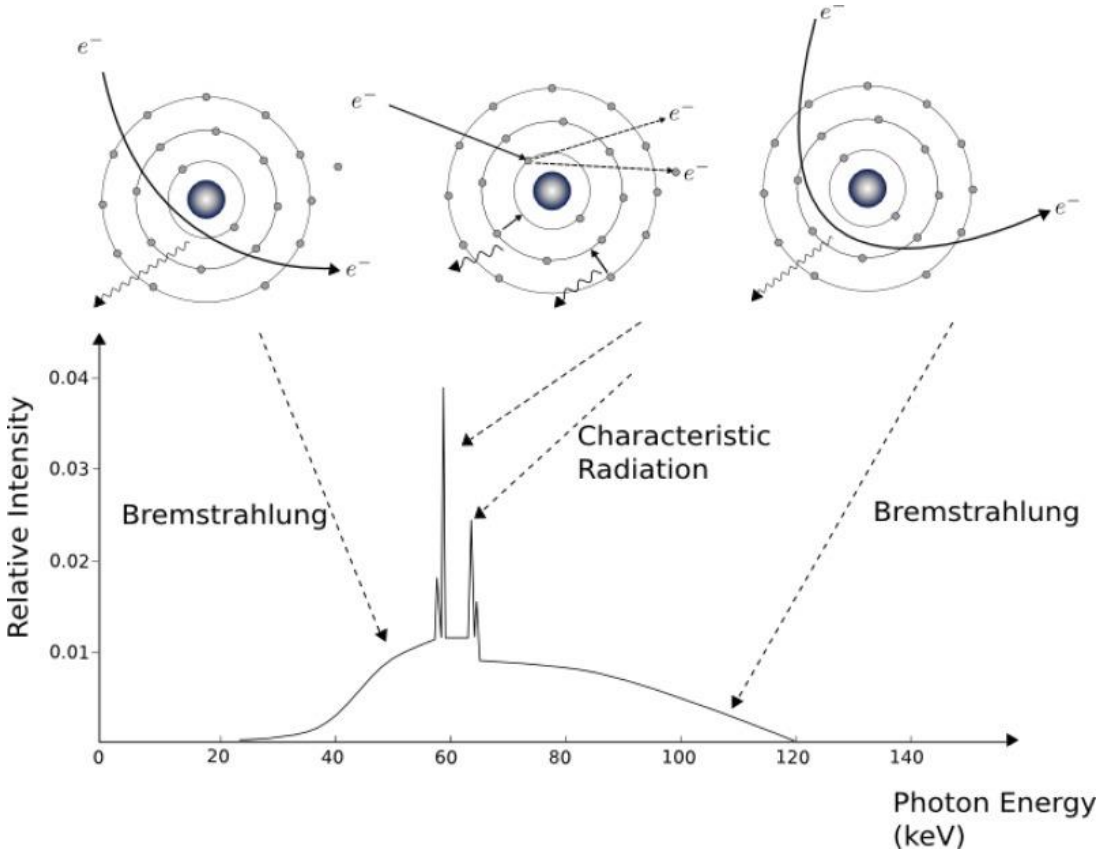

Figure 6 – The X-ray spectrum of a tungsten tube [34].

Gamma rays are also used in the clinics for radiation therapy. Often, gamma rays are obtained from Cobalt-60 (^{60}Co). In this case, radiation is emitted when the excited nucleus of a radionuclide undergoes radioactive decay.

2.2.2. Production of charged particles at the University of Namur

The University of Namur is equipped with a 2 MV tandem accelerator (ALTAIS) (Figure 7). The latest is capable of accelerating several types of ions. In our case, a beam of H+ was produced from the sputtering of a TiH_2 powder in the plasma source. Negative ions are first extracted from the plasma, and these negative ions can be selected with the low energy magnet and accelerated as they are attracted by the positive voltage residing at the center of the accelerator. There, i.e. where the high voltage is applied, nitrogen is released which strips the electrons leading to the production of positive ions. These positive ions are then pushed by the positive voltage and thus accelerated a second time. This is why ALTAIS is a tandem accelerator, the particles are accelerated twice thanks to the charge state change. After the second acceleration, the ions can be deflected to the desire beam line with the high energy magnet [35].

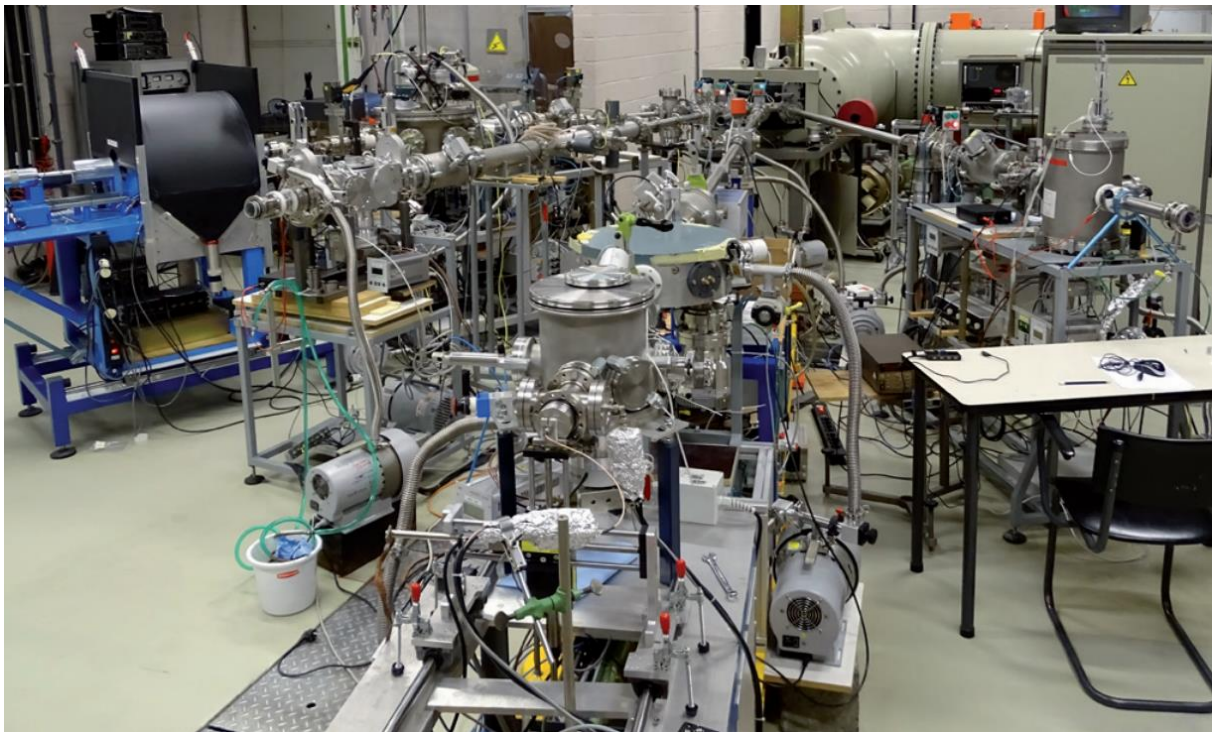

Figure 7 – The ALTAIS at the University of Namur.

2.2.3. Dose distribution

Photons deposit most of their energy close to the surface entrance followed by a continuous decrease characteristic of their attenuation, while charged particles deposit a small fraction of their energy before what is called the Bragg peak, characterizing the maximal energy released when the particles come at rest. The dose sharply decreases beyond this peak, allowing to spare downstream tissues. In order to irradiate a tumor, several Bragg peaks have to be superposed in order to generate the so-called Spread-Out Bragg Peak (SOBP) (Figure 8).

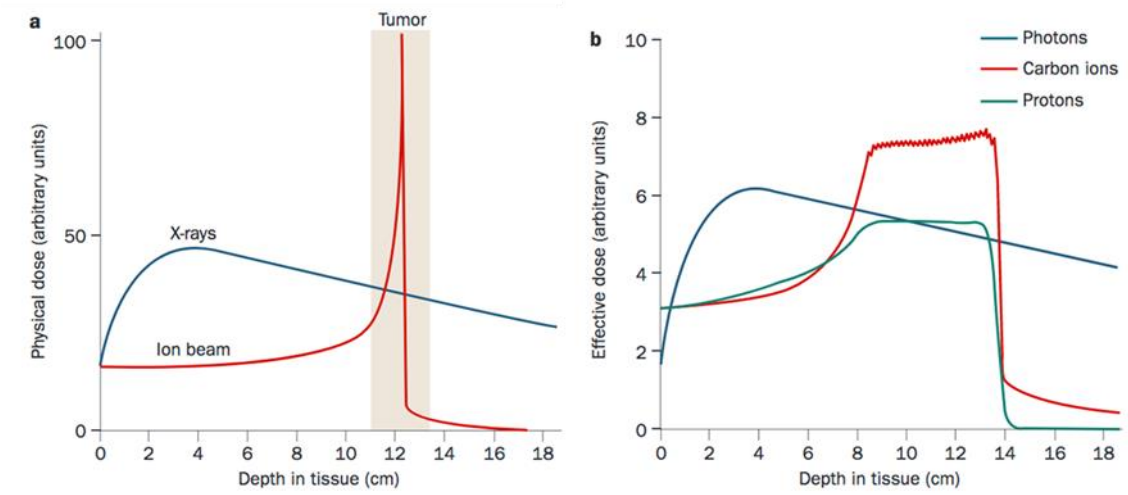

Figure 8 - (A) Comparison of the dose distribution of X-rays (in blue) and charged particles (in red). (B) When tumors are treated, several Bragg peaks must be overlapped to create the SOBP [26].

2.2.4. Absorbed dose

The absorbed dose measures the energy deposited by ionizing radiation in a unit mass of matter being irradiated [36]. The gray (Gy) is a unit in the International System of Units (SI), and is used to measure the absorbed dose. The gray is defined as "the absorption of one joule of radiation energy per kilogram of matter".

Patients receiving radiotherapy are often given 50 Gy over the course of 5 weeks where 2 Gy is given at each treatment, called fraction. For example, the conventional fractionation schedule, also refers as the gold standard, is used to give patients, a dose of 1.8 Gy to 2 Gy per fraction. The patient will receive 5 fractions per week until the total dose is reached. Other schedules exist such as the acceleration schedule, hypofractionation schedule, hyperfractionation schedule and accelerated-hyperfractionated schedule which are often used to increase tumor control [37]. In the laboratory, cells are often exposed to a variety of doses ranging from 0.5 to 20 Gy.

2.2.5. Linear energy transfer

The linear energy transfer (LET) corresponds to the amount of energy transferred by an ionizing particle to the traversed materiel per unit distance for a given medium. It is usually express in keV/µm. Depending on velocity and charge, ionizing particles display a low or high LET. The LET will increase along the particle path as it slows down. Photons are said to be low-LET radiation. In comparison, along their trajectory, the LET of protons varies from a fraction of keV/µm up to 50 keV/µm within the Bragg peak. Protons are thus, described as intermediate LET radiation. Finally, carbon ions and alpha particles are said to be high-LET radiation [37]. In the clinic, carbon ions typically have a LET of 10 to 80 keV/µm while the LET of alpha particles is around 100 keV/µm.

2.2.6. Relative biological effectiveness

The relative biological effectiveness (RBE) of a radiation is defined as: "the dose of reference radiation divided by the dose of test radiation to reach a given biological response". The radiation reference is often a beam of 250 kVp X-rays or ^{60}Co gamma-rays. The RBE depends on several parameters such as the measured end point, dose, dose rate, dose per fractionation, number of fractions, particle charge, velocity, oxygen concentration and cell-cycle phase [37,38]. Particles with a LET of 100 keV/µm possess the highest RBE value (Figure 9). For example, the RBE in the clinic for protons is 1.1 meaning that protons are capable of killing 10% more of cancer cells when compared to X-rays or gamma rays. Of note, in the distal part of the SOBP, the RBE increases above 1.1. At the University of Namur, depending on the chosen LET: 10 keV/µm or 25 keV/µm, the RBE varies from 1 to 3 [39].

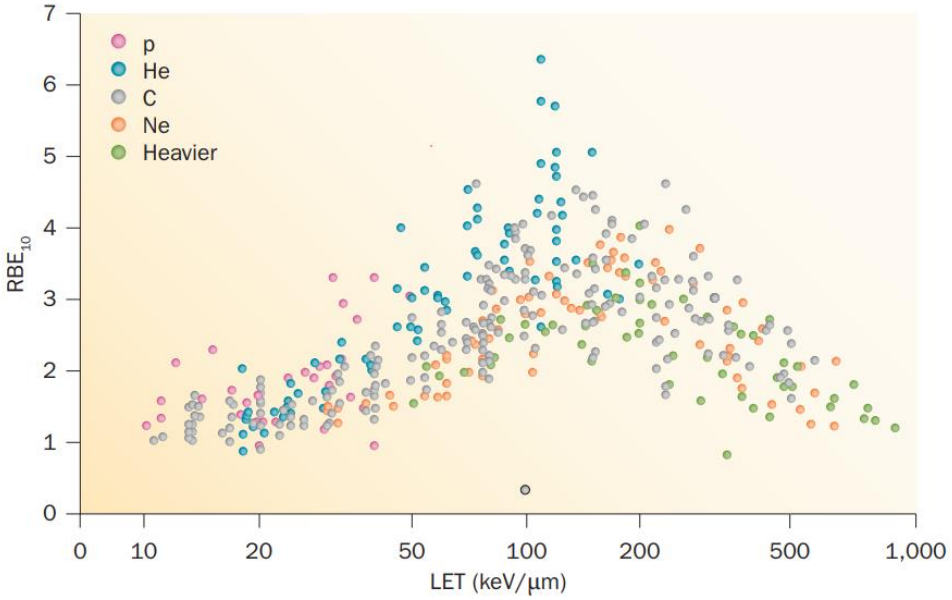

Figure 9 – The RBE calculated at 10% of survival versus the LET from published in vitro experiments. The colors refer to different ions : protons in pink, helium (He) in blue, carbon (C) in gray, neon (Ne) in orange and heavier particle are in green [38].

The RBE value can be calculated using the following equation:

$$RBE = \frac{Dose\ of\ 250\ kVp\ Xrays\ to\ produce\ a\ biological\ effect}{Dose\ of\ a\ test\ radiation\ to\ produce\ the\ same\ biological\ effect}$$

2.2.7. Clonogenic assay

Clonogenic assay or colony formation assay is often seen as the gold standard to determine *in vitro* cell reproductive death following radiation [40]. To calculate the surviving fraction (SF) at a given dose, the number of colonies is divided by the number of seeded cells and normalized to the plating efficiency of the control cells. The log-transformed values of the surviving fractions are plotted against the corresponding irradiation doses.

$$PE = \frac{Number\ of\ colonies\ formed}{Number\ of\ cells\ seeded} * 100\%$$

$$SF = \frac{PEx}{PEcontrol}$$

The linear-quadratic (L-Q) model is then used, and the latest describes the shape of survival curve, which is characterized by two parameters, α and β. For some cell lines at higher LET,

the shape of the survival curve tends to be linear. In that case, the β parameter of the LQ model is set to zero (Figure 10).

The equation of the LQ model is the following:

$$p(survival) = \exp(-\alpha D - \beta/D^2)$$

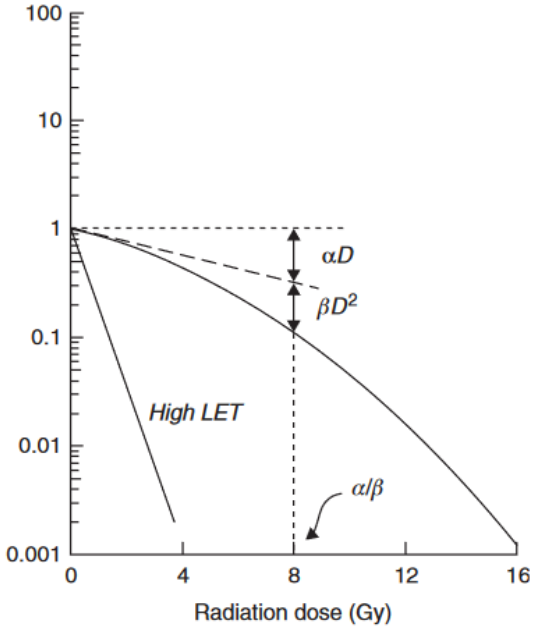

Figure 10 – Survival fraction for cells irradiated with low LET radiation or with high LET radiation fitted with the LQ model [36].

2.3. Factors influencing the success of RT

Withers summarized the factors influencing the success of RT as the four Rs of radiotherapy : recovery from sublethal damage, cell cycle redistribution, cellular repopulation and tumor reoxygenation [41].

Following radiation, DNA damages can be repaired by the cells through several mechanisms which will be detailed in chapter 2.6. The efficacy of the repair determines the ability of the cells to recover from radiation. Second, cells exhibit different levels of radio-resistance as they pass through the different phases of the cell cycle. Indeed, the cells which are in the S phase are known to be the most resistant while the cells in late G2 and mitosis are the most sensitive to radiation. The reason behind this difference is thought to be due to the ability of the cells to repair DNA damages through the homologous recombination (HR) pathway during the S phase as the sister chromatid acts as a repair template. Cellular repopulation is often described as the main cause of radiotherapy failure. Indeed, surviving tumor cells often have the ability to perform rapid proliferation following treatment. The last R refers to tumor

reoxygenation: cancers contain hypoxic zones in which cancer cells are seen as resistant to radiation, especially to conventional radiation. In 1989, Steel et al. proposed to add intrinsic radiosensitivity as a fifth parameter to account for the different tolerance of tissues to radiation [42]. More recently, in 2019, re-activation of the tumor immune response was added as a sixth parameter [43]. Indeed, several studies indicate that radiotherapy is capable of inducing immunogenic cell death (ICD). Immunogenic cell death is defined as a type of cell death capable of inducing an immunogenic response. ICD is characterized by several markers, namely the translocation of calreticulin (CRT) to the cell surface, the release of adenosine triphosphate (ATP) and the release of high mobility group box-1 (HMGB-1) [44]. These events are said to be of high importance in the context of dendritic cell (DC) activation and the priming of T cells. Furthermore, it was also shown that radiotherapy could trigger the release of double-stranded DNA (dsDNA) within the cytoplasm leading to the activation of the cGAS-STING pathway which also is responsible for the induction of the interferon (IFN) type I response, leading to the activation of DC. Interestingly, the induction of the IFN type I response was only observed when cells were irradiated with a dose of 12 Gy or lower. Indeed, the authors demonstrated that higher dose induced the expression of Trex1 leading to the degradation of dsDNA, thus preventing the activation of cGAS-STING [45]. Radiotherapy has also been shown to trigger the induction of PD-L1 [46,47]. Several researches were conducted on the combination of RT to anti-CTLA-4 or anti-PD-L1 or anti-PD-1 antibodies [48,49]. The PACIFIC trial found significantly longer progression free survival (PFS) and overall survival (OS) in patients with stage 3 non-small cell lung cancer (NSCLC) treated with durvalumab, an anti-PD-L1 antibody, compared to placebo group after concurrent chemoradiotherapy. Indeed, the 24-month OS rate was 66.3% in the durvalumab group, as compared with 55.6% in the placebo group. Current research focus on the impact of the dose and fraction regimen which should be adopted, as well as the exploring the schedule for the combination therapy. Indeed, it seems that RT is capable of increasing the expression of PD-L1 at mRNA and protein levels. However, studies also suggest that injecting PD-L1 antibodies before RT could also give good results. Concurrent injection could also work. Thus, the optimal timing remains to be defined [50].

2.4. Comparison between conventional radiotherapy and charged particle therapy

2.4.1. Spatial dose distribution

The depth profile between photons and protons is different and represents one of the major differences between photons and protons. Charged particles are often used to limit the effects on healthy tissues, thus decreasing the chances of secondary cancers.

2.4.2. Direct and Indirect DNA damages

Protons possess a higher LET (higher density of ionization). Protons thus produce more cell killing per Gy. Indeed, charged particles directly interact with the DNA resulting in complex and clustered DNA damages (DSBs) which are more difficult to repair for the cells. In comparison, photon irradiation produces more indirect DNA damages through the production of free radicals. These DNA damages are easier to repair (Figure 11) [36].

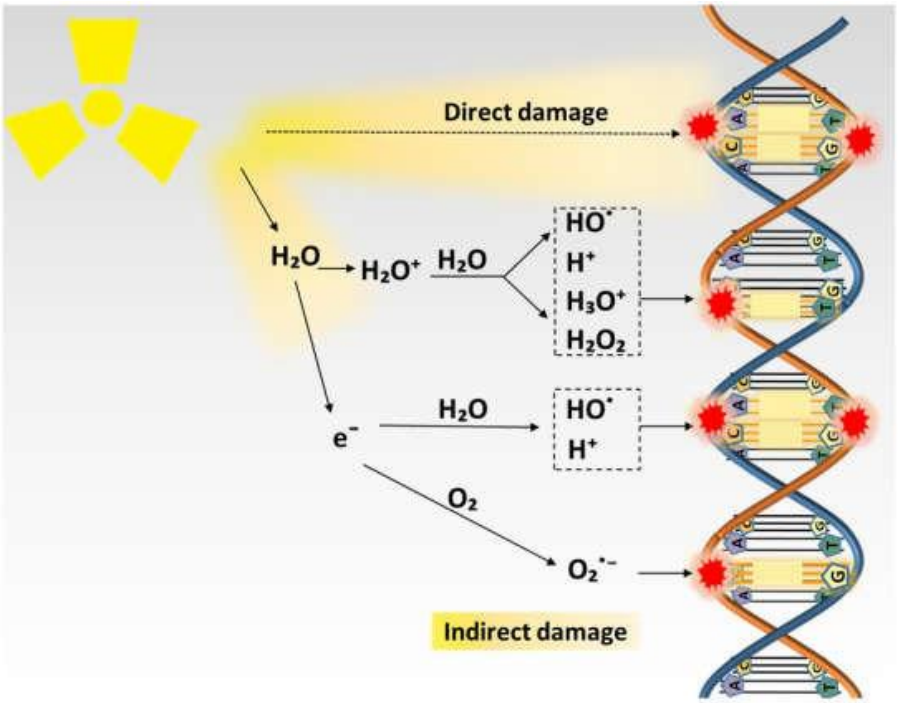

Figure 11 – Radiation produces direct DNA damage and indirect DNA damage. Radiation directly interacts with the DNA resulting in DNA damage. Radiation can also interact with water (H_2O), resulting in the production of free radicals resulting in DNA damages [51].

2.4.3. Oxygen enhancement ratio

Radiosensitivity depends on the amount of oxygen. Indeed, poorly oxygenated cells are more resistant when compared to well oxygenated cells. Interestingly, this effect seems to be less important with high-LET radiations. Since the response of cells to radiotherapy depends on oxygen, it is possible to calculate the oxygen enhancement ratio (OER) in the following manner [52] :

$$OER = \frac{Radiation\ dose\ without\ oxygen}{Radiation\ dose\ with\ oxygen}\ (for\ a\ given\ effect)$$

For cells exposed to X-rays, the OER is around 3.0 meaning that the dose used to kill the same number of cells in hypoxic conditions is three times higher than in normoxia. For protons, the OER is also around 3.0, whereas for carbon ions, the value is around 1 to 2.5. These differences can be explained by the oxygen-fixation hypothesis (Figure 12). Indeed, radiation is known to produce free radicals. These free radicals are highly reactive molecules, which react with

oxygen leading to more DNA damages rendering cells more sensitive to radiation [53]. Furthermore, the complexity of damages is enhanced with increased LET, meaning that high LET radiations are less depend on the formation of ROS, and thus on oxygen concentration [38].

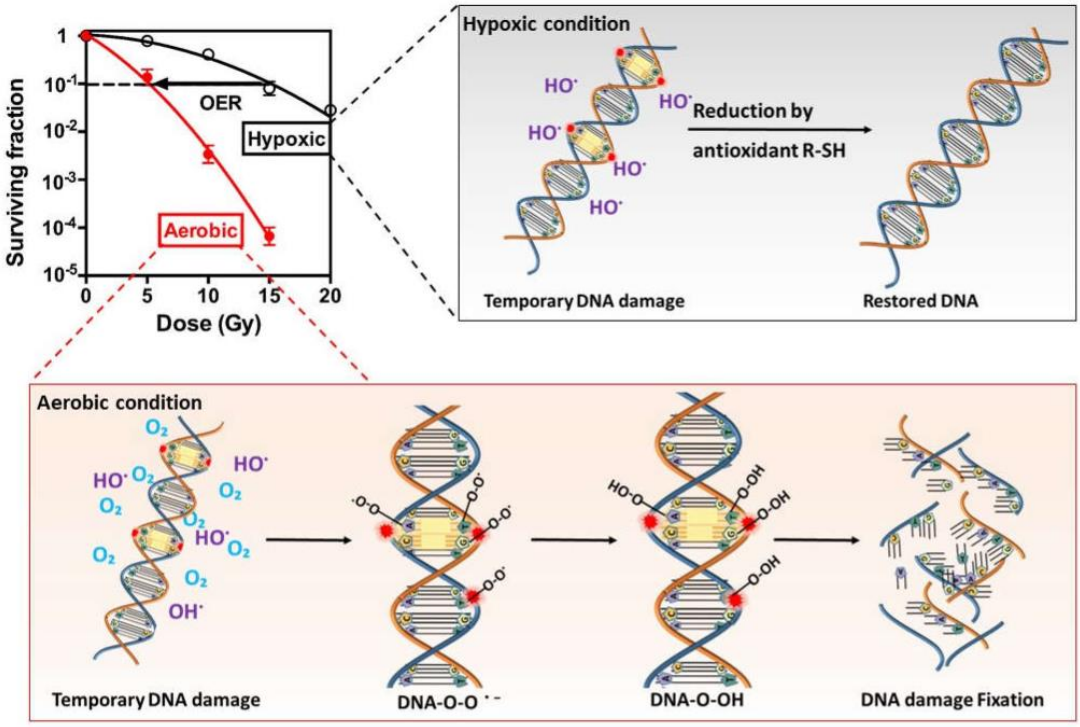

Figure 12 – The oxygen-fixation hypothesis. Under aerobic (normoxic) condition, the free radicals are capable of reacting with oxygen which results in permanent DNA damage. Under hypoxic condition, the free radicals are not capable of reacting with oxygen, thus reducing the amount of DNA damages, explaining why survival fraction is increased in hypoxic condition [51].

2.4.4. Cell cycle

The radiosensibility of cells varies depending on the position of the cell in the cell cycle. Briefly, the process of duplication of the genetic material of a cell and the division of the latest are tightly regulated processes. Indeed, cells have to progress through several phases of the so-called cell cycle: growth phase 0 or 1 (G0/G1), synthesis (S), growth phase 2 (G2) and mitotic (M) phase. The progress through cell cycle is regulated by cyclin-dependent kinases (CDKs). Furthermore, the activity of the CDKs is positively regulated by their cyclin partners and negatively regulated by CDK inhibitors (CDKi) [54].

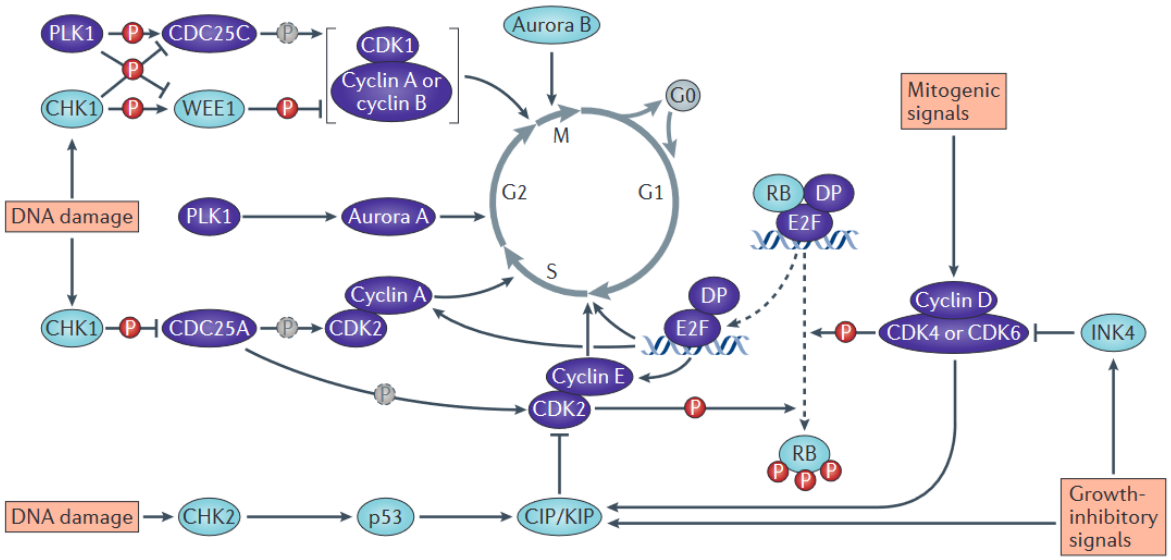

Figure 13 – Major regulatory proteins of the cell cycle. Mitogenic signals activate the complex Cyclin D/CDK4 or Cyclin D/CDK6. The active complex Cyclin D/CDK4 or Cyclin D/CDK6 phosphorylates the retinoblastoma protein (RB) leading to the progression from G1 phase into S phase. In case of detection of growth-inhibitory signals, INK4 and CIP/KIP prevent the progression from G1 phase to S phase to respectively, inhibiting Cyclin D/CDK4 or Cyclin D/CDK6 complex and Cyclin E/CDK2 complex. The progression from the S phase to the G2 is controlled by Cyclin-CDK complexes and Aurora kinases. Furthermore, DNA damages activate CHK1 or CHK2 triggering cell cycle arrest to allow cell to repair DNA damages. The dark blue color indicates positive regulators of cell cycle progression and the light blue color indicates negative regulators of cell cycle progression [55].

The cells undergoing mitosis are more sensitive to radiation, while the cells in the S phase are more resistant to radiation. Interestingly, this difference in radiosensitivity depending on the phase of cell cycle is not as clear when using high LET radiation meaning that high LET radiation could be more efficient to treat slow proliferation tumors [56]. The reason behind the decreased cell cycle dependence following high LET radiation could be explained by the increased DNA damage complexity preventing DNA damage response to occur.

2.4.5. The immune system

As aforementioned, the interest in combining RT to immunotherapy is rising. Indeed, conventional RT seems to possess both immune-stimulating and immune-suppressive properties. Even if the number of studies conducted on the effects of particle therapy on the immune system are limited, it seems that particle therapy could lead to a stronger immune response compared to conventional radiotherapy [57–59].

2.5. Current clinical applications

Currently, charged particles are used to treat pediatric cancers since the precise dose distribution limits exposure to healthy tissue, thus limiting the risk of secondary cancers. Furthermore, high LET radiation is used in the treatment of tumors located near sensitive organs such as: uveal melanoma, chordomas, chondrosarcomas and glioblastoma multiforme (GBM). In the Netherlands, a National Indication Protocol Proton therapy for several cancer types has been developed in order to select patients who might benefit from proton therapy [60]. Despite these clear advantages compared to conventional radiotherapy, the use of charged particle therapies has been slow due to the cost of the treatment. Indeed, the cost of a proton therapy treatment is approximately 2 to 4 times higher than the cost of conventional radiotherapy. Furthermore, no results from randomized phase III clinical trial comparing proton therapy to conventional radiotherapy are currently available.

However, with the construction of several proton centers around the world, proton therapy is being tested in several cancer types such as head and neck, breast, gastrointestinal and lung cancers. One proton center is already in use in Belgium at UZ Leuven, and another Belgian proton center should start treating patients in 2024 in Charleroi.

2.6. DNA damages and DNA damage response

As mentioned above, damages to the DNA structure can arise leading to the formation of DNA damage patterns. DNA damages are often divided into two categories: endogenous and exogenous. Conventional radiotherapy and particle therapy generate exogenous damages as ionizing radiation can directly affect the integrity of the DNA [61]. Furthermore, conventional radiotherapy and particle therapy can also lead to endogenous damages as these therapies produce reactive oxygen species (ROS).

Once DNA damages are detected, the cells initiate a DNA damage repair response (DDR). The repair mechanisms implicated in the DDR vary according to the damage type. Furthermore, double-stranded breaks (DSBs) are considered to be the most complex and difficult DNA damages to repair. Thus, the therapeutic effect of commonly used cancer treatments such as radiotherapy, is based on their ability to generate DSBs leading to cell killing (Table 1). DNA damages are then detected by sensors capable of sensing DNA damage and signaling the presence of DNA damage in order to promote subsequent repair. Two major pathways known as the homologous recombination (HR) and non-homologous end joining (NHEJ) pathways are capable of repairing DSBs. Of note, HR is an error free repair mechanism, while NHEJ is an error prone mechanism.

Table 1 - DNA damages per cell treated with 1 Gy induced by ionising radiations calculated for X-rays, protons (25 keV/µm), alpha particles (100 keV/µm) and carbon ions (282 keV/µm) [62].

	X-rays	Protons	Alpha particles	Carbon ions
Base damage	3100 (74.9%)	1525 (59.6%)	792 (48.6%)	262 (32%)
Single-strand break	1000 (24.1%)	937 (36.6%)	704 (43.1%)	387 (47%)
Double-strand break	40 (1%)	97 (3.8%)	137 (8.3%)	168 (1%)

2.6.1. Detection of DNA damages – Foci formation

An early cellular response to DSBs is the recruitment of a large number of proteins to the sites of DNA damages. The recruitment of these proteins can be visualized microscopically as "foci" in the nucleus of cells with DNA damages. One of the earliest events to occur after DNA damage, is the rapid phosphorylation of H2AX, known as the minor histone H2A variant, at mammalian Ser-139 to produce the phosphorylated H2AX, also called gamma-H2AX (Figure 14). The phosphorylation spreads to adjacent areas of chromatin inducing chromatin relaxation. This event is necessary for other DNA repair proteins to access the site which needs to be repaired [63].

H2AX can be phosphorylated by several proteins: Ataxia Telangiectasia mutated (ATM), DNA-dependent protein kinase (DNA-PKcs) and AT-related kinase (ATR). ATM is mainly responsible for the phosphorylation of H2AX following DNA damages induced by radiotherapy and proton therapy [63]. Indeed, ATM is recruited to the DSB by the protein complex MRN composed of MRE11, RAD50 and NBS1 (also known as NBN). Once recruited, ATM becomes activated leading to the phosphorylation of H2AX [64]. DNA-PKcs is a kinase playing a central role in the NHEJ pathway. As DNA-PKcs is unable to act as sensor of DNA damages, DNA-PKcs is recruited to the sites of damage through the heterodimer Ku70-Ku80. Once recruited, the phosphorylation of H2AX occurs [65]. Finally, ATR can also phosphorylate H2AX. The activation of ATM, DNA-PKcs and ATR leads to the phosphorylation of many proteins in order to activate the various effectors of the DDR. The DDR then block several cellular processes such as cell cycle progression.

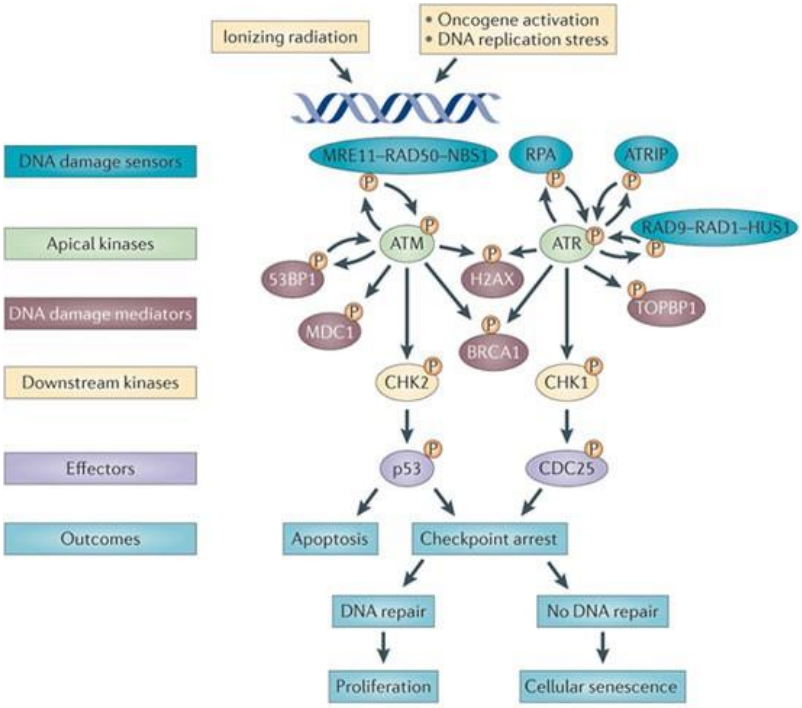

Figure 14 – Radiation induced double-strand breaks which then activate ATM resulting in the phosphorylation of H2AX and the phosphorylation of CHK2 which subsequently phosphorylates H2AX. ATR is also capable of phosphorylating H2AX. The activation of ATM and ATRI results in the phosphorylation of CHK2 and CHK1 respectively. CHK2 can activate p53, whereas CHK1 can activate CDC25. The activation of p53 or CDC25 results in checkpoint arrest or apoptosis [66].

2.6.2. DDR - NHEJ

NHEJ is the primary repair pathway used by mammalian cells. The NHEJ pathway is initiated upon the binding of the Ku heterodimer composed of Ku70 and Ku80 (also known as XRCC6-XRCC5) to the DSB ends [67]. The binding of the Ku heterodimer recruits other NHEJ members, including the DNA-dependent protein kinase catalytic (DNA-PKcs), the DNA ligase IV (LIG4), and the associated scaffolding factors XRCC4, XRCC4-like factor (XLF) and the paralogue of XRCC4 and XLF (PAXX). If necessary, several proteins, including Artemis, the polynucleotide kinase (PNK) and members of the polymerase X family, process the DNA ends to make them compatible for subsequent ligation steps. Finally, the ligation complex, consisting of DNA ligase IV, XRCC4 and XLF ligates the ends of the DNA to repair the break (Figure 15).

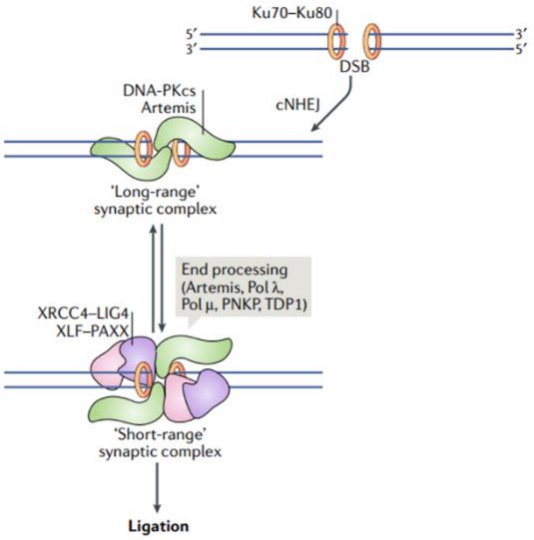

Figure 15 – DSB can be repaired either by conventional non-homologous end joining (cNHEJ) or by homologous recombination (HR). cNHEJ is initiated by the binding of the heterodimer Ku70-Ku80 to the DNA ends. Ku70-Ku80 allows for the recruitment of DNA-PKcs and Artemis. DNA ligation is then performed to repair the DSB (modified from [68]).

2.6.3. DDR - HR

Unlike NHEJ, HR can only operate during the S phase and G2 phase of the cell cycle, since a sister chromatid template with sufficient homology is needed. The process starts with the resection of the DNA ends by the MRN complex composed of MRE11-RAD50-NBS1 together with CtBP-interacting protein (CtIP) and other exonucleases. The action of these proteins generates a 3'-single stranded DNA, which is subsequently coated by the replication protein A (RPA) to remove its secondary structure. Furthermore, BRCA2 mediates the replacement of RPA by RAD51 forming a nucleoprotein filament searching for the homologous sequence on the sister chromatid. After invasion of the strand, the DNA end is extended using the intact sequence of the sister chromatid as a template as already mentioned. After restoration, the second end of the broken DNA is captured and the junctions are resolved to give a precisely repaired DSB (Figure 16) [68].

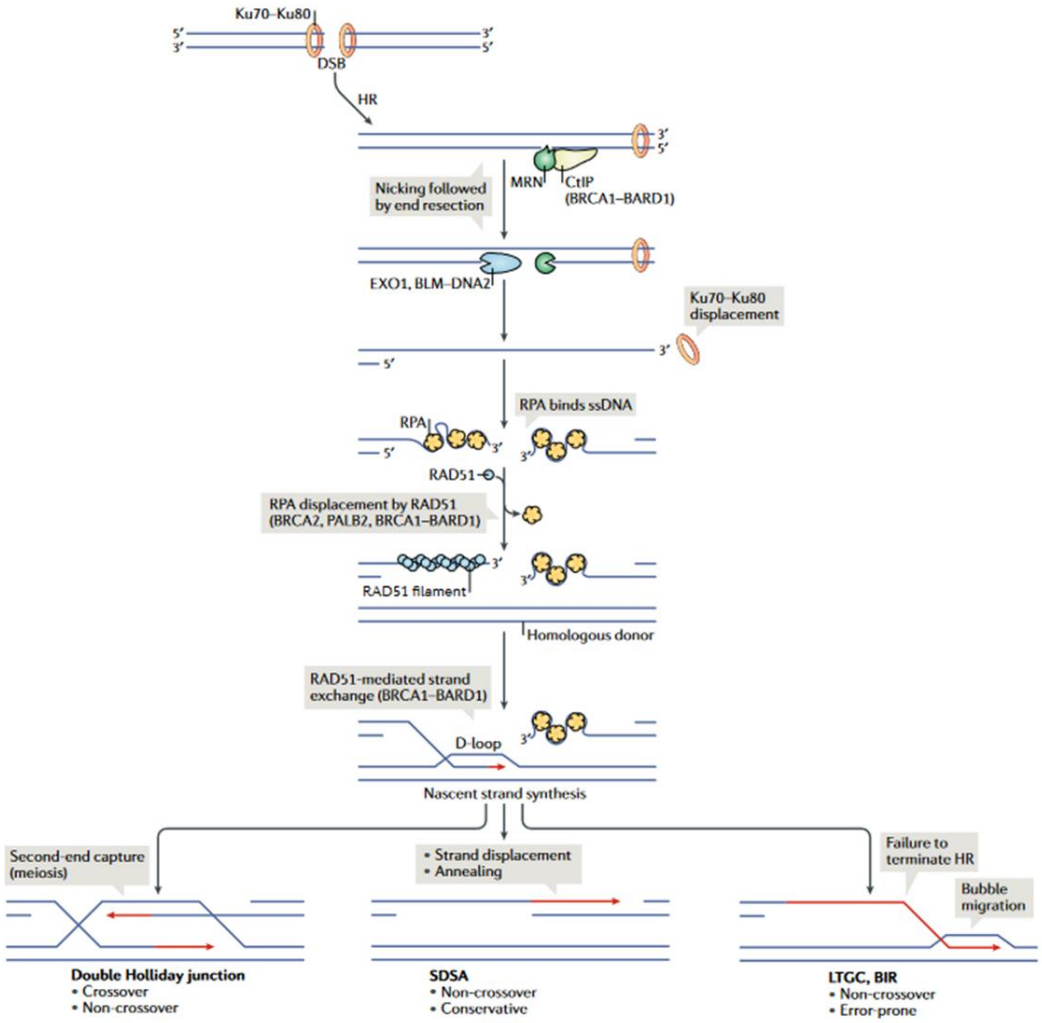

Figure 16 - DSB can be repaired either by conventional non-homologous end joining (cNHEJ) or by homologous recombination (HR). Ku70-Ku80 initiates the repair through HR [68].

2.6.4. The choice between NHEJ and HR

Several factors are implicated in determining the pathway which is going to repair DSBs. First, the MRN complex and the Ku complex compete for DNA ends. The competition between the two complexes is often seen as passive competition. Second, as previously mentioned, HR requires a template provided by the sister chromatid. For this reason, HR is rare or absent in G1 as the sister chromatid is not present. Third, HR is actively regulated as end-resection at the break site is necessary. Of note, researchers demonstrated that end resection is absent in the G1 phase as it relies on specific CDKs which are not active in G1 [36].

2.6.5. Other DNA repair pathways

Even if DSBs are the most lethal, DSBs are not the most common types of DNA damage. Indeed, base damage as well as single-strand breaks are often described as the most frequent DNA damages.

In the context of radiotherapy, approximately 65% of radiation-induced DNA damages are indirect DNA damages. For this reason, radiotherapy induces several types of base lesions, namely 8-oxo-guanine, thymine glycol and formamidopyrimidines. Moreover, radiotherapy induces single-strand breaks. These types of DNA damages are easier to repair and can be repaired by base excision repair (BER) and single strand break repair (SSBR) pathways [69].

2.7. The different types of cell death

Upon irradiation and mostly due to DNA damages, cells are most likely to undergo permanent cell cycle arrest or cell death. Cells entering a permanent cell cycle arrest are said to enter a senescent state. The following chapter is devoted to senescence. However, if the cells do not enter this so-called senescent state, cells can die from different types of cell death, mainly mitotic catastrophe and apoptosis (Figure 17). Apoptosis was first described by Kerr, Wyllie and Currie in 1972 [70]. Apoptosis was described as a programmed cell death mechanism, occurring normally in order to control the growth and the development of an organism. Moreover, apoptosis can also remove cells which have been damaged beyond repair, for example, irradiated cells. Apoptosis is mediated by caspases which are a conserved family of cysteine proteases playing a central role in the regulation of cell death and inflammation responses [71]. Mitotic catastrophe results from a combination of deficient cell cycle checkpoints and cellular damage as defined by Guido Kroemer. Indeed, G2 checkpoint of the cell cycle is supposed to block mitosis if cells are unable to fully repair DNA damage. However, in some cases, the cell is capable of entering mitosis prior complete DNA replication and/or prior DNA damage repair due to defective cell cycle checkpoints. It results in an attempt of aberrant chromosome segregation, which activates the apoptotic pathway leading to cell death [72].

Moreover, cells can also die through immunogenic cell death (ICD) [73]. The concept of ICD was introduced in 2005 to differentiate between cell death capable of inducing antigen-specific immune responses leading to formation of immunological memory and cell death leading to the activation of innate immune system or the activation of immunosuppressive mechanisms. Immunogenic cell death can be assessed *in vitro* through the detection of the translocation of calreticulin (CRT) from the endoplasmic reticulum (ER) to the plasma membrane serving as a “eat-me” signal to the dendritic cells. The secretion of high-mobility group box 1 (HMGB1) can also be assessed, HMGB1 in the extracellular space can easily bind pattern recognition

receptors (PRRs) expressed by myeloid cells. The release of adenosine triphosphate (ATP) is also released serving as a "find-me" signal to the dendritic cells and macrophages [74]. However, the gold standard is to assess the ability of dying cells to initiate an adaptive immune response through vaccination assays [75].

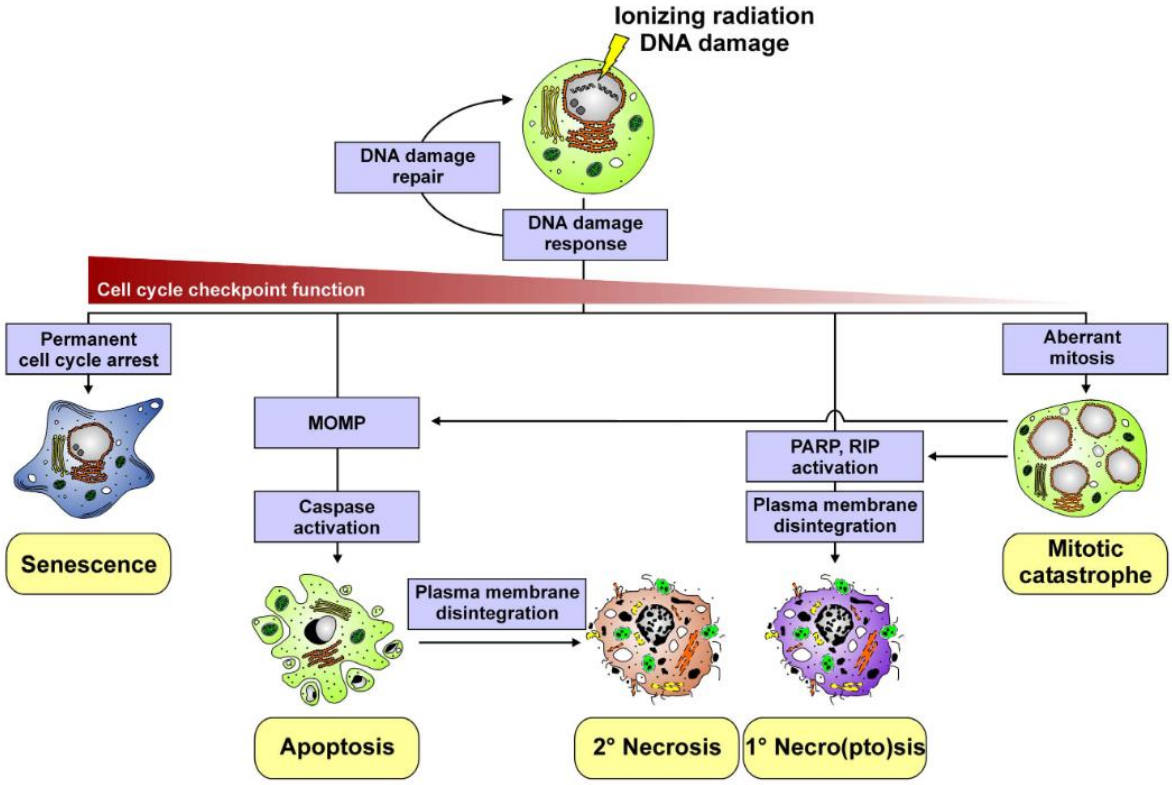

Figure 17 – Different cell death modalities following ionizing radiation. On one hand, cells can enter senescence, a state of permanent cell cycle arrest. On the other hand, cells can die through apoptosis, necrosis, necroptosis and mitotic catastrophe [76].

3. Cellular senescence

Senescence was first described by Hayflick and Moorhead in 1961 [77,78]. The latest demonstrated that human fibroblasts displayed a finite capacity for cell division before entering a permanent growth arrest, also referred to as replicative senescence. However, debate in the literature persists to determine if senescence is permanent or reversible [79,80]. It was further demonstrated that cell types other than fibroblasts can also enter the so-called senescent state.

Over the years, it was shown that cellular senescence can occur after various triggers such as telomere dysfunction, oncogene activation, organelle stresses and anti-cancer therapies. In the context of this PhD thesis, the focus will be solely on therapy-induced senescence (TIS) since numerous anti-cancer therapies have been described as inducers of senescence.

3.1. Therapy-induced senescence

TIS can be induced by several classical cytotoxic therapies such chemotherapies, radiotherapies, immunotherapies and targeted therapies. In this PhD thesis, TIS was induced using ionizing radiation (X-rays and protons) as well as a consequence of inhibition of PARP.

Senescence seems to occur following TIS due to the formation of nuclear DNA damages causing an accumulation of DSBs, which in turn activate the DDR pathway resulting in some cases, in cellular senescence. At the bottom of the DDR cascade, the tumor suppressor p53, which is a target of ATM and its paralogue ATR, is activated and induces the expression of the cyclin-dependent kinase inhibitor p21, an essential mediator of senescence-associated cell cycle arrest. Furthermore, p38 which can also be activated by DNA damages, can further activate p53, p16, an inhibitor of CDK4 and CDK6. p16 is another key player in senescence capable of inhibiting RB through CDK4 and CDK6 [81] (Figure 18).

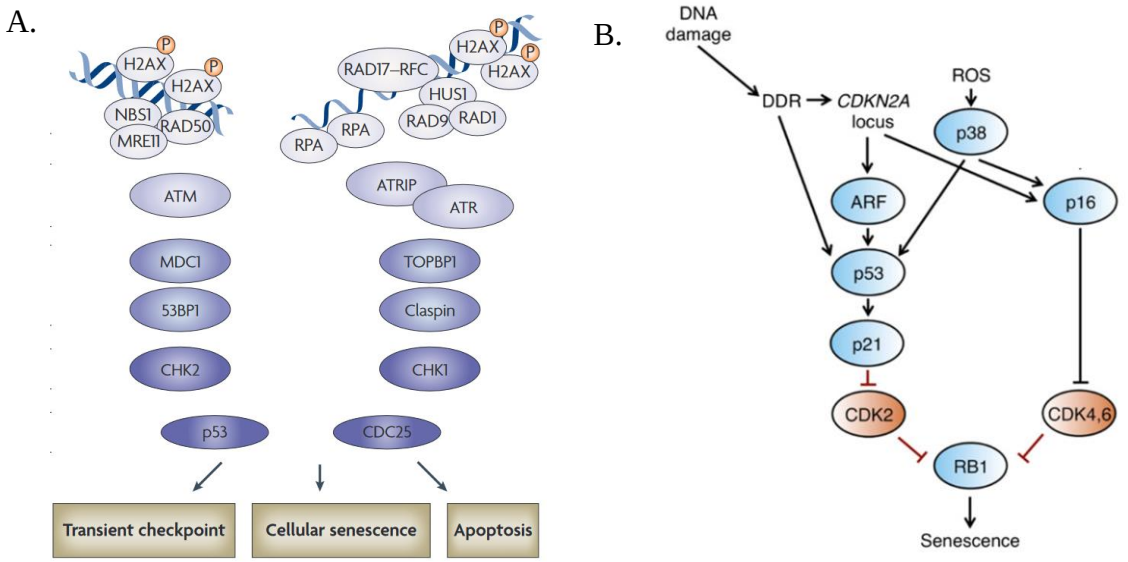

Figure 18 – Therapy-induced senescence through DNA damages. (A) The DNA damage response. The damages can be sensed by several DNA-damage sensors, resulting in the activation of ATM or ATR. Then, CHK2 and CHK1 are activated by ATM and ATR respectively leading to the activation of p53 and CDC25. Cell cycle arrest is mainly induced by p53 and CDC25. The transcription of p21 is activated through p53, while CDC25 activates CDKs, key players in cell proliferation. Cell cycle arrest can be transient if the cell manages to repair its DNA. Cells incapable of DNA repair undergo apoptosis or cellular senescence (modified from [82]). (B) The damage response can also activate p16 leading to the inhibition of CDK4,6 resulting in the inhibition of RB (modified from [83]).

TIS does not only affect cancer cells but it also affects the entire tumor microenvironment including cancer-associated fibroblasts, endothelial cells and immune cells. Senescent stromal cells have also been reported to play an important role in the tumor microenvironment (for a review, see [84]). The first experimental proof for TIS came from the team of J. Campisi. The authors demonstrated that senescent fibroblasts (WI-38 fibroblasts) stimulated pre-neoplastic epithelial cell growth (Sp2, S1, HaCAT and MDA-231 cells). Moreover, the senescent fibroblasts also stimulated tumorigenesis in vivo. Indeed, the authors injected into nude mice, epithelial cells either alone or with pre-senescent fibroblasts or with senescent fibroblasts. The results demonstrated that most of the mice injected with epithelial cells only or with epithelial cells and pre-senescent fibroblasts did not form tumor, whereas most of mice injected with epithelial cells and senescent fibroblasts did form tumor [85].

Senescent immune cells have also be described. Senescent T cells display a reduced expression of CD27 and CD28, two co-stimulatory receptors. Due to this reduced expression of two important co-stimulatory receptors, it is usually hypothetized that senescent T cells have immunosuppressive properties [86].

3.2. The role of ATM, ATR and DNA-PK

To delineate the role of actors involved in the DDR, namely, ATM, ATR and DNA-PK in the induction of senescence, specific inhibitors and/or genetic ablation strategies have been used. In response to DSBs, ATM is often activated. In a similar fashion, ATR is also activated by the

presence of DSBs. Moreover, ATR can be activated by a broad spectrum of DNA damages. DNA-PKcs is activated once it's recruited to the DSB site by the Ku heterodimer. The role of DNA-PKcs is to promote NHEJ. Indeed, senescent BJ cells (fibroblasts derived from the skin) were micro-injected with plasmids expressing kinase dead (KD) forms of ATM, ATR, CHK1 and CHK2. Using bromodeoxyuridine (BrdU), a compound incorporated into the DNA during DNA synthesis, the authors demonstrated that the percentage of proliferating cells increased in cells micro-injected with the combination of ATM-KD, ATR-KD, CHK1-KD and CHK2-KD plasmids as well as in cells micro-injected with the combination of ATM-KD and ATR-KD plasmids or with the combination of CHK1-KD and CHK2-KD plasmids. As BrdU is only incorporated in cells capable of dividing, these results thus demonstrated the importance of DNA damage checkpoints to maintain senescence in BJ cells [87]. To further delineate the role of these DDR players, genetic ablation of ATM was carried out in normal and senescent fibroblasts. The results indicated that ATM is heavily involved in the induction of replicative senescence in normal fibroblasts. Furthermore, in the case of telomere damages, the authors also showed that Chk1 is phosphorylated at Ser317 by ATM and ATR, and that ATM is responsible for the phosphorylation of Chk2 at Thr68 [88]. CC-115, an inhibitor for DNA-PK/mTOR, and AZD0156, an inhibitor for ATM, were shown to decrease senescence induction in irradiated healthy fibroblasts, SBLF9 and SBLF7. However, VE-822, an inhibitor for ATR, was not able to decrease senescence in irradiated SBLF9 and SBLF7 cells [89].

In cancer cells, the role of ATM, ATR and DNA-PK was also investigated in HPV+ and HPV- head and neck cancer cell lines. In HPV+ UM-SCC-47 cells, senescence was barely induced following conventional radiotherapy (2 Gy), and the effects of CC-115 (DNA-PK/mTOR inhibitor), AZD0156 (ATM inhibitor) and VE-822 (ATR inhibitor) were barely visible. Indeed, CC-115 and VE-822 slightly increased senescence in unirradiated cells while, AZD0156 had no effect. However, irradiation induced senescence was reduced in HPV+ UD-SCC-2 when treated with CC-115, VE-822 or AZD0156. In HPV- HSC-4 cells, no effects of the inhibitors were observed, while in HPV- Cal33, a significant increase in senescence induction was observed when cells were treated with AZD0156 [89]. More recently, the actors involved in cellular senescence following temozolomide (TMZ) treatment in glioma cells were characterized. LN229 cells were incubated with 50 µmol/L of TMZ leading to a significant increase in the number of senescence-associated beta-galactosidase (SA-β-Gal) positive cells. LN229 cells were treated with TMZ and KU60019 (inhibitor of ATM) or VE-821 (inhibitor of ATR) or KU0060648 (inhibitor of DNA-PKcs) or Mirin (inhibitor of MRN), and assessed for SA-β-Gal activity. The percentage of SA-β-Gal positive cells was reduced in TMZ treated LN229 when combined with the inhibitor of ATR, the inhibitor of DNA-PKcs as well as with the inhibitor of MRN. These results demonstrate that the induction of senescence with TMZ in LN229 cells is dependent on ATR, DNA-PKcs and MRN [90].

3.3. The role of the CDK inhibitor family

In mammalian cells, two distinct families of CDK inhibitors have been characterized. The first family is composed of three proteins: $p21^{Cip1}$, $p27^{Kip1}$ and $p57^{Kip2}$. The second family includes four proteins: $p16^{INK4a}$, $p15^{INK4b}$, $p18^{INK4c}$ and $p19^{INK4d}$ [91].

The activation of the actors of the DDR activates p53, which regulates CDKN1A expression. CDKN1A encodes the cyclin-dependent kinase inhibitor p21. Several studies have already demonstrated that p21 accumulates during senescence [92]. Furthermore, p21 knockdown or p21 overexpression can respectively prevent senescence [93] or induce senescence [94]. In addition, recent work by Hsu et al. demonstrated that the choice between proliferation or senescence in response to chemotherapy is tightly controlled by a pattern of p21. Indeed, a delayed or an acute drug-induced p21 response leads to senescence, whereas intermediate level of p21 in G1 leads to proliferation. The authors proposed to make use of this "Goldilocks Zone" to reduce proliferative cells through the use of nutlin-3a to increase p21 level or through the abrogation of the G1/S checkpoint by inhibiting ATM (Figure 19) [95]. Of note, nutlin-3a binds Mdm2 thus disrupting the interaction between p53 and Mdm2 leading to the activation of p53.

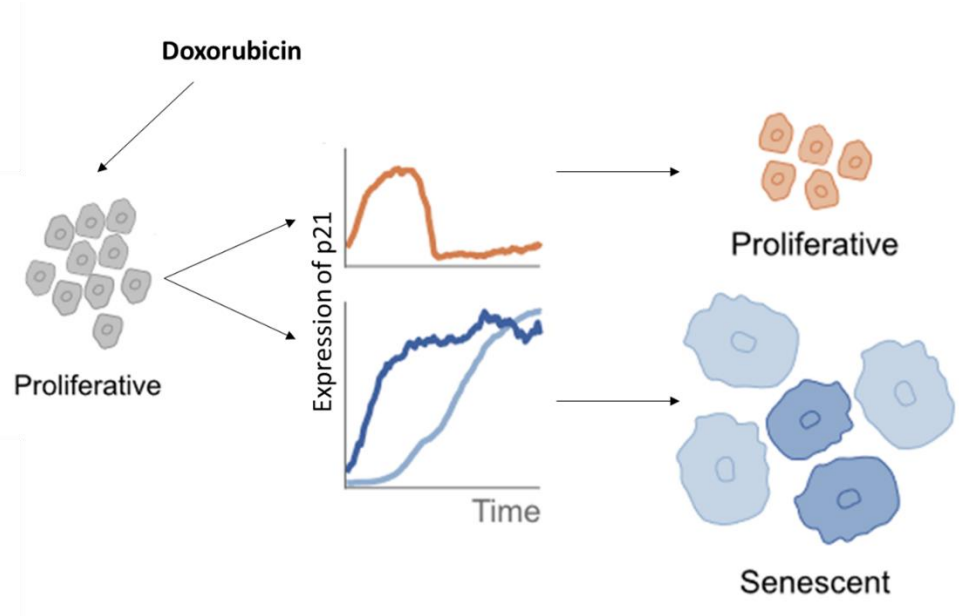

Figure 19 – The model proposed by Chien-Hsiang Hsu et al. Cancer cells treated with chemotherapy (doxorubicin) do not have the same modification in p21 expression. Indeed, cancer cells can either strongly upregulate p21 expression during the G1 phase or the S/G2 phase, leading to a senescent state or strongly decrease p21 expression in the G1 phase leading a proliferative state (adapted from [95]).

Several studies have demonstrated that p16 and p21 are upregulated in senescent human fibroblasts at mRNA and protein levels, namely in senescent NHF1, MRC-5, IMR90 and WI-38 [96,97]. The authors classified the cells based on their proliferative capacity, which they called the labeling index (LI). Interestingly, the expression of p21 reached a peak in senescent cells with a low proliferative capacity (LI = 20 %). Senescent cells with a lower proliferative capacity

(LI < 5 %), the expression of p21 decreased. The expression of p16 is on the other hand was significantly upregulated in senescent cells with a lower proliferative capacity (LI < 5%). Therefore, the authors hypothesized that since p16 is only upregulated in the terminal of stages of senescence, it might explain why p16 but not p21 is often mutated in cancer cells [98].

Finally, p16 and/or p21 indirectly target RB, which is known to prevent excessive cell growth through the control of the cell cycle. RB is hypo-phosphorylated in cells in the G0 phase or the G1 phase, and RB is associated with E2F transcription factors to repress the transcription of E2F target genes. RB becomes phosphorylated during progression through the G1 phase by CDKs allowing E2F target genes to be transcribed. In this case, p16 and p21 prevent the phosphorylation of RB, in order to prevent the transcription of the E2F target genes (such as CCNE1, CDC25A, CDC6). The E2F target genes are implicated in several processes, namely cell cycle, DNA replication, DNA damage repair and apoptosis (a detailed list can be found in [99]).

3.4. The markers of cellular senescence

Senescent cells can be recognized through several key markers (Figure 20).

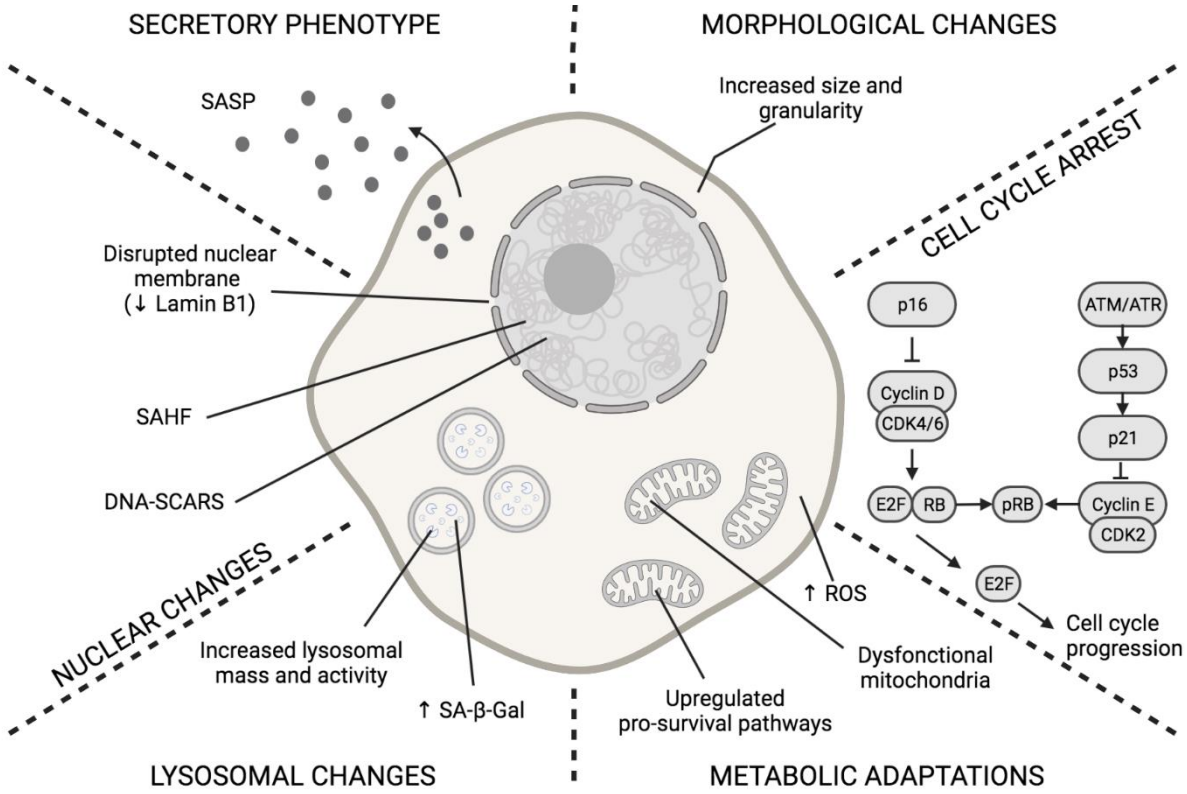

Figure 20 – The key players and markers for cellular senescence. Most common markers are the upregulation of p16 and/or p21 leading to cell cycle arrest, metabolic adaptations, lysosomal changes, nuclear change and morphological changes. The senescent cells also secrete an large variety of factors which are termed senescence-associated secretory phenotype (SASP) (created with BioRender).

3.4.1. Cell size and shape

Changes in morphology are often observed in the context of cellular senescence. Indeed, cells present an enlarged and irregularly shape. Thus, changes in morphology and granularity are often incorporated into the markers of senescence. These morphological markers can easily be assessed *in vitro* through flow cytometry or microscopy [100]. The mechanisms responsible for these changes in morphology are not fully understood.

Several authors demonstrated that the composition of the cytoskeleton is modified. Indeed, an increase in vimentin at the protein level was observed in human fibroblasts which might be responsible for the senescent morphology [101]. Furthermore, it seems that the unfolded protein response (UPR) might also play a role in the control of the size and the shape of a cell. Indeed, silencing ATF6α, one of the three main actors of the UPR, in normal human dermal fibroblasts (NHDFs) restored the fusiform shape of the cells. The change in size was correlated with an increased in protein content. The authors hypothesized that ATF6α controls the size and shape of the cells through ER expansion [102].

3.4.2. Plasma membrane

The composition of the plasma membrane is also affected by senescence. It seems that the most well-known change in the composition of the plasma membrane is the upregulation of caveolin-1. The latest is a component of caveolae which are a special type of lipid raft. Caveolae are implicated in several processes such as signal transduction (for a review, see [103]).

3.4.3. Nuclear envelope

The disruption of the nuclear envelope is also a feature of senescent cells. The protein lamin-B1, which is a major component of the nuclear lamina, is often downregulated in the context of cellular senescence [104]. The integrity of the nucleus is thus often lost in senescent cells, leading to the release of cytoplasmic DNA outside of the nucleus which also might explain why the cGAS/STING pathway is often activated in senescent cells [105].

3.4.4. Lysosomal content

Senescent cells are characterized by the upregulation of several lysosomal proteins. The activity of SA-β-Gal activity is the most frequently used marker to identify senescent cells. Furthermore, the upregulation of SA-β-Gal activity is seen as the most important marker to identify senescent cells. At pH = 4.0, all cells express acidic β-Gal activity, but at pH = 6.0, it is possible to specifically detect the SA-β-Gal activity which is associated with senescent cells, as it has been demonstrated that SA-β-Gal activity is not detected in most quiescent or terminally differentiated cells [106].

It was demonstrated that the GLB1 gene is responsible for encoding the β-Gal enzyme. The GLB1 gene is upregulated in senescent cells at the mRNA and protein levels [107]. Interestingly, the molecular mechanism responsible for the overexpression of the GLB1 gene in senescent cells is to this day, unknown.

3.4.5. DNA damages

Persistent DNA damages is often detectable in senescent cells. Indeed, senescent cells present with DNA segments with chromatin alterations reinforcing senescence, named DNA-SCARS [108] and with senescence-associated heterochromatin foci, named SAHF [109].

DNA-SCARS are associated with the presence of nuclear bodies as well as with the activation of several DDR proteins such as ATM, ATR, CHK2 and p53. Furthermore, DNA-SCARS lack the DNA repair proteins RPA and RAD51 [108].

The heterochromatin foci represent domains of the heterochromatin which contribute to the silencing of several genes such as the E2F target genes.

3.4.6. Cell cycle arrest

Cell cycle arrest is often described as a hallmark of cellular senescence. The actors which are the most characterized to induce this cell cycle arrest are p16, p21, p53 and RB. The activation of the p53/p21 pathway is observed following therapy-induced senescence. The p16/RB pathway is often activated following replicative senescence, reactive oxygen species (ROS) induced senescence- or oncogene-induced senescence. Thus, the mRNA level of p16 and p21 is often evaluated in cells which are thought to be senescent. Moreover, p53, p-p53, RB and p-RB levels are also often evaluated via immunoblot in order to investigate if cells are senescent or not.

It is also possible to evaluate the arrest in proliferation using Incucyte Live-Cell Analysis system. Proliferation can also be assessed through 5-Ethynyl-2'-deoxyuridine (EdU). EdU is a thymine analogue which can be incorporated into the DNA whenever the cells are dividing. EdU can then be revealed through flow cytometry orfluorescence labeling. EdU staining works via a "click" chemistry reaction.

3.4.7. The secretory phenotype

Senescent cells secrete numerous inflammatory, extracellular matrix modifying enzymes, growth factors and lipids, all together called the senescence-associated secretory phenotype (SASP). Furthermore, extracellular vesicles are also emerging as a new class of SASP factors.

However, the secretion of these factors is not specific to senescent cells. The presence of these factors can modulate the tumor microenvironment. For this reason, the SASP is often investigated if cells have been defined as senescent, and the composition of the SASP can easily be evaluated using ELISA and antibody-array. For unbiased analysis, RNA-sequencing, mass spectrometry or lipidomics can be used. The composition of the SASP is diverse and dynamic. It can be influenced by the cell type undergoing senescence, the tissue of origin and the inducer of senescence [110].

3.4.8. Resistance to apoptosis

Several pro-survival genes are also upregulated in senescent cells such as some members of the Bcl-2 family. Indeed, senescent human fibroblasts upregulate Bcl-2 [111]. For this reason, several Bcl-2 inhibitors are currently being investigated to specifically target senescent cells as described below. Moreover, it seems that resistance to apoptotic cell death can also be attributed to a decrease in caspase activity [112]. p53 is also implicated in the resistance to apoptosis of senescent cells. It seems that senescent cells are capable of displaying a reduced p53 level. In the context of fibroblasts, Sturmlechner et al. studied the senescence-associated super enhancers (SASE). The authors demonstrated that SASE promote survival through the prevention of p53 induced apoptosis : modulation of Mdm2 and Ang [113]. Heat shock proteins are also implicated in the resistance to apoptosis. In the context of senescence, HSP90 has been implicated as an anti-apoptotic and pro-survival factor in senescent cells. The authors showed that inhibition of HSP90 destabilize Akt and Erk to increase apoptosis [114]. Furthermore, survivin and phospho-survivin were found to accumulate in aged normal human skin fibroblasts [115]. Ma et al. also determined that survivin expression in senescent cells might be increased due to nuclear accumulation of Yes-associated protein (YAP) which is a known regulator of survivin expression [116]. Finally, apoptosis can be triggered by the binding of death ligands to their death receptors (DR). DR-mediated apoptosis can be inhibited by c-FLIP and decoy receptors which have been shown to be upregulated in senescent cells [117].

3.4.9. Emerging markers

3.4.9.1. Stemness

Milanovic et al. showed that senescent cells are associated with a stem cell signature [80]. Thus, the authors proposed to add senescence-associated stemness (SAS) as a new feature of senescent cells. Furthermore, the acquision of this stem cell signature has been suggested to be strongly implicated in the treatment outcome as it contradicts what was initially thought meaning that senescent cells have limited growth potential unlike these cells with a stem cell signature.

3.4.9.2. Reversibility of the senescence state

Senescence was first thought to be an irreversible cell cycle arrest, at least for replicate senescence. However, several recent discoveries demonstrated that it might be a reversible phenomenon in some cases.

A first proof of this reversibility came from the team of Abbadie. Inded, her team showed that normal primary human epidermal keratinocytes first reached a senescence plateau *in vitro*. If these keratinocytes were kept in culture for longer period of time, some cells emerged from the senescence plateau, started to divide again while displaying transformed and tumorigenic properties [118]. The team of Rodier also showed that cancer cells might exit the senescence state triggered by PARP inhibor treatment [119].

The mechanisms responsible for the exit of the cells from the senescence state are not yet defined. It has been hypothetized that epigenetic remodeling is heavily involved in controlling the choice between entry and exit of the senescence state [120].

3.5. The different types of senescence

The concept of senescence might be further complicated by the presence of different types of senescence. Indeed, some researchers are talking about “premature senescence” or “early senescence” and “mature senescence” or “late senescence” [121]. The difference between these two types relies on the SA-β-Gal staining. Indeed, the cells characterized as being in premature senescence are presenting with a light blue staining while the cells defined as being in mature senescence display a dark blue staining.

Moreover, the emergence of technologies such as single-cell RNA-sequencing technology defined several subsets of senescence as demonstrated in [122]. The use of single-cell RNA-sequencing technology on prostate cancer cells allowed to define at least 7 different signatures of senescence.

Furthermore, results from our laboratory also confirm the aforementioned results. Indeed, K. Bouhjar, a PhD student, is currently studying the induction of senescence using X-rays and Cisplatin in HPV- and HPV+ head and neck cancer cell lines. He demonstrated that HPV- and HPV+ cancer cell lines all display markers of senescence, but the markers are very different between HPV- and HPV+ cell lines which suggest that HPV- and HPV+ cancer cell lines could undergo different types of senescence.

3.6. The interplay between senescent cells and cancer cells

The impacts of senescent cells in the context of tumors are quite blurry. Indeed, senescent cells have been associated with anti-tumoral and pro-tumoral effects (Figure 21).

Senescent cells seem to be able to affect cancer cells, mostly through the SASP. The first evidence of an interplay between senescent cells and cancer cells came from the team of Campisi. Indeed, senescent fibroblasts could promote epithelial cell proliferation. Epithelial cells were cultured in the presence of WI-38 fibroblasts, senescent fibroblasts stimulate pre-neoplastic cell growth unlike young fibroblasts. Furthermore, it seems that cancer cell proliferation is partially attributable to the secretory phenotype of these senescent fibroblasts [85]. The same team latter demonstrated that two breast cancer cell lines, T47D and ZR75.1, displayed EMT when co-cultured with senescent fibroblasts [123]. Similarly, senescent fibroblasts co-transplanted with breast cancer cells (MDA-MB-231) in immunodeficient mice favored the growth of the tumor [124].

Senescence also seems to be responsible for promotion cancer stemness as demonstrated in human cancer cell lines and primary samples of human hematological malignancies [80]. Indeed, Milanovic et al. showed that senescent cells are associated with a stem cell signature. Thus, the authors proposed to add senescence-associated stemness (SAS) as a new feature of senescent cells.

More recently, Baker et al. showed that removing senescent cells delay tumor formation in mice (the study included mice with lymphomas, sarcomas and carcinomas at the time of death) [125]. These results triggered a strong interest for the elimination of senescent cells in the context of cancer therapy.

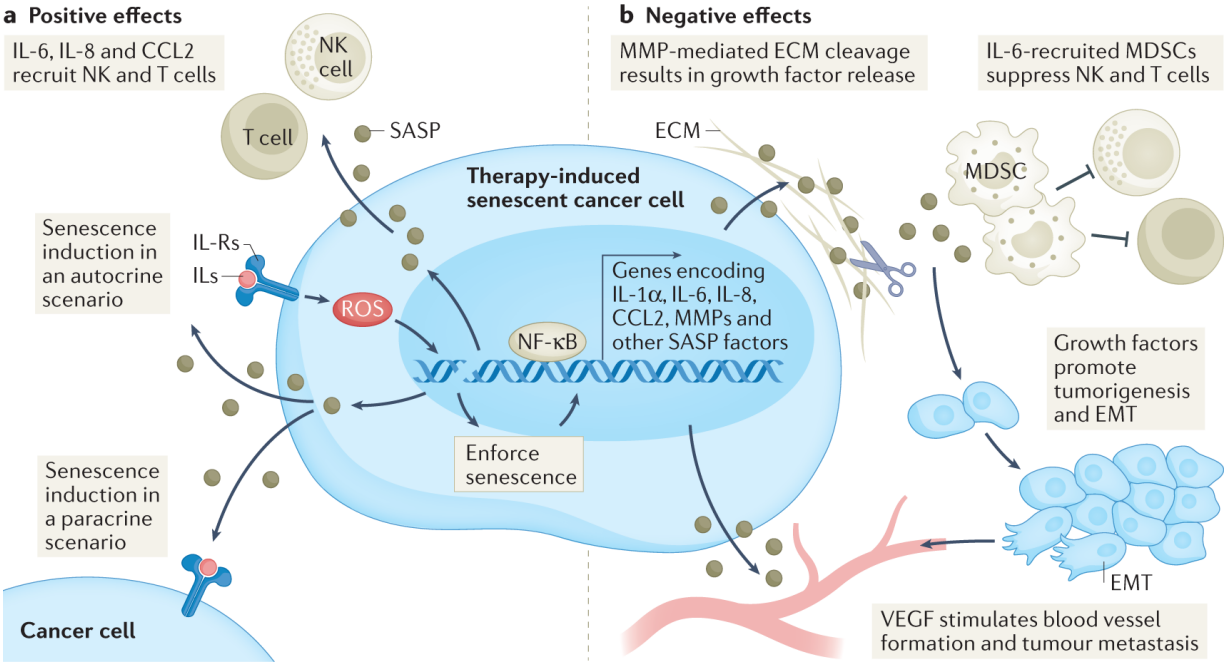

Figure 21 – The positive and negative effects of senescent cells in the context of cancer [126]. Senescent cancer cells mostly exert their effects on the tumor microenvironment through SASP.

3.7. Targeting senescent cells

It was demonstrated that a decrease in the number of senescent cells was associated with increased health span and life span [127]. Furthermore, Baker et al. demonstrated that the clearance of senescent cells delays ageing-associated disorders in mice [128]. In another study, Baker et al. showed that removing p16 positive cells delayed tumor formation [125]. Removal of senescent cells also decreased cancer relapse as demonstrated by Demaria et al [129]. In the context of cancer therapies, these studies indicate that the removal of senescent cells could benefit cancer patients. These discoveries opened the search for compounds capable of killing senescent cells. These therapies are often classified into two groups: senolytic compounds and senomorphic or senostatic compounds. The senolytics are used to specifically target and kill senescent cells while senomorphics antagonize or neutralize the effects of the SASP.

3.7.1. Senolytics

Several senolytics target pro-survival pathways, including the BCL-2/BCL-xL, p53/p21, and PI3K/AKT, and the anti-apoptotic pathways, including serpins (Figure 22).

Dasatinib (D), Quercetin (Q) and Fisetin (F) represent the most famous senolytics. Fisetin and Quercetin are natural flavonoids which can be used in combination with Dasatinib. Fisetin and Quercetin prevent the activation of PI3K, whereas Dasatinib prevents the activation of tyrosine kinase (TK). These molecules are currently in Phase II clinical trials for chronic kidney disease (NCT02848131), skeletal health (NCT04313634), Alzheimer disease (NCT04063124)

and osteoarthritis of the knee (NCT04210986). Forkhead box protein O4 (FOXO4)-DRI is able to promote senolysis by preventing the binding of p53 to FOXO4 resulting in the exclusion of p53 from the nucleus initiating apoptosis [130]. Cardiac glycosides were also identified as senolytic compounds, due to the activation of NOXA, a pro-apoptotic Bcl-2 family protein [131]. Furthermore, members of the Bcl-2 family can be directly targeted by A-1331852 and A-1155463 which inhibit Bcl-XL [132]. ABT-263 (Navitoclax) and ABT-737 inhibit the activity of Bcl-XL, Bcl-2 and Bcl-w [132]. Bcl-2 can be specifically targeted by ABT-199 (Venetoclax) [133].

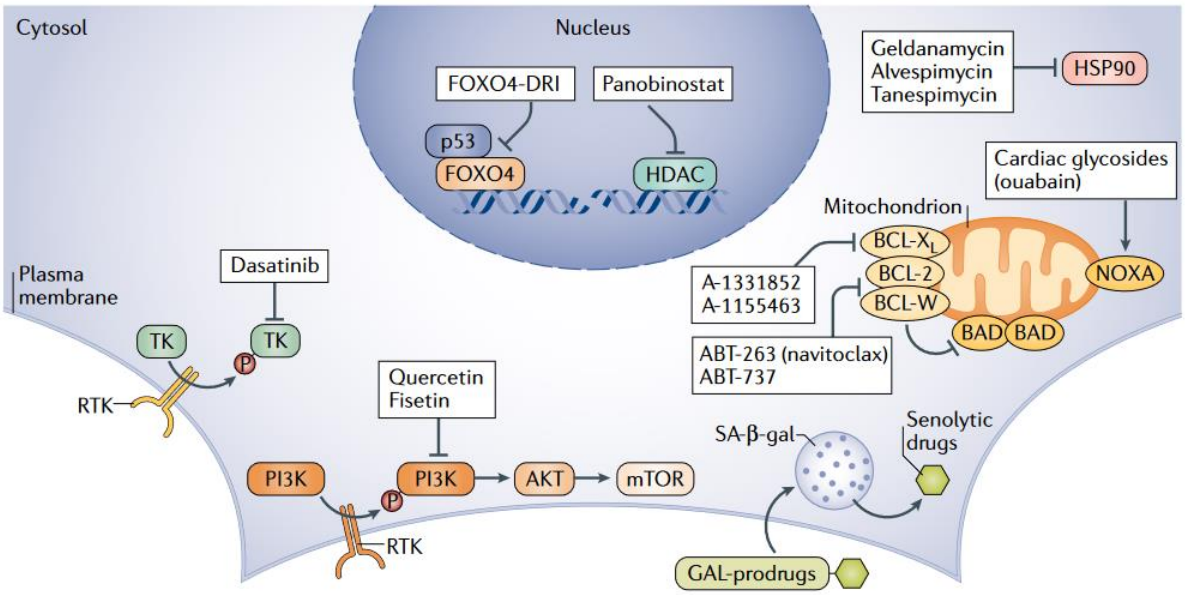

Figure 22 – Schematic representation of different senolytics and of their targets [132].

3.7.2. Senomorphics

It is also possible to specifically target the SASP as it has been shown that the SASP is mainly responsible for the positive and negative effects of senescent cells.

3.8. Conclusion

In conclusion, senescence is a new player in tumors. The role of senescence in the context of cancer is still unclear as it has been shown that senescence exerts anti-tumoral and pro-tumoral functions. Due to the recent discoveries mostly driven by the team of Campisi and Van Deursen, removing senescent cells as a therapy for cancer is currently getting a lot of attention from researchers.

4. The PARP family and the inhibitors of PARP

Poly (ADP-ribose) polymerases (PARPs) are a family of related enzymes that share the ability to catalyze the transfer of ADP-ribose to target proteins. These target proteins are said to be ADP-ribosylated. As PARP is strongly implicated in DNA repair, several inhibitors of PARP were recently approved for the treatment of several cancers.

4.1. The members of the PARP family

The PARP family is currently composed of 17 members (Table 2). PARP1, PARP2 and PARP3 are thought to be the most important members for responses in case of DNA damages. The percentage of homology in the catalytic domain of PARP1, PARP2 and PARP3 is fairly high (around 70%) [134]. PARP5A and PARP5B are said to play a role in the regulation of telomere homeostasis. The CCCH-type PARP subfamily is composed of PARP7, PARP12 and PARP13. The macroPARP subfamily is composed of PARP9, PARP14, PARP15. The rest of the PARP family is composed of PARP4, PARP10, PARP6, PARP8, PARP11 and PARP16 [135].

Table 2 – The 17 members of the PARP family.

Gene name	Other name
PARP1	ARTD1/ADPRT/PPOL
PARP2	ARTD2/ADPRTL2
PARP3	ARTD3/ADPRT3/PADPRT-3
PARP4	VPARP/ARTD4
PARP5A	TNKS/TNKS1
PARP5B	TNKS2
PARP6	ARTD17
PARP7	ARTD14/TIPARP
PARP8	ARTD16
PARP9	ARTD9
PARP10	ARTD10
PARP11	ARTD11
PARP12	ARTD12
PARP13	ZC3HDC2/ARTD13
PARP14	ARTD8
PARP15	ARTD7
PARP16	ARTD15

Most members of the PARP family have been shown to catalyze the transfer of ADP-ribose to substrates [136] (Figure 23). As shown in the Figure, PARP adds ADP-ribose to an acceptor protein, which is said to be MARylated (mono-ADP-ribosylation). The acceptor protein can

become PARylated (poly-ADP-ribosylation). The process is fairly dynamic, and thus the acceptor protein can quickly become free of PAR thanks to poly-ADP-ribose glycohydrolase (PARG) responsible for the catabolism of PAR.

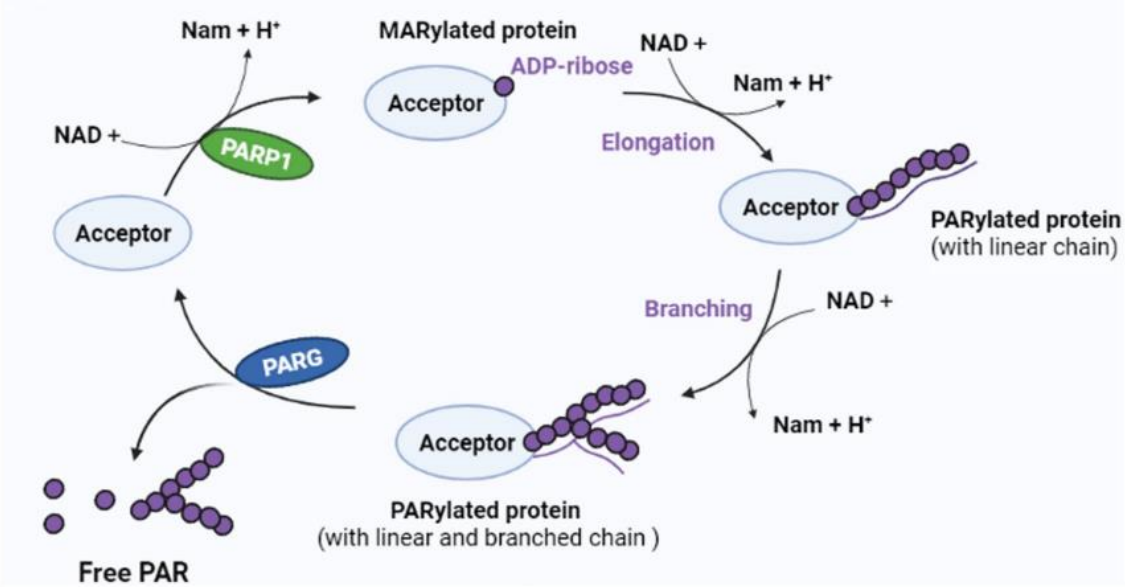

Figure 23 – PARP uses NAD+ to generate Nam + H⁺ resulting in the ADP-ribosylation of the acceptor protein (MARylated protein). Then, the acceptor can become PARylated through elongation with either linear chain or with linear and branched chains. PARG can catalyze the hydrolysis of PAR to free poly(ADP-ribose) or ADP-ribose [137].

In the context of this PhD thesis, the focus is on PARP1 and PARP2, as PARP inhibitors were specifically designed to inhibit PARP1. However, several research papers have already characterized the "off-targets" effects of PARP inhibitors onto PARP2.

4.1.1. PARP1

The functions of PARP1 are extremely diversified. PARP1 is implicated in the repair of single-strand breaks and double-strand breaks. Moreover, PARP1 is also needed in case of replication stress. PARP1 has also been described as a key player in chromatin remodeling and translation.

The domains of the PARP1 protein are the following: DNA-binding domain, automodification domain and PARP domain. As mentioned by its name, the DNA-binding domain allows PARP1 to bind to the DNA at single- and double-strand breaks. The automodification domain contains regions that are extremely important for PARP1 automodification. Finally, the PARP domain is composed of the catalytic domain that is conserved between PARP1, PARP2 and PARP3 and of the ADP-ribosyltransferase (ART) domain [135].

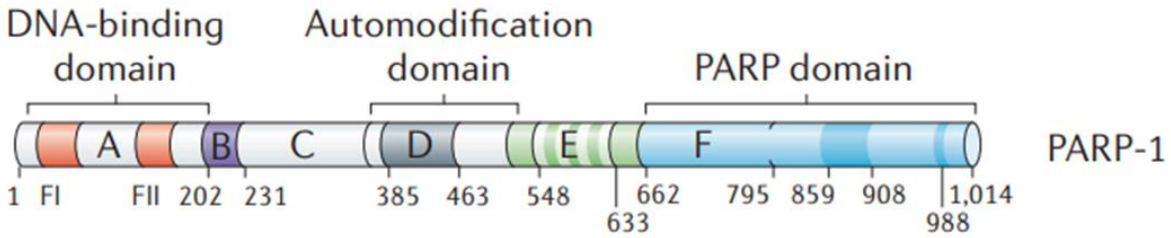

Figure 24 – The different domains composing the human PARP1 protein [135].

4.1.1.1. Implication in DNA damage repair

Upon DNA damage induced by alkylating agents and oxidative stress, PARP1 is activated to synthesize PAR (also named pADPr) [138]. As a consequence, several effectors such as gamma-H2AX, XRCC1, … are recruited to DNA damage sites to facilitate DNA damage repair. However, if DNA damages cannot be repaired, cell death will ensue.

4.1.1.1.1. Single-strand break repair pathway

In the context of SSBR pathway, it has been shown that PARP1 is responsible for promoting the accumulation of XCRR1, a key player in the SSBR pathway. PARP1 also triggers the relaxation of the chromatin through the poly-ADP-ribosylation of histone H1 and H2B facilitating the repair of the damaged DNA [138].

4.1.1.1.2. Double-strand break repair pathway

PARP1 has been described as a sensor of DSBs. Indeed, PARP1 deficiency delayed the activation of DDR such as the phosphorylation of H2AX. Moreover, PARP1 also has a role in the resection of the DNA through the recruitment of MRN to the DSBs. PARP1 has thus been shown to be implicated in HR, cNHEJ and aNHEJ [138].

4.1.1.2. Implication in chromatin remodeling

PARP1 induces chromatin relaxation through PARylation of histones allowing the recruitment of several chromatin remodelers [139,140]. One of the best-known chromatin remodeler is ALC1. The recruitment of ALC1 permits the repositioning of nucleosomes making DNA accessible to DNA damage repair actors [141]. Several other actors can also be recruited in a PARP1 dependent manner, such as CHD2 which is capable of depositing the histone variant H3.3, known to alter chromatin accessibility and to regulate gene transcription (Figure 25) [142].

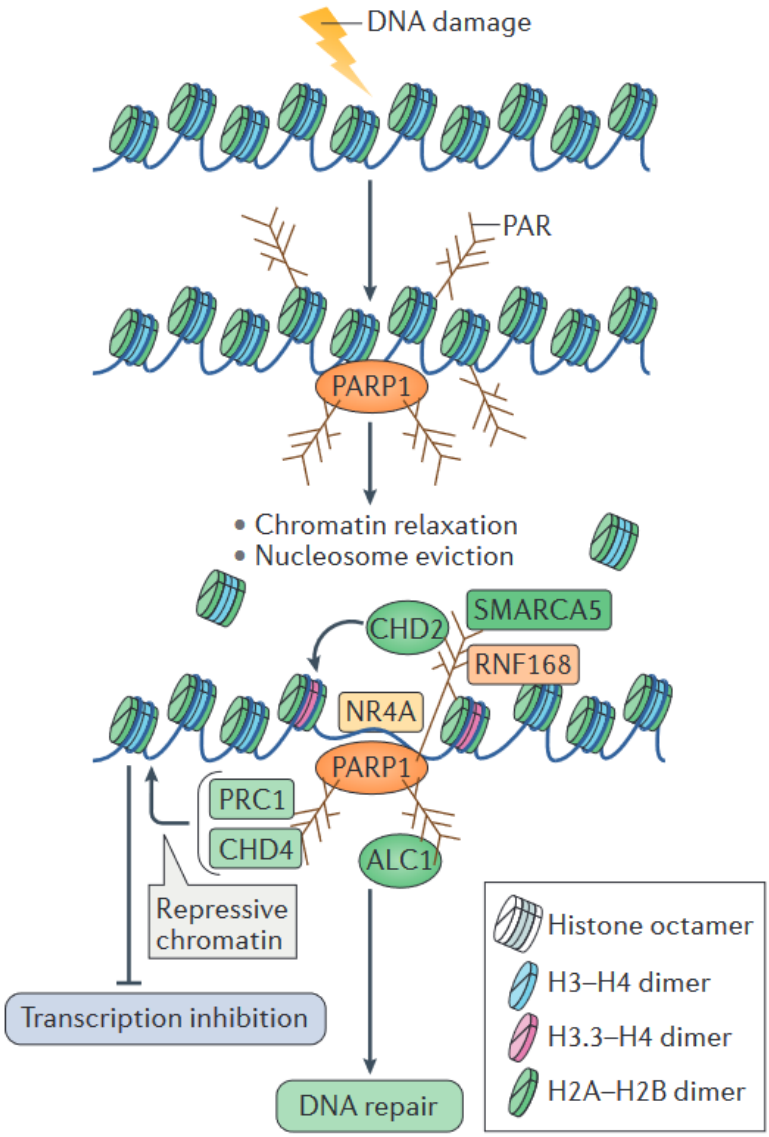

Figure 25 - The role of PARP1 in chromatin remodeling [138].

4.1.1.3. Implication in regulation of transcription

For transcription to occur, RNA polymerase and transcription factors must be capable of accessing the DNA sequence of the promoter of the gene of interest. PARP1 is heavily involved in the regulation of chromatin structure. Thus, PARP1 is also implicated in the regulation of the transcription by triggering or maintaining changes in chromatin and also through the recruitment of several transcription factors. For this reason, PARP1 has been demonstrated to be implicated in the regulation of elongation of RNA polymerase II, of splicing, of RNA binding proteins, … (for a review, see [143]).

4.1.1.4. Parthanatos

Parthanatos (derived from 'par' and 'thanos') is a PARP1-dependent, caspase-independent, cell death pathway. Parthanatos occurs when PARP1 is over-activated usually linked to the presence of a large amount of DNA damages, leading to the accumulation of PAR polymers [144].

Under conditions of overactivation of PARP1, there is a large production of PAR. The large amount of PAR results in a strong reduction of NAD^+ which is necessary for several biochemical reactions such as glycolysis, the Krebs cycle and the pentose phosphate pathway (PPP). The depletion of NAD^+ causes ATP depletion, which promotes the translocation of AIF from the mitochondria to the nucleus. AIF can then recruit the migration inhibitory factor (MIF) to the nucleus, leading to the cleavage of genomic DNA into fragments resulting in cell death (Figure 26) [145]. Parthanatos has been described in pathological processes, including ischemia-reperfusion injury after brain ischemia or myocardial infarction, septic shock and neurodegenerative diseases such as Parkinson's disease and Alzheimer's disease [144].

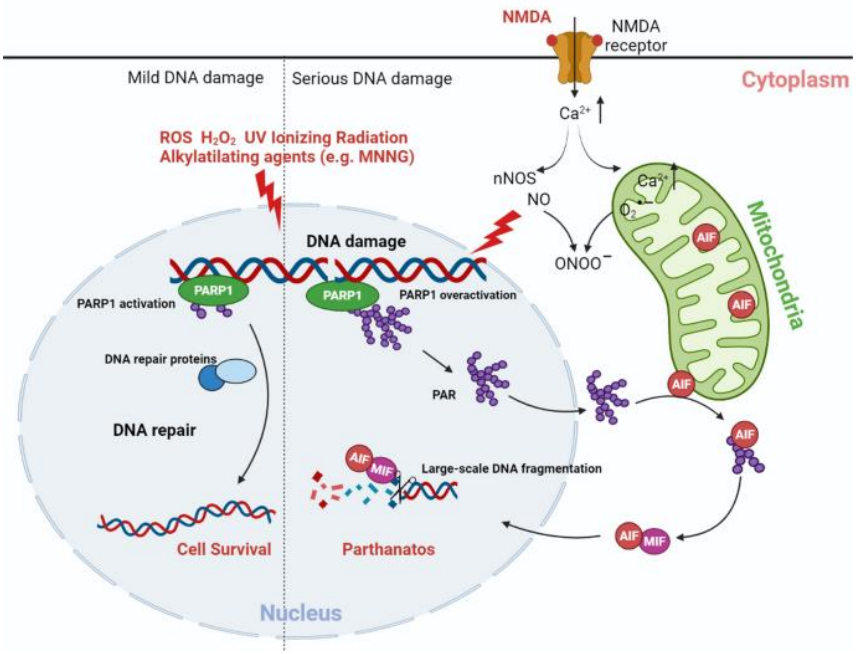

Figure 26 – Schematic representation of Parthanatos [137].

Unpublished data by Demaria et al., presented at the International Cell Senescence Association (ICSA) in 2021, showed the importance of Parthanatos in cellular senescence. Indeed, fibroblasts (IMR90 cells) treated with PJ34 (PARP inhibitor) and H_2O_2 showed a decrease in cell death compared to IMR90 cells treated with H_2O_2 alone. These results demonstrated that a PARP inhibitor was capable of protecting fibroblasts from cell death. Furthermore, it was shown that PJ34 rescued IMR90 cells treated with H_2O_2 by promoting the entrance of the IMR90 cells into senescence. The PJ34 treated IMR90 cells expressed several markers of senescence such as an increased in SA-β -Gal, a decrease in EdU labeling and expression of several key SASP factors at the mRNA level. The authors further demonstrated

that PARP inhibition preserved mitochondrial membrane potential and limited mitochondrial Ca^{2+} overload. Mitochondrial Ca^{2+} overload was reduced through the prevention of the translocation of hexokinase II (HKII) from the mitochondria to the cytoplasm, a process known to result in cell death. These results demonstrated the importance of PARP in the regulation of cell survival.

4.1.2. PARP2

DNA damages lead to PARylation induced by PARP1. The PARylation signal also mediates the recruitment of PARP2 to the damaged site. Although the role of PARP2 has not been fully elucidated yet, it seems that PARP2 is responsible for the expansion of the PARylation signal via the synthesis of branched PAR chain [146,147].

4.2. Agents targeting PARP

Several tumors present mutation in DNA repair genes such as breast cancer antigen (BRCA)-1 and BRCA-2. In these tumors, there is a disruption in the activity of the HR repair pathway meaning that the only pathway available for DNA damage repair is the PARP-mediated DNA repair pathways.

PARP can be inhibited using PARP inhibitors, thus, DNA damages are unable to be repaired resulting in cell death through "synthetic lethality" in the case of BRCA1/2 mutation [148]. Several PARP inhibitors have been approved for the treatment of BRCA1/2 mutated cancers. Indeed, PARP inhibitors are currently approved for the treatment of breast, ovarian, pancreatic and prostate cancers. Due to the relatively low frequency of BRCA1/2 mutations, the inhibitors are only used in 10-15% of breast and ovarian cancers, 4-7% of pancreatic cancers and 1-2% of prostate cancers [149]. Fortunately, several studies demonstrated that PARP inhibitors could be used in combination with other drugs that target DDR proteins [119,150]. Furthermore, PARP inhibitors could also be used as a mono-therapy in cancers presenting with mutations in other DNA damage response genes. Several clinical trials are currently registered to study the efficacy of these inhibitors in monotherapy or in combination with other drugs.

4.2.1. PARP inhibitors

Olaparib (Lynparza), sold by AstraZeneca, was the first PARP inhibitor approved by the Food and Drug Agency as a monotherapy for the treatment of advanced, germline BRCA mutated ovarian cancer in 2014 [151]. The clinical study SOLO-1 (NCT01844986) demonstrated that nearly 50% of the tumor of the patients presenting with advanced ovarian cancers treated with Olaparib did not progress after 5 years compared to 20% in the placebo group [152]. The results of SOLO-2 (NCT01874353) and Study-19 (NCT00753545) demonstrated that Olaparib was

efficient for patients with reoccurring ovarian, fallopian and primary peritoneal tumors, regardless of BRCA mutational status. It was thus approved for these indications [151,153]. Olaparib was also approved for the treatment of germline BRCA1/2 mutated HER2-negative breast [154], germline BRCA1/2 metastatic pancreatic cancer [155] and homologous recombination deficiency (HRD)-positive metastatic castration-resistance prostate cancer [156].

Furthermore, several other PARP inhibitors have been approved for various uses. These inhibitors are named Rucaparib, Niraparib and Talazoparib. Rucaparib (Rubraca) was approved for the treatment of germline or somatic BRCA1/2 mutated advanced ovarian carcinomas following multiple chemotherapy treatments [157]. Rucaparib was further approved for the treatment of reoccurring ovarian, fallopian, primary peritoneal tumors regardless of BRCA mutational status [158]. Rucaparib is also approved for BRCA1/2 mutated metastatic castration-resistant prostate cancer [20]. Patients with reoccurring ovarian, fallopian and primary peritoneal carcinomas that show a complete or partial chemotherapy response can be treated with Niraparib (MK-4827) regardless of BRCA mutational status [160]. Moreover, Niraparib is also used in the late-line treatment of the three aforementioned carcinomas if they are HRD-positive [161]. Talazoparib (BMN673) was approved for the treatment of germline BRCA1/2-mutated advanced or metastatic HER2-negative breast cancer [162]. Finally, Veliparib (ABT-888) is currently undergoing clinical trials for ovarian cancers.

On the 14th of August 2022, 108 clinical trials were registered using Talazoparib, 181 studies using Niraparib, 388 studies with Olaparib, 67 clinical trials with Rucaparib and 106 studies using Veliparib on the ClinicalTrials.gov website.

4.2.1.1. The mechanism of action of PARP inhibitors

The mechanism of action of the PARP inhibitors has not been fully uncovered yet. It is proposed that these inhibitors act through three mechanisms : inhibiting PARylation, inducing PARP trapping onto the DNA and modifying the speed of the replication fork (Figure 27) [163,164]. Furthermore, PARP inhibitors were designed to inhibit PARP1, but these inhibitors might also target other members of the PARP family such as PARP2. Interestingly, deletion of PARP1, but not PARP2, reduces the sensitivity of U2OS cells to Talazoparib and to Niraparib [165] meaning that the role of PARP2 might be negligible, at least in an *in vitro* setting.

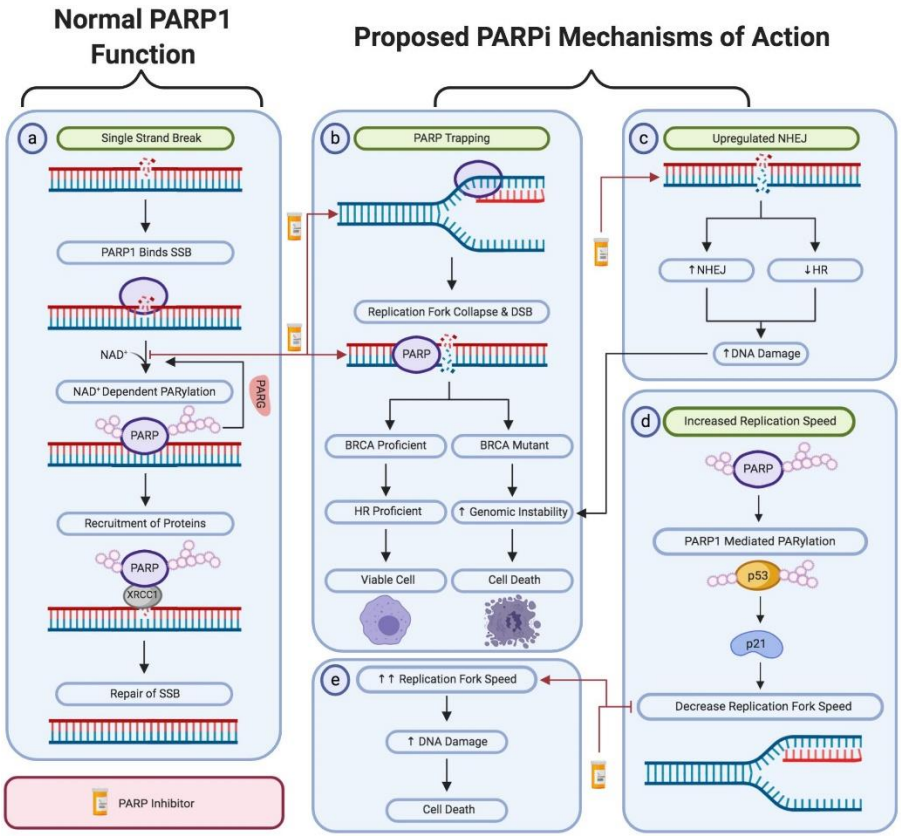

Figure 27 – Schematic representation of the normal function of PARP1 and the proposed mechanism of action of the inhibitors of PARP [149].

4.2.1.1.1. Inhibition of PARylation

As PARP1 is a key player in the repair of single-strand breaks via the base excision repair pathway, it seems rationale to hypothesize that PARP inhibitors induce lethality by impairing the repair of DNA single-strand breaks, thus leading to the accumulation of DNA damages. Indeed, the post-translational modification PARylation promotes the recruitment of DNA repair proteins, necessary for repair of single-strand breaks. The inhibitors compete with NAD+ at the catalytic pocket of PARP (PARP1/PARP2), thus preventing PARylation. It seems that all the inhibitors present the same ability to prevent PARylation [166]. Indeed, the inhibition constant (Ki) for Veliparib (ABT-888) is 5.2 nM for PARP1 and 2.9 nM for PARP2 [167]. Rucaparib (Rubraca, AG014699, PF01367338) demonstrates a Ki value of 1.4 nM for PARP1 [168]. Olaparib (AZD2281) presents Ki values of 5 nM and 1 nM for PARP1 and PARP2 respectively [169]. Ki value for PARP1 was 3.8 nM and 2.1 nM for PARP2 for Niraparib [170]. Talazoparib (BMN 673) has been described as the most potent and selective inhibitor of PARP so far, with a Ki value of 0.57 nM for PARP1 [171].

4.2.1.1.2. PARP trapping

The PARP inhibitors competitively bind to the NAD^+ binding domain on PARP1. This results in PARP1 becoming trapped on the DNA due to the inability to auto-PARylate PARP1. The

correlation between PARP trapping and tumor sensitivity has also been investigated and it seems that the ability to trap PARP onto the DNA correlates with toxicity [172]. Interestingly, all the inhibitors of PARP do not possess the same ability to trap PARP onto the DNA. Researchers noticed that the cytotoxicity profile of the inhibitors greatly differs. Rucaparib, Olaparib and Niraparib have comparable toxicity while Talazoparib is 25 to 100-fold more potent. Veliparib is 1000 to 10000-fold less potent than Talazoparib [166]. These differences cannot be explained solely by off-target effects, as Olaparib and Veliparib have similar selectivity profile against 13 members of the PARP family [173]. In addition, DT40 cells knockout for PARP1 demonstrated a high resistance to Talazoparib, indicating that the cytotoxicity of Talazoparib is mediated primarily by PARP1 [174]. Talazoparib demonstrated a stronger ability to trap PARP1 and PARP2 compared to Rucaparib and Olaparib in DT40 and DU145 cells [174]. Further studies showed that Talazoparib is the most potent PARP trapper to date [163]. Recently, Lin et al. demonstrated that PARP inhibitors are also capable of trapping PARP2 at DNA damage sites. Indeed, RPE-1 cells treated with methyl methanesulfonate (MMS) (0.1 mg/mL) and Niraparib (1 µM) demonstrated strong trapping of PARP1 but also, of PARP2. Furthermore, Olaparib and Talazoparib induce PARP2 trapping but Niraparib and Talazoparib possessing a higher ability to trap PARP2 compared to Olaparib [175]. These results thus indicate that inhibitors of PARP might also exert their functions through the trapping of PARP1 and PARP2, and not solely through the trapping of PARP1. This latest discovery has to be taken into account, knowing that some researchers do not usually check PARP2 following treatment of cells with inhibitors of PARP.

Furthermore, Krastev et al. performed mass spectrometry to determine which proteins were linked to PARP1 when PARP1 was trapped onto the DNA. To this purpose, CAL51 cells were exposed to PARP inhibitors combined to MMS to permit PARP1 trapping. The proteins interacting with trapped PARP1 were identified through mass spectrometry. The KEGG Gene Ontology enrichment analysis demonstrated an enrichment for spliceosome, RNA transport, ribosome biogenesis, protein processing in ER, base excision repair, sulfur metabolism, cysteine and methionine metabolism, autophagy, tight junction, vitamin B6 metabolism, mRNA surveillance pathway, fatty acid degradation, sulfur relay system, proteasome and adherens junction (Figure 28) [176]. These results demonstrate that trapping of PARP1 is extremely important in the context of ribosome biogenesis and mRNA processing. Thus, trapping of PARP1 onto the DNA by Talazoparib might strongly affect several important processes in cancer cells, which might be responsible for the reprogrammation of these cancer cells: from cancer cell death to senescence.

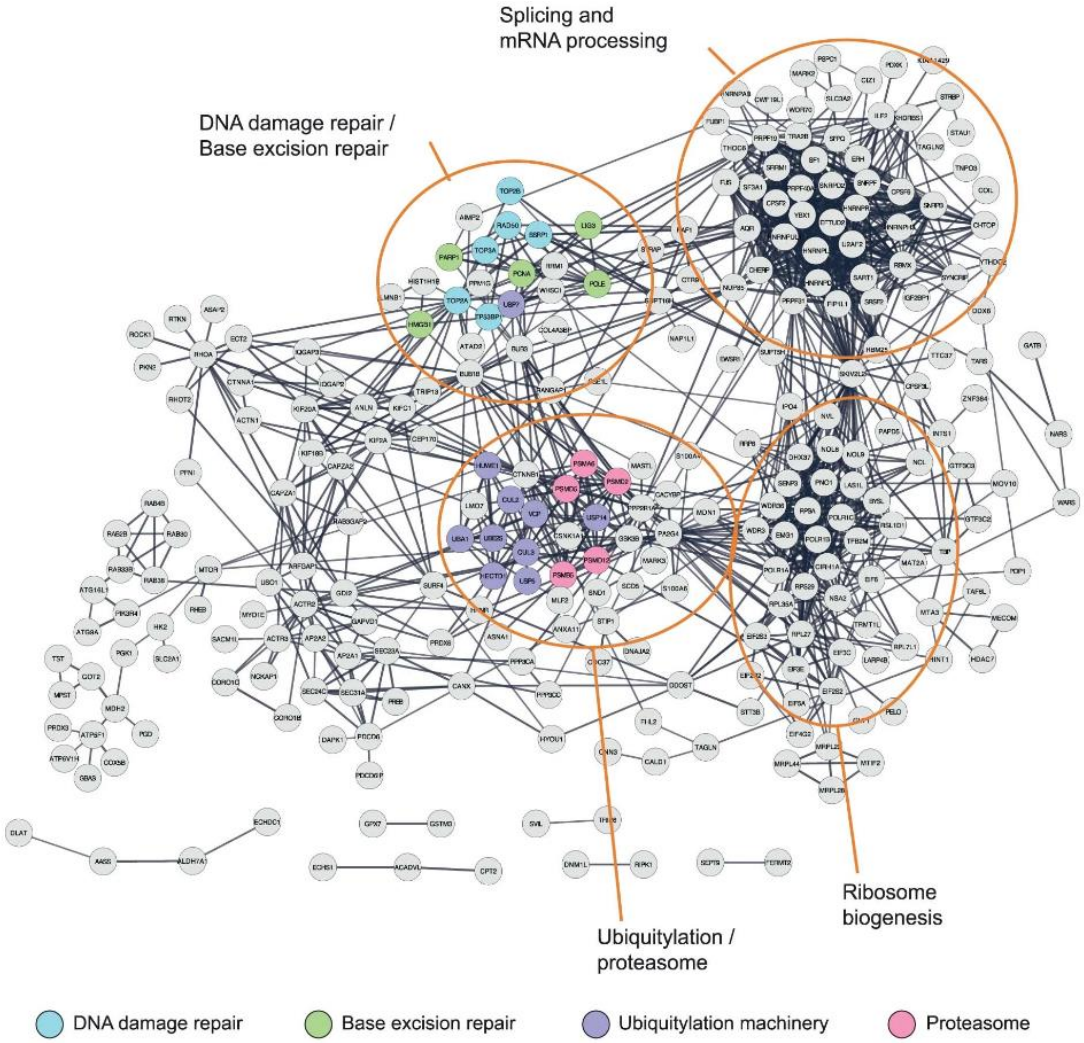

Figure 28 - Identified trapped PARP1 proteins through STRING network analysis [176].

4.2.1.1.3. Dysregulation of the replication fork

At the moment, it is unknown if the inhibition of PARP directly dysregulates the replication fork or if the dysregulation of the replication fork might be a consequence of the trapping of PARP onto the DNA.

It was initially thought that inhibition of PARP could induce replication fork stalling. The proposed theory was disproved by Maya-Mendoza et al. in 2018. Indeed, the inhibition of PARP actually increases the speed of fork elongation. Fork speed was compared in U2OS cells treated with 10 µM of Olaparib or with 30 µM of cisplatin for 24 hours: the fork speed was significantly increased in U2OS cells treated with Olaparib compared to untreated cells or cells treated with cisplatin. Furthermore, the authors demonstrated that Olaparib treated cells accumulated in mid-to-late S phase and activated the DDR. The authors showed that Olaparib treatment led to an increase in γH2AX, RAD51, RPA, 53BP1 and phosphorylation of RPA and CHK1. These results suggest that the absence of PARylation accelerates fork speed leading to the activation of the DDR. Interestingly, the authors also demonstrated that the presence of

PARP1 is necessary for increasing the speed of the replication fork. Indeed, knockdown of PARP1 did not significantly affect fork speed and did not activate DDR. It seems that, in order to increase fork speed, PARP1 is thus required.

Furthermore, the authors investigated the interaction between PARP1, PARylation and the p53-p21 pathway in the regulation of fork speed. Knockdown of PARP1 in U2OS cells resulted in increased p21 abundance. Interestingly, depletion of p21 also increased total fork speed without modifying PARylation level. In contrast, PARPi slightly decreased the nuclear level of p21. Knockdown of p53 did not modify PARylation level while total fork speed was decreased [177]. These results thus demonstrated that PARP is the initial sensor of replication stress-associated DNA damage. PARylation suppresses fork progression, leading to the activation of p53 which can in turn, activate p21 to further suppress fork progression (Figure 29).

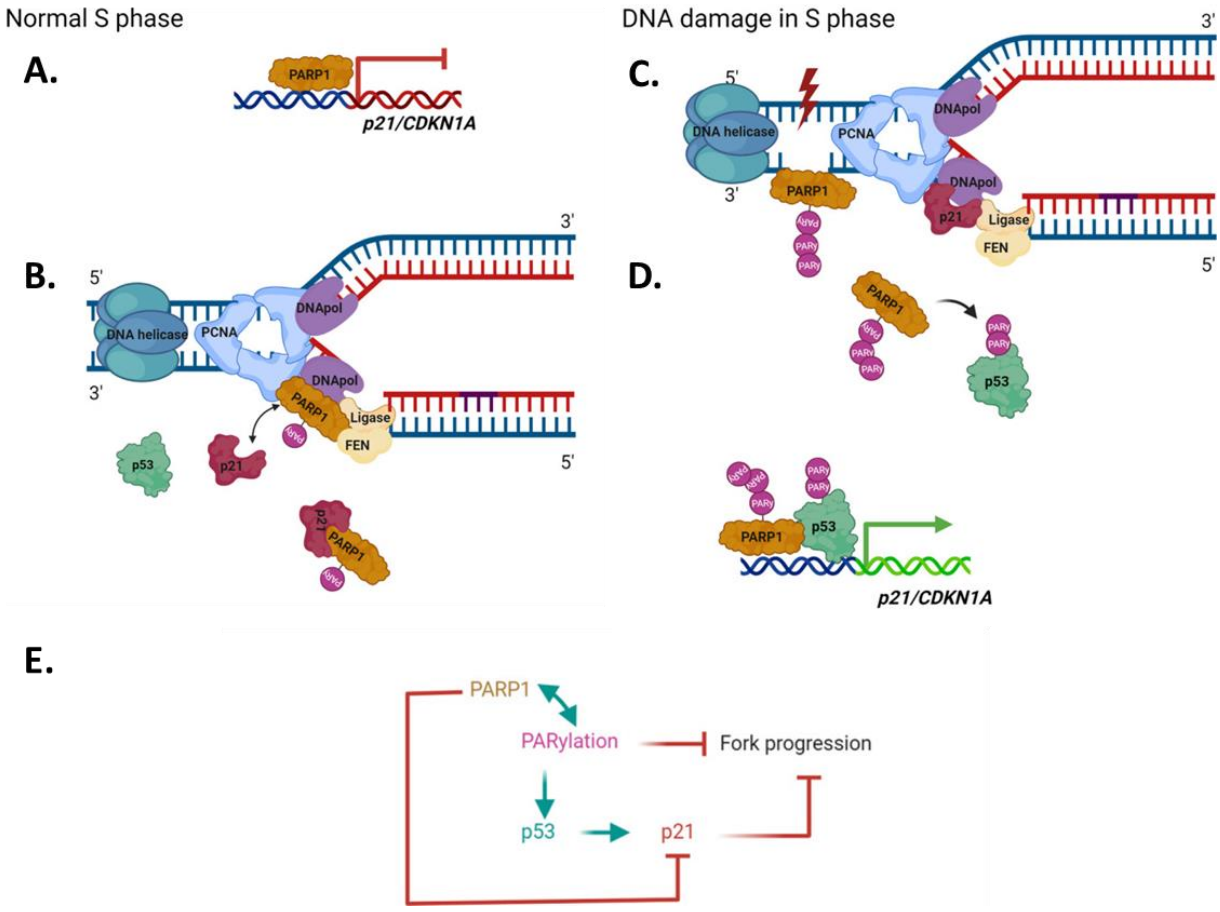

Figure 29 – (A) During normal S phase, PARP1 inhibits the transcription of the CDKN1A gene. (B) During normal S phase, a low level of PARylation is maintained. (C) In the presence of DNA damages, PARP1 recognizes these DNA damages, resulting in increased PARylation levels triggering the recruitment of DDR proteins. (D) p53 is PARylated by PARP1 and forms a complex with PARylated PARP1 to trigger the transcription of CDKN1A gene. (E) The proposed model to maintain normal speed of replication fork (modified from [178]).

4.2.2. PARP degraders

PARP1 is often hyperactivated upon genotoxic stresses linked with various pathologies, namely ischemia-reperfusion injury and neurological disorders [179–181]. For this reason, the inhibition of PARP is being evaluated for the treatment of these pathologies [163]. However, the aforementioned inhibitors might not be useful as they are highly cytotoxic due to mostly to their ability to trap PARP1 and/or PARP2 onto the DNA. In order to circumvent this limitation, compounds mimicking PARP1 genetic deletion are currently being investigated.

The proteolysis targeting chimera (PROTAC) technology might be of interest in this case. The technology is designed to degrade proteins by directing them to the ubiquitin-proteasome system. A small molecule which is the ligand of a protein of interest is linked to a binder of ubiquitin E3 ligase. Thus, upon binding of the protein of interest, it brings the E3 ligase in close proximity of the targeted protein, leading to its ubiquitination and subsequent degradation through the proteasome (Figure 30) [182].

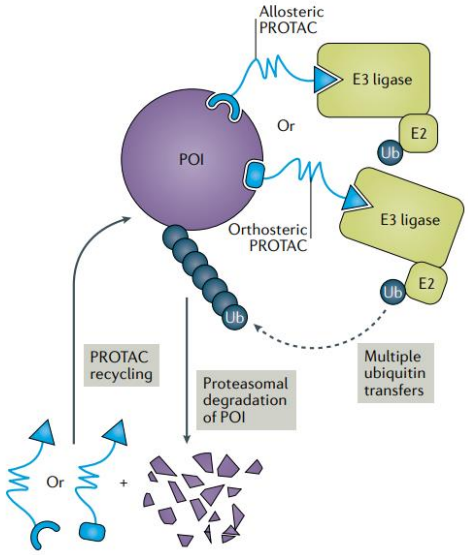

Figure 30 – Schematic representation of the PROTAC technology. The protein of interest (POI) is bound to the E3 ligase via the orthosteric PROTAC (the binding occurs at the active site of the POI) or the allosteric PROTAC (the binding does not occur at the active site of the POI). The E3 ligase mediates the transfer of ubiquitin (Ub) from the E2 enzyme to the POI. The ubiquitinylated POI is then degraded by the proteasome. The PROTAC is available to bind to another POI when the interaction between the POI and the PROTAC is a non-covalent interaction (modified from [182]).

Wang et al. used the PROTAC technology for targeting on PARP1 and PARP2. They used the PARP inhibitor Rucaparib to develop several compounds with the ability to induce the degradation of PARP. One of these compounds is iRucaparib-AP6 which selectively targets PARP1 for degradation as in primary rat neonatal cardiomyocytes using multiplexed quantitative mass spectrometry. Indeed, concentrations ranging from 0.05 µM to 10 µM of iRucaparib-AP6 led to significant reduction of PARP1. Furthermore, HeLa cells were treated with Rucaparib or iRucaparib-AP6 for 24 hours. HeLa cells treated with Rucaparib

demonstrated PARP1 trapping whereas HeLa cells treated with iRucaparib-AP6 showed no PARP1 trapping [183]. Several authors have also designed, synthetized and evaluated compounds for PARP degradation [184–186]. Thus, the development of PARP degraders might be of interest in several pathologies as aforementioned, but it might also permit to dissect the contribution of PARP1 trapping from the catalytic inhibition of PARP1.

4.3. Conclusion

To sum up, the current role of the members of the PARP family is extremely diversified and complex. The role of PARP1 ranges from DNA damage repair to mRNA processing. Even if the functions of PARP1 are not fully understood, in the context of cancer therapy, PARP inhibitors are showing great promises for patients presenting with BRCA1/2 mutations. Indeed, four PARP inhibitors are already approved for cancer patient treatment. Developing a better understanding of the role of PARP1 and the molecular mechanisms of action of these PARP inhibitors would certainly be beneficial for cancer patients, allowing an improvement in cancer therapy.

5. The induction of cellular senescence following radiotherapy and PARP inhibition

5.1. Cellular senescence following radiotherapy

Several reports demonstrated that conventional radiotherapy may induce cellular senescence in cancer cells [4,187–192]. Efimova et al. demonstrated that X-rays induce senescence in a breast cancer cell line (MCF7) and a murine melanoma cell line (B16.SIY). The phenotype was characterized by an increase in SA-β-Gal activity [190]. Lafontaine et al. also showed that photons induce a senescent-like phenotype in sarcoma cell lines. Indeed, three sarcoma cell lines, STS93, STS117 and STS109, demonstrated an increase in SA-β-Gal activity, IL-6 and IL-8 mRNA expression as well as a decrease in proliferation shown through 5-ethynyl-2'-deoxyuridine (EdU) incorporation after irradiation (2, 4, 6, 8 and 10 Gy). The authors also evidenced that irradiation induced a significant increase in the expression of Bcl-2 and Bcl-XL at mRNA and protein levels [191]. Similar results were observed in prostate cancer cell lines, LNCaP and PC-3. 8 Gy of X-rays triggered senescence which was characterized by an increase in the number of cells positive for SA-β-Gal, a significant increase in the mRNA expression of the genes coding for p15 and p21 as well as a decrease in the number of cells positive for EdU incorporation [193]. Photon irradiation was also shown to induce a senescent phenotype in several glioblastoma cell lines and human patient-derived glioblastoma cell lines. An increase in the number of cells positive for SA-β-Gal was observed in GB40, GB48, GBM39, U87MG, U87, LN229, U251 and U373 cells following photon irradiation. Interestingly, PTEN influenced the fate of GBM cell lines following photon irradiation. Indeed, it seems that wild-type PTEN GBM cell lines were not capable of undergoing senescence as LN18 and LN428 did not express senescence markers following photon irradiation [194]. The authors thus proposed that senescence would be a fail-safe option for cells incapable of undergoing apoptosis. In non-mutated GBM cell lines, p21 and Bcl-2 expression increased following photon irradiation at the protein level [195]. Senescence was also examined in several head and neck cancer cell lines, namely, UDSCC2, UPCISCC 040, Cal27, Cal33, UPCISCC 099, UPCISCC 131, UPCISCC 154, UMSCC1, HN30, Detroit, HN31 following photon irradiation. The authors demonstrated an increase in the number of cells positive for SA-β-Gal as well as a decrease in Lamin B1 expression at the protein level. Furthermore, the SASP was also increased following photon irradiation.

5.1.1. Radio-sensitization and radio-resistance

It is unclear if senescence induces radio-sensitization (meaning that cellular senescence would increase the lethal effect of radiation) or to radio-resistance (meaning that cellular senescence would decrease the lethal effect of radiation) in cancer cells. The induction of senescence is often correlated with the presence of p53, which is then able to activate p21 [196]. The importance of p53 in the induction of cellular senescence following radiation was also highlighted in prostate cancer cell lines. It was shown that mutation of even one p53 allele is

capable of preventing entry of prostate cancer cell lines into senescence [197]. It seems that the entry into senescence is a mechanism of radio-sensitization in p53 wild-type and p53 mutant lung cancer cell lines. The authors showed that treatment with epidermal growth factor receptor (EGFR) radiosensitized lung cancer cell lines. This effect was linked to the induction of DSBs in p53 wild-type and p53 mutant cell lines [198].

Radiation-induced senescence seems to be lower in HPV+ head and neck cancer cell lines, namely, UDSCC2 and UPCISCC-154 than in HPV- head and neck cancer cell lines. Conversely to what is mentioned above, the authors demonstrated that TIS strongly correlates with radio-resistance, providing a first explanation regarding the radio-sensitive status of HPV+ head and neck cancer cell lines [199]. Also, in the context of human head and neck squamous cancer cells, Taichi Nyui et al. demonstrated that X-ray irradiation strongly increased the percentage of senescent cells defined by increased SA-β-Gal staining and increased p21 expression at protein level in Ca9-22 cancer cells. Interestingly, the authors proposed that cGAS regulates the radio-resistance. cGAS negatively regulates the expression of p21 which in turn, regulates cellular senescence. The absence of cGAS prevents the regulation of p21 allowing the cells to enter senescence leading to a strong increase in cellular senescence, leading in this context, to radio-sensitivity [200]. In cervical cancer cell lines depleted for HPV18 (E6 or E6/E7), a strong induction in radiation induced SA-β-Gal staining was observed when compared to wild type cells. Combination of radiation and E6/E7 silencing in cervical cancer cell lines seems to enhance the anti-tumor effect of radiation [201], demonstrating the potential role of senescence as a radio-sensitizer. Radio-resistant nasopharyngeal carcinoma cell line demonstrated feature of “premature” cellular senescence following X-ray irradiation. It seems that radio-resistant cancer cells over-expressed CDC6, which in turn, led to increased “pre-mature” cellular senescence. However, depletion of CDC6 sensitized the nasopharyngeal carcinoma cell line, CNE2, to radiation and promoted “mature” cellular senescence in the remaining CNE2 cells. The “mature” cellular senescence was described as the cells possessing a typical morphology of a senescent cell. Furthermore, the cells also showed dark blue positive β-galactosidase staining in the cytoplasm. CDC6 depletion increased p16 and p21 protein abundance, but did not modify p53 protein level. The depletion of CDC6 also sensitized radio-resistant clones, promoting significant tumor regression [121]. In conclusion, these research articles suggest an important role for senescence in the regulation of radio-resistance and radio-sensitization. The role of senescence might be further complicated by the different types of senescence.

5.1.2. Abscopal effect

Senescence is also involved in the abscopal effect which describes the disappearance of cancer cells which were not directly irradiated. Indeed, senescent cells were detected in non-irradiated contralateral tumors of mice xenografted with A549 cells wild-type for p53. The authors demonstrated that irradiated A549 cancer cells delivered signals through senescence-

associated secretory phenotype leading to the production of vesicles containing RNA:DNA hybrids. Interestingly, co-culture of these vesicles with unirradiated A549 cells induced a significant inhibition of colony-forming ability and increased expression of several markers of senescence in these unirradiated cells. Moreover, the vesicles secreted by irradiated A549 cells reprogrammed macrophages (Raw 264.7) towards the M1 phenotype characterized by a decrease in Egr2 and an increase in IL6 and IL-1β at the mRNA level [202]. Furthermore, cellular senescence can also drive a potent immune response. Induction of cellular senescence by radiation in PANC-01 and SK-Mel-28 cells led to the release of IL-8. The latest is capable of activating natural killers expressing IL-8 receptor, CXCR1. The activation of these natural killers led to a strong anti-tumor response in mice grafted with PANC-01 or SK-Mel-28 cells [203].

5.1.3. Particle therapy

Induction of senescence following particle therapy has also been described. Li Wang et al. compared the percentage of SA-β-Gal positive cells in 4 head and neck cancer cell lines (SqCC/Y1, HN5, UPCI-SCC-154 and UMSCC-47) after an irradiation of 4 Gy with photons or protons. The authors showed that 4 Gy of protons resulted in a stronger increase in SA-β-Gal staining compared to 4 Gy of photons [204]. Moreover, senescence after proton irradiation was also demonstrated in non-small lung cancer cell line as A549 cells irradiated with protons showed SA-β-Gal staining [205,206]. Moreover, proton irradiation also showed a decreased induction of senescence in DU145 and PC3 prostate cancer cell lines as well as LN229 and U87MG glioblastoma cancer cell lines when compared to conventional radiotherapy. Interestingly, the induction of senescence following protons was not modified in FaDu and Cal33 head and neck cancer cell lines in comparison to conventional radiotherapy. This difference might be explained by the result of the 3D colony-formation assay. Indeed, the authors investigated the induction of senescence following 4 Gy of photons or protons. However, proton irradiation led to a significant reduction of clonogenic survival in LN229, U87MG, DU145 and PC3 cancer cell lines in comparison with photons whereas no difference in clonogenic survival was observed between FaDu and Cal33 cancer cell lines [207]. High-LET radiation such as carbon ions are also capable of increasing several markers associated to senescence in human glioma cancer cell lines and in a lung cancer cell line [208,209]. The induction of SA-β-Gal in U87 cancer cells was also reported following irradiation with neutrons [210]. In H460 cells, the percentage of SA-β-Gal positive cells was similar after an irradiation of 9 Gy with X-rays and with 4 Gy of carbon ions, which led to a similar survival fraction [208]. Induction of senescence following X-rays and carbon ions was also compared in A549 and H1299 cells. The percentage of senescent cells was higher in cells treated with 4 Gy of carbon ions compared to cells treated with 4 Gy of X-rays, especially in A549 cells. Moreover, survival fraction was lower when cells were irradiated with 4 Gy of carbon ions than with 4 Gy of X-rays which might explain the stronger induction in senescence observed after carbon irradiation [211]. Finally, senescence induction following irradiation with X-rays, carbon ions or

iron ions was compared in 92-1 cancer cells. The authors showed that, at similar doses, iron ions are more efficient than carbon ions and X-rays to induce senescence in 92-1 cells. These differences can be explained by the strong induction of DNA damages following high-LET radiation [212]. However, as no survival curve is given, it remains to be determined if the induction of senescence is based on the quality of DNA damages, or simply on their quantity leading to different levels of activation of downstream targets.

5.1.4. The role of reactive oxygen species

ROS are important for senescence to occur after irradiation. Indeed, the use of anti-oxidants (N-acetyl cysteine) caused a significant decrease in senescence in head and neck cancer cell lines after irradiation. Furthermore, the protein level of p21, p53 and p-p53 was also reduced in cancer cells treated with anti-oxidants [213]. These effects of the ROS on induction of cellular senescence, can probably be explained by the induction of DNA damages in the presence of ROS.

5.1.5. The dose rate

The dose rate also seems to affect the induction of senescence in cancer cells. 2 Gy was delivered to one rhabdomyosarcoma cell line (RH30) and two prostate cancer cell lines (PC3 and DU145) at a dose rate of 1.5 Gy/min or 10.1 Gy/min. Interestingly, the percentage of senescent cells was lower in cells irradiated at a dose rate of 10.1 Gy/min compared to cells irradiated at a dose rate of 1.5 Gy/min. Modulation of the dose-rate does not change the ability of X-rays to produce ROS, which was assessed through MitoSox staining. However, the expression of several miRNAs involved in the anti-oxidant response, namely miR-34a, miR-22, miR-126, miR-210 and miR-375 was strongly induced in RH30 cells irradiated with 10.1 Gy/min compared to cells irradiated with 1.5 Gy/min. The expression of miR-375 was strongly upregulated in PC3 cells irradiated with 10.1 Gy/min and the expression of miR-210 was also strongly increased in DU145 cells irradiated with 10.1 Gy/min. The activation of several DNA repair pathways was also differentially regulated depending on the dose rate. Indeed, in RH30 cells, 10.1 Gy/min efficiently induced phosphorylation of Ku80 while in both prostate cancer cell lines, 1.5 Gy/min efficiently induced phosphorylation of ATM and DNA-PK [214]. In conclusion, it seems that a higher dose rate reduced the amount of cellular senescence. However, the molecular mechanisms behind this difference in induction is not clearly understood.

Induction of cellular senescence was also compared between cancer cells treated with synchrotron microbeam radiation therapy (MRT) and uniform broad beam (BB) radiation therapy. MRT spatially distributes the X-ray beam into several microbeams of very high dose, regularly separated by low-dose intervals. The authors applied a similar BB to the MRT valley

dose deposited in the tumors. In the context of melanoma, MRT led to a stronger reduction in tumor volume compared to BB. Furthermore, Ki-67 at protein level was strongly decreased in MRT compared to BB, and SA-β-Gal staining was increased in MRT compared to BB. MRT enhanced the presence of immune cells, notably CD8, CD4, NK and macrophages [215]. Interestingly, these results thus demonstrated that MRT significantly delayed tumor growth compared to BB. Furthermore, MRT significantly increased the percentage of senescent cells, and the authors also demonstrated a strong impact of MRT on the immune system. It remains to be investigated if senescent cancer cells are responsible for the pro-inflammatory effects observed in the tumor microenvironment.

5.1.6. Fractionation

Fractionation is also implicated in the induction of cellular senescence following radiation. Indeed, A549 cells were either treated with 10 Gy or with 8x2 Gy, whereas H460 cells were either treated with 10 Gy or with 13x2 Gy. The survival fraction for A549 cells and H460 cells was similar for the two types of fractionations. However, 10 Gy led to a stronger increase in the number of SA-β-Gal positive cells in A549 cells (36.84% versus 3.915%) and H460 cells (43.010% versus 2.965%). Moreover, cells irradiated with 10 Gy also demonstrated a stronger cell cycle arrest and a stronger staining for gH2AX [216]. These results thus suggest that fractionation strongly reduced the induction of cellular senescence.

5.2. Cellular senescence following PARP inhibition

Fleury et al. reported that PARP inhibition using Olaparib induced a senescent-like phenotype in ovarian and breast cancer cell lines. OV1369(R2), OV90, OV4453 and OV1946 cells were exposed to several concentrations of Olaparib leading to the induction of senescent-like phenotype characterized by an increase in SA-β-Gal positive cells, morphological changes, an increase in the secretion of IL-6 and IL-8 and proliferation arrest. Furthermore, these results were also reproduced in MDA-MB-231 cells which also showed a senescent-like phenotype following treatment with Olaparib. The authors demonstrated that the senescent-like phenotype induced by the inhibitor of PARP was p53 independent but p21 dependent. It was also demonstrated that the induction of senescence is not Olaparib dependent as ovarian cancer cells treated with Niraparib and Talazoparib, two other PARP inhibitors, also showed senescent-like features [119]. Similar results were also obtained when prostate cancer cell lines, LNCaP and PC-3 cells, were treated with Olaparib [193]. Interestingly, it was shown that senescence was induced in prostate cancer cells sensitive to Olaparib, but not in resistant prostate cancer cells. In sensitive prostate cancer cells, p21 was increased at protein level and the authors hypothesized that senescence was an alternative to cell death and that senescent cancer cells which could have escape cell death could then promote treatment resistance [217]. Senescence following inhibition of PARP was reversible, as ovarian cancer cells re-started

proliferation if left untreated for 3 days. As the authors stated, these cells might contribute to therapy resistance [119].

5.3. Cellular senescence following radiotherapy and PARP inhibition

The induction of senescence following RT combined to PARP inhibitors was demonstrated in 2010. Veliparib (ABT-888) combined to irradiation significantly increased the number of senescent MCF7 cells. Interestingly, the authors already demonstrated that the induction of senescence following treatment with PARP inhibitor and radiation was not limited to p53 wild-type cancer cell lines [218]. Furthermore, HCT116 and HCT116 Ligase $IV^{-/-}$ cells treated with RT (4 Gy) and Niraparib (MK-4827) or Olaparib (AZD-2281) showed stronger percentage of SA-β-Gal positive cells compared to cells treated only with RT or with MK-4827 or AZD-2281 [219].

Glioblastoma cells treated with radiotherapy at a dose of 8 Gy demonstrated a strong increase in cells positive for SA-β-Gal. The authors showed that the use of radiotherapy combined to Olaparib further increased the number of cells positive for SA-β-Gal. The same results were also observed when irradiated cells were treated with a siRNA targeting PARP1. Moreover, the combination of Olaparib with radiation induced a strong increase in mRNA levels of several SASP factors, namely, IL-8, CXCL5, CSF2 and TIMP1. The authors also demonstrated the importance of reduced PARP-1 activity to facilitate senescence. Indeed, a significant reduction in PARylation of proteins was detected by western blots in radio-resistant cells. Radio-resistant cells treated with Olaparib were more sensitive to radiation demonstrating the importance of reduced PARP-1 activity to maintain senescence.

5.4. One-two punch approach: targeting cellular senescence with senolytics

As mentioned in Chapter 3, senescence can either be beneficial or detrimental to cancer cells. Several researchers demonstrated the interest in targeting senescent cells to increase cell death. Radiotherapy and/or inhibitors of PARP have already been combined to senolytics to further improve cancer treatments. Fleury et al. confirmed the results of Yokoyama et al., which demonstrated that apoptosis was increased when PARP inhibitor was combined to Navitoclax (ABT-263) in ovarian cancers [119,220]. Several senolytics namely, Dasatinib, Querceting, Fisetin, A-1155463 and Piperlongumine (PPL) demonstrated a synergistic effect for cancer cell death when combined with Olaparib in ovarian cancer cells. Moreover, the effect was not only observed in ovarian cancer cells. Indeed, Navitoclax, A-1155463 and PPL also demonstrated a synergistic effect for cancer cell death in combination with Olaparib in MDA-MB-231 cancer cell line [119]. Navitoclax and A-1155463 also led to a synergistic effect in LNCaP and PC-3 cells treated with Olaparib. Navitoclax (ABT-263) was also combined with X-rays in A549 and Ca9-22 cancer cells, leading to increased cancer cell death [221]. Esophageal cancer cell lines demonstrated an increase in SA-β-Gal activity following X-ray irradiation.

These senescent cancer cells could further be targeted by YM155, an inhibitor of the survivin protein. The inhibition of the survivin protein pushed senescent cells towards apoptosis [222].

However, PPL was unable to trigger cell death in Olaparib treated LNCaP and PC-3 cancer cell lines. In a similar fashion, PPL was also unable to induce cell death in X-ray treated LNCaP and PC-3 cancer cell lines [193]. These results demonstrated that the regulation of apoptosis resistance following TIS in context-dependent, which might explain why PPL was unable to induce cell death in combination with Olaparib.

B. Objectives of the PhD thesis

As aforementioned, senescence is a new hallmark in the context of cancer. Furthermore, it has already been characterized that senescence can be induced through several current cancer therapies such as chemotherapy, radiotherapy and targeted therapy. In this context, we decided to evaluate the induction of senescence following irradiation with photons and with protons in combination or not with PARP inhibitors.

The first purpose of the project was to determine if radiotherapy and protontherapy alone are capable of triggering cellular senescence in cancer cells. To this purpose, several cancer cell lines were chosen: A549, MDA-MB-231, KP4 and HCT-116. A549 cells were irradiated with X-rays and protons whereas, MDA-MB-231, KP4 and HCT-116 were irradiated with X-rays. Markers of senescence were then evaluated.

The second purpose of the project was to define if radiotherapy and protontherapy could be combined to an inhibitor of PARP to trigger a stronger induction of cellular senescence compared to radiotherapy or protontherapy alone. In this case, radiotherapy and protontherapy were combined to the most described inhibitor of PARP: Olaparib. The same cancer cell lines as mentioned above were used. Markers of senescence were also evaluated to determine if senescence was induced.

The third purpose was to determine the mechanisms behind the induction of cellular senescence by PARP inhibitors. Indeed, several PARP inhibitors have already been described to induce cellular senescence in various cancer cell lines but the mechanism has yet to be discovered. To this purpose, several non-small cell lung cancer cell lines were used: A549, H460 and Calu1. These cancer cell lines were treated with various PARP inhibitors: Veliparib, Rucaparib, Olaparib, Niraparib and Talazoparib.

The final objective was to determine if conventional radiotherapy, protontherapy and inhibitors of PARP could be combined with senolytics in order to improve the outcome of these cancer treatments.

A better understanding of senescence in the context of cancer is currently required to improve outcomes. Furthermore, senolytics have already shown some benefits for pathologies linked to ageing, but these compounds might also bring a new therapeutic venue in the context of cancer. We thus hope that our work will permit a better comprehension of the field of cancer and senescence.

C. Results

1. Taking Advantage of the Senescence-Promoting Effect of Olaparib after X-ray and Proton Irradiation Using the Senolytic Drug, ABT-263

In this first article published in Cancers in March 2022, we described that irradiation with photons or protons led to a senescent-like phenotype in A549, MDA-MB-231 and to a lesser extent, in HCT-116 and KP4 cancer cells. The senescent-like phenotype could be further increased when cells were treated with photons or protons combined with Olaparib, an inhibitor of PARP. The inhibitor of PARP alone did not increase the percentage of senescent-like cells. It has to be mentioned that the inhibitor was used at non-toxic concentration. Interestingly, we also demonstrated that the senescent cancer cells could further be targeted by Navitoclax (ABT-263) to increase cell death. These results thus demonstrate that particle therapies (high-LET protons) induce senescent cancer cells similarly to what is observed with photons. Furthermore, these preliminary data indicate that senolytics used in combination with radiation could improve the outcome in cancer patients.

Taking Advantage of the Senescence-Promoting Effect of Olaparib after X-ray and Proton Irradiation Using the Senolytic Drug, ABT-263

Camille Huart [1], Maude Fransolet [1], Catherine Demazy [1], Benjamin Le Calvé [1], Stéphane Lucas [2], Carine Michiels [1] and Anne-Catherine Wéra [1,3,*]

[1] Cellular Biology Research Unit (URBC), Namur Research Institute for Life Sciences (NARILIS), University of Namur (UNamur), 5000 Namur, Belgium

[2] Laboratory of Analysis by Nuclear Reaction (LARN), Namur Research Institute for Life Sciences (NARILIS), University of Namur (UNamur), 5000 Namur, Belgium

[3] Molecular Imaging, Radiation and Oncology (MIRO) Lab, Institut de Recherche Expérimentale et Clinique (IREC), Université Catholique de Louvain (UCLouvain), 1200 Woluwe-Saint-Lambert, Belgium

* Correspondence: anne-catherine.wera@uclouvain.be

Simple Summary: Radiotherapy is one of the most common treatments for cancer. Overcoming the failure and side effects of radiotherapy are current challenges. It has been recently demonstrated that senescence contributes to radioresistance. Cellular senescence is a permanent arrest in cell proliferation induced by various factors, such as radiation. Here, we aimed to assess the potential of combining the radiation and DNA damage repair inhibitor, Olaparib to a senolytic drug, ABT-263. We demonstrated that combining radiation, Olaparib and ABT-263 successfully targeted the radio- induced senescent cells resulting in increased cell death and reduced senescence-associated secretory phenotype. These results paved the way towards a new therapeutic combination for patients treated with radiotherapy and Olaparib.

Abstract: Radiotherapy (RT) is a key component of cancer treatment. Although improvements have been made over the years, radioresistance remains a challenge. For this reason, a better understanding of cell fates in response to RT could improve therapeutic options to enhance cell death and reduce adverse effects. Here, we showed that combining RT (photons and protons) to noncytotoxic concentration of PARP inhibitor, Olaparib, induced a cell line-dependent senescence- like phenotype. The senescent cells were characterized by morphological changes, an increase in p21 mRNA expression as well as an increase in senescence-associated β-galactosidase activity. We demonstrated that these senescent cells could be specifically targeted by Navitoclax (ABT-263), a Bcl-2 family inhibitor. This senolytic drug led to significant cell death when combined with RT and Olaparib, while limited cytotoxicity was observed when used alone.

These results demonstrate that a combination of RT with PARP inhibition and senolytics could be a promising therapeutic approach for cancer patients.

Keywords: cancer; PARP; proton radiation; X-ray radiation; senescence; senolytics

Introduction

About 50% of cancer patients undergo radiotherapy during the course of their treatment either for curative prospect or palliative assistance [1]. In order to improve patient outcome, treatments usually combine surgery, chemotherapy and radiotherapy. Although improvements have been made over the last decades to optimize the therapeutic index, resistance to treatment is still a major issue. Amongst the strategies to optimize cell response to radiation, it is worth mentioning the improvement of radiation dose conformity, higher effectiveness radiation and biological strategies [2,3,4].

The improvement of dose spatial distribution aims at dose escalation, hypofractionation and the sparing of healthy tissues. For photons, techniques such as IMRT must be favored as well as stereotactic body radiotherapy (SBRT), which is being pushed forward. In the seeking of dose conformation, charged particles, such as protons or carbon ions, present a clear advantage compared to photons due to their depth dose profile [5,6]. While photons deposit most of their energy close to the surface entrance, followed by a continuous decrease characteristic in their attenuation, charged particles deposit a small fraction of their energy before what is called the Bragg peak. This peak characterizes the maximal energy released when the particles come to rest. For photons, dose deposition upstream and downstream the tumor is observed, but for charged particles, the dose sharply decreases beyond the Bragg peak, allowing the downstream tissues to be spared. Highly conformal dose deposition profiles can be obtained as the position of the Bragg peak can be tuned with the incident beam energy to coincide with the tumor position.

A wide range of biological strategies are under study as well as in clinical assessment for charged particles and conventional photon irradiation [7,8]. One of the most promising strategies is that of DNA repair inhibitors. Amongst them, the most widely used is poly(ADP-ribose)polymerase (PARP) inhibitor (PARPi) [9,10]. PARPi are able to stabilize the single strand breaks (SSBs) induced by radiation, which are then translated into double-strand breaks (DSBs) at the replication fork leading to increased cell death. This is particularly observed for homologous recombination (HR) deficient cell lines as these DSBs are usually processed with the HR machinery during the S phase of the cell cycle. This is generally referred to as synthetic lethality [11]. PARPi are currently approved by the FDA for patients with germline BRCA-mutated cancers, such as ovarian cancer, breast cancer, pancreatic cancer and prostate cancer [12–15]. Combination strategies with RT and/or chemotherapy might extend the therapeutic indications of PARPi to patients

with BRCA wild-type tumors, as sensitization has been observed in several studies [16–19]. Although the literature is scarce for proton irradiation [19,20], several authors have demonstrated that treatment with radiotherapy and/or PARPi triggers cell senescence [21–24]. Senescence is marked by changes in cell morphology, irreversible cell cycle arrest characterized by an increase in $p16^{INK4A}$ and $p21^{Waf1/Cip1}$ expression, increased senescence-associated β-galactosidase (SA-β-gal) activity, changes in gene expression, Lamin B1 loss, presence of senescence-associated heterochromatin foci (SAHF) and a common mitochondrial DNA deletion of 4977 bp [25,26]. In addition, senescent cells are characterized by a specific senescence-associated secretory phenotype (SASP). SASP factors include chemokines, inflammatory cytokines, matrix-remodeling proteases, growth factors and associated proteins, as well as insoluble secreted proteins [27]. Senescent cells exhibit an increased resistance to apoptosis, thereby impacting tumor growth [28]. Chronic accumulation of senescent cells has been proposed to support SASP signaling as well as to promote pro-tumoral effects on the surrounding microenvironment [29]. The pro-tumoral ability of senescent cells was discovered when senescent fibroblasts were co-cultured with pre-neoplastic epithelial cells, which led to an increased proliferation rate of the epithelial cells. These pro-tumoral abilities have been, in part, linked to the secretion of SASP factors, notably IL6 and IL8 [30–33]. In addition, although senescence is often described as an irreversible state, several studies have reported proliferation in the recovery of cells from their induced senescence status. For example, Fleury et al. recently demonstrated the need for sustained PARPi therapy as drug withdrawal permitted senescent cells to escape the senescent state and to re-initiate proliferation [21]. Alotaibi and colleagues demonstrated in HCT-116 cells that Olaparib promoted senescence induced by radiation and that a sub-population of these cells was able to re-enter proliferation [24]. It is now suggested that senescence could represent a form of tumor dormancy [34]. Associated with its pro-tumoral secretory phenotype, this population could ultimately lead to treatment failure.

For this reason, the clearance of senescent cells has become an interesting new pharmacological strategy. These molecules which are able to kill senescent cells are called senolytics [35]. The goal of these drugs is to selectively eliminate senescent cells while sparing normal cells. Several companies are currently developing senolytics, exploiting the dependence of senescent cells for specific pro-survival pathways [36]. Examples are ABT-263 and TW-37, which inhibit pro-survival genes in the Bcl-2 family [37]. These drugs specifically induce apoptosis in RT- and PARP inhibitor-induced senescent cells [21–23].

In this work, we examined the effects of X-rays and protons combined with Olaparib on BRCA wild-type cancer cells. We showed that the combination of Olaparib with radiation (both photons and protons) increased the number of senescent cells, which can subsequently be

targeted by ABT-263. Importantly, the concentration of Olaparib and ABT-263 used did not induce cellular senescence or cell death if not combined to radiation. While Olaparib radiosensitized all cell lines, the proportion of senescence induced when combined with radiation was cell line-dependent and the efficiency of the combined treatment with ABT-263 varied accordingly. Together, our results propose a new therapeutic approach combining protons or X-rays and Olaparib with senolytic agents to decrease the number of senescent cells, enhancing cell death and reducing the risk of treatment failure.

Materials and Methods

- Cell Culture, Olaparib and ABT-263

Human A549 non-small-cell lung cancer (NSCLC) cells were sub-cultured in Glutamax Modified Eagle's Medium (Gibco Life Technologies, Carlsbad, CA, USA) supplemented with 10% fetal bovine serum (FBS) (Gibco Life Technologies). KP4 pancreatic cancer cells and HCT-116 colon cancer cells were sub-cultured in 4500 mg/L glucose Dulbecco's Modified Eagle's Medium (Gibco Life Technologies) supplemented with 10% FBS. For the experiments, the medium was supplemented with 0.1% penicillin/streptomycin (Sigma, Saint Louis, MO, USA). Olaparib (AZD2281, S1060, Selleckchem, Houston, TX, USA), a poly(ADP-ribose)polymerase inhibitor, was used at 0.5 µM final concentration. ABT-263 (Navitoclax, MedChemExpress, HY-10087, MedChemExpress, Monmouth Junction, NJ, USA), a Bcl-2 family inhibitor, was used at 1 µM final concentration. Cells were incubated in the presence of the Olaparib for a total duration of 24 h. ABT-263 was added 24 h after irradiation and was left up to the end of the assay. The concentration chosen for Olaparib is based on previous work [19]. For ABT-263, 1 µM concentration allowed to limit the clonogenic toxicity when combined with Olaparib in cells unexposed to radiations.

- Irradiation: Protons and X-rays

The experimental set-up and irradiation procedure for protons using a 2MV tandem accelerator are described in [38,39]. Briefly, 24 h before irradiation, A549 cells were seeded as a 38 µL drop (800 c/µL) in designed irradiation chambers and left to attach to a Mylar foil for 4 h. The chambers were then filled with medium and left in the incubator before the irradiation. A proton beam energy of 1.3 MeV was used for the experiments, which corresponds to a fixed linear energy transfer (LET) of 25 keV/µm within the cell monolayer. Such LET is found at the end of each particle's track composing the proton beams found in clinic. This high LET leads to the highest effect of protons in cells [40]. Dose rates ranging from 2 to 8 Gy/min were used.

For X-ray irradiation, cells were seeded in 24 well-plates 24 h before irradiation to obtain the same density as for proton irradiation (200 x 10^3, 250 x 100^3 and 300 x 10^3 cells/well for A549, KP4 and HCT-116, respectively). Irradiations were performed at 225 kV (X-RAD 225-XL, PXI) and the dose rate set to 2 Gy/min.

For proton and X-ray irradiations, 2 h before irradiation, the culture medium was replaced with medium containing: no inhibitor (CTL) or 0.5 µM Olaparib (Ola.). Within 30 min after the irradiation, cells were detached using trypsin, then counted and seeded in cell culture plates. After 24 h, the medium was refreshed with FBS-supplemented medium containing or not containing ABT-263 at 1 µM and cells were left to proliferate.

- Senescence-Associated Beta-Galactosidase

Six days post-irradiation, cells were detached and around 15,000 cells were reseeded in 12 well-plates in duplicates. The next day, cells were fixed with 2% formaldehyde, 0.2% glutaraldehyde in PBS for 5 min. Cells were rinsed twice with PBS and incubated at 37 °C for 18 h (A549 cells) to 24 h (KP4 and HCT-116 cells) in the staining solution containing: x-gal (20 mg/mL) (No. 0428-1G, Amresco, Fountain Parkway Solon, OH, USA), phosphate buffer (pH 5.8), potassium ferricyanide (100 mM), potassium ferrocyanide (100 mM), NaCl (2.5 M) and $MgCl_2$ (1 M). After incubation, cells were rinsed twice with PBS and twice with methanol before observation under optical microscope [41]. At least 200 cells were counted. At least three independent experiments were performed, and data are presented as mean ± 1 SD.

- EdU Labelling

Six days after irradiation (5 Gy for A549 and KP4 cells and 3 Gy for HCT-116 cells due to a higher radiosensitivity), cells were detached and reseeded onto a glass coverslip. The next day, cells were incubated for 8 h with 10 µM EdU before 4% formaldehyde fixation.The EdU staining was performed following the manufacturer's instructions (BCK-EDU488, Sigma, Saint Louis, MO, USA). The nuclei were stained with 2.5 mg/mL DAPI (Sigma) for 10 min. Following PBS washes, the coverslips were mounted on microscope slides with Mowiol. The observations were performed by confocal microscopy by keeping the photomultiplier at a constant gain (Leica SP5, Leica Microsystems, Wetzlar, Germany). ImageJ software was used to quantify the green signal intensity in each nucleus. Each cell with an integrated density value above 1 was scored as positive. At least three independent experiments were performed, and data are presented as mean ± 1 SD.

- RNA Extraction and RT-qPCR

Three and six days post-irradiation, total RNA was isolated from cells with ReliaPrep™ RNA Tissue Miniprep System (Promega, Z6111, Madison, WI, USA) according to the manufacturer's instructions. RNA concentration was quantified using the Nanophotometer N60 (Implen, Munich, Germany). cDNA was synthetized with GoScript™ Reverse Tran- scription Mix (Promega, A2790) according to the manufacturer's instructions using random primers. 2 µg of RNA was used per reaction. The primers used for the qPCR are described in Table S1. Linear relationships between Ct values and cDNA

concentration expressed in log2 were checked for all primer pairs. All real-time PCR reactions were performed in duplicates with GoTaq™ qPCR Master Mix (Promega, A6001) on a ViiA 7 Real-Time PCR System (Applied Biosystems, Waltham, MA, USA) using a standard run. The gene expression level of each messenger RNA (mRNA) was calculated, further normalized to glyceraldehyde 3 phosphate dehydrogenase (GAPDH) mRNA, and related to the control condition. Specific amplification was confirmed by melting curve analysis. At least three independent experiments were performed, and data are presented as mean ± 1 SD.

- Measurement of IL6 Secretion

Secreted IL6 was assessed in cell-free supernatants collected 6 days after irradiation using ELISA kit, according to the manufacturer's recommendations (Quantikine, R&D Sytems D6050, Minneapolis, MN, USA). For all samples, measured concentrations were normalized by the number of viable cells. At least three independent experiments were performed, and data are presented as mean ± 1 SD.

- Flow Cytometry

The apoptotic fraction was assessed with a FITC Annexin V detection kit (BD Pharmignen, Franklin Lakes, NJ, USA, No. 556547) 72 h after irradiation. The samples (composed of both cells present in the supernatant and adherent to the bottom of the wells) were handled following the manufacturer's instructions. Data acquisitions were performed using FACS Verse (BD Biosciences, Franklin Lakes, NJ, USA) and quantifications using FlowJo software. Based on the intensity of Annexin V and propidium iodide fluorescence, the proportion of dead cells can be determined. Annexin V positive cells were considered as dead cells. The PI fluorescence intensity of Annexin V positive cells differentiated early apoptosis (PI negative) to late apoptosis or post-apoptotic necrosis (PI positive). At least three independent experiments were performed, and data are presented as mean ± 1 SD.

- Colony Formation Assay and Survival Fraction

After irradiation, cells were detached using trypsin and seeded in 12-well plates at desired concentrations in medium (with or without 0.5 µM Olaparib) supplemented with 10% FBS. More precision on the procedure can be found in [38,39]. After 24 h, the medium was refreshed with FBS-supplemented medium containing or not ABT-263 at 1 µM and cells were left to proliferate (8 days for KP4 cells and 12 days for A549 and HCT-116 cells). The cells were then stained with crystal violet in 2% ethanol and the number of visible colonies (containing more than 50 cells) was counted. The plating efficiency (PE) was calculated for each irradiation dose and drug condition as the ratio of the number of colonies to the number of cells seeded. The survival fraction at a dose D is then obtained with comparison to un-irradiated cells:

$$SF_D = \frac{PE_D}{PE_0}$$

With PE_D and PE_0 the plating efficiency calculated at a dose *D* and 0 Gy (no irradiation), respectively. Survival fraction can be calculated from un-irradiated cells that have not been in the presence of neither Olaparib nor ABT-263 (CTL cells) or from un-irradiated cells exposed to Olaparib, ABT-263 or both. At least three independent experiments were performed, and data are presented as mean ± SD.

The coefficient of drug interaction (CDI) highlighting the potentiation obtained when combining two drugs can be calculated from the survival fractions:

$$CDI = \frac{SF_{Ola+ABT}}{SF_{Ola}\ x\ SF_{ABT}}\ x\ SF_{CTL}$$

where SF is the survival fraction associated with a chosen dose in the case of control, i.e., no drugs, (SF_{CTL}), Olaparib (SF_{Ola}), ABT-263 (SF_{ABT}) and the combination Olaparib plus ABT-263 ($SF_{Ola+ABT}$). These SF are calculated from the corresponding un-irradiated cells (CTL, ABT-263, Olaparib or both). A CDI below 0.9 considers the combination as synergic, between 0.9 and 1.1 as additive and above 1.1 as antagonist.

The amplification factor (AF) at a dose *D* is calculated as:

$$AF_D = \frac{SF_{D,CTL} - SF_{D,drug}}{SFD,CTL}\ x\ 100\ (\%)$$

where $SF_{D,CTL}$ is the survival fraction at dose *D* without either Olaparib nor ABT-263 and $SF_{D,drug}$ corresponds to the survival fraction at dose *D* of cells exposed to either Olaparib, ABT-263 or both. The amplification factor highlights the increase in cell death when using drugs compared to irradiation alone.

- Statistical Analysis

Statistical analyses were performed with GraphPad Prism. The unpaired two-tail Student *t*-test was applied considering that the data were normally distributed. If the variance between groups were not similar, Welch's correction was applied. The groups compared are CTL vs. 1 µM ABT-263, CTL vs. 0.5 µM Olaparib and 0.5 µM Olaparib vs.0.5 µM Olaparib plus 1 µM ABT-263. All experiments were repeated at least three times (*n* = 3).

Results

- ABT-263 Hampers the Senescence-Promoting Effect of Olaparib after X-ray and Proton Radiation in A549 Cells

A549 cells were irradiated with X-rays at 3 and 5 Gy or with 1.3 MeV protons at 2.5 Gy. 2 h before irradiation, 0.5 µM Olaparib was added and left for 24 h. ABT-263 (1 µM) was then added and 3 to 12 days post-irradiation, cells were analyzed for senescence markers (Figure 1). These concentrations of Olaparib and ABT-263 led to limited (although significant)

toxicity in un-irradiated cells with survival close to that of the control cells (Table S2).

The induction of senescence was investigated in A549 cells exposed to irradiation with or without these different drugs. For that purpose, SA-β-Gal activity was evaluated, EdU incorporation (indicating DNA synthesis) was assessed and CDKN1A mRNA level (related to cell cycle arrest) was determined. Figure 1a presents pictures of SA-β-Gal staining in cells obtained at 12 days after 5 Gy X-rays (end time for clonogenic survival assays).

The presence of senescent cells after irradiation was observed, especially if Olaparib was used. These senescent cells in between colonies were no longer observed in the presence of ABT-263. Quantifications of SA-β-Gal activity in A549 cells 6 days after irradiation are presented in Figure 1b, showing that X-ray irradiation induced an increase in the proportion of senescent cells in a dose-dependent manner and that Olaparib significantly increased it further. Moreover, the addition of ABT-263 reduced the proportion of senescent cells down to the level of the one observed for irradiation alone. At 3 days, the mRNA level of CDKN1A was increased after X-ray irradiation and was reduced in the presence of ABT-263 (Figure 1c, data at day 6 post-irradiation presented in Supplemental Figure S1a). Figure 1d displays confocal images of A549 cells exposed to an 8 h pulse of 10 µM EdU 6 days post-irradiation. A decreased incorporation in irradiated cells and a recovery in the presence of ABT-263 were observed. The quantification of EdU incorporation (Figure 1e) showed a reduced cell proliferation after irradiation. As for SA-β-Gal activity, Olaparib treatment accentuated this effect. In this case also, ABT-263 partly relieved the induction of cell cycle arrest. As it was reported by others in senescent cells [42], a nuclear enlargement was also observed after irradiation (Supplemental Figure S1c). It was reduced in the presence of ABT-263.

Although to a lesser extent, similar results were obtained after 2.5 Gy proton irradiation with increased SA-β-Gal activity (Figure 1f). A higher level of CDKN1A mRNA (Figure 1g, data for day 6 in Supplemental Figure S1b), reduced EdU incorporation (Figure 1h) and nuclear enlargement (Supplemental Figure S1d) were observed. The increase in CDKN1A mRNA level was still significant for the proton at 6 days. As for X-rays, the combination of Olaparib with proton irradiation strengthened the senescence phenotype and ABT-263 was able to counteract the effect of Olaparib.

Together, these results showed that Olaparib promoted the senescence induced by X-ray and proton radiation in A549 cells and that ABT-263 was able to revert it.

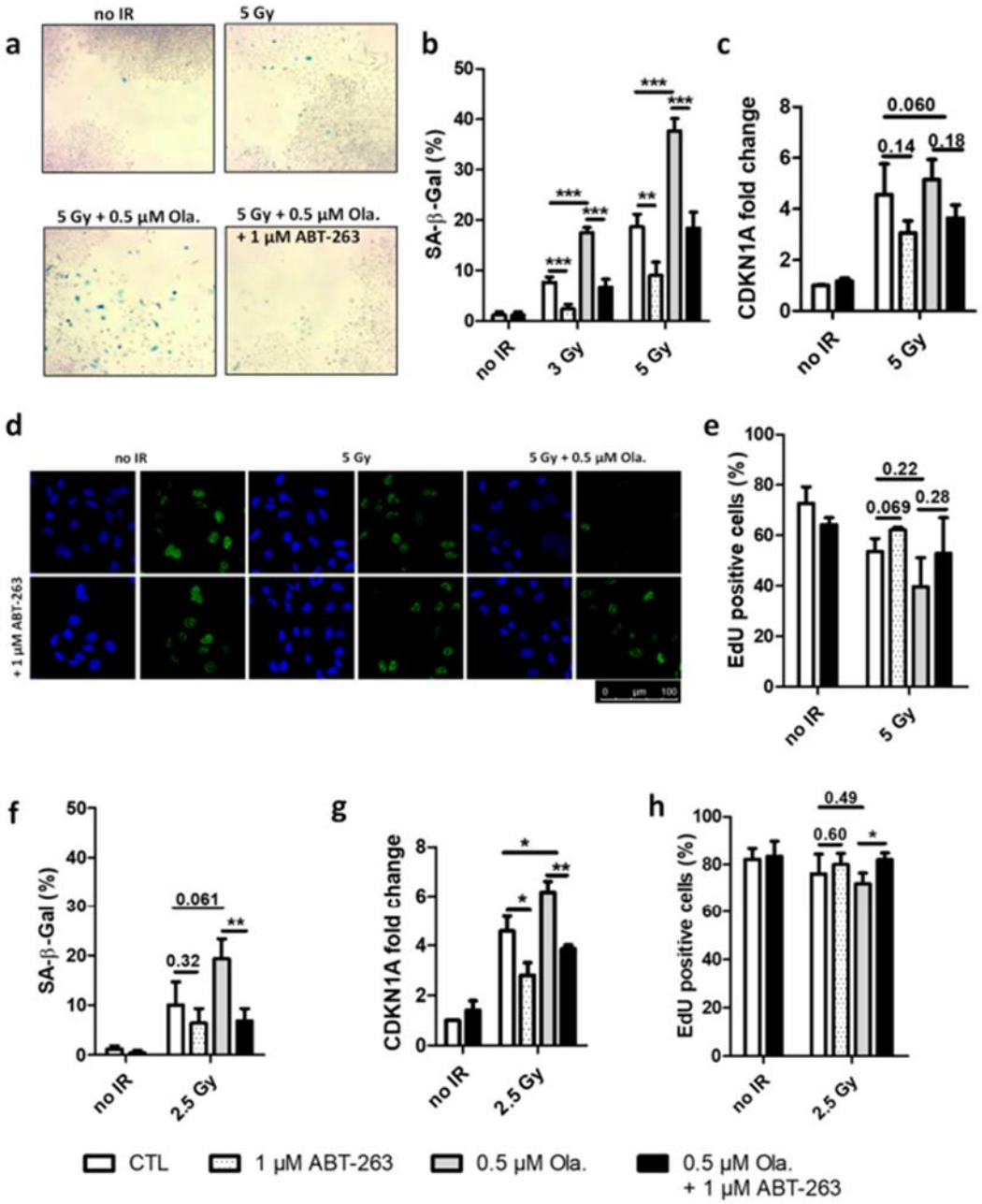

Figure 1 - ABT-263 hampers the senescence-promoting effect of Olaparib after X-ray and proton radiation in A549 cells. A549 cells were irradiated with 3 and 5 Gy X-rays or 2.5 Gy protons with or without 0.5 µM of Olaparib; The medium was replaced 22 h after irradiation, and 1 µM of ABT-263 was added. (a) Bright field microscopic images were obtained 12 days after X-ray irradiation. Blue cells are positive for senescence associated beta-galactosidase activity. (b,f) Quantification of SA-β- Gal positive cells 6 days after irradiation ((b): X-rays; (f): protons). (c,g) CDKNA1 mRNA level 3 days after treatment ((c): X-rays; (g): protons). (d) Representative confocal images of A549 cells 6 days post-irradiation after an 8 h pulse of 10 µM EdU: nucleus (blue), EdU (green). (e,h) Quantification of EdU incorporation after irradiation ((e): X-rays; (h): protons). At least three independent experiments were performed, and data are presented as mean ± 1 SD. Unpaired t-tests were performed (*: $p < 0.05$;**: $p < 0.01$; ***: $p < 0.001$) for CTL vs. ABT, CTL vs. Ola and Ola vs. Ola + ABT.

- The Effect of ABT-263 Is Lower for Cell Lines with Limited Radio-Induced Senescence

HCT-116 and KP4 cells were irradiated with 3 and 5 Gy X-rays. Two hours before irradiation, 0.5 µM Olaparib was added for 24 h. ABT-263 (1 µM) was then added and 6 days post-irradiation, cells were analyzed for senescence markers (Figure 2). These concentrations of Olaparib and ABT-263 led to limited toxicity (although significant for HCT-116 cells) with cell survival without irradiation close to the one of control cells (Table S2).

For HCT-116 cells, the proportion of SA-β-Gal positive cells, even if lower than for A549 cells, also increased with Olaparib (~25% at 5 Gy vs. ~40% for A549 cells) (Figure 2a). The CDKN1A mRNA level markedly increased 3 days after 5 Gy irradiation with slight effects on Olaparib and ABT-263 (Figure 2b). At 6 days, the CDKN1A mRNA level was diminished (Supplemental Figure S2a). The EdU incorporation assay (Figure 2c) followed the same trend. The addition of ABT-263 reduced the proportion of senescent cells in HCT- 116 cells, but to a lesser extent than what was observed for A549 cells. The enlargement of the nuclear area varied accordingly (Supplemental Figure S2c). For KP4 cells, SA-β-Gal activity moderately increased with irradiation and Olaparib (Figure 2d). In agreement with the low proportion of SA-β-Gal positive cells (10% at 5 Gy), CDKN1A mRNA levels were very slightly increased after irradiation (Figure 2e and Supplemental Figure S2b at 6 days). As for HCT-116 cells, EdU (Figure 2f) labeling in irradiated cells was close to the one of un-irradiated cells and the exposure to Olaparib and/or ABT-263 did not lead to notable changes, as it was noticed for nuclear enlargement (Supplemental Figure S2d).

These results showed that although Olaparib promoted the senescence induced by X-ray irradiation in HCT-116 and KP4 cell lines, the induction of senescence is cell line-dependent with a lower effect in HCT-116 and KP4 cells compared to the pro-senescence phenotype observed in A549 cells.

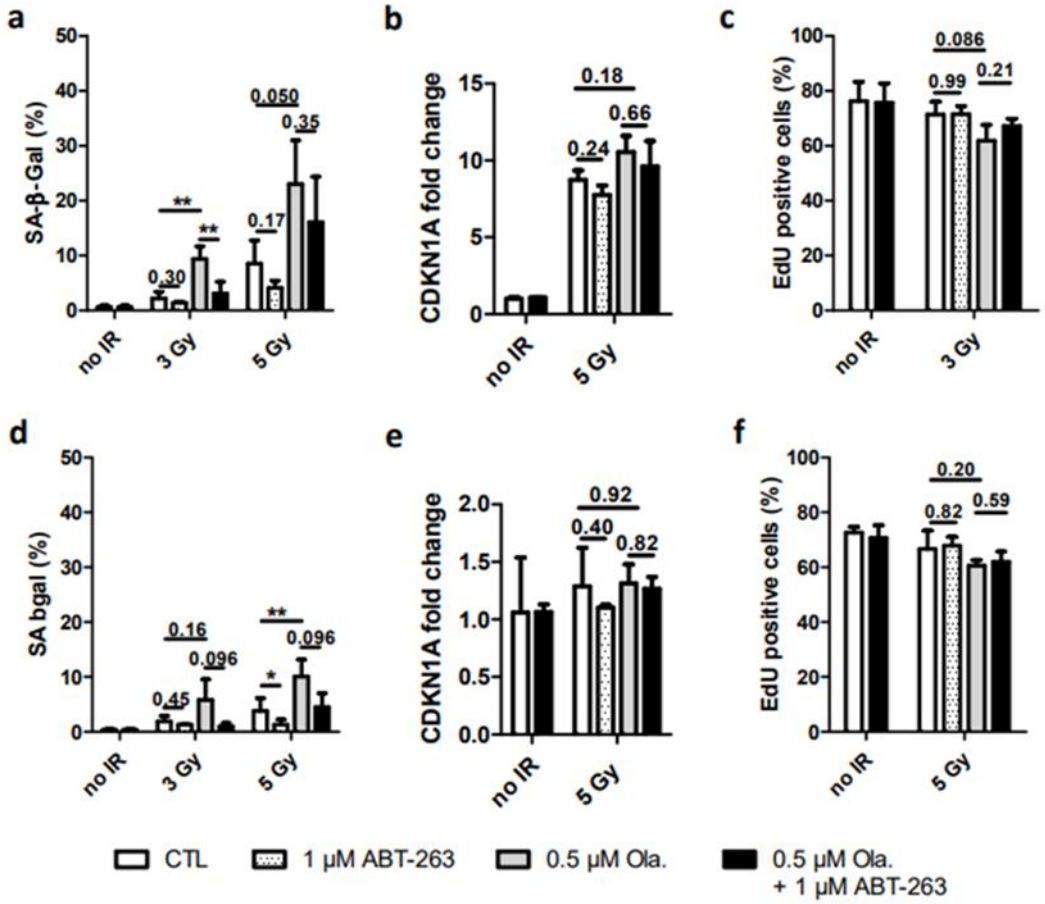

Figure 2 - The effect of ABT-263 is reduced for cell lines with limited radio-induced senescence. HCT-116 and KP4 cells were irradiated with 3 and 5 Gy X-rays with or without 0.5 µM of Olaparib. The medium was replaced 22 h after irradiation, and 1 µM of ABT-263 was added. (a,d) Quantification of SA-β-Gal positive cells 6 days after irradiation ((a): HCT-116; (d): KP4). (b,e) CDKNA1 mRNA level 3 days after treatment ((b): HCT-116; (e): KP4). (c,f) Quantification of EdU incorporation after a 10 µM 8 h pulse ((c): HCT-116; (f): KP4). At least three independent experiments were performed, and data are presented as mean ± 1 SD. Unpaired t-tests were performed (*: $p < 0.05$; **: $p < 0.01$) for CTL vs. ABT, CTL vs. Ola and Ola vs. Ola + ABT.

- ABT-263 Induces Cell Death in Cell Lines Displaying Radiation-Induced Senescence

Cumulative cell death was measured by flow cytometry 72 h after 5 Gy X-ray irradiation for A549, HCT-116 and KP4 cells (Figure 3). Representative distributions for A549 cells are presented in Figure a. The proportion of Annexin V positive cells was quantified for each cell line. For A549 cells (Figure 3b), irradiation alone or irradiation combined with Olaparib led to a slight increase in cumulative cell death. The Annexin V positive fraction significantly increased in the presence of ABT-263. The highest percentage, reaching approximately 60% of dead cells, was observed when Olaparib and ABT-263 were combined after irradiation. The level of cumulative cell death in HCT-116 cells (Figure 3c) after irradiation was higher compared to A549 cells and the effect of ABT-263 was also highlighted but to a lower extent than for A549 cells. For KP4 cells, on the other hand, the fraction of dead cells in irradiated cells only slightly increased compared to un-irradiated cells and no effect of Olaparib, ABT-263 or their combination was noticeable (Figure 3d).

For A549 cells, the distribution between early and late apoptosis was about 50–50%, while for HCT and KP4 cell lines, dead cells were mostly in late apoptosis or necrosis.

PARP cleavage was analyzed by Western blot 6 days post-irradiation in A549 cells exposed to 5 Gy X-rays (Supplemental Figure S3a,b). The ratio of the cleaved over full length forms of PARP was higher in irradiated cells in the presence of ABT-263, especially when combined with Olaparib. A slight increase in Bcl-XL mRNA levels 3 and 6 days after X-ray or proton irradiation was observed in the presence of Olaparib (Supplemental Figure S3c–f). In both cases, the addition of ABT-263 was able to reduce, to a small extent, this increase.

These results showed that ABT-263 was able to promote cell death after irradiation in cell lines displaying radiation-induced senescence.

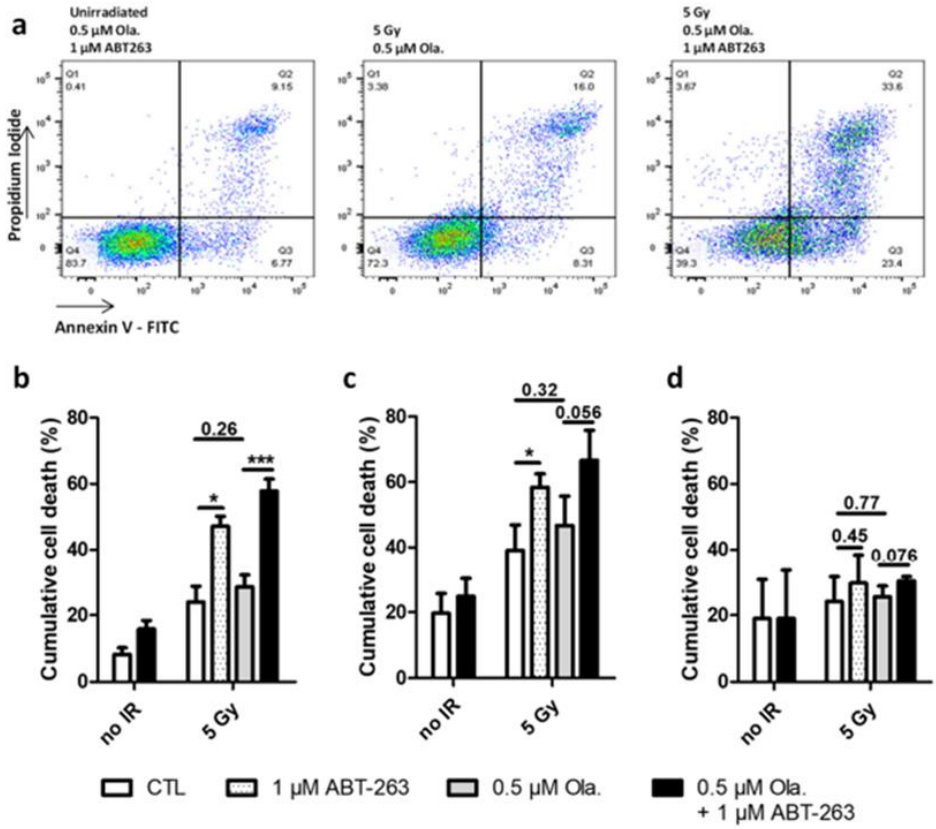

Figure 3 - ABT-263 can induce cell death in cell lines displaying radiation-induced senescence. A549, HCT-116 and KP4 cells were irradiated with 5 Gy X-rays with or without 0.5 µM of Olaparib. The medium was replaced 22 h after irradiation, and 1 µM of ABT-263 was added. (a) Representative flow cytometry results for Annexin V assessment in A549 cells 72 h after irradiation. (b–d) Cumulativecell death 72 h after X-rays ((b): A549 cells; (c): HCT-116 cells, (d): KP4 cells). At least three independent experiments were performed, and data are presented as mean ± 1 SD. Unpaired *t*-tests were performed (*: $p < 0.05$; ***: $p < 0.001$) for CTL vs. ABT, CTL vs. Ola and Ola vs. Ola + ABT.

- Non-Toxic Combination of ABT-263 and Olaparib Can Synergize after X-ray and Proton Irradiation to Increase Clonogenic Cell Death

Clonogenic fractions were assessed after 3 and 5 Gy X-ray irradiation in A549, HCT-116 and KP4 cell lines as well as after 1 and 2.5 Gy proton irradiation for A549 cells (Figure 4). For all cell lines, the combination of Olaparib and ABT-263 led to limited toxicity in un-irradiated cells as shown in Figure 4 (values are presented in Table S2). HCT-116 cells were more radiosensitive than A549 and KP4 cells.

For A549 cells, after X-ray irradiation, a decrease in survival fraction upon the addition of Olaparib was observed for each irradiation dose (Figure 4a). While the addition of ABT-263 significantly decreased survival, the combination with Olaparib reduced survival to a much higher extent compared to Olaparib and ABT-263 alone. The same observation was made after proton irradiation (Figure 4b), with a pronounced radiosensitization when Olaparib and ABT-263 were combined. For HCT-116 cells (Figure 4c), a decrease in the survival fraction with the irradiation dose and with the addition of Olaparib was observed. The addition of ABT-263 did not further increase the clonogenic death. KP4 cells were radiosensitized by Olaparib but the combination with ABT-263 did not lead to a higher clonogenic cell death (Figure 4d).

The interaction of Olaparib and ABT-263 was characterized using the coefficient of drug interaction (CDI) and the amplification factor (AF) (Table 1). For A549 cells, a synergistic effect was obtained in most cases, with an increased AF for the combination of the drugs compared to Olaparib alone. For HCT-116 cells, the CDI calculated corresponded to an additive effect of the drugs with a slightly increased AF for the combination compared to Olaparib alone. For KP4 cells, CDI and AF did not highlight a potentiation of the drugs when combined. Moreover, an antagonist effect was calculated at 5 Gy.

These results showed that Olaparib sensitized A549, HCT-116 and KP4 cells to radiation. ABT-263 alone slightly increased cell death after X-rays or protons compared to Olaparib. ABT-263 and Olaparib can synergize in A549 cells to reduce clonogenic cell death after X-ray and proton irradiation. For HCT-116 cells, the combination was slightly less efficient than for A549 cells. For KP4 cells, the combination was not effective with a CDI above 1.1 at 5 Gy and a smaller amplification factor compared to Olaparib alone.

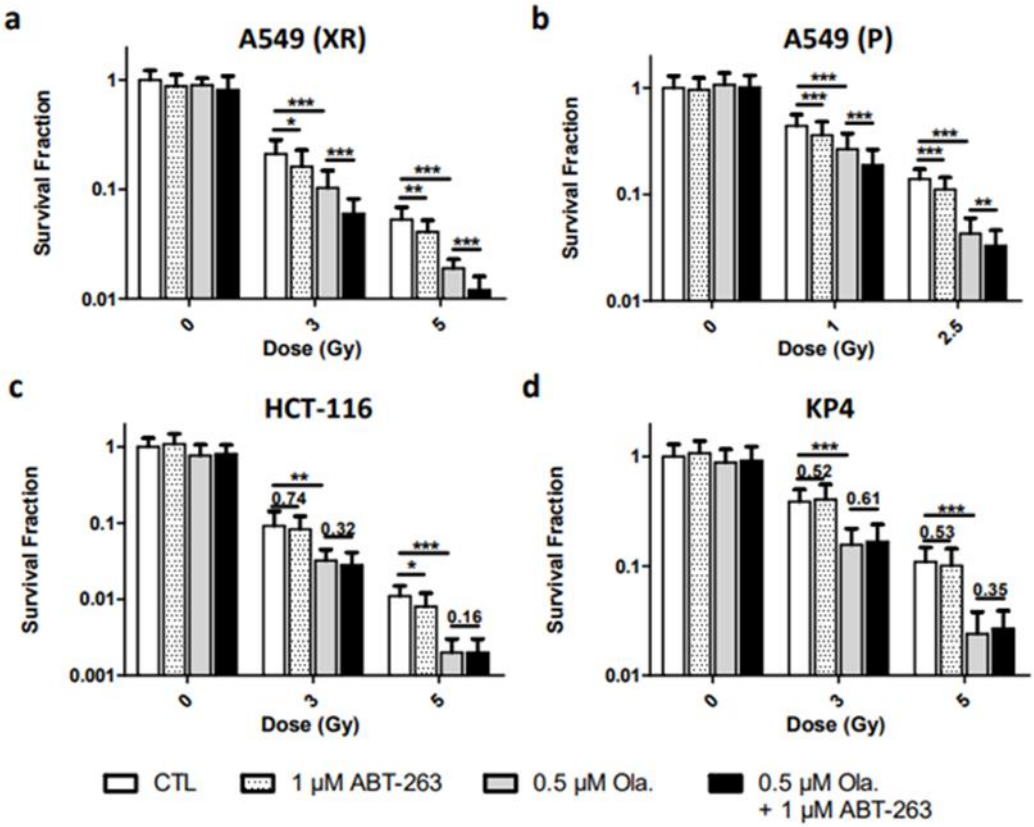

Figure 4 - Non-toxic combination of ABT-263 and Olaparib can synergize after X-ray and proton irradiation to increase clonogenic cell death. A549, HCT-116 and KP4 cells were irradiated with 3 and 5 Gy X-rays or 1 and 2.5 Gy protons with or without 0.5 µM of Olaparib. The medium was replaced 22 h after irradiation, and 1 µM of ABT-263 was added. Colonies were stained and counted 8 days (KP4 cells) or 12 days (A549, HCT-116 cells) post-irradiation. (a) A549 cells after X-rays. (b) A549 cells after protons. (c) HCT-116 cells after X-rays. (d) KP4 cells after X-rays. At least three independent experiments were performed, and data are presented as mean ± 1 SD. Unpaired *t*-tests were performed (*: $p < 0.05$; **: $p < 0.01$; ***: $p < 0.001$) for CTL vs. ABT, CTL vs. Ola and Ola vs.Ola + ABT.

Table 1 - Coefficient of drug interaction and amplification factor calculated with the survival fraction of A549, HCT-116 and KP4 cells after irradiation with 3 and 5 Gy X-rays (XR) or 1 and 2.5 Gy protons (P). The survival fractions were evaluated in comparison to un-irradiated cells.

		CDI		AF		
				1 µM ABT-263	0.5 µM Olaparib	Ola. + ABT-263
A549 (XR)	3 Gy	0.74	Syn.	13	46	65
	5 Gy	0.84	Syn.	13	61	71
A549 (P)	1 Gy	0.88	Syn.	15	43	58
	2.5 Gy	0.98	Add.	18	71	77
HCT-116	3 Gy	1.01	Add.	17	55	62
	5 Gy	1.08	Add.	31	72	79
KP4	3 Gy	1.04	Add.	2	54	53
	5 Gy	1.28	Anta.	14	76	73

- ABT-263 Reduces the SASP Induced by Olaparib after X-ray and Proton Irradiation in A549 Cells

Three days after irradiation, mRNA levels for IL-6, IL-8, IGFB5 and CCL2 (MCP1) were determined in A549 cells exposed to X-rays (Figure 5a) and protons (Figure 5b). These genes have been reported as genes associated with the SASP and are upregulated upon stress-induced senescence [33,42]. Results at 6 days are presented in Supplemental Figure S4. The levels of mRNAs in these genes increased with radiation (photons and protons). The addition of Olaparib seemed to further increase mRNA levels but not significantly. ABT-263 was able to lower this effect, especially for IL6. As for the level of SA-β-Gal activity, the induction of SASP genes after 2.5 Gy is smaller than 5 Gy X-rays.

The results obtained for the mRNA levels for IL6 were confirmed at protein level (Figure 5c). Six days post-irradiation, the level of IL6 in the culture medium was higher for X-ray irradiated cells compared to un-irradiated cells. The presence of Olaparib enhanced this effect. The addition of ABT-263 22 h after irradiation was able to reduce it.

The mRNA levels of these genes were also assessed in HCT-116 and KP4 cells after 5 Gy X-rays (Supplemental Figure S5). The effect of irradiation was limited for most genes and as expected, because of the lower induction of senescence and the lower effect of ABT-263: the responses to Olaparib or ABT-263 were rather small and not observed for all genes.

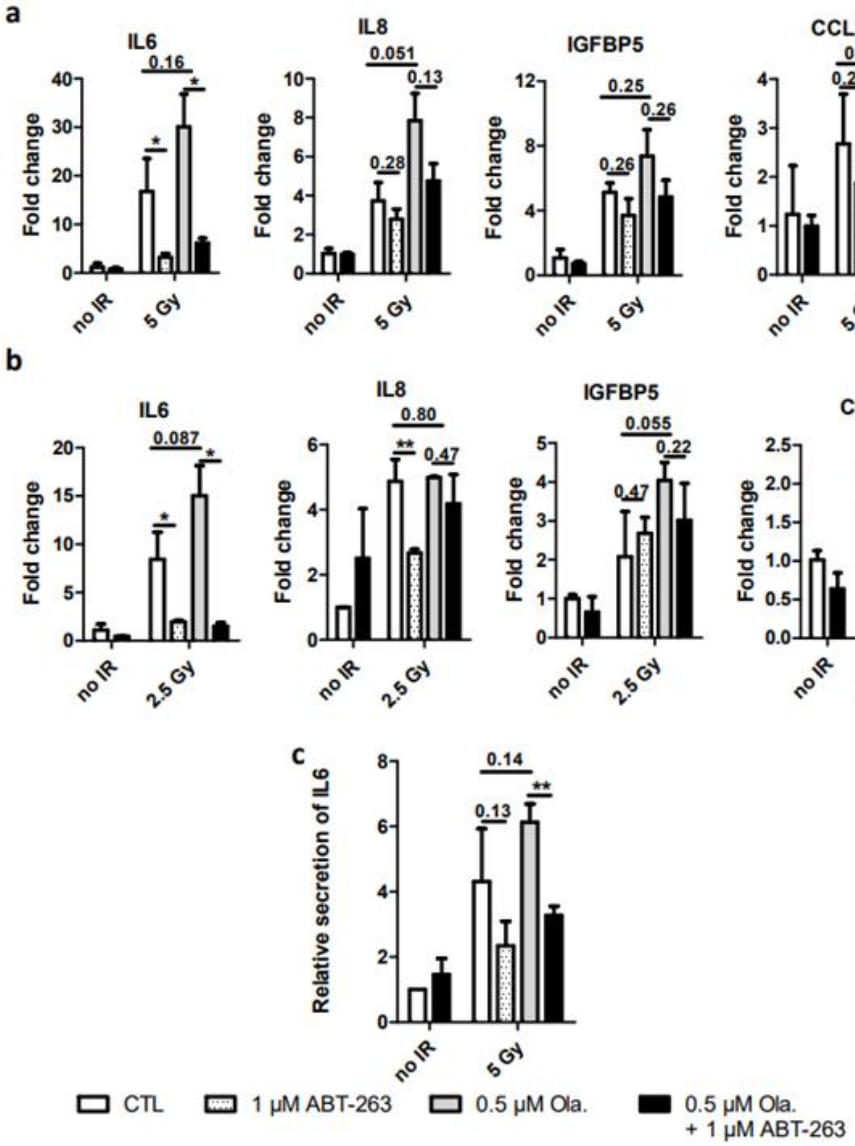

Figure 5 - ABT-263 reduces the SASP promoted by Olaparib and radiations in A549 cells. A549 cellswere irradiated with 5 Gy X-rays or 2.5 Gy protons with or without 0.5 µM of Olaparib. The mediumwas replaced 22 h after irradiation, and 1 µM of ABT-263 was added. (a,b) 3 days post-irradiation,mRNA level of genes implicated in SASP were determined. Fold changes, calculated as $2^{-\Delta\Delta ct}$, are presented after X-rays (a) and protons (b) radiation. (c) Relative secretion of IL6 six days after X-rays. At least three independent experiments were performed, and data are presented as mean ± 1 SD. Unpaired *t*-tests were performed (*: $p < 0.05$; **: $p < 0.01$) for CTL vs. ABT, CTL vs. Ola and Ola vs. Ola + ABT.

Discussion

In this work, we proposed taking advantage of the senolytic drug, ABT-263, to enhance the effects of the combination of radiation (X-rays or protons) and a PARPi, Olaparib.

Even though the use of Olaparib is currently recommended for cancer patients with germline BRCA mutations, PARPi have been demonstrated to be efficient as sensitizing agents in cell lines with BRCA1/2 wild-type tumors. In this work, HR proficient cell lines have been studied, namely A549, HCT-116 and KP4 cells. These three cell lines are TP53 wild-type and KRAS-mutated cancer cells. A549 and HCT-116 cells are CDKN2A deficient. Previous works from our team and others showed that both A549 and HCT-116cells can be radiosensitized by Olaparib and undergo senescence after irradiation. On the other hand, KP4 cells are not known to display a stress-induced senescent response. The increase in senescence following irradiation and treatment with PARPi has already been reported [22,24,43]. Recently, Fleury et al. also demonstrated that ovarian and breast cancer cells treated with Olaparib acquired a senescent-like phenotype [21]. The mechanisms of action regarding the induction of senescence following the inhibition of PARP are not well known. However, it was demonstrated that the induction of p21 is necessary for senescence to occur following treatment with PARPi [21]. Several high-grade serous epithelial ovarian cancer cells (HGSOC) were treated with PARPi, namely Olaparib, Talazoparib and Niraparib. These molecules induced a senescence-like phenotype in these cells, meaning the findings are likely not limited to Olaparib [21]. Senescence has often been seen as a double-edged sword in cancer [29,33]. For this reason, we proposed to eliminate these senescent cells using senolytic drugs such as ABT-263, an inhibitor of Bcl2, Bcl-x_L and Bcl-w in order to enhance treatment efficacy.

We showed that X-ray irradiation induced a cell line-dependent senescence. In addition, Olaparib further enhanced the X-ray-induced senescence phenotype. Moreover, our results demonstrated that the use of ABT-263 was able to counteract the senescence-promoting effect of Olaparib after irradiation. The literature on proton irradiation induced senescence is limited. However, we confirmed here our previous results and we showed that proton irradiation, at a LET of 25 keV/µm, induced senescence [19]. The induction of senescence by protons was also recently observed by Schniewind et al. [20]. These authors exposed glioblastoma, prostate and head-and-neck cancer cells to 3.7 keV/µm protons and photons. They observed that 4 Gy irradiation led to an increased SA-β-Gal activity for both types of radiations. For prostate cancer and glioblastoma cells, the induction was less pronounced after proton irradiation compared to photon irradiation. It would be interesting to study whether the radiation quality (using particles of various LETs) could influence the induction of senescence. In this work, as for photons, the combination with Olaparib enhanced the proton-induced senescent phenotype and the addition of ABT-263 prevented this effect.

p21 (CDKN1A) is an inhibitor of cyclin-dependent-kinases and its induction by p53 leads to cell cycle arrest in G1 due to the inhibition of CDK4 and CDK6, while it also prevents G2/M transition initiated by CDK1-cyclinB complex. It is already known that the induction of senescence by PARPi and radiation is mediated by p21 (CDKN1A) [21]. Our results showed that the mRNA expression of CDKN1A was increased following combined treatments (PARPi and radiation), while the use of ABT-263 decreased the mRNA expression of CDKN1A. Our results also indicate that the effect of this senolytic drug depends on the ability of radiation and PARPi to induce senescence. Indeed, the effect of ABT-263 was lower in KP4 cells, as the percentage of SA-β-Gal positive cells only reached 10% following radiation and PARP inhibition. This is also confirmed by the lack of cells in between colonies (data not shown) that were observed for A549 cells (Figure 1a). The lower induction of senescence could be explained by the fact that the Chk2-p53-p21 pathway may not have been activated since we did not observe a significant increase in mRNA expression of CDKN1A following radiation and PARP inhibition in KP4 cells. However, the induction of p21 is a dynamic process that can determine cell fate [44]. In this later work, the authors followed, at a single cell level, the induction of p21 in A549 and HCT-116 cells before, during and days after (up to 96 h) drug treatment. They highlighted three different patterns: (i) cells exhibiting early and transient acute p21 response (level back to control within 36 h) were found to proliferate, (ii) cells exhibiting an early acute high level of p21 maintained over time became senescent, (iii) cells exhibiting a delayed but increasing (from 24 h) induction of p21 over time became senescent. The first two patterns were found in G1 cells while the last was associated with S/G2 cells. Hsu and colleagues showed that ATM signaling is required for high levels of drug-induced p21 expression in G1. Regarding the unexpectedly lower levels of p21 expression in S/G2, they evidenced a p21 expression repression mediated by Chk1 signaling and proteasomal degradation [44]. The low level of CDKN1A mRNA in KP4 cells 72 h after treatment could indicate an early and transient induction of p21 that is associated with proliferation and not to senescence as proposed in Hsu's work.

The induction of senescence after radiation (with or without Olaparib) was also observed in TP53-mutated MDA-MB-231 cells (Supplemental Figure S6a). As for A549 cells, Olaparib promoted SA-β-Gal activity after irradiation. Although ABT-263 led to a strong reduction of SA-β-Gal activity, no effect of Olaparib or of ABT-263 was detected on the induction of CDKN1A mRNA level at 3 days (Supplemental Figure S6b). At day 6 (Supplemental Figure S6c), the mRNA level of CDKN1A was higher for cells irradiated in the presence of Olaparib, but again, the effect of ABT-263 was negligible. In TP53 mutant cells, Chk2 is responsible for p21 induction and senescence [45]. Despite a possible correlation between the induction of cell death (Annexin V positive cells) and the reduction of SA-β-Gal positive cells proportion with the addition of ABT-263 when considering A549, HCT-116 and KP4 cells, no remarkable difference in cell death quantification was

observed in MDA-MB-231 cells with the addition of ABT-263 (Supplemental Figure S6d). Still, the implication of p21 in apoptosis has been evidenced by others and notably for A549 and HCT-116 cells [46,47]. These authors showed that downregulation of p21 using p21 antisense oligodeoxynucleotide led to increased apoptosis. Here, we observed, at 72 h, a strong correlation between the increase in Annexin V positive cells and the reduction of CDKN1A mRNA level when ABT-263 was added (Supplemental Figure S7). The low decrease in CDKN1A mRNA level of MDA-MB-231 cells with the addition of ABT-263 could thus explain the lack of Annexin V positive cells in comparison to A549 cells.

We demonstrated that further sensitization by ABT-263 is correlated with the ability ofthe treatment to induce senescence. As presented above, the use of ABT-263 alone did not induce immediate nor clonogenic cell death, indicating that this drug specifically targets senescent cells. While A549, HCT-116 and KP4 cells were sensitized by Olaparib after X-ray or proton irradiation, the combination with ABT-263 led to a synergic increased cell death only for A549 cells. For KP4 cells, with very limited radio-induced senescence, the combination of ABT-263 with Olaparib did not reduce survival fraction. For MDA-MB-231 cells, the radiosensitizing effect of Olaparib was limited while ABT-263 significantly affected cell survival (Supplemental Figure S6e). This could be due to the lack of p53 in these cells. Nonetheless, as for A549 cells, the combination of ABT-263 with Olaparib led to a synergistic effect upon 5 Gy X-ray irradiation (CDI = 0.87). This synergistic effect is in agreement with SA-β-Gal activity results. Furthermore, a correlation was observed between the reduction in SA-β-Gal activity with the addition of ABT-263 and the calculated CDI as shown in Supplemental Figure S8.

The release of SASP factors is able to modulate several aspects, including prolifera- tion, metastasis, treatment resistance and immunosuppression. SASP factors can induce epithelial–mesenchymal transition (EMT) as reported by Coppé et al. [48]. It was also evidenced that IL6 and IL8 can promote proliferation through the activation of STAT3 [49,50]. The activation of the latest STAT3 regulates c-myc, c-Fos, cyclin D1 and mammalian target of rapamycin complex 1 (mTORC1) expression. Moreover, these pro-tumorigenic SASP factors have also been implicated in the regulation of invasive properties of cancer cells. Cancer cells incubated with a conditioned medium of senescent cells demonstrated a higher capacity to invade the basement membrane [48]. IL6 and IL8 blocking antibodies reduced the invasion capability of the cells exposed to these conditioned media. Our results demonstrated that irradiation (X-rays and protons), and notably in the presence of Olaparib, led to increased mRNA levels of SASP genes in A549 cells (Figure 5a,b, respectively) and MDA-MB-231 cells (Supplemental Figure S6f). This was especially the case for IL6 and IL8 mRNAs. The incubation in the presence of ABT-263 decreased IL6 and IL8 mRNA expression. The decrease in IL6 mRNA expression was confirmed at the protein level for A549 cells. Overall, these results demonstrate that ABT-263 can successfully decrease the

expression of SASP factors and could ultimately prevent its pro-tumorigenic role.

Conclusions

Our results constitute a first step to further preclinical investigation in order to combine PARP inhibitors to proton or photon irradiation and inhibitors of the Bcl-2 or Bcl-xL family. Clinical limitations of this strategy are risks for ABT-263 to induce side effects such as thrombocytopenia and neutropenia [51]. Nonetheless, a study has mentioned the safety of ABT199 (Venetoclax), a Bcl-2 inhibitor [52]. Furthermore, the proteolysis-targeting chimera (PROTAC) technology was recently used to decrease the platelet toxicity of ABT-263 [53].

We worked with BRCA1/2 will type cells and demonstrated that both TP53 wild-type and mutant cell lines could be targeted by this strategy as long as senescence induction is observed. More work and more cell lines are needed to further characterize the effect ofOlaparib and ABT-263 on radio-induced senescence.

The concentration of Olaparib (0.5 µM) and ABT-263 (1 µM) chosen aimed at limited toxicities in un-irradiated cells even though higher doses should lead to stronger effects.

Furthermore, studying the establishment of senescence, in the presence or not of Olaparib, could point out a better schedule for the combination. For that purpose, single cell analysis using live cell imaging could be of particular interest. In our case, the cells were incubated 24 h with Olaparib before it was replaced by ABT-263. A longer incubation time and even a co-incubation could be of interest.

This study could be extended to other senolytics. Indeed, in the context of senescence, it was demonstrated that several anti-apoptotic pathways are upregulated. A senolytic panel composed of dasatinib, querceting, fisetin and piperlongumine (PPL) has already been used in combination with Olaparib in HGSOC cells. The authors demonstrated that synergy occurred between Olaparib and the different senolytics that were tested [21]. Interestingly, ABT-263, A-1155463 and PPL were also tested in combination with X-rays or Olaparib in LNCaP and PC-3 cells. Combining ABT-263 or A-1155463 to Olaparib or X-rays increased cell death in LNCaP and PC-3 cells. However, it was not the case for PPL supporting the fact that the upregulation of anti-apoptotic genes following senescence depends on the inducer and on the cell type [23].

To conclude, the use of such senescence-targeting inhibitors could enhance the effects of combining PARP inhibitors to conventional or proton radiotherapy and prevent adverse effects associated with senescence induction.

Supplementary Materials: The following supporting information can be downloaded at: https:// www.mdpi.com/article/10.3390/cancers14061460/s1, Table S1: Primers sequences. Figure S1: ABT- 263 hampers the senescence-promoting effect of Olaparib after X-ray and proton irradiation in A549 cells. Figure S2: The effect of ABT-263 is reduced for cell lines with limited radio-induced senescence. Figure S3: ABT-263 induces cell death in cell lines displaying radiation-induced senescence. Table S2: Survival fraction of A549 cells exposed to 0.5 µM Olaparib and/or 1 µM ABT-263 without irradiation. Figure S4: ABT-263 reverts the SASP promoted by Olaparib after X-ray and proton irradiation in A549 cells. Figure S5: X-rays, Olaparib and ABT-263 effect on SASP genes in HCT-116 and KP4 cells. Figure S6: Induction of senescence in MDA-MB-231: effect of Olaparib and ABT-263. Figure S7: Correlation between increased Annexin V and CDKN1A fold change reduction. Figure S8: Correlation between CDI and reduction of SA-β-Gal by ABT-263. Reference [54] is cited in the supplementary materials.

Author Contributions: C.H. and A.-C.W., conceptualization and data analysis; M.F. and C.D., data curation; B.L.C. and C.M., conceptualization and data analysis; A.-C.W. and S.L., proton irradiation expertise; C.H., A.-C.W. and C.M., writing of original draft; C.H., M.F., C.D., B.L.C., S.L., C.M. and A.-C.W., final writing revision. All authors have read and agreed to the published version of the manuscript.

Funding: This research was supported by the Walloon Region in the framework of the PIT program Prother-wal under grant agreement No. 7289. C. Huart is recipient of a Fonds National de la Recherche Scientifique (F.R.S.-FNRS, Belgium) fellowship. The X-ray irradiator was acquired with the support of the University of Namur, Oncobeth and Solidarité-Espoir (CHU-UCL Namur, Sainte-Elisabeth).

Institutional Review Board Statement: Not applicable.

Informed Consent Statement: Not applicable.

Data Availability Statement: The data presented in this study are available upon request to the authors.

Acknowledgments: The authors acknowledge T. Tabarrant for technical support. The authors are thankful to the technological platforms SIAM and Morph-Im (UNamur).

Conflicts of Interest: The authors declare no conflict of interest.

References

1. Delaney, G.; Jacob, S.; Featherstone, C.; Barton, M. The role of radiotherapy in cancer treatment. *Cancer* 2005, *104*, 1129–1137. [CrossRef] [PubMed]
2. Baumann, M.; Krause, M.; Overgaard, J.; Debus, J.; Bentzen, S.M.; Daartz, J.; Richter, C.; Zips, D.; Bortfeld, T. Radiation oncology in the era of precision medicine. *Nat. Rev.* 2016, *16*, 234–249. [CrossRef] [PubMed]
3. Chargari, C.; Magne, N.; Guy, J.B.; Rancoule, C.; Levy, A.; Goodman, K.A.; Deutsch, E. Optimize and refine therapeutic index in radiation therapy: Overview of a century. *Cancer Treat. Rev.* 2016, *45*, 58–67. [CrossRef] [PubMed]
4. Thariat, J.; Hannoun-Levi, J.M.; Sun Myint, A.; Vuong, T.; Gerard, J.P. Past, present, and future of radiotherapy for the benefit of patients. *Nat. Rev. Clin. Oncol.* 2013, *10*, 52–60. [CrossRef] [PubMed]
5. Durante, M.; Loeffler, J.S. Charged particles in radiation oncology. *Nat. Rev. Clin. Oncol.* 2010, *7*, 37–43. [CrossRef] [PubMed]
6. Loeffler, J.S.; Durante, M. Charged particle therapy—Optimization, challenges and future directions. *Nat. Rev. Clin. Oncol.* 2013, *10*, 411–424. [CrossRef] [PubMed]
7. Konings, K.; Vandevoorde, C.; Baselet, B.; Baatout, S.; Moreels, M. Combination Therapy With Charged Particles and Molecular Targeting: A Promising Avenue to Overcome Radioresistance. *Front. Oncol.* 2020, *10*, 128. [CrossRef] [PubMed]
8. Marx, S.; Van Gysel, M.; Breuer, A.; Dal Maso, T.; Michiels, C.; Wouters, J.; Le Calve, B. Potentialization of anticancer agents by identification of new chemosensitizers active under hypoxia. *Biochem. Pharmacol.* 2019, *162*, 224–236. [CrossRef] [PubMed]
9. Bryant, H.E.; Schultz, N.; Thomas, H.D.; Parker, K.M.; Flower, D.; Lopez, E.; Kyle, S.; Meuth, M.; Curtin, N.J.; Helleday, T. Specific killing of BRCA2-deficient tumours with inhibitors of poly(ADP-ribose) polymerase. *Nature* 2005, *434*, 913–917. [CrossRef] [PubMed]
10. Lesueur, P.; Chevalier, F.; Austry, J.B.; Waissi, W.; Burckel, H.; Noel, G.; Habrand, J.L.; Saintigny, Y.; Joly, F. Poly-(ADP-ribose)- polymerase inhibitors as radiosensitizers: A systematic review of pre-clinical and clinical human studies. *Oncotarget* 2017, *8*, 69105–69124. [CrossRef]
11. Lord, C.J.; Ashworth, A. PARP inhibitors: Synthetic lethality in the clinic. *Science* 2017, *355*, 1152–1158. [CrossRef] [PubMed]
12. Golan, T.; Hammel, P.; Reni, M.; Van Cutsem, E.; Macarulla, T.; Hall, M.J.; Park, J.O.; Hochhauser, D.; Arnold, D.; Oh, D.Y.; et al. Maintenance Olaparib for Germline BRCA-Mutated Metastatic Pancreatic Cancer. *N. Engl. J. Med.* 2019, *381*, 317–327. [PubMed]
13. Robson, M.E.; Tung, N.; Conte, P.; Im, S.A.; Senkus, E.; Xu, B.; Masuda, N.; Delaloge, S.; Li, W.; Armstrong, A.; et al. OlympiAD final overall survival and tolerability results: Olaparib versus chemotherapy treatment of physician's choice in patients with a germline BRCA mutation and HER2-negative metastatic breast cancer. *Ann.*

Oncol. 2019, *30*, 558–566. [CrossRef] [PubMed]
14. Hussain, M.; Mateo, J.; Fizazi, K.; Saad, F.; Shore, N.; Sandhu, S.; Chi, K.N.; Sartor, O.; Agarwal, N.; Olmos, D.; et al. Survival with Olaparib in Metastatic Castration-Resistant Prostate Cancer. *N. Engl. J. Med.* 2020, *383*, 2345–2357. [CrossRef] [PubMed]
15. Arora, S.; Balasubramaniam, S.; Zhang, H.; Berman, T.; Narayan, P.; Suzman, D.; Bloomquist, E.; Tang, S.; Gong, Y.; Sridhara, R.; et al. FDA Approval Summary: Olaparib Monotherapy or in Combination with Bevacizumab for the Maintenance Treatment of Patients with Advanced Ovarian Cancer. *Oncologist* 2021, *26*, e164–e172. [CrossRef] [PubMed]
16. Miura, K.; Sakata, K.; Someya, M.; Matsumoto, Y.; Matsumoto, H.; Takahashi, A.; Hareyama, M. The combination of olaparib and camptothecin for effective radiosensitization. *Radiat. Oncol.* 2012, *7*, 62. [CrossRef] [PubMed]
17. Michels, J.; Vitale, I.; Senovilla, L.; Enot, D.P.; Garcia, P.; Lissa, D.; Olaussen, K.A.; Brenner, C.; Soria, J.C.; Castedo, M.; et al. Synergistic interaction between cisplatin and PARP inhibitors in non-small cell lung cancer. *Cell Cycle* 2013, *12*, 877–883. [CrossRef] [PubMed]
18. Bridges, K.A.; Toniatti, C.; Buser, C.A.; Liu, H.; Buchholz, T.A.; Meyn, R.E. Niraparib (MK-4827), a novel poly(ADP-Ribose) polymerase inhibitor, radiosensitizes human lung and breast cancer cells. *Oncotarget* 2014, *5*, 5076–5086. [CrossRef] [PubMed]
19. Wera, A.C.; Lobbens, A.; Stoyanov, M.; Lucas, S.; Michiels, C. Radiation-induced synthetic lethality: Combination of poly(ADP- ribose) polymerase and RAD51 inhibitors to sensitize cells to proton irradiation. *Cell Cycle* 2019, *18*, 1770–1783. [CrossRef] [PubMed]
20. Schniewind, I.; Hadiwikarta, W.W.; Grajek, J.; Poleszczuk, J.; Richter, S.; Peitzsch, M.; Muller, J.; Klusa, D.; Beyreuther, E.; Lock, S.; et al. Cellular plasticity upon proton irradiation determines tumor cell radiosensitivity. *Cell Rep.* 2022, *38*, 110422. [CrossRef] [PubMed]
21. Fleury, H.; Malaquin, N.; Tu, V.; Gilbert, S.; Martinez, A.; Olivier, M.A.; Sauriol, A.; Communal, L.; Leclerc-Desaulniers, K.; Carmona, E.; et al. Exploiting interconnected synthetic lethal interactions between PARP inhibition and cancer cell reversible senescence. *Nat. Commun.* 2019, *10*, 2556. [CrossRef] [PubMed]
22. Efimova, E.V.; Mauceri, H.J.; Golden, D.W.; Labay, E.; Bindokas, V.P.; Darga, T.E.; Chakraborty, C.; Barreto-Andrade, J.C.; Crawley, C.; Sutton, H.G.; et al. Poly(ADP-ribose) polymerase inhibitor induces accelerated senescence in irradiated breast cancer cells and tumors. *Cancer Res.* 2010, *70*, 6277–6282. [CrossRef] [PubMed]
23. Malaquin, N.; Vancayseele, A.; Gilbert, S.; Antenor-Habazac, L.; Olivier, M.A.; Ait Ali Brahem, Z.; Saad, F.; Delouya, G.; Rodier, F. DNA Damage- But Not Enzalutamide-Induced Senescence in Prostate Cancer Promotes Senolytic Bcl-xL Inhibitor Sensitivity. *Cells* 2020, *9*, 1593. [CrossRef] [PubMed]

24. Alotaibi, M.; Sharma, K.; Saleh, T.; Povirk, L.F.; Hendrickson, E.A.; Gewirtz, D.A. Radiosensitization by PARP Inhibition in DNA Repair Proficient and Deficient Tumor Cells: Proliferative Recovery in Senescent Cells. *Radiat. Res.* 2016, *185*, 229–245. [CrossRef] [PubMed]
25. Hernandez-Segura, A.; Nehme, J.; Demaria, M. Hallmarks of Cellular Senescence. *Trends Cell Biol.* 2018, *28*, 436–453. [CrossRef] [PubMed]
26. Zheng, Y.; Luo, X.; Zhu, J.; Zhang, X.; Zhu, Y.; Cheng, H.; Xia, Z.; Su, N.; Zhang, N.; Zhou, J. Mitochondrial DNA 4977 bp deletion is a common phenomenon in hair and increases with age. *Bosn. J. Basic Med. Sci.* 2012, *12*, 187–192. [CrossRef] [PubMed]
27. Freund, A.; Orjalo, A.V.; Desprez, P.Y.; Campisi, J. Inflammatory networks during cellular senescence: Causes and consequences.
Trends Mol. Med. 2010, *16*, 238–246. [CrossRef] [PubMed]
28. Soto-Gamez, A.; Quax, W.J.; Demaria, M. Regulation of Survival Networks in Senescent Cells: From Mechanisms to Interventions.
J. Mol. Biol. 2019, *431*, 2629–2643. [CrossRef] [PubMed]
29. Wang, B.; Kohli, J.; Demaria, M. Senescent Cells in Cancer Therapy: Friends or Foes? *Trends Cancer* 2020, *6*, 838–857. [CrossRef] [PubMed]
30. Fisher, D.T.; Appenheimer, M.M.; Evans, S.S. The two faces of IL-6 in the tumor microenvironment. *Semin. Immunol.* 2014, *26*, 38–47. [CrossRef]
31. Krtolica, A.; Parrinello, S.; Lockett, S.; Desprez, P.Y.; Campisi, J. Senescent fibroblasts promote epithelial cell growth and tumorigenesis: A link between cancer and aging. *Proc. Natl. Acad. Sci. USA* 2001, *98*, 12072–12077. [CrossRef] [PubMed]
32. Waugh, D.J.; Wilson, C. The interleukin-8 pathway in cancer. *Clin. Cancer Res.* 2008, *14*, 6735–6741. [CrossRef] [PubMed]
33. Coppe, J.P.; Desprez, P.Y.; Krtolica, A.; Campisi, J. The senescence-associated secretory phenotype: The dark side of tumor suppression. *Annu. Rev. Pathol.* 2010, *5*, 99–118. [CrossRef] [PubMed]
34. Saleh, T.; Tyutyunyk-Massey, L.; Gewirtz, D.A. Tumor Cell Escape from Therapy-Induced Senescence as a Model of Disease Recurrence after Dormancy. *Cancer Res.* 2019, *79*, 1044–1046. [CrossRef] [PubMed]
35. Zhu, Y.; Tchkonia, T.; Pirtskhalava, T.; Gower, A.C.; Ding, H.; Giorgadze, N.; Palmer, A.K.; Ikeno, Y.; Hubbard, G.B.; Lenburg, M.; et al. The Achilles' heel of senescent cells: From transcriptome to senolytic drugs. *Aging Cell* 2015, *14*, 644–658. [CrossRef]
36. Dolgin, E. Send in the senolytics. *Nat. Biotechnol.* 2020, *38*, 1371–1377. [CrossRef] [PubMed]
37. Zhu, Y.; Tchkonia, T.; Fuhrmann-Stroissnigg, H.; Dai, H.M.; Ling, Y.Y.; Stout, M.B.; Pirtskhalava, T.; Giorgadze, N.; Johnson, K.O.; Giles, C.B.; et al. Identification of a novel senolytic agent, navitoclax, targeting the Bcl-2 family of anti-apoptotic factors. *Aging Cell* 2016, *15*, 428–435. [CrossRef] [PubMed]
38. Wéra, A.C.; Riquier, H.; Heuskin, A.C.; Michiels, C.; Lucas, S. In vitro irradiation

station for broad beam radiobiological experiments. *Nucl. Instrum. Methods Phys. Res. Sect. B Beam Interact. Mater. At.* 2011, *269*, 3120–3124. [CrossRef]
39. Wéra, A.-C.; Heuskin, A.-C.; Riquier, H.; Michiels, C.; Lucas, S. Low-LET Proton Irradiation of A549 Non-small Cell Lung Adenocarcinoma Cells: Dose Response and RBE Determination. *Radiat. Res.* 2013, *179*, 273–281. [CrossRef]
40. Folkard, M.; Prise, K.M.; Vojnovic, B.; Newman, H.C.; Roper, M.J.; Michael, B.D. Inactivation of V79 cells by low-energy protons, deuterons and helium-3 ions. *Int. J. Radiat. Biol.* 1996, *69*, 729–738. [CrossRef] [PubMed]
41. Debacq-Chainiaux, F.; Erusalimsky, J.D.; Campisi, J.; Toussaint, O. Protocols to detect senescence-associated beta-galactosidase (SA-betagal) activity, a biomarker of senescent cells in culture and in vivo. *Nat. Protoc.* 2009, *4*, 1798–1806. [CrossRef] [PubMed]
42. Gonzalez-Gualda, E.; Baker, A.G.; Fruk, L.; Munoz-Espin, D. A guide to assessing cellular senescence in vitro and in vivo. *FEBS J.* 2021, *288*, 56–80. [CrossRef] [PubMed]
43. Gewirtz, D.A.; Alotaibi, M.; Yakovlev, V.A.; Povirk, L.F. Tumor Cell Recovery from Senescence Induced by Radiation with PARP Inhibition. *Radiat. Res.* 2016, *186*, 327–332. [CrossRef] [PubMed]
44. Hsu, C.H.; Altschuler, S.J.; Wu, L.F. Patterns of Early p21 Dynamics Determine Proliferation-Senescence Cell Fate after Chemother- apy. *Cell* 2019, *178*, 361–373.e312. [CrossRef]
45. Aliouat-Denis, C.M.; Dendouga, N.; Van den Wyngaert, I.; Goehlmann, H.; Steller, U.; van de Weyer, I.; Van Slycken, N.; Andries, L.; Kass, S.; Luyten, W.; et al. p53-independent regulation of p21Waf1/Cip1 expression and senescence by Chk2. *Mol. Cancer Res.* 2005, *3*, 627–634. [CrossRef] [PubMed]
46. Sak, A.; Wurm, R.; Elo, B.; Grehl, S.; Pottgen, C.; Stuben, G.; Sinn, B.; Wolf, G.; Budach, V.; Stuschke, M. Increased radiation- induced apoptosis and altered cell cycle progression of human lung cancer cell lines by antisense oligodeoxynucleotides targeting p53 and p21(WAF1/CIP1). *Cancer Gene Ther.* 2003, *10*, 926–934. [CrossRef] [PubMed]
47. Tian, H.; Wittmack, E.K.; Jorgensen, T.J. p21WAF1/CIP1 antisense therapy radiosensitizes human colon cancer by converting growth arrest to apoptosis. *Cancer Res.* 2000, *60*, 679–684.
48. Coppe, J.P.; Patil, C.K.; Rodier, F.; Sun, Y.; Munoz, D.P.; Goldstein, J.; Nelson, P.S.; Desprez, P.Y.; Campisi, J. Senescence-associated secretory phenotypes reveal cell-nonautonomous functions of oncogenic RAS and the p53 tumor suppressor. *PLoS Biol.* 2008, *6*, 2853–2868. [CrossRef] [PubMed]
49. Kojima, H.; Inoue, T.; Kunimoto, H.; Nakajima, K. IL-6-STAT3 signaling and premature senescence. *Jak-Stat* 2013, *2*, e25763. [CrossRef]
50. Ortiz-Montero, P.; Londono-Vallejo, A.; Vernot, J.P. Senescence-associated IL-6 and

IL-8 cytokines induce a self- and cross- reinforced senescence/inflammatory milieu strengthening tumorigenic capabilities in the MCF-7 breast cancer cell line. *Cell Commun. Signal.* 2017, *15*, 17. [CrossRef] [PubMed]

51. Rudin, C.M.; Hann, C.L.; Garon, E.B.; Ribeiro de Oliveira, M.; Bonomi, P.D.; Camidge, D.R.; Chu, Q.; Giaccone, G.; Khaira, D.; Ramalingam, S.S.; et al. Phase II study of single-agent navitoclax (ABT-263) and biomarker correlates in patients with relapsed small cell lung cancer. *Clin. Cancer Res.* 2012, *18*, 3163–3169. [CrossRef] [PubMed]
52. Souers, A.J.; Leverson, J.D.; Boghaert, E.R.; Ackler, S.L.; Catron, N.D.; Chen, J.; Dayton, B.D.; Ding, H.; Enschede, S.H.; Fairbrother, W.J.; et al. ABT-199, a potent and selective BCL-2 inhibitor, achieves antitumor activity while sparing platelets. *Nat. Med.* 2013, *19*, 202–208. [CrossRef] [PubMed]
53. He, Y.; Zhang, X.; Chang, J.; Kim, H.N.; Zhang, P.; Wang, Y.; Khan, S.; Liu, X.; Lv, D.; Song, L.; et al. Using proteolysis-targeting chimera technology to reduce navitoclax platelet toxicity and improve its senolytic activity. *Nat. Commun.* 2020, *11*, 1996. [CrossRef] [PubMed]
54. Sermeus, A.; Rebucci, M.; Fransolet, M.; Flamant, L.; Desmet, D.; Delaive, E.; Arnould, T.; Michiels, C. Differential effect of hypoxia on etoposide-induced DNA damage response and p53 regulation in different cell types. *J. Cell. Physiol.* 2013, *228*, 2365–2376. [CrossRef] [PubMed]

Supplementary information

- **MDA-MB-231: Cell Culture, Olaparib and ABT-263**

MDA-MB-231 cells were sub-cultured in RPMI medium supplemented with 10% FBS. For the experiments, the medium was supplemented with 0.1% penicillin/streptomycin (Sigma). Olaparib was used at 0.5 μM final concentration. ABT-263 was used at 1 μM final concentration. Cells were incubated in the presence of the Olaparib for total duration of 24 h, while ABT-263 was added 24 h after irradiation and was left up to the end of the assay.

- **Western blot analysis**

Six days after irradiation, A549 cells were lysed as described in [1]. The western blot analyses were performed as described in [2]. Primary antibody against cleaved and full-length PARP (9548, mouse, Bioke) was used at 1/1000 and β-actin (A5441, mouse, Sigma) at 1/10,000. Anti-mouse secondary antibody, IRDye 680RD and IRDye 800CW Goat anti-mouse IgG (Li-Cor Biosiences) were used at 1/10,000. The membranes were scanned with the Amersham Typhoon. β-actin was used as loading control. Three independent experiments were performed and data are presented as mean ± 1 SD.

- **RNA extraction and RT-qPCR**

Table S1: Primer sequences

Primers	Forward sequence (5' - 3')	Reverse sequence (3' - 5')
CDKN1A	GTGGACCTGTCACTGTCTTG	GGCGTTTGGAGTGGTAGAAA
IL6	CCTGAACCTTCCAAAGATGGC	CACCAGGCAAGTCTCCTCATT
IL8	CTGGCCGTGGCTCTCTTG	GGGTGGAAAGGTTTGGAGTATG
IGFBP5	TGTGACCGCAAAGGATTCTACA	TCCCCGTCAACGTACTCCAT
CCL2	AAGTGTCCCAAAGAAGCTGT	TGGGTTGTGGAGTGAGTGTT
GAPDH	TGAAGGTCGGAGTCAACGG	GCAACAATATCCACTTTACCAGAGT

- **Combination of ABT-263 and Olaparib led to limited clonogenic cell death in un-irradiated cells.**

Table S2: Survival fraction of A549 cells exposed to 0.5 µM Olaparib and/or 1 µM ABT-263 without irradiation. Thesurvival fraction was evaluated related to unexposed cells. p values calculated with t-tests (unpaired with Welch'scorrection in case of significantly different variance).

	Survival fraction from CTL cells at 0 Gy		
	1 µM ABT-263	**0.5 µM Olaparib**	**Ola. + ABT-263**
A549 (XR)	0.88 ±0.24 (p=0.0675)	0.90 ±0.14 (p=0.0271*)	0.81 ±0.28 (p=0.0035**)
A549 (p)	0.96 ±0.28 (p=0.4844)	1.08 ±0.31 (p=0.1537)	1.02 ±0.30 (p=0.7629)
HCt-116	1.08 ±0.39 (p=0.4198)	0.77 ±0.29 (p=0.0192*)	0.80 ±0.25 (p=0.0153*)
KP4	1.08 ±0.32 (p=0.2467)	0.89 ±0.28 (p=0.0784)	0.92 ±0.32 (p=0.2516)

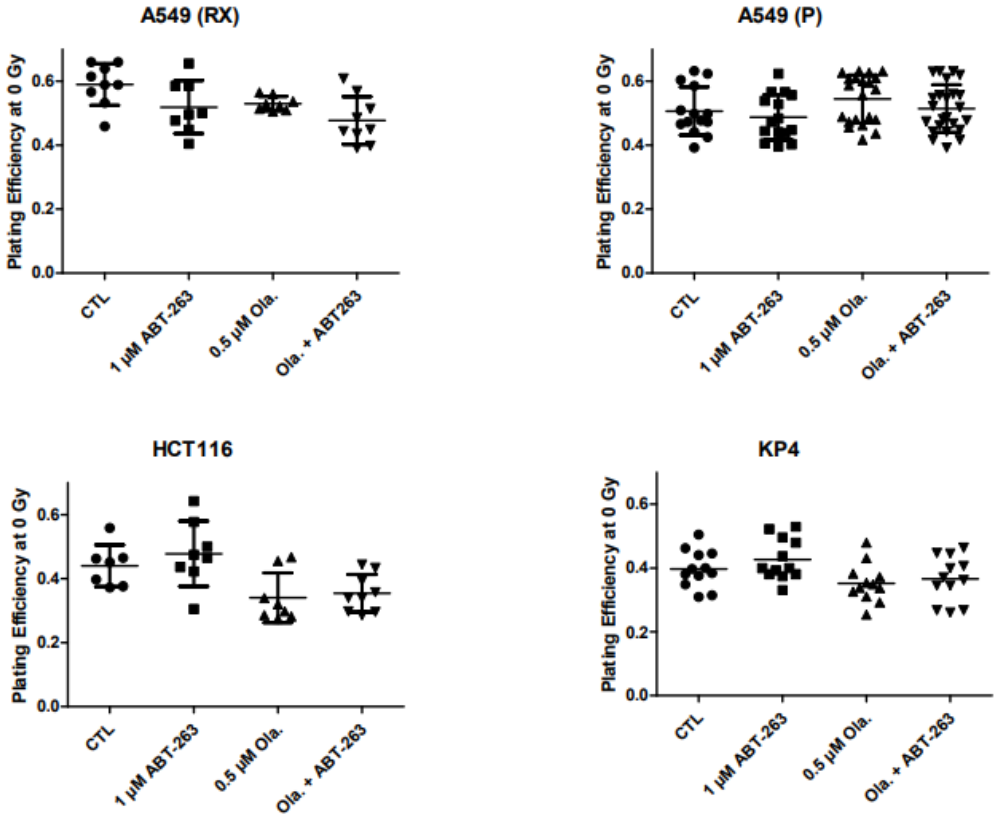

- **ABT-263 hampers the senescence inducing effect of Olaparib after X-ray and proton radiation in A549 cells**

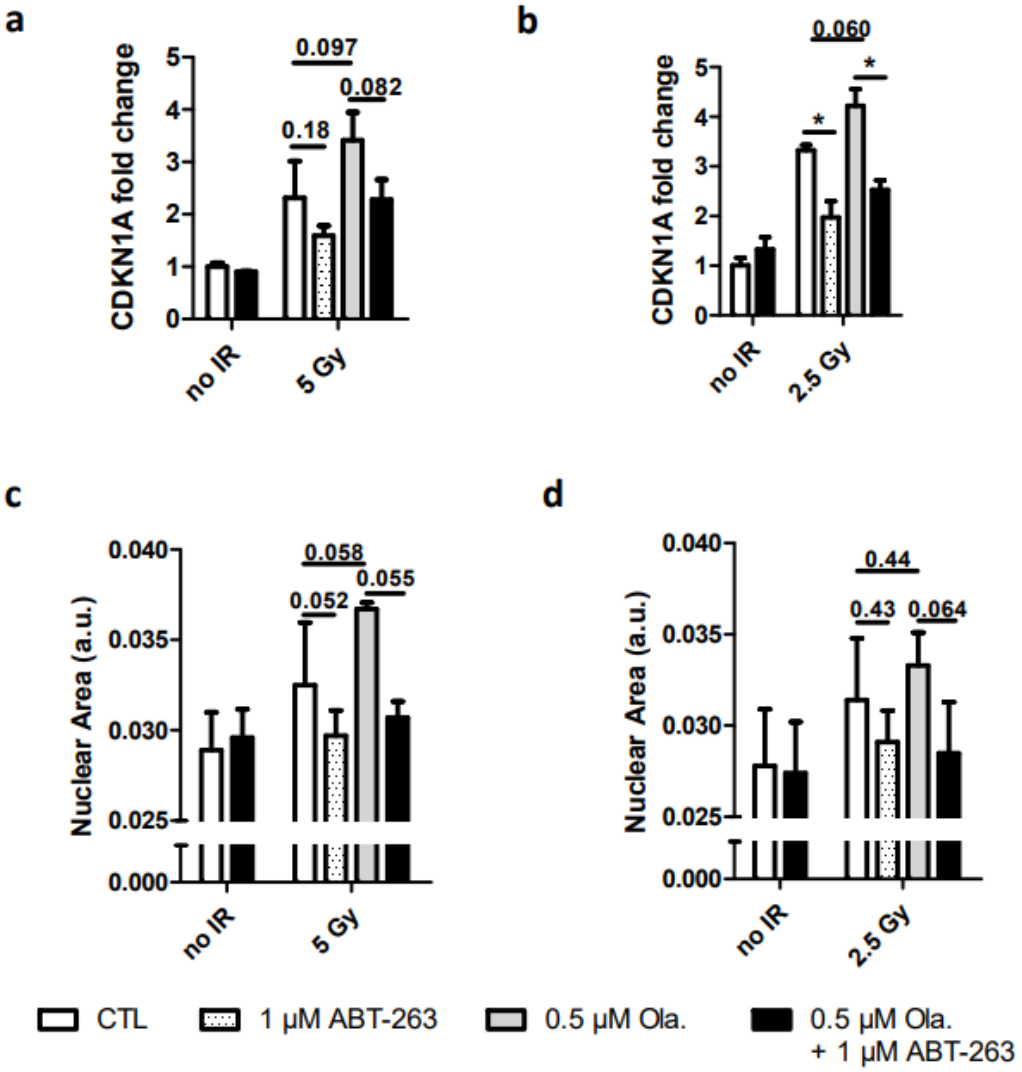

Figure S1: ABT-263 hampers the senescence promoting effect of Olaparib after X-ray and proton irradiation in A549 cells. A549 cells were irradiated with 5 Gy X-rays or 2.5 Gy protons with or without 0.5 µM of Olaparib. 22h after irradiation, the medium was replaced and 1 µM of ABT-263 was added. 6 days after irradiation, mRNA level of CDKN1A was evaluated (a: X-rays; b: protons). 6 days post-irradiation, cells were fixed and the nuclei stained with DAPI. The nucleus mean area of at least 100 cells was recorded (c: X-rays; d: protons). At least three independent experiments were performed and data are presented as mean ± 1 SD. Unpaired t-tests were performed (*: $p<0.05$; **: $p<0.01$; ***: $p<0.001$) CTL vs ABT, CTL vs Ola and Ola vs Ola+ABT.

- **The effect of ABT-263 is reduced for cell lines with limited radio-induced senescence**

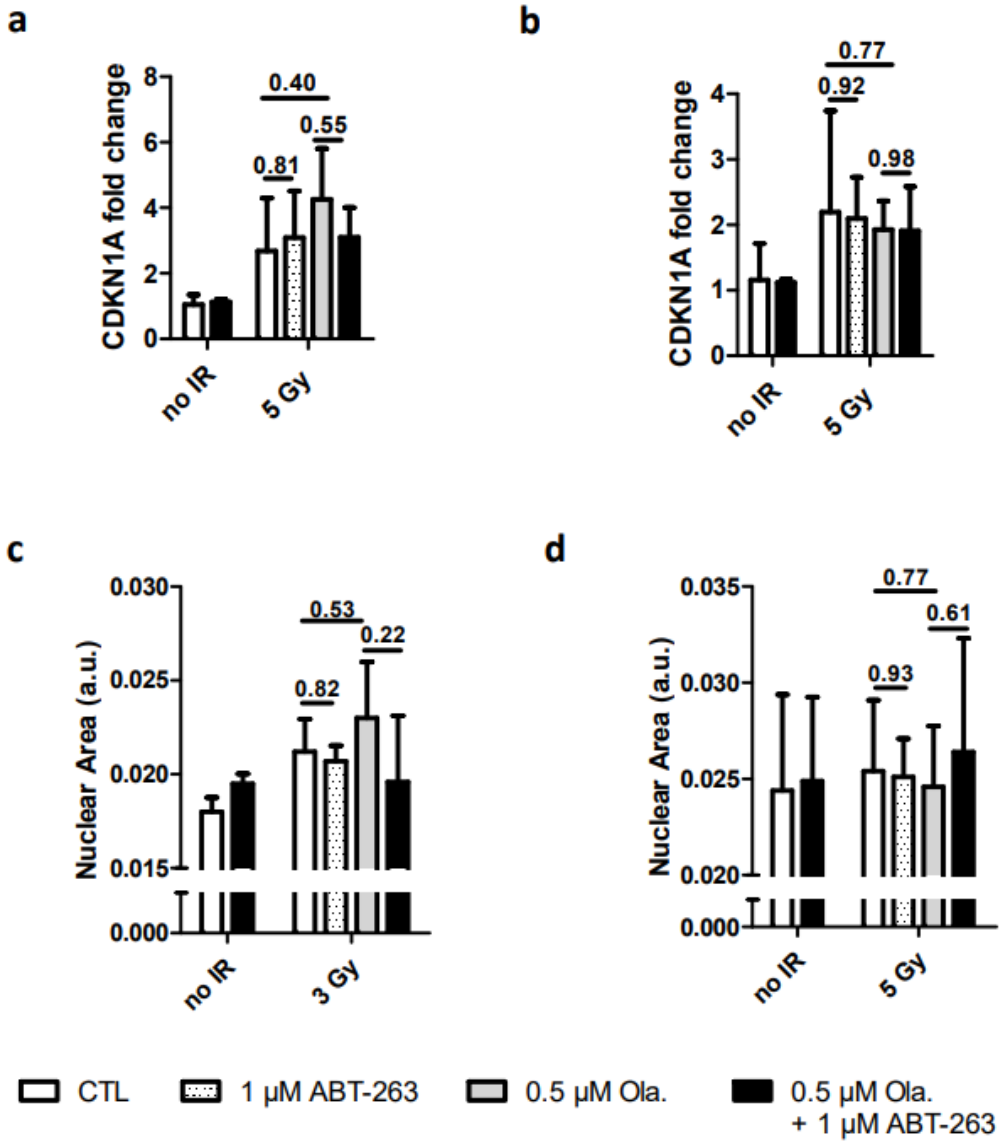

Figure S2: The effect of ABT-263 is reduced for cell lines with limited radio-induced senescence. HCT-116 and KP4 cells were irradiated with 5 Gy X-rays with or without 0.5 µM of Olaparib. 22h after irradiation, the medium was replaced and 1 µM of ABT-263 was added. 6 days after irradiation, mRNA level of CDKN1A was evaluated (a: HCT-116; b: KP4). 6 days post-irradiation, cells were fixed and the nuclei stained with DAPI. The nuclear mean area of at least 100 cells was recorded (c: HCT-116; d: KP4). At least three independent experiments were performed and data are presented as mean ± 1 SD. Unpaired t-tests were performed (*: p<0.05; **: p<0.01; ***: p<0.001) CTL vs ABT, CTL vs Ola and Ola vs Ola+ABT.

- **ABT-263 induces cell death in cell lines displaying radiation-induced senescence**

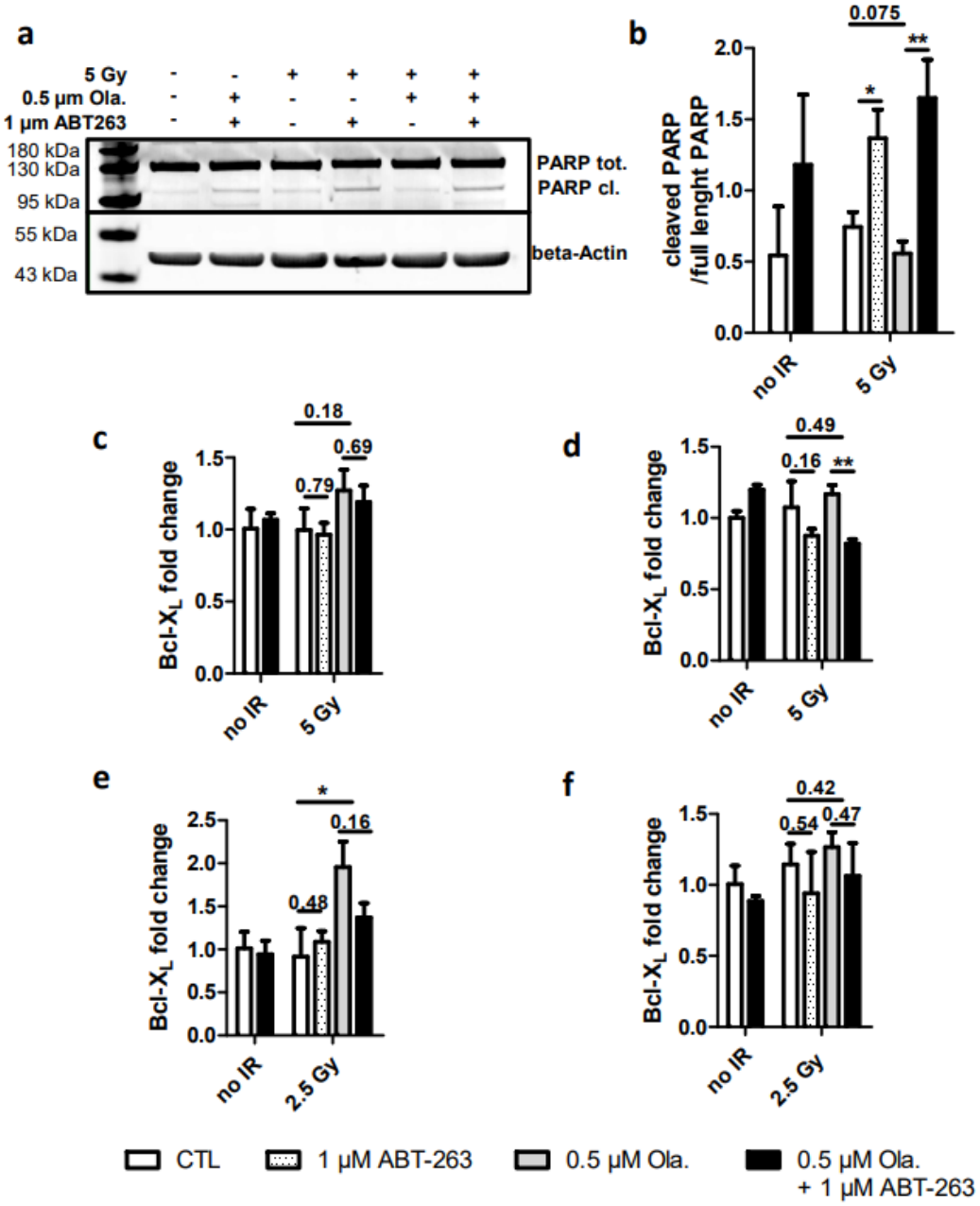

Figure S3: Induction of apoptosis by ABT-263 in A549 cells. A549 cells were irradiated with 5 Gy X-rays with or without 0.5 µM of Olaparib. 22h after irradiation, the medium was replaced and 1 µM of ABT-263 was added. a) Representative western blot results of total and cleaved forms of PARP 6 days after X-ray irradiation. b) Cleaved over full-length PARP ratio in A549 cells. At least three independent experiments were performed and data are presented as mean ± 1 SD. c-d) Bcl-XL mRNA level 3 (c) and 6 (d) days after X-ray irradiation. e-f) Bcl-XL mRNA level 3 (e) and 6 (f) days after proton irradiation At least three independent experiments were performed and data are presented as mean ± 1 SD. Unpaired t-tests were performed (*: p<0.05; **: p<0.01;***: p<0.001) for CTL vs ABT, CTL vs Ola and Ola vs Ola+ABT.

- **ABT-263 reverts the SASP induced by Olaparib after X-ray and proton irradiation in A549 cells**

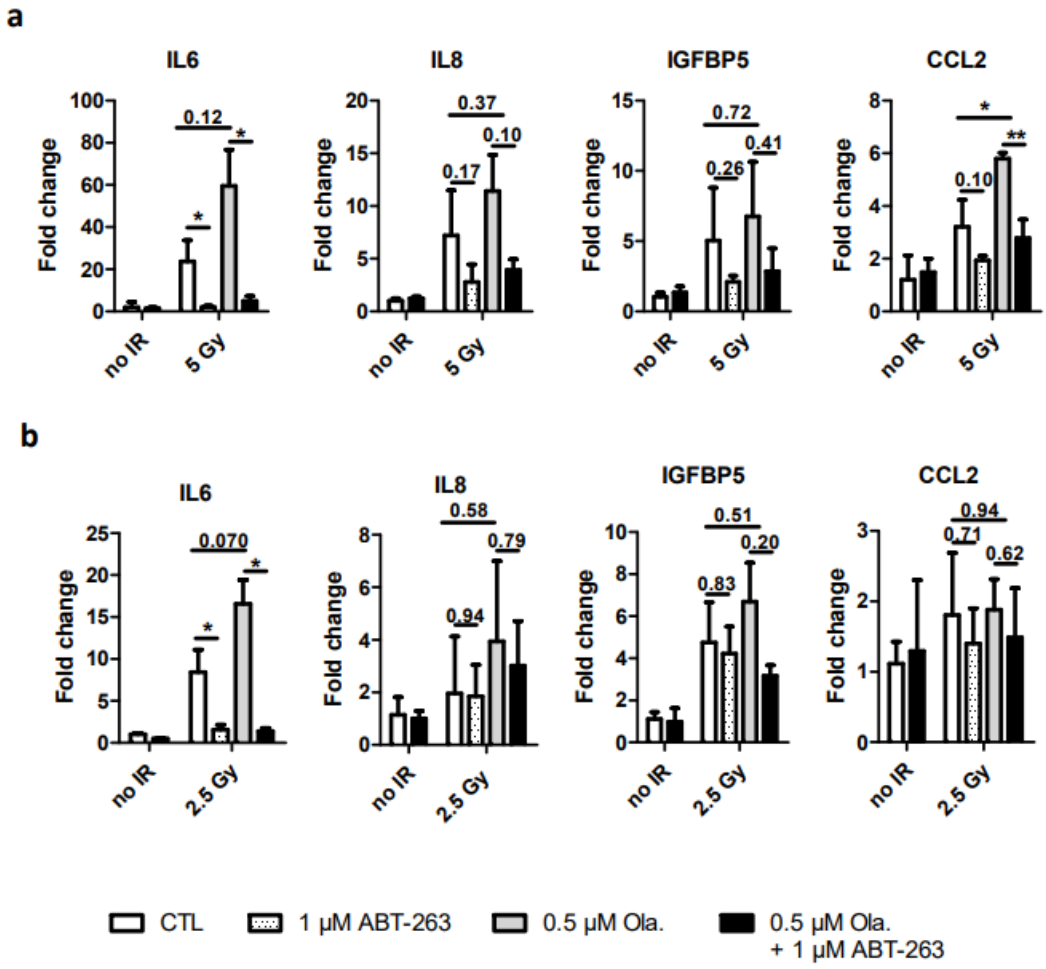

Figure S4: ABT-263 reverts the SASP promoted by Olaparib after X-ray and proton irradiation in A549 cells. A549 cells were irradiated with 5 Gy X-rays or 2.5 Gy protons with or without 0.5 µM of Olaparib. 22h after irradiation, the mediumwas replaced and 1 µM of ABT-263 was added. a, b) 6 days post-irradiation, mRNA levels of genes implicated in SASP were determined. Fold change, calculated as 2-ΔΔct, are presented after X-rays (a) and protons (b) radiation. At least three independent experiments were performed and data are presented as mean ± 1 SD. Unpaired t-tests were performed (*: p<0.05; **: p<0.01; ***: p<0.001) CTL vs ABT, CTL vs Ola and Ola vs Ola+ABT.

- **X-rays, Olaparib and ABT-263 effects on mRNA level of SASP genes in HCT-116 and KP4 cells**

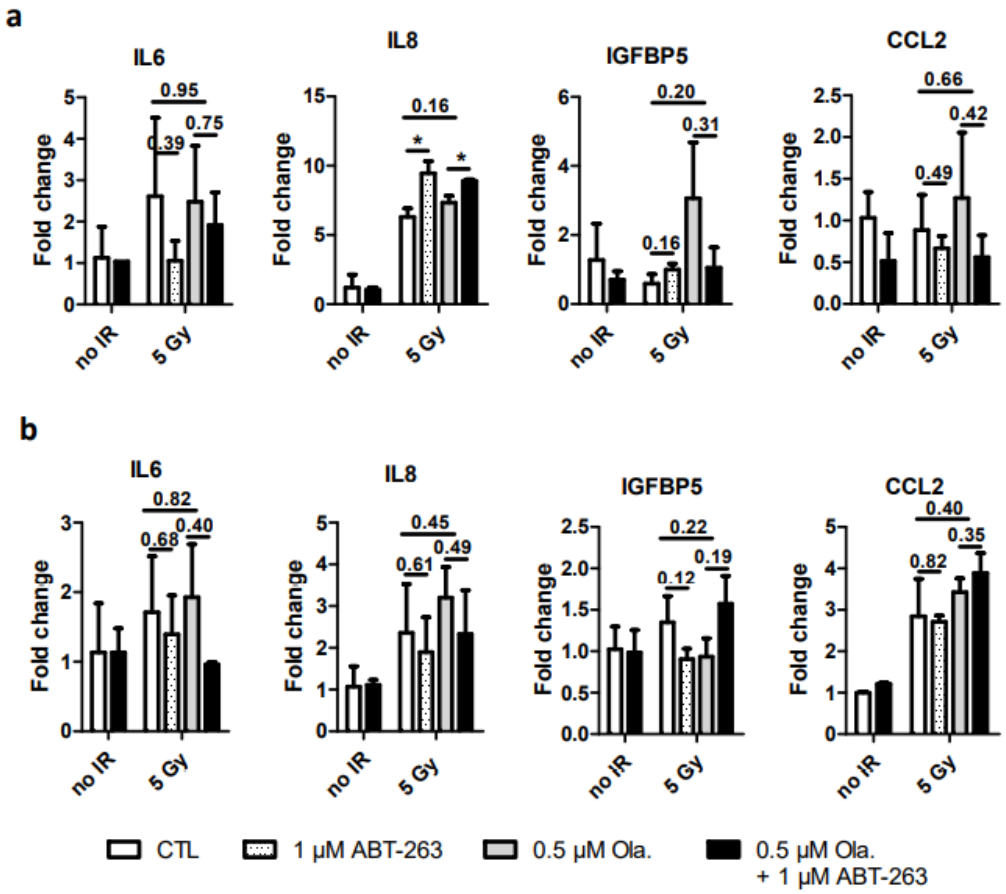

Figure S5: HCT-116 and KP4 cells were irradiated with 5 Gy X-rays with or without 0.5 µM of Olaparib. 22h after irradiation, the medium was replaced and 1 µM of ABT-263 was added. a, b) 6 days post-irradiation, mRNA levels of genes implicated in SASP were determined. Fold change, calculated as 2-ΔΔct, are presented for HCT-116 (a) and KP4 (b) cells. At least three independent experiments were performed and data are presented as mean ± 1 SD. Unpaired t-test were performed (*: p<0.05; **: p<0.01; ***: p<0.001) CTL vs ABT, CTL vs Ola and Ola vs Ola+ABT.

- **Induction of senescence in MDA-MB-231: Effects of Olaparib and ABT-263**

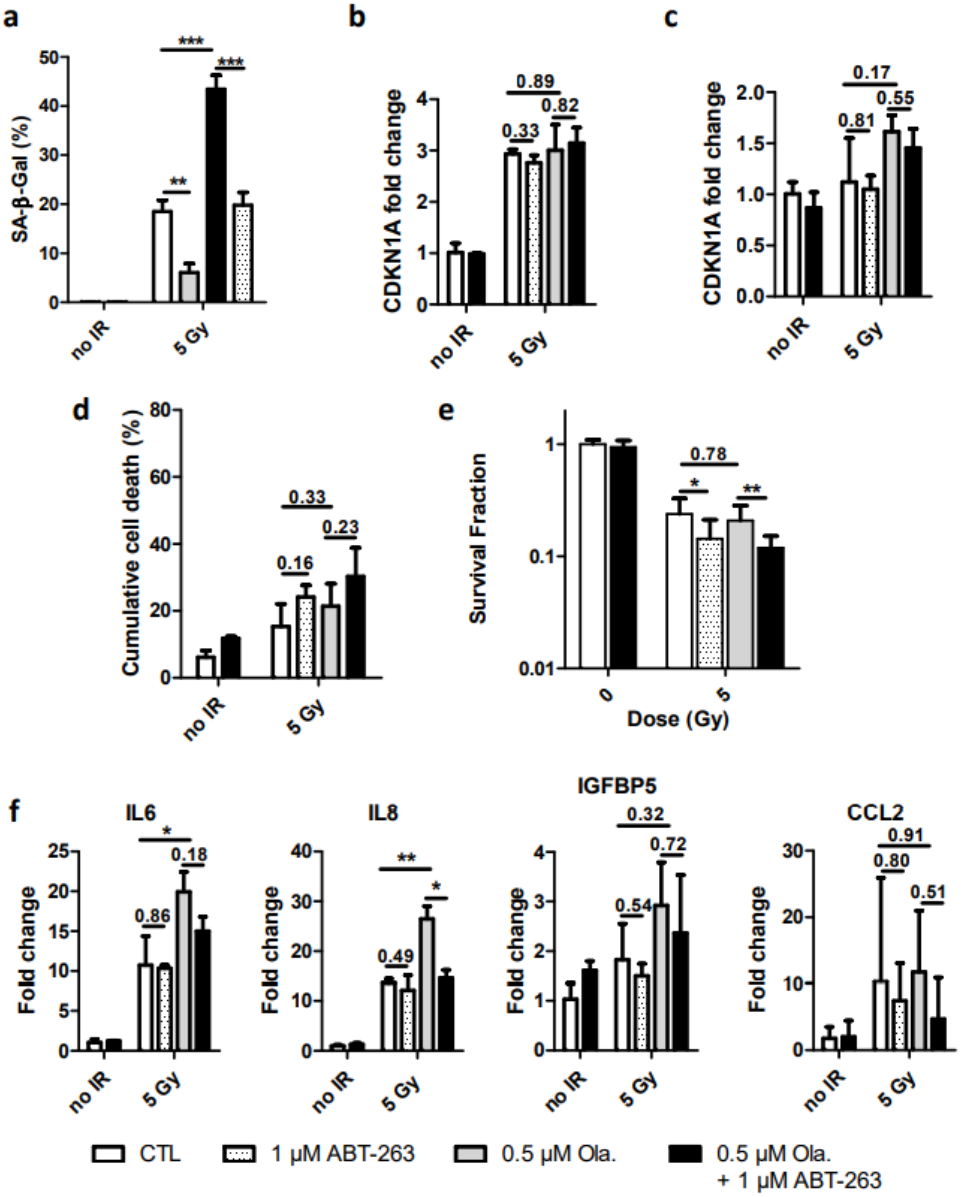

Figure S6: MDA-MB-231 cells were irradiated with 5 Gy X-rays with or without 0.5 µM of Olaparib. 22h after irradiation, the medium was replaced and 1 µM of ABT-263 was added. a) Quantification of SA-β-Gal positive cells 6 days after irradiation. b) CDKN1A mRNA level 3 days after irradiation. c) CDKN1A mRNA level 6 days after irradiation. d) Cumulative cell death 72 h after X-rays. e) Clonogenic survival fraction. F) mRNA levels of genes implicated in SASP were determined 3 days after irradiation. Fold change were calculated as 2-ΔΔct. At least three independent experiments were performed and data are presented as mean ± 1 SD. Unpaired t-tests were performed (*: p<0.05; **: p<0.01; ***: p<0.001) CTL vs ABT, CTL vs Ola and Ola vs Ola+ABT.

- **Correlation between increase in Annexin V and CDKN1A fold change reduction**

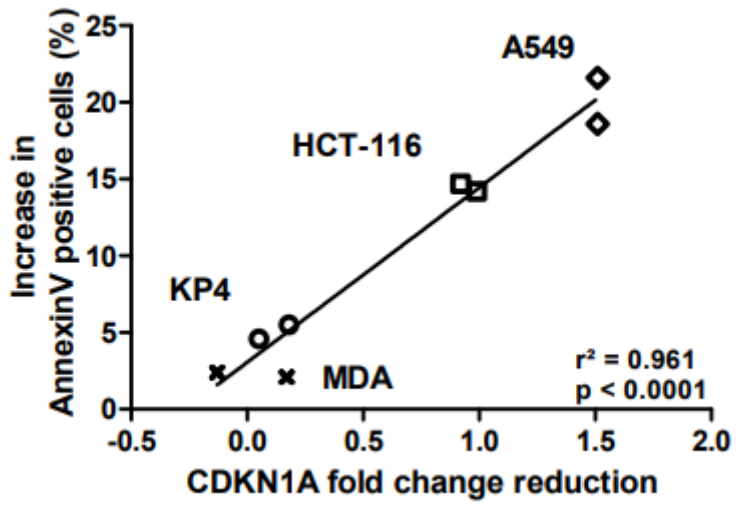

Figure S7: Correlation between the increase in Annexin V and the reduction of CDKN1A fold change at day 3 with the addition of ABT-263. Circle: KP4 cells, square: HCT-116 cells, diamond: A549 cells (X-rays), cross: MDA-MB-231 cells. r^2 and p value obtained with a Pearson's correlation test.

- **Correlation between CDI and reduction of SA-β-Gal by ABT-263**

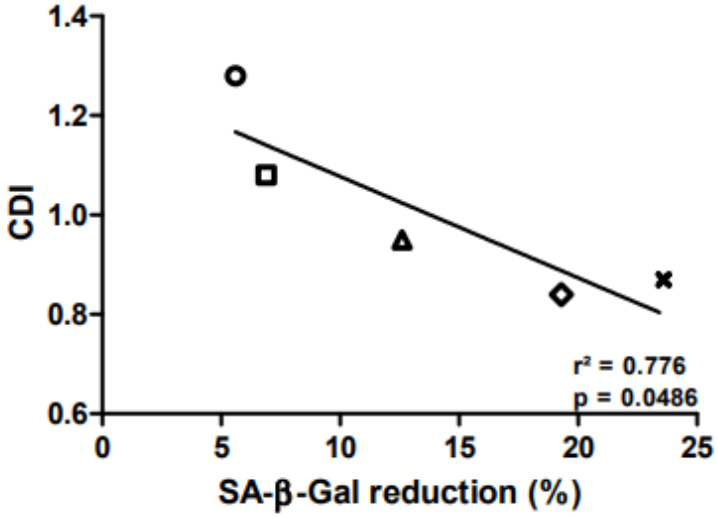

Figure S8: Correlation between CDI and SA-β-Gal activity reduction at 5 Gy with Olaparib with the addition of ABT-263.Circle: KP4 cells, square: HCT-116 cells, triangle: A549 cells (protons), diamond: A549 cells (X-rays), cross: MDA-MB-231cells. r^2 and p value obtained with a Pearson's correlation test.

- Percentage of SA-β-Gal positive cells in non-irradiated cells incubated with ABT-263 or with Olaparib alone or with Olaparib and ABT-263

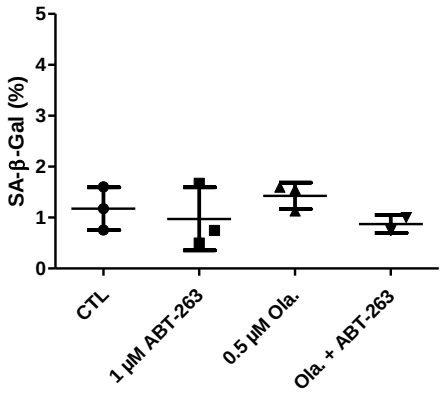

Figure S9: Percentage of SA-β-Gal positive cells in non-irradiated A549 cells incubated with ABT-263 or with Olaparib alone or with Olaparib and ABT-263 at 6 days.

- mRNA expression level of CDKN1A and IL6 in non-irradiated and irradiated cells incubated with ABT-263 or with Olaparib alone or with Olaparib and ABT-263

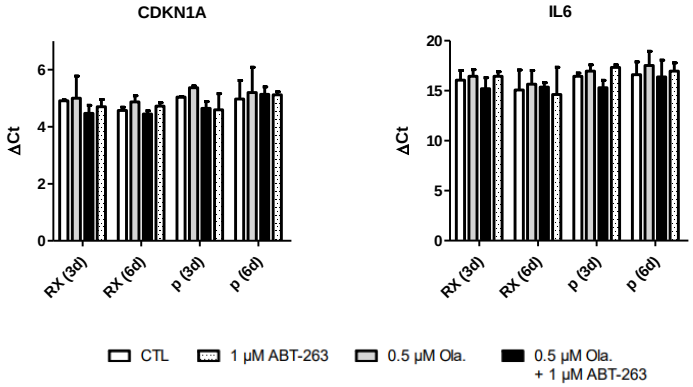

Figure S10: Delta Ct of CDKN1A and IL6 in non-irradiated and irradiated A549 cells incubated with ABT-263 or with Olaparib alone or with Olaparib and ABT-263 at 3 or 6 days.

Supplementary reference

1. Marx, S.; Van Gysel, M.; Breuer, A.; Dal Maso, T.; Michiels, C.; Wouters, J.; Le Calve, B. Potentialization of anticancer agents by identification of new chemosensitizers active under hypoxia. *Biochemical pharmacology* **2019**, *162*, 224-236, doi:10.1016/j.bcp.2019.01.004.
2. Sermeus, A.; Rebucci, M.; Fransolet, M.; Flamant, L.; Desmet, D.; Delaive, E.; Arnould, T.; Michiels, C. Differential effect of hypoxia on etoposide-induced DNA damage response and p53 regulation in different cell types. *Journal of cellular physiology* **2013**, *228*, 2365-2376, doi:10.1002/jcp.24409.

2. PARP inhibitors induce a senescent phenotype in non-small cell lung carcinoma cell lines

In this second part of the thesis, we tried to decipher the induction of the senescent phenotype induced by PARP inhibitors. To this purpose, the induction of senescence was compared in three NSCLC cell lines: A549, H460 and Calu1, using five different PARP inhibitors.

We showed that Talazoparib was the strongest inducer of senescence in A549, H460 and Calu1 cells compared to Niraparib, Olaparib, Rucaparib and Veliparib. Interestingly, all the five inhibitors completely abrogated the formation of PAR (pADPr). This result seems to indicate that the inhibition of the catalytic site of PARP1 is not implicated in the induction of senescent cancer cells.

In conclusion, further research is needed to decipher in depth the induction of the senescent phenotype. Moreover, it remains to be determined if Talazoparib can be used in combination with senolytics in order to enhance cancer cell death which could bring new hopes for cancer patients.

PARP inhibitors induce a senescent phenotype in non-small cell lung carcinoma cell lines

Camille HUART [1], Alexis KHELFI [2], Anne-Catherine WERA [1] and Carine MICHIELS [1*]

[1] Biochemistry and Cellular Biology Research Unit (URBC), Namur Research Institute for Life Sciences (NARILIS), University of Namur (UNamur), 61 Rue de Bruxelles, B-5000, Namur, Belgium

[2] Molecular Physiology Research Unit (URPhyM), Namur Research Institute for Life Sciences (NARILIS), University of Namur (UNamur), 61 Rue de Bruxelles, B-5000, Namur, Belgium

***** Corresponding author: carine.michiels@unamur.be

Introduction

The Poly-ADP-ribose polymerase (PARP) family is composed of 17 members [223]. Poly-ADP-ribose polymerase 1 (PARP1) is the most-well known member of the PARP family. This enzyme is notably heavily involved in the DNA damage response (DDR). Upon genotoxic stress, PARP1 is recruited and uses nicotinamide adenine dinucleotide (NAD+) as a substrate to synthesize poly-ADP-ribose (PAR) polymers. These PAR polymers attach to PARP1 itself and to multiple target proteins, serving as a platform to recruit among others, the DDR machinery [138].

Due to the importance of PARP1 into the DDR, PARP inhibitors (PARPi) have been designed. These PARPi are currently approved as anti-cancer agents due to their ability to induce "synthetic lethality" in cancer patients presenting with BRCA1/2 mutations. PARPi are being studied in many other solid tumors as single agent or in combination with chemo- and radio-therapy [224]. PARPi inhibit PARP1 activity through NAD+ competition, thus preventing the formation of PAR polymers. Interestingly, even if PARP1 is often considered to be the major target of PARPi, some off-target effects on other PARP members such as PARP2 and PARP3 cannot be excluded as the structure of the NAD-binding domain is similar.

Initially, it was thought that the cytotoxicity of the inhibitors came from the catalytic inhibition of PARP1. However, recent studies demonstrated that cytotoxicity of these inhibitors derive from their ability to trap PARP, mostly PARP1, onto the DNA [225]. In the absence of PARPi, the negative charge of the PAR polymers which are present onto PARP1 allow the release of PARP1 from the chromatin. In the presence of PARPi, the formation of PAR polymers is prevented leading to the trapping of PARP1 onto the chromatin. The PARP-DNA complexes are highly toxic as these complexes have been proposed to interfere with the DDR [225].

As aforementioned, PARPi are used to catalytically inhibit PARP1. However, these inhibitors can also affect other members of the PARP family, in particular PARP2. The inhibition constant (Ki) for Veliparib (ABT-888) is 5.2 nM for PARP1 and 2.9 nM for PARP2 [167]. Rucaparib (Rubraca, AG014699, PF01367338) demonstrated a Ki value of 1.4 nM for PARP1 [168]. Olaparib (AZD2281)

presented Ki values of 5 nM and 1 nM for PARP1 and PARP2 respectively [169]. Ki values for Niraparib (MK-4827) are 3.8 nM and 2.1 nM for PARP1 and PARP2 respectively [170]. Talazoparib (BMN 673) has been described as the most potent and selective inhibitor of PARP so far, with a Ki value of 0.57 nM for PARP1 [171]. Research further demonstrated that PARPi do not present with the same ability to trap PARP onto the chromatin. The level of PARP1 trapping elicited by the inhibitors of PARP can be classified in the following manner: Talazoparib > Niraparib > Olaparib ≈ Rucaparib > Veliparib [226].

Recent studies have demonstrated that treatments capable of activating the DDR can often lead to therapy-induced senescence (TIS) [227]. PARPi, mainly Olaparib, have been described to induce senescence which is regarded as a state of irreversible proliferation arrest maintained by p16/RB and/or p21/p53 [228–230]. Senescent cells are characterized by several features *in vitro* and *in vivo* such as morphological modification. Moreover, senescent cells display an enlarged shape, the integrity of their nucleus is compromised due to a decrease in the expression of Lamin B1 (LMNB1) and an increased activity of senescence-associated beta-galactosidase (SA-β-Gal). Senescent cells also activate several pro-survival factors in order to resist to apoptosis. Indeed, increased translation of anti-apoptotic proteins, namely Bcl-2 and Bcl-XL, is observed [132,231,232]. Senescent cells exert several effects on surrounding cells mainly through a specific secretory phenotype, called the secretory associated senescence phenotype (SASP). The SASP is composed of cytokines, chemokines, proteinases, … [110,233].

In the context of cancer, senescent cells exert dual effects: pro-tumoral or anti-tumoral [234]. Baker et al. showed that the clearance of $p16^{Ink4a}$ positive cells resulted in reduced incidences of spontaneous tumorigenesis and cancer-associated death in aged mice [125]. The interest in targeting senescent cells in the context of cancer further increased as senescence was recently added as a Hallmark of Cancer [235]. Senescent cells can be specifically targeted by senolytics or senomorphics. Senolytics refer to the lysis of senescent cells, whereas senomorphics refer to the inhibition of the SASP without damaging the senescent cells. Presently, senolytics have shown positive effects in mouse models presenting with atherosclerosis, osteoarthritis, cataracts, cardiac hypertrophy, renal dysfunction, lipodystrophy and sarcopenia [125,236–239].

In the context of cancer, ovarian cancer cell lines (OVCAR3, OVCAR8 and OV90) showed decreased cell viability when treated with Talazoparib and Navitoclax (ABT-263) compared to cells treated with Talazoparib or Navitoclax alone. The combination of Talazoparib and Navitoclax induced an accumulation of ovarian cancer cells in the sub-G1 phase indicating an increase in DNA fragmentation. Furthermore, more apoptosis was observed in the presence of Talazoparib and Navitoclax compared to Talazoparib alone. The increased apoptosis was demonstrated by an increase in the percentage of cells positive for annexin V, an increase in caspase 3/7 activity, an increase in cleaved PARP and an increase in the protein abundance of some members of the Bcl-2 family [240]. Fleury et al. confirmed these results *in vitro* and *vivo.* Indeed, human cell lines derived from the ascites of patients diagnosed with high grade serous epithelial ovarian cancer (OV4453 and OV1946) were injected into NOD-$Rag1^{null}$ $IL2rg^{null}$, NOD

rag gamma (NRG) mice. The mice demonstrated decreased tumor size when treated with Olaparib and Navitoclax compared to Olaparib alone. Similar conclusion could be drawn in NRG mice injected with breast cancer MDA-MB-231 cells [228].

In this work, in order to decipher how PARPi induce senescence in cancer cell lines, five clinically relevant inhibitors were tested: Veliparib, Rucaparib, Olariparib, Niraparib and Talazoparib. We showed that these inhibitors induce a senescent-like phenotype in non-small cell lung carcinoma (NSCLC) cell lines. Interestingly, we showed that Talazoparib induced a stronger senescent phenotype compared to the other PARPi. Our results suggest that the senescent phenotype is not linked to the ability of the PARPi to inhibit the formation of pADPr.

Materials and Methods

- Cell lines and culture procedures

Human A549 NSCLC cells and human Calu-1 NSCLC cells were sub-cultured in Glutamax Modified Eagle's Medium (Gibco Life Technologies) supplemented with 10% fetal bovine serum (FBS) (Gibco Life Technologies). Human H460 NSCLC cells were sub-cultured in Roswell Park Memorial Institute 1640 (RPMI 1640) (Gibco Life Technologies) supplemented with 10% FBS. For the experiments, the medium was supplemented with 0.5% penicillin/streptomycin (Sigma). Cell lines were maintained at 37°C in 5% CO2. All cell lines were tested negative for mycoplasma using MycoAlert™ Mycoplasma Detection Kit (Lonza).

- Reagents

The following reagents were used: Olaparib (AZD2281, S1060, Selleckchem), Talazoparib (BMN673, S07048, Selleckchem), Niraparib (MK-4827, S2741, Selleckchem), Rucaparib (AG-014699, S1098, Selleckchem) and Veliparib (ABT-888, S1004, Selleckchem).

- Immunoblot analysis

Cells were lysed in NP-40 buffer (Tris 40 mM pH 7.5, KCl 150 mM, EDTA 1 mM, Triton X-100 1%) containing protease inhibitors and phosphatase inhibitors. The lysate was then centrifuged 15 min at 15,000 rpm at 4 °C and the supernatant was collected. 10-15 µg of proteins was separated on home-made gel, and then, transferred onto a low fluorescence background polyvinylidene fluoride (PVDF) membrane (Millipore) using the wet blotting procedure. Membranes were blocked with Odyssey blocking buffer (Li-Cor Biosciences) for 1 hour at room temperature. Primary antibody against full-length PARP1 (Cell Signaling, #9542), pADPR (Abcam, ab14459) were used at 1/1.000 and GAPDH (Abcam, ab8245) at 1/10.000. Anti-mouse secondary antibody, IRDye 680RD and IRDye 800CW Goat anti-mouse IgG (Li-Cor Biosiences) and anti-rabbit secondary antibody, IRDye 680RD and IRDye 800CW Goat anti-rabbit IgG (Li-Cor Biosciences) were used at 1/10.000. The membranes were scanned with the Li-Cor Odyssey Infrared Imager (Li-Cor Biosciences).

- Senescence-associated beta-galactosidase

Detection of senescence-associated beta-galactosidase was described in Debacq-Chainiaux et al [241]. Briefly, cells were fixed with 2 % formaldehyde and 0.2 % glutaraldehyde diluted in PBS for 5 minutes. Cells were rinsed with PBS and with phosphate buffer (pH 5.8) before incubation at 37°C for 18 hours in the staining solution containing: 5-bromo-4-chloro-3-inolyl-β-galactosidase in dimethylformamide (20 mg/ml) (#0428-1G, Amresco), phosphate buffer (pH 5.8), potassium ferricyanide (100 mM), potassium ferrocyanide (100 mM), NaCl (2.5 M) and MgCl2 (1 M). After the incubation, cells were rinsed twice with PBS and with methanol before observation under optical microscope for quantification. At least, 200 cells per well were counted.

- RNA extraction and RT-qPCR

Total RNA was isolated from cells with ReliaPrep™ RNA Tissue Miniprep System (Promega, Z6111) according to the manufacturer's instructions. RNA concentrations were quantified using the Nanophotometer N60 (Implen). cDNA was synthetized with GoScript™ Reverse Transcription Mix (Promega, A2790) according to the manufacturer's instructions using random primers. 0.5-2 µg of RNA was used per reaction. The primers used for the qPCR are described in Table 1. Linear relationship between Ct values and cDNA concentration expressed in log2 were checked for all primer pairs. All real-time PCR reactions were performed using 3 ng of cDNA. Reactions were performed in duplicates with GoTaq™ qPCR Master Mix (Promega, A6001) on a ViiA 7 Real-Time PCR System (Applied Biosystems) using a standard run. The gene expression level of each messenger RNA (mRNA) was calculated, further normalized to glyceraldehyde 3 phosphate dehydrogenase enzyme (GAPDH) mRNA, and related to the control condition. Specific amplification was confirmed by melting curve analysis.

Table 1 – Primer sequences

Gene	**Forward sequence (5'-3')**	**Reverse sequence (5'-3')**
PARP1	GGGAGGGTCTGATGATAGC	CTGTCAACCACCTTAATGTCAG
CDKN1A	GTGGACCTGTCACTGTCTTG	GGCGTTTGGAGTGGTAGAAA
MKI67	AGAAGACAGTACCGCAGATGA	CGCCTCACTAATTTAACGCTGG
LMNB1	ACTGGCGAAGATGTGAAGGTTAT	CCCTGCTGGTGGAAAAGTTC
CCL2	AAGTGTCCCAAAGAAGCTGT	TGGGTTGTGGAGTGAGTGTT
CCL5	AGCCTCTCCCACAGGTACCAT	GCGGGCAATGTAGGCAAA
CXCL10	CCAGTCTCAGCACCATGAATC	GAGGTACTCCTTGAATGCCACT
IL6	CCTGAACCTTCCAAAGATGGC	CACCAGGCAAGTCTCCTCATT
IL8	CTGGCCGTGGCTCTCTTG	GGGTGGAAAGGTTTGGAGTATG

IGFBP5	TGTGACCGCAAAGGATTCTACA	TCCCCGTCAACGTACTCCAT
GAPDH	TGAAGGTCGGAGTCAACGG	GCAACAATATCCACTTTACCAGAGT

- **Generation of knock-out PARP1 cell line**

To generate A549 cells knock-out for PARP1, two crRNAs were used (Table 2). crRNA (IDT) were annealed to tracrRNA (IDT) using a thermocycler. In order to form the ribonucleoprotein (RNP) complex, Cas9 (IDT) was added to the crRNA:tracrRNA duplex. Approximately 1 x 10^6 cells were harvested and resuspended in Nucleofector solution (IDT) supplemented with the RNP complex. The suspension was then placed in an Axama cuvette nucleocuvette for electroporation using program C-09 (Amaxa). Cells were then plated in a 6-wells plate. 24 hours after electroporation, the medium was changed. 48 hours after electroporation, the cells were placed in 96 wells plate for limit dilution. The knock-out clones were identified via Sanger sequencing and immunoblot.

Table 2 – crRNA sequences

crRNA	**Forward sequence (5'-3')**
PARP1 (exon 1)	CGAGTCGAGTACGCCAAGAG
PARP1 (exon 11)	AACTCGGGGGGAAGTTGACG

- **Statistical analyses**

Statistical analyses were performed with GraphPad Prism. The unpaired two-tail Student *t*-test was applied considering that the data were normally distributed. If the variance between groups was not similar, Welch's correction was applied. The ANOVA I was applied considering that the data were normally distributed. If the variance between groups was not similar, Kruskal-Wallis test was performed. The number of independent replicates for each experiment is indicated in the corresponding figure.

Results

- Talazoparib induces a senescent-like phenotype in non-small cell lung carcinoma cell lines

In a previous work, we investigated the induction of senescence in human A549 NSCLC treated with radiotherapy or radiotherapy combined to PARPi Olaparib [242]. Knowing that senescence is dependent on the inducer, we first assessed if another PARPi, namely Talazoparib, could also induce senescence in A549 cells. In addition, other NSCLC cell lines were used to confirm the results: Calu1 and H460. These cells were incubated with 1 or 10 µM of Talazoparib for 6 days. Treated cells showed a strong decrease in cell proliferation (**Fig. S1**). As aforementioned, senescent cells are characterized by several features such as morphological changes, cell cycle arrest, increase lysosomal mass and the secretion of specific cytokines and chemokines. Senescent markers were observed in cancer cells after 6 days. A549, Calu1 and H460 cells demonstrated an increase in the percentage of senescence-associated beta-galactosidase (SABGAL) positive cells after treatment with 1 or 10 µM of Talazoparib (**Fig. 1A**). For A549 cells, the percentage was respectively 76% and 96% for cells incubated with Talazoparib 1 µM and Talazoparib 10 µM respectively compared to control cells exhibiting a negligeable percentage of SABGAL positive cells. To a lesser extent, the increase could also be observed in H460 cells since 1 µM of Talazoparib and 10 µM of Talazoparib respectively induced 50% and 52% of positive cells for SABGAL, while the percentage of SABGAL positive cells was negligeable in control cells. Calu1 cells showed 61% and 89% of SABGAL positive cells after incubation with 1 µM of Talazoparib and 10 µM of Talazoparib in comparison the percentage of SABGAL positive cells was around 10%.

In addition, the shape of cells was modified as demonstrated by the significative increase in nucleus area observed after incubation with 1 and 10 µM of Talazoparib in A549, H460 and Calu1 cells (**Fig. 1B**). All three NSCLC cell lines also demonstrated a significant increase in cyclin dependent kinase inhibitor 1 (CDKN1A) expression at mRNA level after three and six days of incubation with Talazoparib (**Fig. S2A and Fig. 1C**). The CDKN1A gene encodes for a cyclin-dependent kinase inhibitor, which is known to inhibit the activity of cyclin-dependent kinase 2 (CDK2), CDK3, CDK4 and CDK6. The function of the CDKN1A gene is thus, to act as a regulator of the cell cycle. The overexpression of CDKN1A is known to induce a G1 arrest [243]. Reduced proliferation following three or six days of Talazoparib treatment was also evidenced by the significant decrease in MKI67 at mRNA level in A549 and H460 cells (**Fig. S2B and Fig. 1D**). Indeed, MKI67 is described as being only present in proliferating cells [244]. The expression of LMNB1 was significantly decreased following three or six days of incubation with Talazoparib in A549 and H460 cells at mRNA level (**Fig. S2C and Fig. 1E**). As aforementioned, decreased LMNB1 expression is observed in senescent cells. It indicates a ruptured of the nuclear membrane, a known hallmark of cellular senescence. Interestingly, the significant decrease in MKI67 and LMNB1 mRNA expression was not observed in Calu1 cells following the incubation

with Talazoparib. The absence of a decreased expression of LMNB1 and MKI67, two senescent markers, in Calu1 cells might be linked to the lack of TP53 gene (homozygous deletion) [245], while A549 and H460 cells are wild-type for TP53.

The expression of SASP genes was also increased in A549, H460 and Calu1 cells following Talazoparib incubation. As stated in the literature [110], the composition of SASP seems to rely on the cancer cell line analyzed. In line with literature, we observed the overexpression of different genes according to the cell type. Indeed, the expression of CCL2, IL6, IL8 and CXCL10 mRNA was significantly increased in A549 cells incubated with Talazoparib. CCL2 mRNA level was also significantly increased in H460 cells incubated with Talazoparib. Calu1 cells demonstrated a significant increase in the mRNA level of CCL2, CCL5, IL6 and IL8 (**Fig. S3 and S4**). Thus, these results demonstrate that the induction of senescence is not limited to Olaparib, as Talazoparib induced a senescent phenotype with several features of well recognized cellular senescence in three NSCLC cell lines.

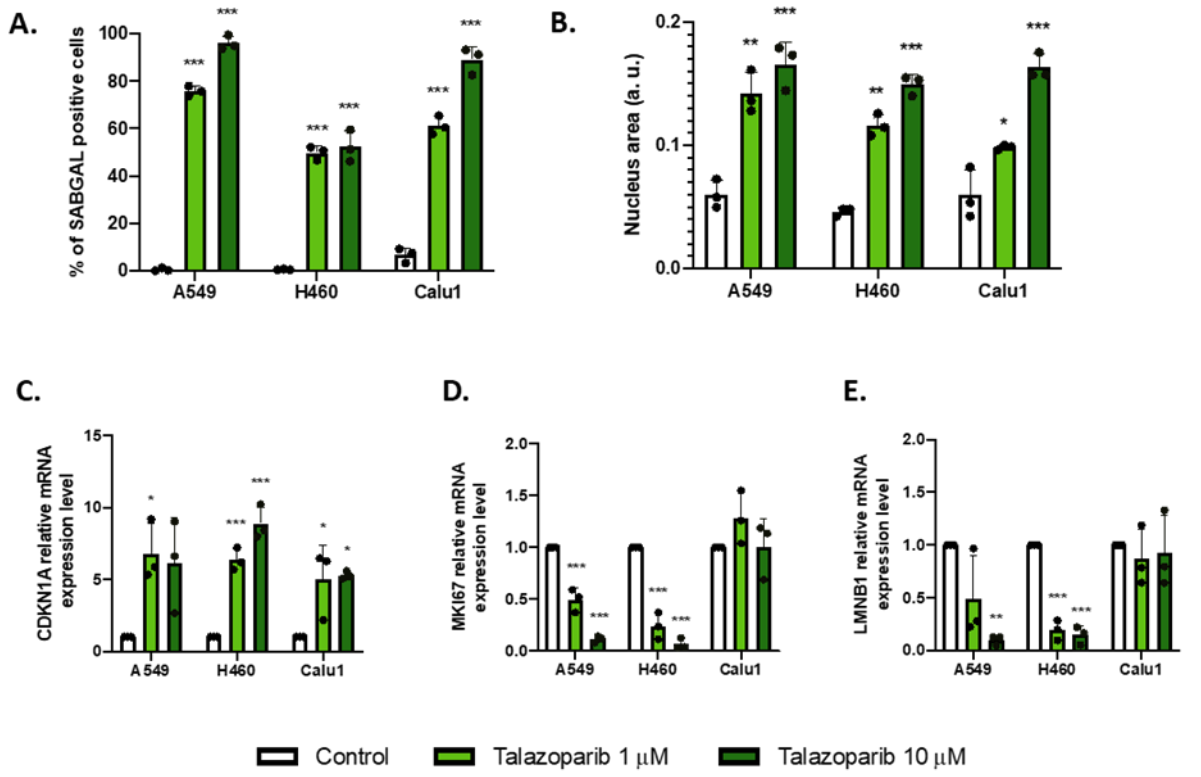

Figure 1 - Talazoparib induces a senescent phenotype in non-small cell lung carcinoma cell lines. *(A) Percentage of SABGAL positive cells for A549, H460 and Calu1 cells incubated with DMSO (control), Talazoparib 1 µM or Talazoparib 10 µM. (B) Nucleus area for A549, H460 and Calu1 cells incubated for 6 days with DMSO (control), Talazoparib 1 µM or Talazoparib 10 µM. (C) CDKN1A relative mRNA expression level, (D) LMNB1 relative mRNA expression level and (E) MKI67 relative mRNA expression level in A549, H460 and Calu1 cells incubated with DMSO (control), Talazoparib 1 µM or Talazoparib 10 µM. Data are shown as mean + S.D. At least, 3 independent experiments were performed. * p < 0.01, ** p < 0.01 and *** p < 0.001.*

- Senescence is differentially induced by different PARP inhibitors

To better understand how senescence is induced following treatment with PARPi, five inhibitors were compared: Talazoparib, Niraparib, Olaparib, Rucaparib and Veliparib. NSCLC cells were incubated with 5 µM of Talazoparib, Niraparib, Olaparib, Rucaparib and Veliparib. Cell proliferation was impacted in all the three cell lines (**Fig. S5**). The strongest impact on cell proliferation was observed in cells incubated with Talazoparib or with Niraparib. Rucaparib and Olaparib induced a similar moderate impact on cell proliferation, whereas Veliparib only slightly affected cell proliferation.

The proportion of SABGAL positive cells were then assessed following incubation with the different PARPi. The percentage of SABGAL positive cells was significantly increased in A549 and H460 cells incubated with Rucaparib, Olaparib, Niraparib or Talazoparib. For Calu1 cells, only Niraparib and Talazoparib significantly increased the proportion of SABGAL-positive cells (**Fig. 2A**). Furthermore, the percentage of SABGAL positive cells was significantly higher when A549, H460 and Calu1 cells were incubated with 5 µM of Talazoparib compared to other PARPi.

All three cell lines were also analyzed for the expression of CDKN1A at mRNA level (**Fig. 2B**). CDKN1A expression significantly increased in A549 and Calu1 cells incubated with 5 µM of Talazoparib when compared to control cells. In A549 cells, Talazoparib significantly increased the expression of CDKN1A mRNA when compared to other PARPi, while in Calu1 cells, Talazoparib significantly increased CDKN1A expression when compared to Veliparib, Rucaparib and Olaparib. In H460 cells, the expression of CDKN1A was significantly increased after exposure to 5 µM of Talazoparib or 5 µM of Niraparib. Moreover, the expression of CDKN1A was significantly more increased after Talazoparib incubation when compared to other PARPi. The expression of MKI67 was significantly decreased in A549 and H460 cells incubated with Talazoparib compared to control cells and to other PARPi (**Fig. 2C**). The expression of LMNB1 was significantly decreased in A549 and H460 cells incubated with Talazoparib compared to control cells (**Fig. 2D**). Moreover, A549 cells incubated with Talazoparib demonstrated a significant reduction in LMNB1 expression when compared to cells exposed to the other PARPi. A significant reduction in LMNB1 expression was observed in H460 cells incubated with Talazoparib compared to H460 cells incubated with Veliparib, Rucaparib or Olaparib. We also observed an increase in 53BP1 foci in A549, Calu1 and H460 cells incubated with Talazoparib (**Fig. S7A-C**). These results demonstrated for the first time that inhibitors of PARP are not all equal in the induction of senescence.

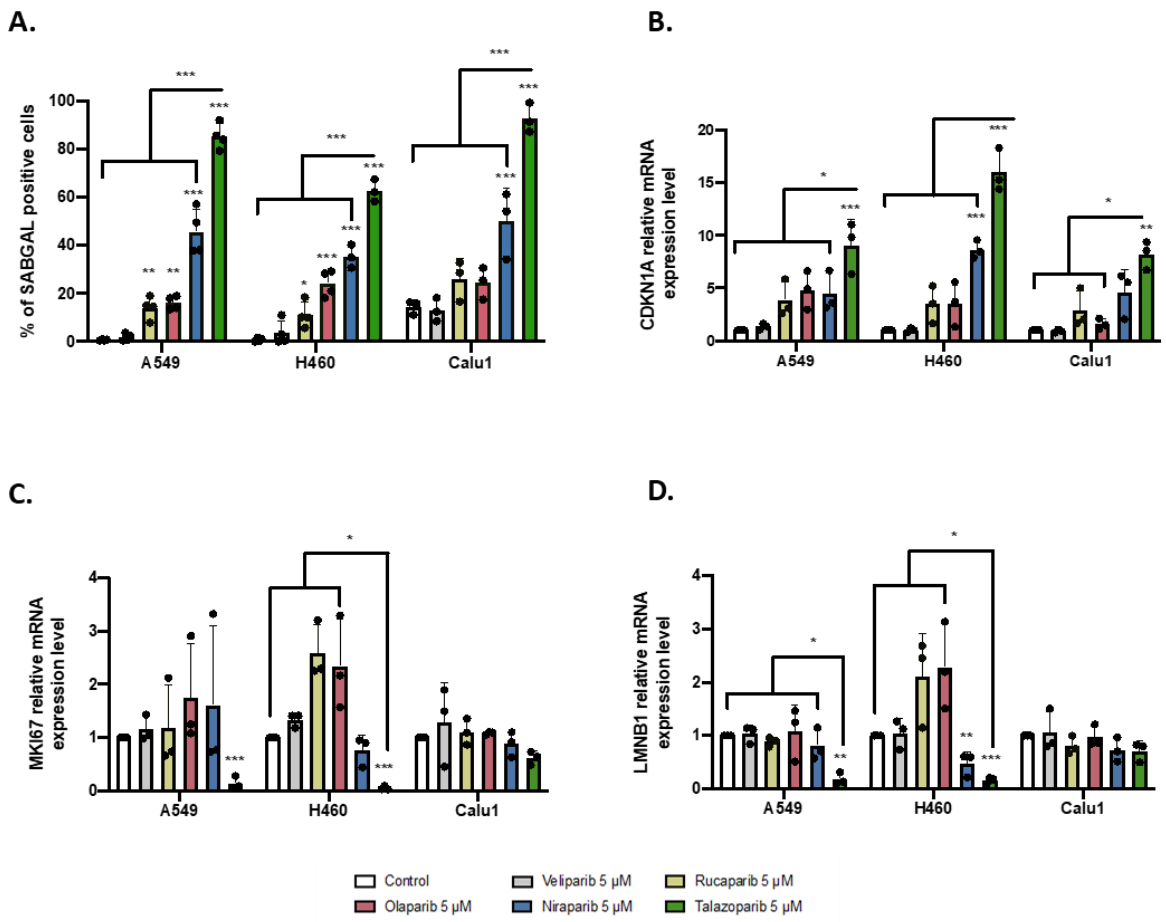

Figure 2 - The induction of senescence by the different PARP inhibitors. *(A) Percentage of SABGAL positive cells in A549, H460 and Calu1 cells incubated with DMSO (control), Veliparib 5 µM, Rucaparib 5 µM, Olaparib 5 µM, Niraparib 5 µM or Talazoparib 5 µM. (B) CDKN1A relative mRNA expression level, (C) LMNB1 relative mRNA expression level and (D) MKI67 relative mRNA expression level in A549, H460 and Calu1 cells incubated for 6 days with DMSO (control), Veliparib 5 µM, Rucaparib 5 µM, Olaparib 5 µM, Niraparib 5 µM or Talazoparib 5 µM. Data are shown as mean + S.D. At least, 3 independent experiments were performed. * p < 0.01, ** p < 0.01 and *** p < 0.001.*

- The inhibition of PARP1 catalytic activity by the different inhibitors is similar

To define if the inhibition of PARP1 catalytic activity is responsible for the senescent phenotype, the formation of pADPr was assessed in cells incubated or not with each of the PARPi. We showed that the five PARPi completely abrogated the formation of pADPr in A549, H460 and Calu1 cancer cells (**Fig. 3**). This result thus indicates that the catalytic inhibition is not responsible for the differential induction, according to the inhibitor, of the senescent phenotype observed in NSCLC cells.

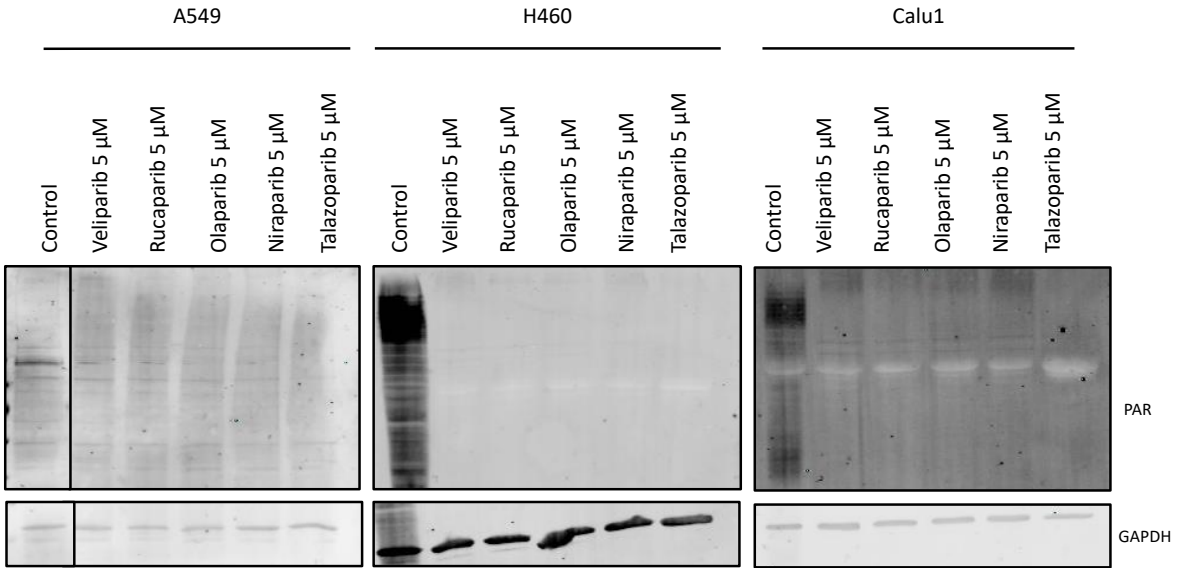

Figure 3 - The catalytic inhibition of PARP is similar for the different inhibitors. *Formation of PAR in A549, H460 and Calu1 cells incubated for 6 days with DMSO (control), Veliparib 5 µM, Rucaparib 5 µM, Olaparib 5 µM, Niraparib 5 µM or Talazoparib 5 µM. GAPDH was used as a loading control. At least, 3 independent biological replicates were performed.*

- The inhibitors of PARP do not induce the same level of cell death

A549, H460 and Calu1 cells were incubated with the different PARP inhibitors for 6 days, and cell survival was measured using MTT (Figure 4). The results demonstrated that Niraparib and Talazoparib were the most toxic molecules in all three cell lines.

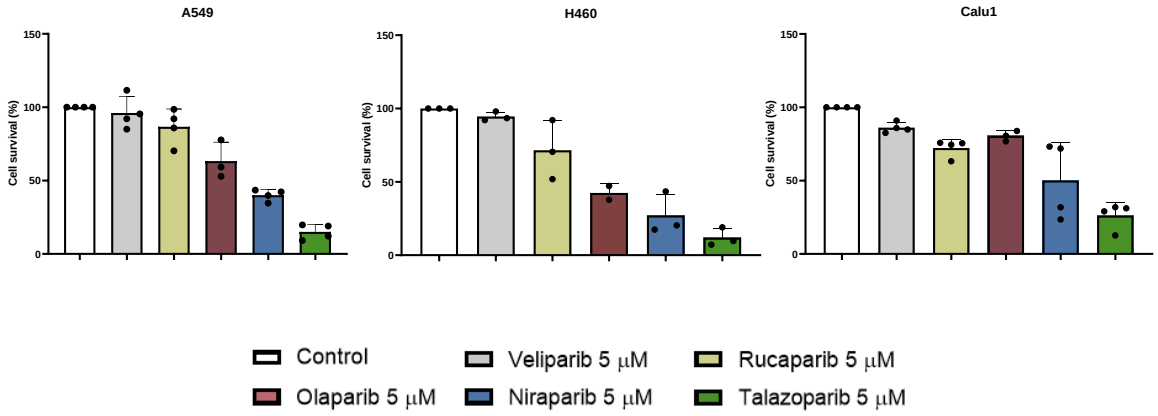

Figure 4 - The inhibitors of PARP do not induce the same level of cell death. *Cell survival of A549, H460 and Calu1 cells incubated for 6 days with DMSO (control), Veliparib 5 µM, Rucaparib 5 µM, Olaparib 5 µM, Niraparib 5 µM or Talazoparib 5 µM.*

- The presence of PARP1 is required for the induction of the senescent phenotype

In order to determine if the knockdown of PARP1 would lead to a senescent-like phenotype similar to what is observed with some PARP inhibitors, short hairpin RNA (shRNA) targeting PARP1 were used. Of note, the four shRNAs used target the two transcripts coding for PARP1 protein (ENST00000366794.10 and ENST00000677203.1). The four shRNAs targeting PARP1 induced a knock-down at mRNA and protein level of PARP1 (**Fig. S8A and S8B**). shRNAs targeting PARP1 alone in A549 cells did not induce a senescent phenotype (**Fig. S8C**). A549 transduced with shRNAs targeting PARP1 and incubated for six days with Talazoparib presented with a reduced senescent phenotype compared to A549 transduced with shRNA control and incubated for six days with Talazoparib (**Fig. S8C**). Similar results were obtained in H460 cancer cell line (**Fig. S9A-C**).

Thus, to determine if PARP1 is the sole contributor to the senescent phenotype, CRISPR/Cas9 genome editing method was used in order to introduce short frameshift insertions-deletions (indels) in the DNA sequence of PARP1 leading to a knock-out for PARP1. Two single-guide RNA (sgRNA) were designed respectively targeting exon 1 and exon 11 (**Fig. 5A**). Several clones could be isolated, and for subsequent analyses, one wild-type clone (50G4) and two knock-out clones were used (50A6 and 50B6). The clones were validated using Sanger sequencing and immunoblot (Fig. 5B).

When the wild-type clone is exposed to Talazoparib (1 µM or 10 µM), the percentage of cells positive for SABG increased (Fig. 6A). Moreover, the expression of CDKN1A was also increased (Fig. 6B) whereas the expression of MKI67 and LMNB1 was decreased at mRNA level (Fig. 6C-D). These results confirmed the previously obtained results in A549 cells. Interestingly, the percentage of SABG positive cells in non-exposed knock-out clones was similar to the percentage observed for the wild-type cells indicating that the absence of PARP1 did not induce a senescent phenotype per se in A549 cells (Fig. 6A). Furthermore, when the knock-out clones were exposed to Talazoparib (1 µM or 10 µM), the percentage of SABG positive cells was strongly reduced compared to the wild-type clone (Fig. 6A). The increase in the expression of CDKN1A at mRNA level was also reduced in the two knock-out clones (Fig. 6B). The decrease in the expression of MKI67 and LMNB1 was reduced in knock-out clones compared to the wild-type clone (Fig. 6C-D). Altogether, these results indicate that PARP1 is necessary for the senescent phenotype to occur.

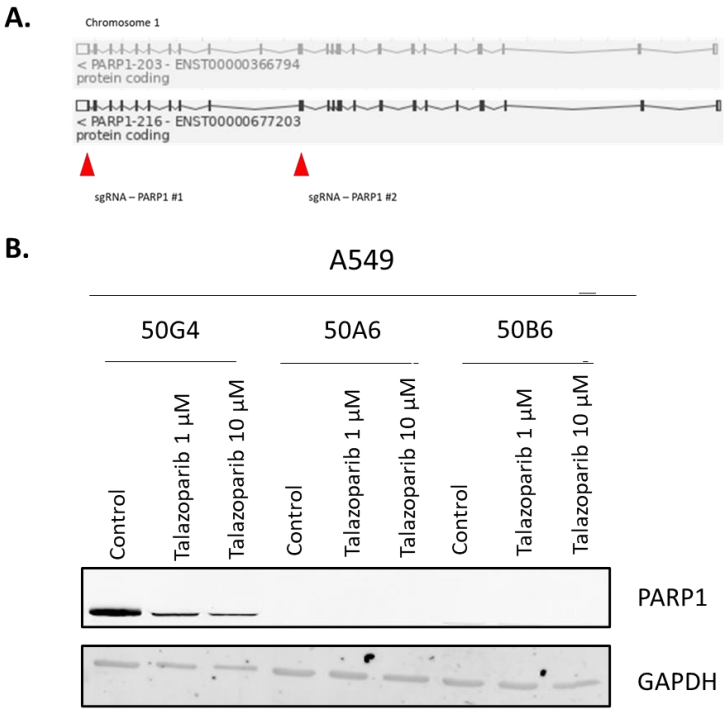

Figure 5 - Validation of the knock-out for PARP1 in individual clones.*(A) Representation of the CRISPR/Cas9 strategy used to induce indels in the DNA sequence of PARP1. (B) Immunoblot of PARP1 of the chosen CRISPR/Cas9 clones incubated for 6 days with DMSO (control) or Talazoparib 1 µM or Talazoparib 10 µM. GAPDH was used as a loading control.*

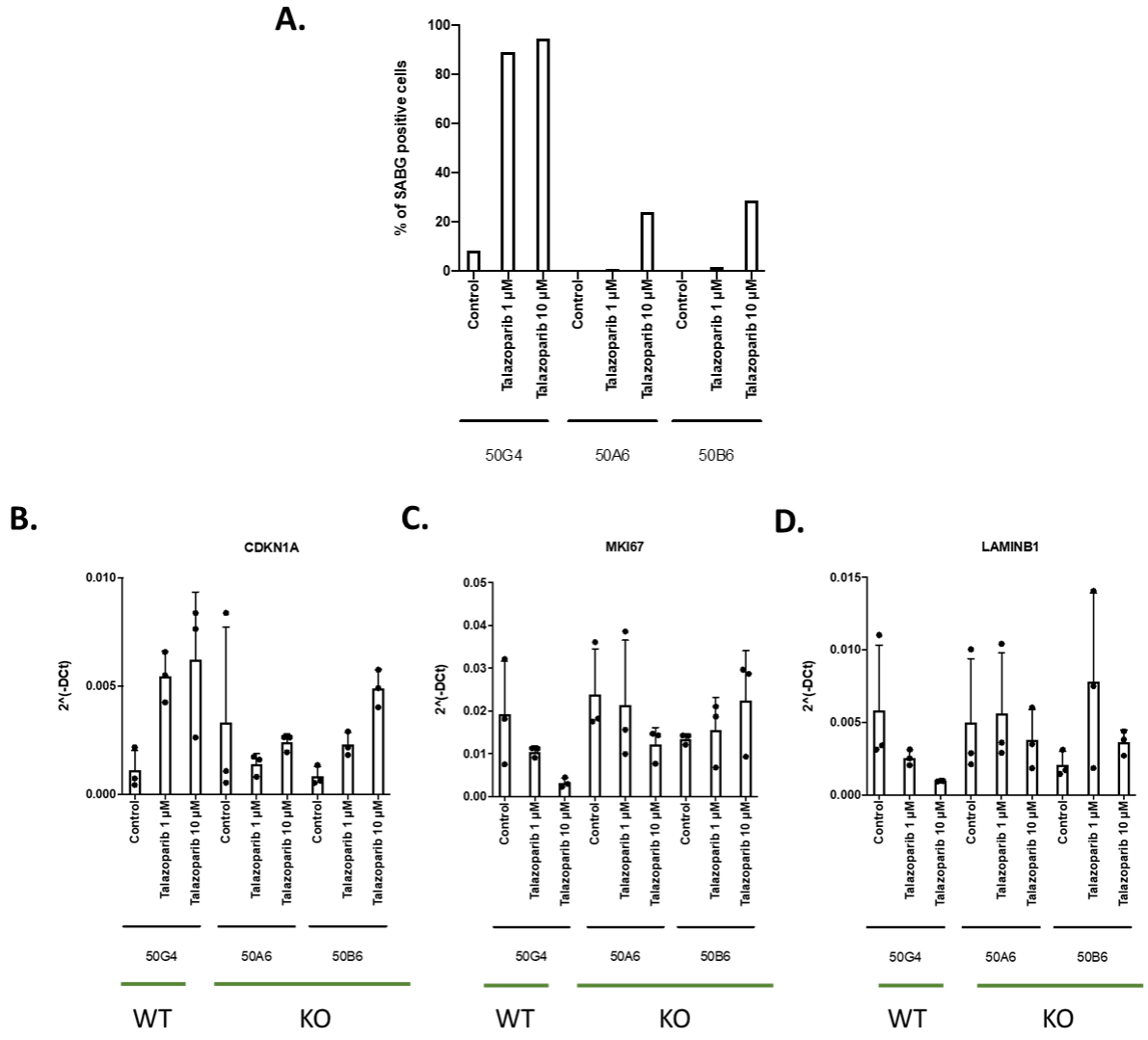

Figure 6 - PARP1 is necessary for the senescent-like phenotype to occur in A549 cancer cell line*. (A) Percentage of SABGAL positive cells in A549 CRISPR/Cas9 clones incubated for 6 days with DMSO (control), Talazoparib 1 µM or Talazoparib 10 µM. (B) CDKN1A relative mRNA expression level, (C) MKI67 relative mRNA expression level and (D) LMNB1 relative mRNA expression level in A549 CRISPR/Cas9 clones incubated for 6 days with DMSO (control), Talazoparib 1 µM or Talazoparib 10 µM. Data are shown as mean + S.D.*

- The presence of CDKN1A is required for the induction of the senescent phenotype

Fleury et al. described the importance of CDKN1A in the induction of the senescent phenotype following treatment with Olaparib in ovarian cancer cells as aforementioned. In order to determine if CDKN1A was also necessary for the senescent phenotype to occur following Talazoparib treatment, shRNA targeting CDKN1A were used. Of note, five transcripts (ENST00000244741.10, ENST00000405375.5, ENST00000448526.6, ENST00000615513.4 and ENST00000373711.3) of CDKN1A are encoding proteins, and these five transcripts are all targeted by the three shRNAs. The knockdown of CDKN1A was verified at mRNA level, and the three shRNAs induced a knockdown of CDKN1A. The mRNA expression was reduced by two-fold in H460 cells (**Fig. S10A**). Moreover, treatment with Talazoparib of H460 transduced with

shRNA targeting CDKN1A demonstrated a reduction in the percentage of SABGAL positive cells compared to H460 transduced with shControl (**Fig. S10B**). This preliminary result suggests that CDKN1A is implicated in the induction of the senescent phenotype following treatment with PARP inhibitors. However, this result has to be repeated as it was only performed once, and more senescent markers should be assessed. Furthermore, this result also has to be validated in A549 and Calu1 cell lines.

- ATM is required for the induction of the senescent phenotype

To determine if ATM was necessary for the senescent phenotype to occur following Talazoparib treatment, two inhibitors of ATM were used: Ku-60019 and AZD1390. A549, H460 and Calu1 cells were incubated for 6 days with Talazoparib either alone or in combination with Ku-60019 or AZD1390. We evaluated the mRNA expression of CDKN1A, MKI67 and LMNB1 in A549, H460 and Calu1 cells (**Fig. S11A-C and Fig. S12A-C**). In A549 cells, we demonstrated that the incubation in the presence of Ku-60019 or Talazoparib for 6 days induced a significant reduction in the expression of CDKN1A at mRNA level compared the incubation with Talazoparib alone (**Fig. S11A**). The expression of CDKN1A was also slightly reduced in H460 cells incubated with Ku-60019 and Talazoparib compared to H460 cells incubated with Talazoparib alone (**Fig. S11A**). However, the expression of CDKN1A showed a non-significant increase in Calu1 cells exposed to Ku-60019 and Talazoparib compared to Calu1 cells exposed to Talazoparib alone (**Fig. S11A**). No significant change in the mRNA expression level of MKI67 (**Fig. S11B**) and LMNB1 (**Fig. S11C**) was observed in cells incuabted with Ku-60019 and Talazoparib compared to cells incubated with Talazoparib alone . When cells were incubated with AZD1390 and Talazoparib, a non-significant decrease in the expression of CDKN1A at mRNA level in A549, H460 and Calu1 cells compared to cells incubated with Talazoparib alone was observed (**Fig. S12A**). A significant increase in the expression of MKI67 in A549 cells incubated with AZD1390 and Talazoparib compared to A549 cells incubated with Talazoparib alone was shown (**Fig. S12B**). These preliminary results indicated that ATM is, at least in part, implicated in the induction of several senescent markers, namely, CDKN1A and MKI67.

- Senescence confers protection against cell death

Incubation of A549, H460 and Calu1 cells with Olaparib and Ku-60019 or AZD1390 showed a strong impact on cell survival (**Fig. S13**). As the senescent phenotype seems reduced in the presence of Ku-60019 or AZD1390, these preliminary results thus show a potential protective effect of the senescent phenotype on cancer cells. These results seem to indicate that when ATM is inhibited, cancer cells cannot enter the “protective” senescent phenotype leading to increased cell death.

Discussion

The purpose of this work was to define how PARPi induce a senescent phenotype in cancer cells. We showed that Talazoparib induced a stronger senescent-like phenotype in cancer cells compared to Niraparib, Olaparib, Rucaparib and Veliparib. We could demonstrate an increased senescent phenotype in three different NSCLC cell lines. Interestingly, A549 and H460 cancer cells are known as TP53 wild-type, whereas Calu1 cancer cells lack TP53 (homozygous deletion). It thus seems that PARPi can induce a senescent-like phenotype in a p53-independent manner. These results are similar to what was described by Fleury et al. [228]. The authors used four different ovarian cancer cells, namely OV1369(R2), OV90, OV4453 and OV1946, and these cancer cells have TP53 mutations. Nonetheless, the four ovarian cancer cell lines demonstrated a senescent-like phenotype induced by Olaparib.

Our results demonstrated that cancer cell lines exposed to Talazoparib displayed a much higher increase in the expression of CDKN1A gene than when exposed to the other PARPi. We incubated the three cell lines with the same concentrations: 1 µM and 10 µM of Talazoparib.

Fleury at al. reported that CDKN1A is necessary for the senescent-like phenotype to occur in ovarian cancer cells [228]. In a similar fashion, our preliminary data indicated that CDKN1A contributes to the senescent phenotype observed when cells are incubated with Talazoparib. These results have to be validated in A549 and Calu1 cells. Furthermore, it seems that ATM also plays a role in the induction of the senescent phenotype. Indeed, treatment of the cells with inhibitors of ATM reduced the mRNA expression of several senescent markers induced by Talazoparib. These results would also have to be investigated further using knock-down or knock-out strategies.

Furthermore, we showed that the percentage of SABGAL positive cells was different in the different cell lines. A549 and Calu1 cells showed a strong induction in the percentage of SABGAL positive cells. Indeed, the percentage of SABGAL positive cells was close to 100% in A549 and Calu1 cells incubated with 10 µM of Talazoparib. In H460 cells, the percentage of SABGAL positive cells only reached about 50% when exposed to 10 µM of Talazoparib. These differences could be explained by differences in sensitivity to Talazoparib. Indeed, Fleury et al. showed that low sensivity to treatment measured by cell death led to a high induction of SABGAL positive cells [228]. However, we showed that the percentage of cell death was very similar in A549, H460 and Calu1 cells incubated with Talazoparib for six days. Hence, another mechanism is underlying these effects.

Interestingly, we demonstrated that the inhibition of the catalytic site of PARP1 is not responsible for the induction of the phenotype. As aforementioned, PARPi exert their effects through the inhibition of the catalytic site of PARP1, but also through the formation of PARP1-DNA complexes. We are currently trying to determine if the formation of PARP1-DNA complexes is responsible for the senescent-like phenotype observed in NSCLC cell lines.

These preliminary results thus indicate that not all senescent inducers are equal. With the strong interest surrounding the use of senolytics in the context of cancer, these results demonstrate the importance of characterizing the induction of the senescent phenotype observed following treatment with cancer therapies. In the end, deepening current understanding regarding senescence in the context of cancer might bring new therapeutic venues for cancer patients.

Supplementary information

Material & Method :

- **Transduction**

shRNAs for PARP1 and CDKN1A were respectively ordered from Horizon and Sigma-Aldrich. The sequences are available in Table S1.

Table S1 – shRNA sequences

shRNA	**Sequence (5'-3')**
shp21 – 1	GACAGATTTCTACCACTCCAA
shp21 – 2	GACACCACTGGAGGGTGACTT
shp21 – 3	CGCTCTACATCTTCTGCCTTA
shPARP1 – 1	AATCTTCGGTTATGAAGCTGC
shPARP1 – 2	AAGGCAGACATTCTAACGAAG
shPARP1 – 3	TTGAGGTAAGAGATTTCTCGG
shPARP1 – 4	TTGATGTTCCAGATCAGGTCG

For lentivirus production, HEK293T cells were seeded in appropriate culture flasks. The next day, the following components were added to the HEK293T: the envelope-encoding vector pCMV-VSVG (Addgene, #8454), the packaging vector psPAX2 (Addgene, #12260), the DNA of interest and $CaCl_2$. 24 hours after, the medium was removed and renewed. 24 hours after media renewal, the medium was collected and filtered using 0.45 µm steriflip (Millipore, SE1M003M00). Particles were concentrated using Lenti Concentrator Lentivirus Concentration Solution 5X (OriGene, TR30025-OR). Particles were titrated using RT-qPCR according to manufacturer's recommendations (Lentivirus qPCR Titer Kit, Applied Biological Materials, LV900). Subconfluent cells were transduced with the adequate lentiviruses in the presence of polybrene, and selected for 3 days using puromycin at a concentration of 1.5 µg/µl.

- **MTT assay**

Cell viability was determined using MTT (3-[4,5-dimethylthiazol-2-yl]-2,5-diphenyltetrazolium bromide) (Sigma). Briefly, MTT was diluted in PBS at 2.5 mg/mL, and added to the cell media at a ratio of 1:1 for 2 hours at 37°C. After incubation, cells were lysed with dimethyl sulfoxide (DMSO) (Sigma). The optic density was read using a spectrophotometer at 570 nm.

- **Immunofluorescence labeling**

Cells were plated on coverslips. Cells were fixed with PFA 4%. Cells were incubated with PBS-BSA 2% for 1 hour at room temperature. Cells were then, incubated with primary antibody: 53BP1 (Novus) overnight at 4°C. The next day, the cells were incubated with secondary antibody for 1 hour at room temperature. The nuclei were stained with 2.5 mg/ml DAPI (Sigma) for 10 minutes. Following PBS washes, coverslips were mounted on microscope slides with Mowiol. The observations were performed by confocal microscopy by keeping the photomultiplier at a constant gain (Leica SP5).

Supplementary Figures

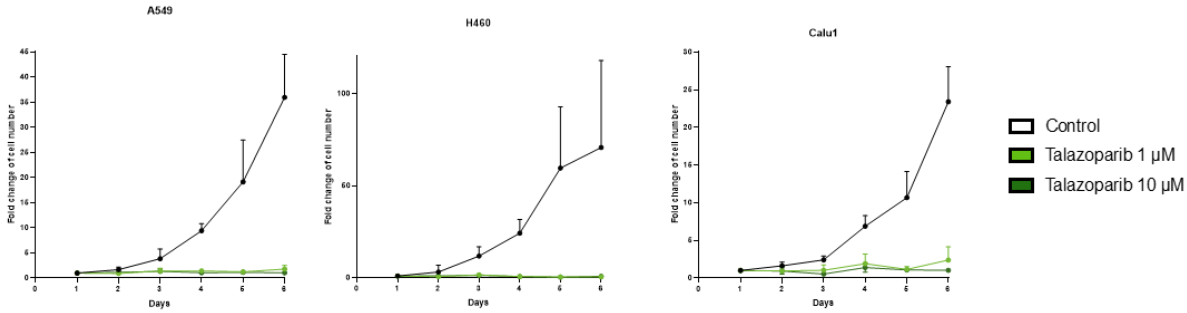

Figure S1 – Talazoparib induces a senescent phenotype in non-small cell lung carcinoma cell lines. *Proliferation arrest in A549, H460 and Calu1 cells incubated for 6 days with DMSO (control), Talazoparib 1 µM or Talazoparib 5 µM. Data are shown as mean + S.D. At least, 3 independent experiments were performed.*

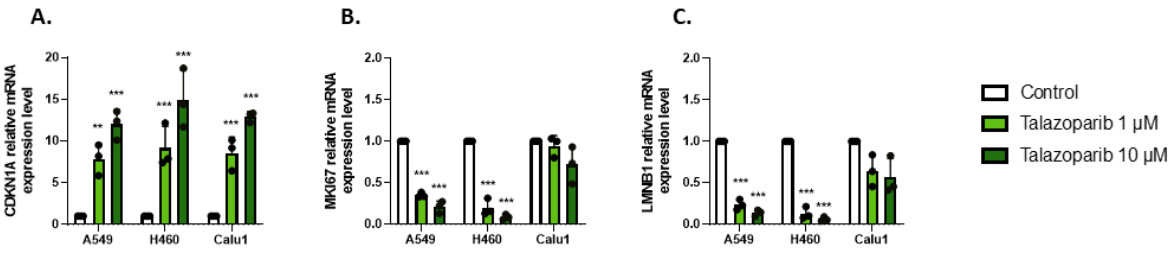

Figure S2 – Talazoparib induces a senescent phenotype in non-small cell lung carcinoma cell lines. *(A) CDKN1A, (B) MKI67 and (C) LMNB1 relative mRNA expression level in A549, H460 and Calu1 cells incubated for 3 days with DMSO (control), Talazoparib 1 µM or Talazoparib 5 µM. Data are shown as mean + S.D. At least, 3 independent experiments were performed. ** $p < 0.01$ and *** $p < 0.001$.*

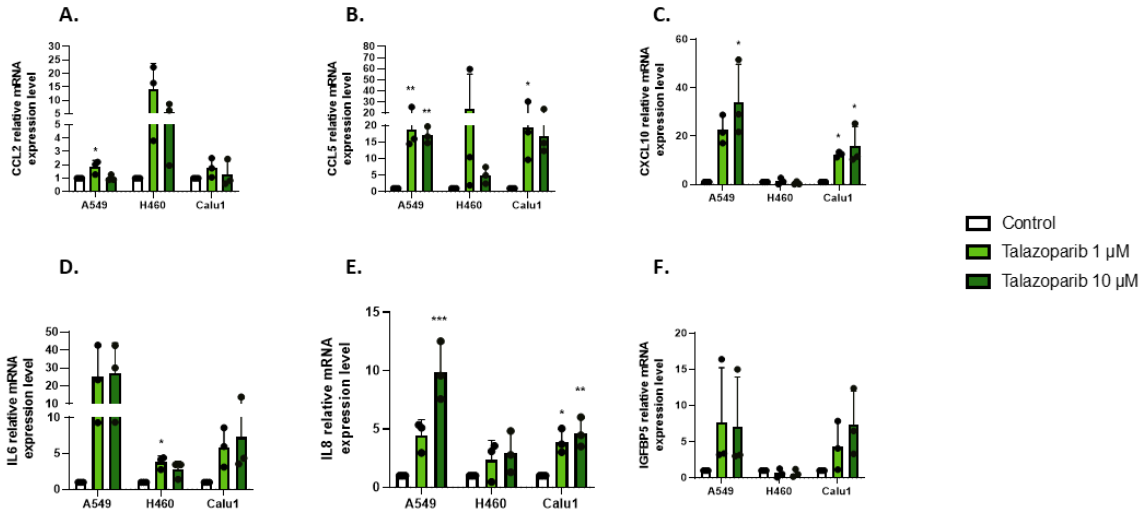

Figure S3 – Talazoparib induces a senescent phenotype in non-small cell lung carcinoma cell lines. *(A) CCL2, (B) CCL5, (C) CXCL10, (D) IL6, (E) IL8 and (F) IGFBP5 relative mRNA expression level in A549, H460 and Calu1 cells incubated for 3 days with DMSO (control), Talazoparib 1 µM or Talazoparib 5 µM. Data are shown as mean + S.D. At least, 3 independent experiments were performed. * p < 0.01, ** p < 0.01 and *** p < 0.001.*

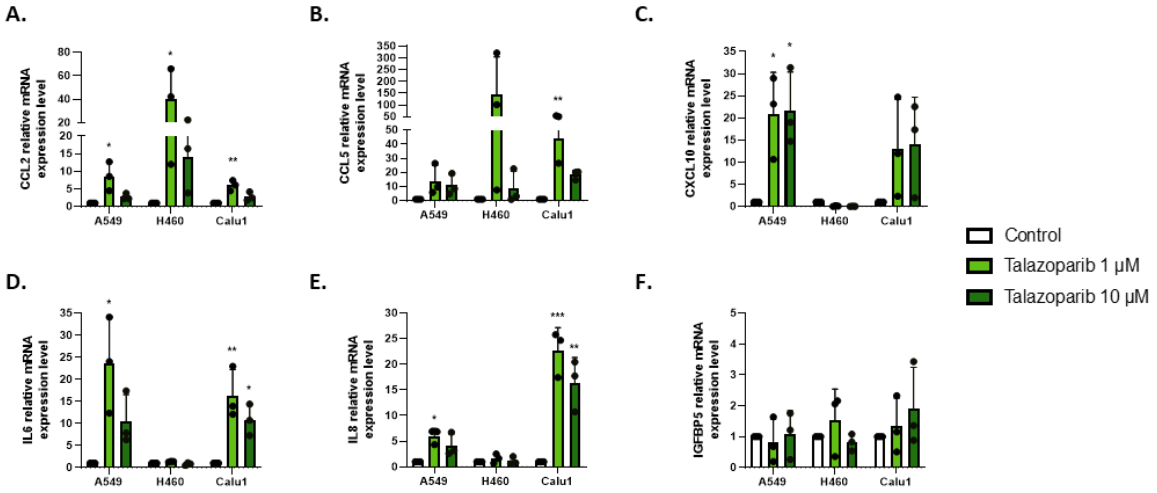

Figure S4 – Talazoparib induces a senescent phenotype in non-small cell lung carcinoma cell lines. *(A) CCL2, (B) CCL5, (C) CXCL10, (D) IL6, (E) IL8 and (F) IGFBP5 relative mRNA expression level in A549, H460 and Calu1 cells incubated for 6 days with DMSO (control), Talazoparib 1 µM or Talazoparib 5 µM. Data are shown as mean + S.D. At least, 3 independent experiments were performed. * p < 0.01, ** p < 0.01 and *** p < 0.001.*

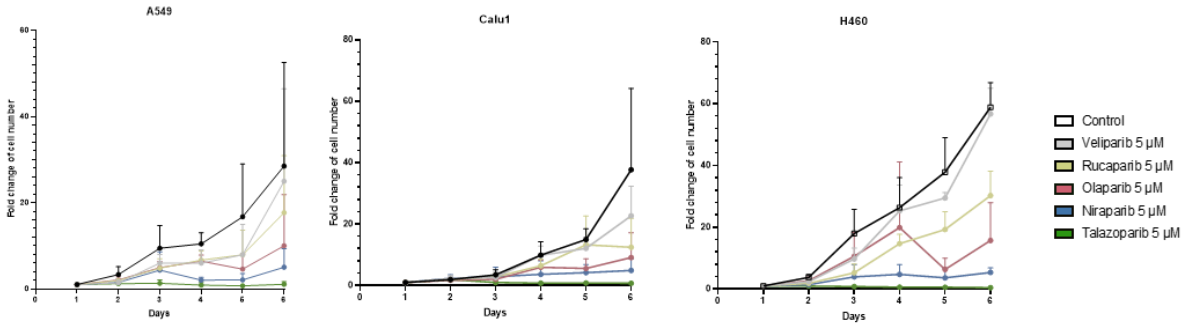

Figure S5 – The induction of senescence by the different PARP inhibitors. *Proliferation arrest in A549, H460 and Calu1 cells incubated for 6 days with DMSO (control), Veliparib 5 µM, Rucaparib 5 µM, Olaparib 5 µM, Niraparib 5 µM or Talazoparib 5 µM. Data are shown as mean + S.D. At least, 3 independent experiments were performed.*

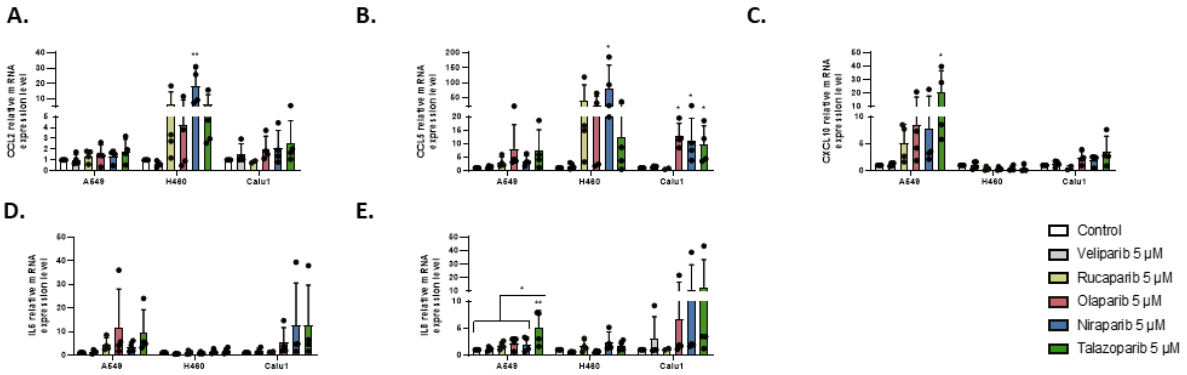

Figure S6 – The induction of senescence by the different PARP inhibitors. *(A) CCL2, (B) CCL5, (C) CXCL10, (D) IL6, and (E) IL8 relative mRNA expression level in A549, H460 and Calu1 cells incubated for 6 days with DMSO (control), Veliparib 5 µM, Rucaparib 5 µM, Olaparib 5 µM, Niraparib 5 µM or Talazoparib 5 µM. Data are shown as mean + S.D. At least, 3 independent experiments were performed. * p < 0.01 and ** p < 0.01.*

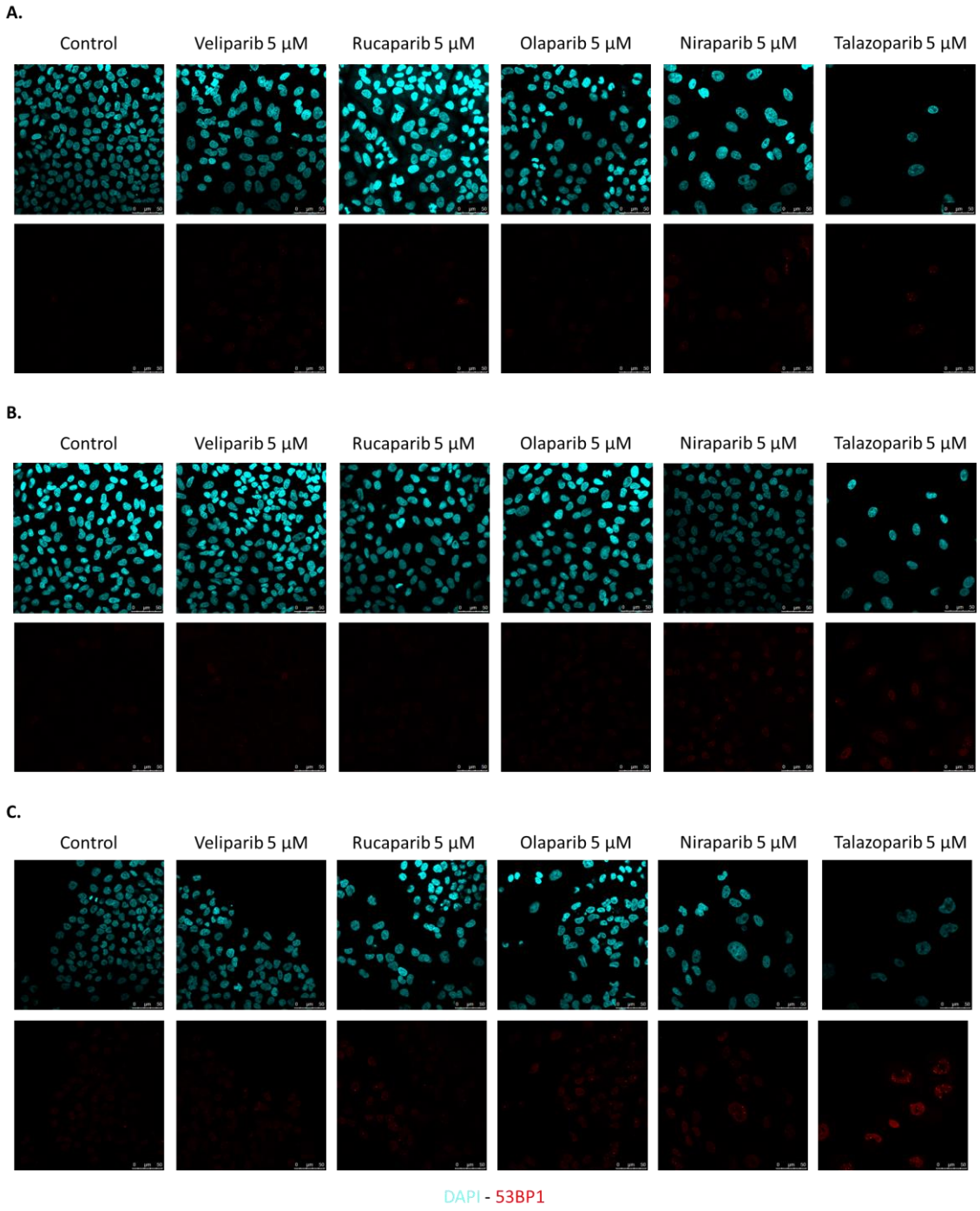

Figure S7 – The induction of senescence by the different PARP inhibitors. *Immunofluorescence labeling of 53BP1 in (A) A549, (B) Calu1 and (C) H460 cells incubated for 6 days with DMSO (control), Veliparib 5 µM, Rucaparib 5 µM, Olaparib 5 µM, Niraparib 5 µM or Talazoparib 5 µM. 2 independent experiments were performed.*

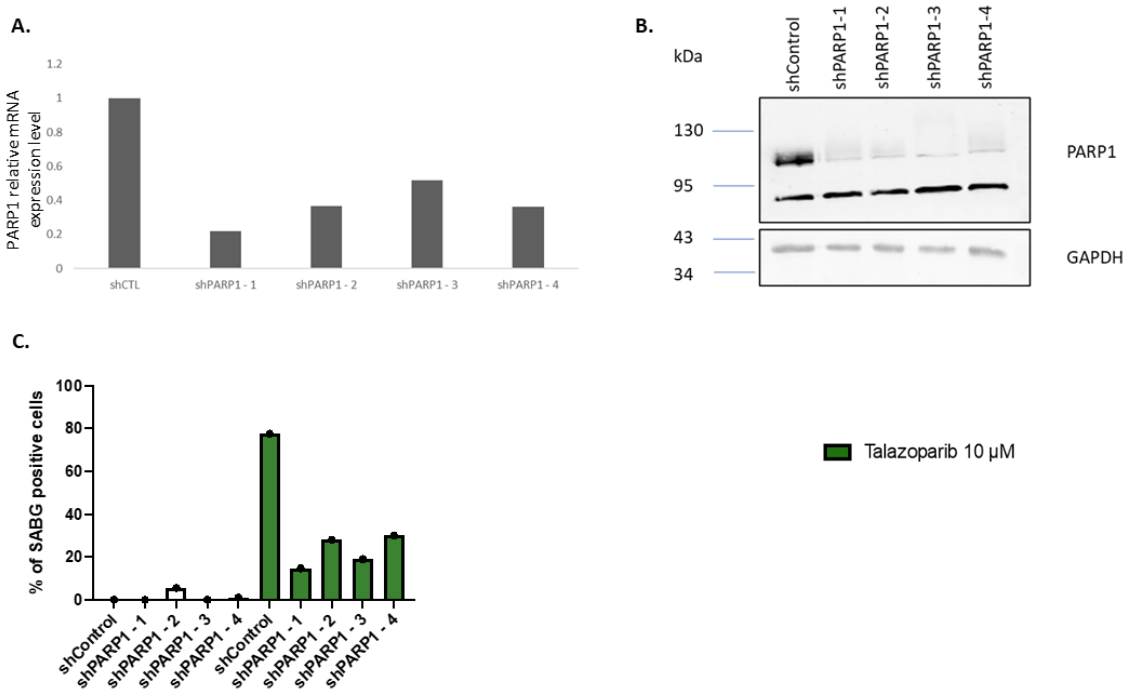

Figure S8 – The presence of PARP1 is required for the induction of the senescent-like phenotype. *(A) PARP1 relative mRNA expression level in A549 cells transduced with shControl, shPARP1 – 1, shPARP1 – 2, shPARP1 – 3 and shPARP1 – 4. (B) Protein level of PARP1 in A549 cells transduced with shControl, shPARP1 – 1, shPARP1 – 2, shPARP1 – 3 and shPARP1 – 4. (C) Percentage of SABGAL positive cells in A549 cells transduced with shControl, shPARP1 – 1, shPARP1 – 2, shPARP1 – 3 and shPARP1 – 4 incubated or not for 6 days with Talazoparib 10 µM. Data are shown as mean for one independent experiment.*

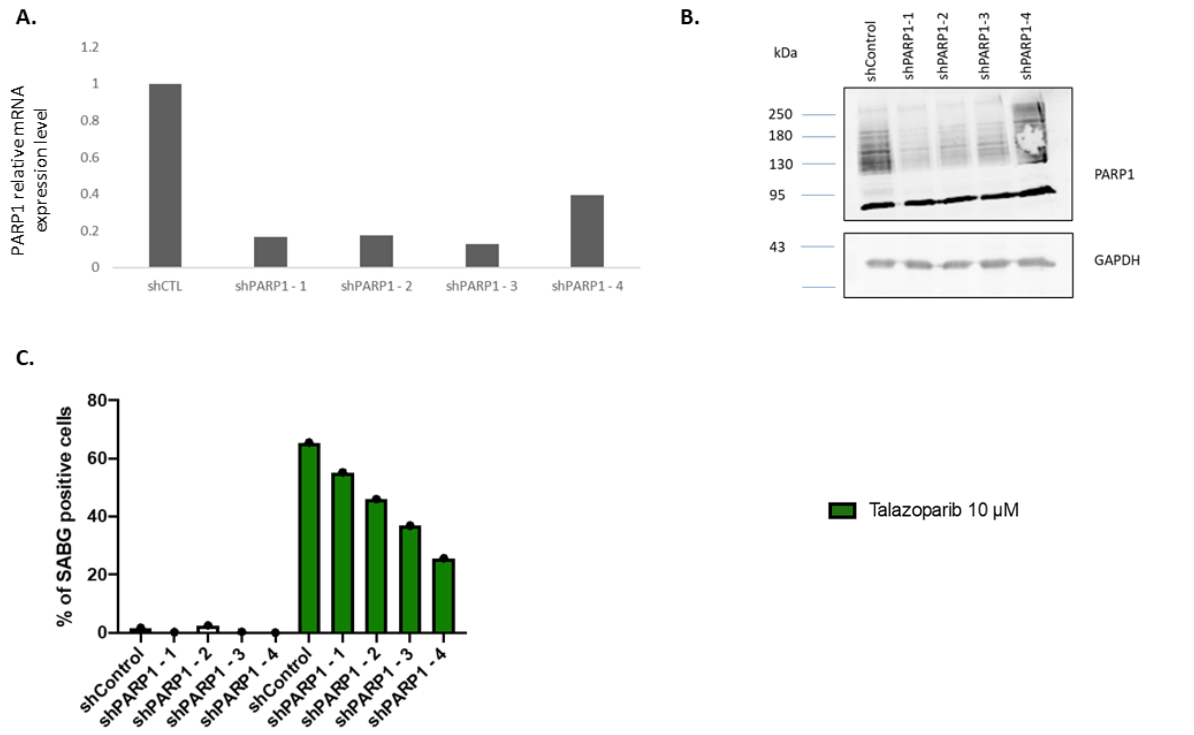

Figure S9 – The presence of PARP1 is required for the induction of the senescent phenotype. *(A) PARP1 relative mRNA expression level in H460 cells transduced with shControl, shPARP1 – 1, shPARP1 – 2, shPARP1 – 3 and shPARP1 – 4. (B) Protein level of PARP1 in H460 cells transduced with shControl, shPARP1 – 1, shPARP1 – 2, shPARP1 – 3 and shPARP1 – 4. (C) Percentage of SABGAL positive cells in H460 cells transduced with shControl, shPARP1 – 1, shPARP1 – 2, shPARP1 – 3 and shPARP1 – 4 incubated or not for 6 days with Talazoparib 10 µM. Data are shown as mean for one independent experiment.*

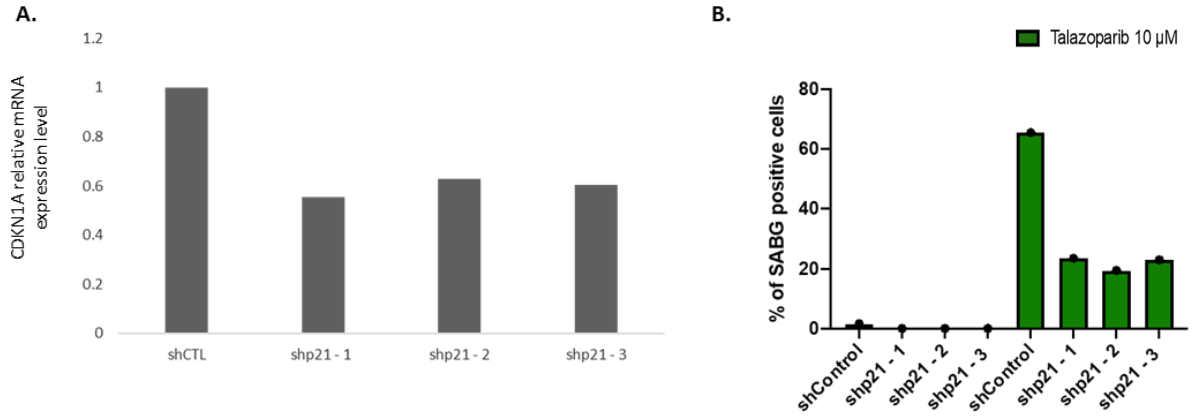

Figure S10 – The presence of CDKN1A is required for the induction of the senescent phenotype. *(A) CDKN1A relative mRNA expression level in H460 cells transduced with shControl, shp21 – 1, shp21 – 2 and shp21 – 3. (B) Percentage of SABGAL positive cells in H460 cells transduced with shControl, shp21 – 1, shp21 – 2 and shp21 – 3 incubated or not for 6 days with Talazoparib 10 µM. Data are shown as mean for one independent experiment.*

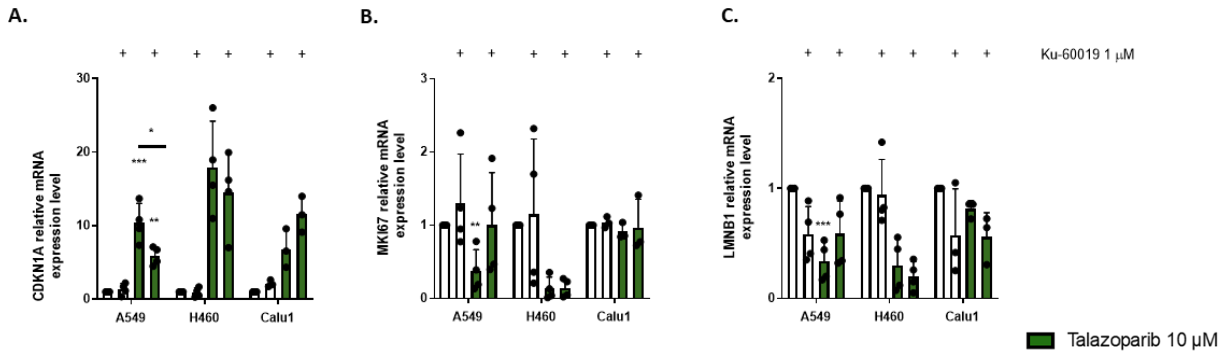

Figure S11 – ATM is required for the induction of the senescent phenotype. *(A) CDKN1A, (B) MKI67 and (C) LMNB1 relative mRNA expression level in A549 cells incubated for 6 days with DMSO (control), Ku-60019 (inhibitor of ATM) 1 µM, Talazoparib 10 µM or Ku-60019 1 µM combined to Talazoparib 10 µM. Data are shown as mean + SD. 3 independent experiments were performed. * p < 0.01, ** p < 0.01 and *** p < 0.001.*

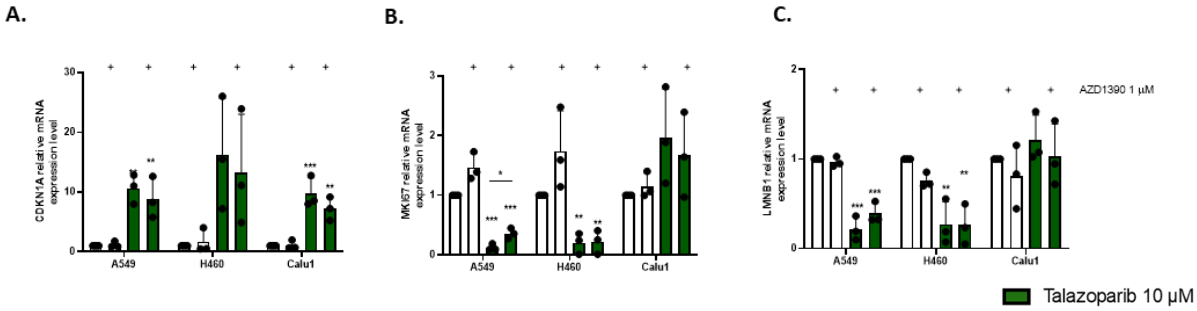

Figure S12 – ATM is required for the induction of the senescent phenotype. *(A) CDKN1A, (B) MKI67 and (C) LMNB1 relative mRNA expression level in A549 cells incubated for 6 days with DMSO (control), AZD1390 (inhibitor of ATM) 1 µM, Talazoparib 10 µM or AZD1390 1 µM combined to Talazoparib 10 µM. Data are shown as mean + SD. 3 independent experiments were performed. * p < 0.01, ** p < 0.01 and *** p < 0.001.*

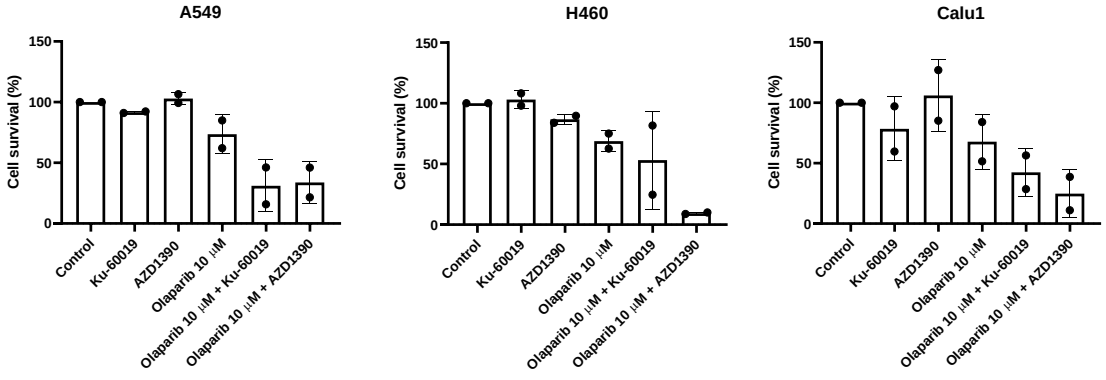

Figure S13 – Senescence protects against cell death. *A549, H460 and Calu1 cells were incubated for 6 days with DMSO (control), Ku-60019 1 µM, AZD1390 1 µM, Olaparib 10 µM, Olaparib 10 µM + Ku-60019 1 µM and Olaparib 10 µM + AZD1390 1 µM. Cell survival was evaluated with MTT. Data are shown as mean + SD. 2 independent experiments were performed.*

D. Discussion

The goal of this PhD thesis was to decipher the induction of senescence by irradiation with photons or protons combined or not with inhibitors of PARP in cancer cells. To this purpose, several cancer cell lines were irradiated with photons or protons or treated with inhibitors of PARP. Cancer cells were then assessed for several senescent markers. We demonstrated that photons and protons can induce a senescent-like phenotype in several cancer cell lines. Moreover, the senescent-like cancer cells could be further targeted by Navitoclax, an inhibitor of the Bcl-2 family members, to further increase cell death.

We also showed that inhibitors of PARP induced a senescent-like phenotype in several cancer cell lines. However, the senescent-like phenotype was not induced to the same extent when comparing the different inhibitors. Interestingly, the different inhibitors used possess the same ability to inhibit the catalytic site of PARP. Thus, our results indicated the ability to inhibit the catalytic site of PARP is not responsible for the induction of senescence in cancer cells. We are currently investigating if the trapping of PARP onto the DNA is responsible for the induction of the senescent-like phenotype observed in cancer cells incubated with the inhibitors of PARP. Indeed, the chosen inhibitors do not have the same capacity to induce PARP trapping. Furthermore, we have also designed a CRISPR/Cas9 experiment in order to knock-out PARP1 to determine if PARP1 is the sole contributor to the induction of the senescent-like phenotype by the inhibitors of PARP in cancer cells.

1. Definition of senescence in cancer cells

The current understanding of senescence is mainly derived from studies in fibroblasts. As demonstrated by several researchers, senescence can also be induced in several other cell types. In this work, we try to develop a better understanding of the induction of the senescent phenotype in cancer cells.

Senescence is associated with several markers: a change in morphology, cell cycle arrest, an increase in SA-β-Gal activity, a decreased expression in Lamin B1 at mRNA and protein levels, secretion of SASP, ... Interestingly, these senescent markers are not all visible depending on the inducer of senescence as well as depending on the cell line which is being studied. Furthermore, these markers are dynamics, for example, SASP is known to change over time.

SA-β-Gal is often considered as the most useful marker in the context of senescence. However, this dogma is currently evolving as SA-β-Gal might just be a marker of senescence similar to other markers. For these reasons, there is a growing interest in better characterizing the induction of cellular senescence in the context of cancer cells. Moreover, the growing interest in single-cell omic technologies recently made it possible to characterize the cells undergoing

senescence at single-cell level [246,247]. Furthermore, it seems that senescence is more heterogenous than what was once thought. For example, Troiani et al. showed that prostate cancer cells isolated from several mouse models could be gathered in eight distinct clusters according to their mRNA expression profile determined by single-cell RNA-sequencing analysis [122].

Senescence has often been regarded as being irreversible based on the pioneer research of Hayflick [77,78]. However, recent research demonstrated that at least in the context of therapy-induced senescence, the senescent state might be reversible. Indeed, Fleury et al. showed *in vitro* that ovarian cancer cells treated with Olaparib that became senescent could re-enter cell cycle if Olaparib treatment was removed [228]. In future studies, it would be necessary to characterize if the so-called senescent state is also reversible when induced by different molecules. It also remains to be determined if cancer cells enter a senescent state to protect themselves from cell death, how these cancer cells are capable of entering a senescent state and of exiting the senescent state.

2. Discovery of the new senescent markers

The markers which are currently used to define if cells are senescent are extremely heterogenous. Furthermore, the current markers are not specific to senescent cells. The use of single-cell RNA-sequencing analysis could allow researchers to discover new markers. Moreover, the use of these omic technologies would also allow to deeply characterize emerging markers such as markers of stemness. Indeed, Milanovic et al. proposed to add stemness as a new marker of cellular senescence [80].

Furthermore, interest in epi-transcriptomics is currently emerging due to the improvements made in omic technologies. Interestingly, epi-transcriptomics have been described as dynamic marks. In the context of stem cell research, m6A, one of the well-studied RNA modifications, is highly implicated in the plasticity of stem cells [248]. For this reason, RNA modifications might also be strongly implicated in the ability of cancer cells to undergo senescence. The field of RNA modifications remains, to this day, largely unexplored.

3. Induction of senescence in cancer cells

In this PhD project, senescence was successfully induced in A549, HCT-116, KP4 and MDA-MB-231 cancer cell lines following irradiation with photons and protons alone or combined with Olaparib. However, the percentage of SA-β-Gal positive cells was different depending on the cancer cell line which was analyzed. Furthermore, senescence was also observed after proton therapy in A549 cancer cell line, and after inhibition of PARP in A549, Calu-1, H460 cancer cell

lines. However, induction of senescence was not observed in H838 and H520 cells treated with PARP inhibitors (data not shown).

It remains to be determined if the induction of senescence depends on the treatment chosen. A549 cells were treated with conventional radiotherapy alone and with inhibitors of PARP alone showed different percentages in SA-β-Gal. 10% and 20% of A549 cells were positive for SA-β-Gal following 3 Gy and 5 Gy of X-rays, respectively. 80% and 95% of A549 cells were positive for SA-β-Gal following 1 µM and 10 µM of Talazoparib, respectively. However, cell survival was not equal between these treatments. Jochems et al. compared senescence induction by alisertib and etoposide in 13 cancer cell lines, and demonstrated that these 13 cancer cell lines entered senescence with percentage in SA-β-Gal reaching between 80 to 100%. The percentage in the number of cancer cells positive for SA-β-Gal was quite similar when induced by alisertib and etoposide. Only the PC9 cancer cell line demonstrated a different response. Indeed, the percentage of SA-β-Gal positive PC9 cancer cells was above 80% following etoposide, and around 50% following alisertib [249]. However, the authors do not specify the percentage of cell death following treatment with etoposide and alisertib in PC9 cancer cells. It thus remained to be determined if the induction of senescence is treatment dependent or not.

The percentage of senescence also seems to vary greatly between cancer cell lines. Indeed, we showed that induction of senescence following radiotherapy varied greatly between A549, HCT-116, KP4 and MDA-MB-231 cancer cell lines. We showed that A549 and MDA-MB-231 cancer cells exhibited the strongest senescent phenotype, HCT-116 cells demonstrated a mild induction of senescence while the induction of senescence was extremely limited in KP4 cells. In a similar fashion, the induction of senescence following inhibition of PARP greatly varied between A549, H460 and Calu1 cancer cell lines. Indeed, A549 and Calu1 cells showed a strong increase in the percentage of cells positive for SA-β-Gal reaching almost 100% after treatment with Talazoparib at 10 µM, whereas the percentage for H460 cells was around 50-60%.

SASP gene expression is heterogenous among senescent cancer cells. As previously mentioned, the SASP can have beneficial and deleterious effects in the context of cancer. The components of the SASP have been described in depth for fibroblasts, while the components are harder to define in the context of cancer cells. Indeed, we showed that A549 cells treated with photons or protons expressed IL-6, IL-8, IGFBP5 and to a lesser extent, CCL2. For HCT-116 cells treated with photons or protons, the expression of IL-6 and IL-8 was increased while the effect of irradiation was barely visible for IGFBP5 and CCL2. For KP4 cells treated with photons or protons, the expression of IL-6, IL-8 and IGFBP5 was not impacted by irradiation while the expression of CCL2 was increased. A549 cells incubated with Talazoparib demonstrated an increase in the expression of CCL2, IL-6, IL-8 while the expression of IGFBP5 was not changed. It thus seems that the components of the SASP can be influenced by the inducer of senescence

and the cell type. It has been noted that the SASP is more influenced by the cancer cell type than the inducer of senescence. Indeed, the authors showed that the SASP was fairly similar between cancer cells treated with etoposide and with cancer cells treated with alisertinib. The same cell lines were also treated with doxorubicin or with a CDK2/4/6 inhibitor, the expression of IL-6 and IL-8 was analyzed. Alisertinib, doxorubicin, CDK/2/4/6 inhibitor and etoposide induced a similar increase in the expression of IL-6 in A549 and Huh7 cells while, the expression of IL-6 was not increased in HCT-116 and MCF7 cells. Similar results were shown for the expression of IL-8 [249]. As the effects of senescent cancer cells on the tumor microenvironment is said to be mediated by the SASP, a better characterization of the SASP and its effects in the context of cancer is needed. The components of the SASP can be studied through ELISA, multiplex ELISA or mass spectrometry.

All of these observations seem to indicate that, in order to better understand therapy-induced senescence, it would be highly necessary to design studies comparing the induction of the senescent phenotype across cancer cell lines allowing researchers to determine the influence of the inducer and the influence of the cancer cell types. It is also necessary to design experiments in which compounds induce similar cell death as the activation of the DDR is highly implicated in determining cellular fate. The exposure of the cancer cells to the drug would also be carefully considered as Fleury at al. demonstrated that releasing treatment led to an escape from the senescent phenotype in ovarian cancer cells [119]. Furthermore, it also seems necessary to investigate the molecular mechanisms leading senescence in cancer cell lines following TIS. This should allow to better select compounds used in the context of cancer therapy and to either limit or increase the number of senescent cells following treatment. Furthermore, a better understanding of the SASP would allow to select or design compounds capable of neutralizing the negative effects of senescent cells on the tumor microenvironment.

4. Induction of senescence following proton therapy

Literature regarding the induction of senescence following particle therapy is extremely rare. Thus, comparison between the induction of senescence after conventional radiotherapy and proton therapy is of interest as more and more patients are being treated with proton therapy. 8% and 20% of A549 cells were positive for SA-β-Gal after irradiation with 3 Gy or 5 Gy of X-rays, respectively. In comparison, 12% of A549 cells were positive for SA-β-Gal in after irradiation with protons at a dose of 2.5 Gy. These results demonstrated that protons could induce senescence similarly to X-rays.

Schniewind et al. demonstrated that proton therapy induces less senescence in DU145 and PC3 prostate cancer cell lines as well as LN229 and U87MG GBM cancer cell lines when compared to conventional radiotherapy. The induction of senescence following proton

therapy was not different in FaDu and Cal33 head and neck cancer cell lines in comparison to conventional radiotherapy. This difference might be explained by the result of the 3D colony-formation assay. Indeed, the authors investigated the induction of senescence following 4 Gy of photons or protons. However, proton irradiation led to a significant reduction of clonogenic survival in LN229, U87MG, DU145 and PC3 cancer cell lines in comparison with photons whereas no difference in clonogenic survival was observed between FaDu and Cal33 cancer cell lines [207]. Results from our studies are different since the RBE of the proton beam was around 1.8-1.9, we can multiply 2.5 Gy by 1.8-1.9 to obtain 4.5-4.75 Gy. Thus, the percentage of SA-β-Gal in A549 cells is less important in protons than in X-rays for a biologically equivalent dose.

Further studies are thus required to determine if the induction of senescence is based on the quality of DNA damages or on their quantity which will then activate downstream targets. Further studies should also investigate other particles such as carbon ions since they are capable of inducing severe DNA double-strand breaks, which could result in a strong activation of ATM, a key player of the DDR implicated in the induction of senescence. Indeed, ATM has been defined as a strong inducer of CDKN1A. These investigations should be carried out *in vitro* to assess several markers of senescence. Results should then be verified *in vivo* as several senescent markers can be assessed both *in vitro* and *in vivo*.

Furthermore, the role of the dose rate and the fractionation schedule should also be investigated. Indeed, comparison between synchrotron microbeam radiation therapy (MRT) and conventional uniform broad beam (BB) was performed, and MRT significantly increased cellular senescence in melanoma cancer cells compared to BB. The researchers used a homogeneous beam which delivered a dose of 6.2 Gy to the tumor with a dose rate of 20.74 Gy/s/mA whereas, for the MRT, the same irradiation field was covered by 37 microbeams leading to a peak dose deposited in the tumor of 407.6 Gy, and the valley dose was 6.2 Gy with a dose rate of 68.78 Gy/s/mA. The BB which was applied as similar to the valley dose observed with MRT [215]. In a similar fashion, FLASH radiotherapy (FLASH-RT) uses a single ultra-high dose rate (40 Gy/s). FLASH-RT has been shown to strongly limit the effects to healthy tissues. In the context of lung progenitor cells, Fouillade et al. demonstrated that FLASH-RT limits the percentage of DNA damages in normal human lung cells *in vitro*. Furthermore, FLASH-RT also limits radio-induced senescence in the lungs of irradiated mice. However, it remains to be determined how high dose rate limits cellular senescence [250].

Fractionation also seems to have a different impact of the induction of senescence. Indeed, Zhang et al. demonstrated that 8 x 2 Gy and 1 x 10 Gy in A549 cancer cells led to a similar cell survival. However, the percentage of SA-β-Gal positive cells was strongly reduced in A549 cells irradiated with 8 x 2 Gy. Similar results were observed in H460 cancer cells [216].

It remains to be understood if these conclusions can also be drawn with other cancer cell lines as well as with high-LET particles.

5. Induction of senescence following PARP inhibition

Inhibitors of PARP are currently approved for the treatment of ovarian, breast, prostate and pancreatic cancers. Fleury et al. showed that the use of these inhibitors, namely, Olaparib, Niraparib and Talazoparib resulted in a strong induction of a senescent-like phenotype in ovarian and breast cancer cells [228]. We demonstrated that Olaparib could be used at sub-cytotoxic concentration in combination with conventional radiotherapy and proton therapy to induce senescence in A549, MDA-MB-231 and to a lesser extent in HCT-116 and KP4 cancer cells.

In order to observe if the induction of cellular senescence could occur following inhibition of PARP outside of ovarian and breast cancer cells, we used three NSCLC cancer cell lines: A549, Calu1 and H460. These three cell lines were incubated with Talazoparib. Following incubation with Talazoparib, a senescent-like phenotype was observed in the three chosen cancer cell lines. The senescent-like phenotype was characterized by a decrease in proliferation, an increase in the percentage of SA-β-Gal positive cells, a change in morphology, an increase in CDKN1A mRNA level and a decrease in MKI67 and LMNB1 mRNA levels.

The role of senescence following treatment with PARP inhibitors remained to be deciphered. Indeed, comparison between cells presenting with BRCA mutations (or mutations in DDR genes) and wild-type cells should be used. This experiment should allow to understand if senescence is used as a protective mechanism for cancer cells. If so, it would be highly interesting to determine the actors regulating the threshold behind the decision to switch cancer cells from cell death to senescence.

5.1. Molecular mechanisms

The intensity of the senescence was different in A549, Calu1 and H460 cells depending on the PARP inhibitor used. Indeed, treatments with 5 µM of Veliparib, Rucaparib, Olaparib, Niraparib and Talazoparib were compared in A549, Calu1 and H460 cells. Talazoparib demonstrated the strongest increase in senescence, followed by Niraparib, Olaparib, Rucaparib and Veliparib.

Of note, the mechanism of action of the inhibitors of PARP are not fully understood but it seems that these inhibitors exert their action through two distinct mechanisms. The first mechanism is the inhibition of the single-strand break repair which is characterized by a rapid synthesis of poly(ADP-ribose) (PAR). It seems that this mechanism is not implicated in the induction of senescence as A549, Calu1 and H460 cells incubated with the inhibitors since all

of them demonstrated a strong reduction in the synthesis of PAR. Talazoparib, Niraparib, Olaparib, Rucaparib and Veliparib, all provoked a complete abrogation of the PAR signal assayed by immunoblot. The second mechanism of action is through the trapping of PARP onto the DNA. Recently, Kim et al. demonstrated that the trapping of PARP1 onto the DNA by the inhibitors of PARP was responsible for the activation of PARP1-induced innate immune signaling in HeLa cells. Indeed, the authors demonstrated that Talazoparib, which is the strongest PARP trapper, led to the strongest innate immune signaling, followed by Niraparib, Olaparib, Rucaparib and Veliparib [226]. As Talazoparib and Niraparib have the highest ability to trap PARP onto the DNA, it seems reasonable to assume that the trapping of PARP could be responsible for the induction of the senescent-like phenotype we observed in this work. To test this hypothesis, we are currently using a fractionation assay in order to isolate proteins linked to the chromatin. The isolated proteins will then be revolved via immunoblot, and the amount of PARP1 linked to the chromatin will be quantified. We also tried to investigate the trapping of PARP through immunofluorescence staining. No difference was observed in A549 cells exposed or not with Talazoparib. However, the experiment was performed after 6 days of incubation with the inhibitor. It would be necessary to investigate the localization of PARP1 at earlier time points. Furthermore, it would also be possible to investigate the localization of PARP1 using live microscopy. If a difference in the trapping intensity between the inhibitors is observed as stated in the literature, the importance of PARP1 trapping for the induction of the senescent phenotype will further be investigated.

Interestingly, the trapping of PARP onto the DNA has been shown to be linked with the cytotoxicity of these inhibitors. It would thus be interesting to investigate the induction of senescence when the different inhibitors are used at their IC50. Furthermore, the increased cytotoxicity of Niraparib and Talazoparib could mean that increased trapping of PARP onto the DNA is linked with a higher number of DNA damages which could in turn, trigger the DDR. We are currently performing an immunolabeling for 53BP1 and gamma-H2AX, two markers of DSBs. We are also performing immunoblot for ATM and phospho-ATM. These two experiments will allow to compare the activation of the DDR between the different PARP inhibitors. Furthermore, to understand if the DDR is involved in senescence triggered by the inhibitors of PARP, several inhibitors of ATM, ATR and DNA-PK can be used. We showed that the inhibition of ATM significantly altered the expression of some markers of senescence. Indeed, the mRNA expression of CDKN1A was decreased and the mRNA expression of MKI67 and LMNB1 was increased in cancer cells treated with Talazoparib and ATM inhibitor compared to cancer cells treated with Talazoparib only. These preliminary results showed that ATM is important in the induction of the senescent-like phenotype. Moreover, treatment of cancer cells with inhibitors of PARP (Olaparib) and ATM inhibitor showed a strong impact on cell survival, thus showing a potential protective effect of the senescent phenotype on cancer cells. These results seem to indicate that when ATM is inhibited, cancer cells cannot enter the “protective” senescent-like phenotype leading to increased cell death.

The DDR is also implicated in the activation of the p53-p21 axis. These proteins are key actors in the induction of the senescent-like phenotype. In our work, the induction of senescence following inhibition of PARP seems to be independent of p53 as senescence was observed in Calu1 cells, which presents a homozygous deletion of p53. Interestingly, Calu1 cells did not demonstrate a decrease in the mRNA expression of MKI67 and LMNB1 compared to p53 wild type A549 and H460 cells. Interestingly, the MDA-MB-231 breast cancer cell line, which present a homozygous mutation in the p53 gene, also presented with a senescent-like phenotype when treated with Talazoparib but the MDA-MB-231 cells did not show a reduced expression in MKI67 and LMNB1 at mRNA levels. These results might indicate that p53 is involved in the induction of several features of senescence. To further understand in which senescent features, p53 is involved, it would be necessary to use a knock-out cell line for p53. For this reason, we used a CRISPR/Cas9 technique to delete the p53 gene from the A549 cancer cell lines using several CRISPR guides to create a large deletion in the gene. Unfortunately, several clones were isolated but at least, one wild-type copy of p53 remained in the isolated clones. Furthermore, according to the CCLE database, the A549 cancer cell line possesses 4 copies of the p53 gene. It is thus extremely difficult to target the p53 gene in A549 cells. To obtain a KO cell line, a frame-shift strategy could be adopted which is supposed to be a more efficient strategy than trying to create a large deletion in the gene. It could also be possible to re-perform a CRISPR KO on the isolated clones to remove the remaining copies of p53.

Moreover, Fleury et al. demonstrated that the senescent-like phenotype was p21-dependent [228]. Indeed, the authors showed that ovarian cancer cells transduced with a shRNA targeting CDKN1A showed a strong decrease in features of senescence (increase in EdU, increase in gamma-H2AX, decrease in clonogenicity and a strong increase in the percentage of clones with abnormal DNA). In this PhD project, A549 and H460 cells were also transduced with shRNA targeting CDKN1A to determine the importance of p21 in the observed phenotype. Preliminary data indicated that A549 and H460 cells transduced with shRNA targeting CDKN1A, presented a decreased senescent phenotype.

We also have to determine if PARP1 is the sole contributor to the senescent phenotype. Indeed, the inhibitors of PARP do not only target PARP1. To this purpose, we developed a CRISPR/Cas9 approach in order to knock-out (KO) PARP1. If a KO cell line is obtained, it would thus be possible to verify if the KO cell line treated with Talazoparib is still demonstrating a senescent phenotype. If Talazoparib does not induce a senescent phenotype in the KO cell line, it would mean that PARP1 is the sole contributor to the senescent phenotype. Moreover, it would be possible to introduce wild-type PARP1 in the KO cell line to verify if the presence of PARP1 can rescue the senescent phenotype. Furthermore, it would also be possible to introduce a trapping-deficient PARP1 into the KO cells as performed in [176]. If the trapping of

PARP1 onto the DNA is responsible for the senescent phenotype, the introduction of a wild-type PARP1 into the KO cell line should rescue the phenotype meaning that cells treated with Talazoparib should become senescent, whereas the introduction of the trapping-deficient PARP1 should not be able to rescue the phenotype meaning that cells treated with Talazoparib should not become senescent.

Furthermore, if the trapping of PARP1 onto the chromatin is demonstrated to be implicated in the senescent phenotype, the impact of the trapping of PARP1 could be further characterized. Indeed, the trapping of PARP onto the DNA is also known to severely impact the compaction of the chromatin [138]. Krastev et al. recently determined the proteins associated with PARP1 when PARP1 was trapped onto the DNA. They showed that there is an enrichment in spliceosome, RNA transport, ribosome biogenesis, protein processing in ER, base excision repair, sulfur metabolism, cysteine and methionine metabolism, autophagy, tight junctions, vitamin B6 metabolism, mRNA surveillance pathway, fatty acid degradation, sulfur relay system, proteasome and adherens junctions. Thus, the results demonstrated that PARP1 is tighly linked to mRNA processing and ribosome biogenesis which might strongly affect the transcription of genes implicated in the regulation of the senescent-like phenotype. It would be interesting to determine the compaction of the chromatin following treatment with PARP inhibitors using for example, with the MNase technique. The approach could then be completed using state of the art technologies such as CHIP-seq and/or ATAC-seq. Furthermore, to characterize the ribosome biogenesis, approaches such as Ribo-seq and polysome profiling could be used.

6. Improving cancer outcomes with senolytics

Baker et al. showed that the removal of senescent cells could strongly decrease the percentage of mice developing cancer [125]. This discovery led a strong interest in using senolytic agents to try to improve outcome in cancer patients. Several clinical trials with senolytics are currently on-going, but these clinical trials are focusing on the benefits of senolytics in the context of Alzheimer's disease, osteoarthritis, chronic kidney disease (for a review, see [251]). However, to our knowledge, no clinical trials is on-going in the context of cancer even though premises are being established by several teams to start clinical trials to evaluate the interest of using senolytics in the context of cancer.

Several senolytics namely, Dasatinib, Quercetin, Fisetin, A-1155463 and Piperlongumine (PPL) demonstrated a synergistic effect when combined with Olaparib in ovarian cancer cells. Similar effect was observed in MDA-MB-231 cancer cell line incubated with Navitoclax, A-1155463 and PPL in combination with Olaparib. Our results demonstrated that Navitoclax could trigger cell death in cancer cells treated with photons and protons. However, PPL was also unable to induce cell death in X-ray treated LNCaP and PC-3 cancer cell lines. These results

demonstrated that the regulation of apoptosis resistance following TIS is context-dependent. Senescent cells often display an upregulatation of several genes implicated in apoptosis that prevent them to undergo cell death. Moreover, the mechanism underlying the alteration of the expression of these genes are not clearly understood.

However, it has to be noted that senolytics also induce side effects. Thus, it is important to choose the senolytic with the highest ability to work in synergy with the senescent inducer, and then, to define the side effects of the senolytics. These side effects are mostly linked to thrombocytopenia (decrease in the number of platelets) [252]. Navitoclax has been associated with thrombocytopenia. Interestingly, the side effects of Navitoclax could be reduced thanks to the PROTAC technology. The PROTAC technology allows the targeted protein to be first, ubiquitinylated and then, to be in closed proximity to the proteasome to induce the specific degradation of the target. In the context of senolytic, He et al. demonstrated that Navitoclax could be converted to PZ15227 leading to the targeting of Bcl-XL to the cereblon E3 ligase for degradation. The convertion of Navitoclax to PZ15227 led to a reduced platelet toxicity while keeping similar senolytic activity of the initial compound [253].

7. Application to other cancer types

Treatment with agents inducing TIS combined with a senolytic could be applicable to several cancer types. It would be interesting to validate these results in ovarian cancer cells with and without BRCA mutation. Moreover, as mentioned above, several cancer cell lines did not enter in a senescent-like phenotype. It is thus highly important to further understand TIS. To this end, it would be possible to carry out a CRISPR/Cas9 screen to identify genes responsible for the induction of senescence in cancer cells as performed in [254].

8. Validation using mouse models

As all experiments performed in the context of this PhD thesis were performed *in vitro*, it would be highly important to see if these results can be recapitulated *in vivo*.

8.1. Immunocompromised models

To this end, nude mice should be implanted with A549, HCT-116, KP4 or MDA-MB-231 cancer cells. Mice will then be left alone until the tumor reaches a diameter of approximately 400 mm^3. Once the appropriate diameter is reached, the mice can be irradiated with photons or protons. These irradiations should be performed at the same dose rate as well as at biologically equivalent doses. Tumor samples should then be removed at different time post-irradiation (3 days, 7 days and 15 days) to evaluate the percentage of senescent in the tumor samples. This experiment would allow to determine the impact of the quality of radiation on

the induction of senescence. Then, it would be extremely important to perform similar experiments but in combination with an appropriate senolytic, meaning that the senolytic can work in synergy with the inducer of senescence, in this case, radiation. The appropriate sequence for the combination should be determined: before, at the same time or after radiation. Afterwards, it is also necessary to determine if the senolytic has to be given more than once. The tumor should then be removed and should be evaluated for percentage of senescence to determine if the senolytic is efficient *in vivo*. Furthermore, the mice have to be evaluated for side effects linked to the use of senolytic. Mice should be evaluated for tumor growth to determine if removing the senescent cells can improve survival of the mice. If survival is improved, it would be interesting to determine how the senescent cells drive tumor growth in the mice. For example, it could be possible to isolate senescent cells through flow cytometry, to define if the negative impact is being driven by SASP. If the impact is mainly being driven by the SASP, it would be interesting to analyze the composition of the SASP through mass spectrometry and lipidomics. It could also be interesting to determine the impact of senescent cells in a more complex environment, in an immune-competent model. These results could then be reproduced in an immune-competent mouse model such as the lewis lung carcinoma (LLC) mouse model.

The second part of the project dealing with the induction of senescence thanks to the use of PARP inhibitors should also be confirmed in an *in vivo* mouse model. In a similar fashion, nude mice should be implanted with A549 or H460 or Calu1 cancer cells. Mice should be left alone until the tumor reaches a diameter of 400 mm^3, then, mice can be injected with each of the PARP inhibitors alone in order to determine if Talazoparib is also leading to a stronger increase in the number of cells presenting with a senescent phenotype compared to other PARP inhibitors *in vivo*. Then, if PARP1 is responsible for the induction of senescence, nude mice can be implanted with A549 cells wild-type or with A549 cells knock-out for PARP1, and the level of senescence has to be compared between these two models. Then, both models have to be injected with the appropriate senolytic agent. Mice have to be checked for side effects. Tumor growth should then be followed until the diameter of the tumor reaches approximately 800 mm^3, which would lead to the sacrifice of the mice. These results would allow to define if senolytic can be used in combination with PARP inhibitors capable of inducing senescence.

8.2. Immunocompetent models

It would also be interesting to determine if the effects can be recapitulated in an *in vivo* model which is immunocompetent. Indeed, senescent cells are known to secrete several compounds referred as the SASP. Interestingly, the compounds of the SASP are often pro-inflammatory and thus, could have strong immuno-modulatory properties. In the context of this PhD thesis, we showed that several compounds of the SASP were upregulated. Indeed, we showed that A549, H460 and Calu1 cancer cell lines significantly upregulated the expression of CCL2 at

mRNA level. Interestingly, CCL2 can bind to CCR2 which is expressed at the surface of monocytes leading to their recruitment. These recruited monocytes will differentiate into macrophages, and can have a strong influence on the tumor microenvironment. Knowing the importance of the immune tumor microenvironment, defining the impact of the senescent cells onto the immune cells would thus be on great importance.

Furthermore, the immune cells are also known to be affected by senescence themselves which could also strongly impact the results mentioned above.

9. Validation using patient samples

Finally, the results could be validated using samples from patients treated with several PARP inhibitors as well as using samples from patients treated with conventional radiotherapy or protontherapy. However, obtaining samples of patients treated with conventional radiotherapy and protontherapy is extremely difficult. Moreover, the doses used in the context of conventional radiotherapy and protontherapy are often not comparable.

Depending on the type of fixation of the sample, different experiments can be performed [255]. Paraffin samples can be stained for Ki-67 and GL13 or for GL13 and p21. Senescent cells are Ki-67$^-$ and GL13$^+$ and p21$^+$. If the sample was placed in OCT, the percentage of SA-β-Gal positive cells can be determined. Moreover, several senescent markers can be determined through RT-qPCR for assessing the mRNA levels of genes such as LMNB1, IL-6, IL-8.

E. Conclusion

To sum up, the purpose of this PhD project was to characterize the induction of senescence following different inducers, namely irradiation with photons or protons as well as with the use of inhibitors of PARP.

In the first part of this PhD project, we demonstrated that irradiation with photons and protons led to a senescent phenotype in several cancer cell lines: A549 and MDA-MB-231 cells and to a lesser extent in: HCT-116 and KP4 cells. The senescent-like phenotype was characterized by an increase in the percentage of cells positive for SA-β-Gal, a decrease in proliferation as noted by the decrease in EdU labeling, an increase in CDKN1A at mRNA level and an increase in the expression of several components of the SASP at mRNA level. We also showed that combining radiation to an inhibitor of PARP, Olaparib, further enhanced the senescent-like phenotype which was observed. Moreover, these senescent-like cells could be further targeted by the use of Navitoclax to increase cell death (Figure 31).

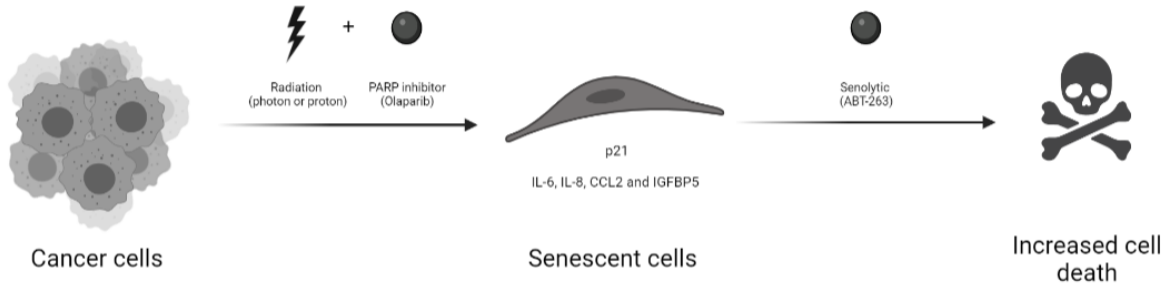

Figure 31 – Representation of the main findings of the first research article. Treatment of cancer cells with ionizing radiation (photons or protons) combined or not to PARP inhibitor (Olaparib) can induce senescence characterized by an increase at the mRNA level of CDKN1A (p21), IL-6, IL-8, CCL2 and IGFBP5. The senescent cells can be further targeted by a senolytic, ABT-263 in order to increase cell death.

In the second part of this PhD project, we wanted to decipher how PARP inhibitors are capable of inducing a senescent-like phenotype in cancer cells. To this purpose, A549, H460 and Calu1 cancer cells were treated with several inhibitors: Talazoparib, Niraparib, Olaparib, Rucaparib and Veliparib. We showed that Talazoparib is the strongest inducer of senescence in the three cancer cell lines. The catalytic inhibition of PARP was similar for the five inhibitors. Indeed, the five inhibitors completely abrogated the PAR signal as demonstrated through immunoblot. We are currently trying to determine if the trapping of PARP onto the DNA is responsible for the senescent-like phenotype. Furthermore, as inhibitors of PARP have been shown to not only target PARP1 but also PARP2, we are trying to determine PARP1 is the sole contributor to the senescent phenotype. To this end, a CRISPR/Cas9 experiment to knock-out PARP1 in A549 cancer cells was performed. With this technique, we generated two clones which are KO

for PARP1. The absence of PARP1 did not lead to a senescent phenotype in A549 cancer cells. This result demonstrated that PARP1 has to be present for a senescent phenotype to occur. (Figure 32). To decipher how PARP inhibitors induce a senescent phenotype, we have to determine if this effect is due to the trapping of PARP1 onto the chromatin. To this end, we will follow the localization of PARP1 within the cancer cells.

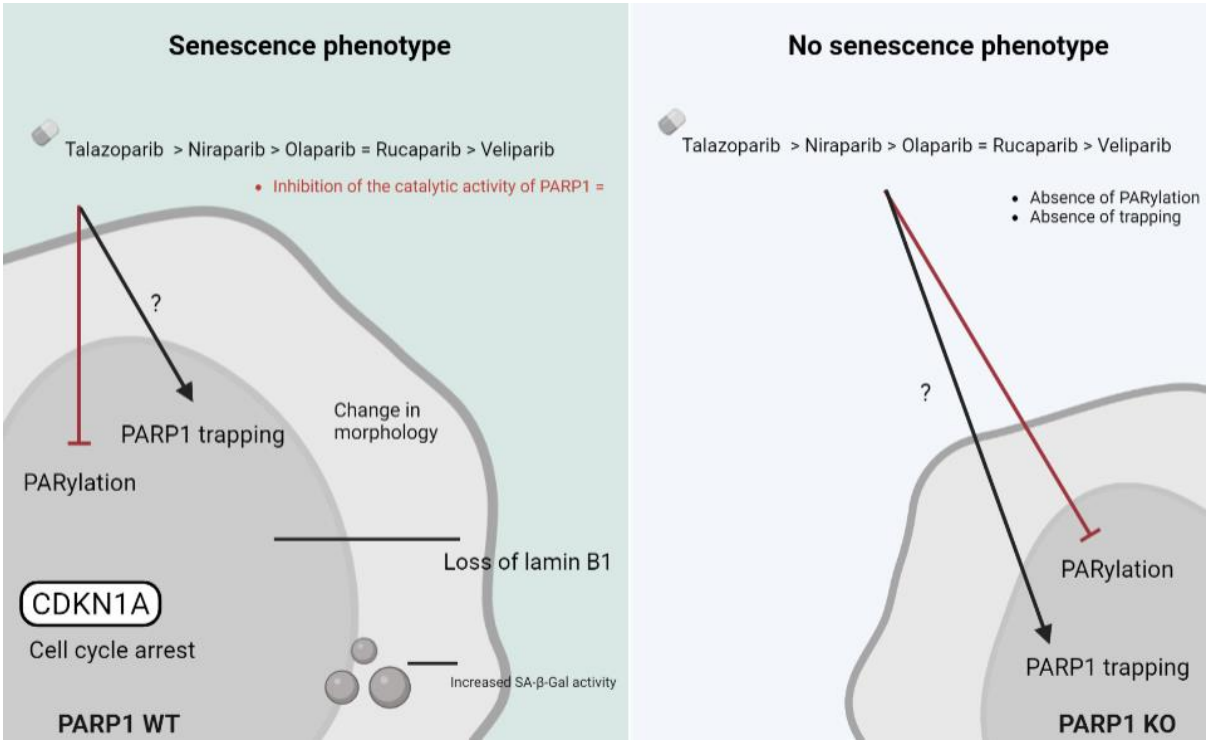

Figure 32 – Representation of the main findings of the second research article. In the presence of PARP1, Takazoparib induces a stronger senescent phenotype than counterparts (Niraparib, Olaparib, Rucaparib and Veliparib). The senescent phneotype is characterized by an increase in the expression of CDKN1A at mRNA level, a decrease in the expression of LMNB1 at mRNA level, a change in the area of nucleus and an increased senescence-associated beta-galactosidase activity. However, in the absence of PARP1, the PARP inhibitors did not induce the senescent.

This project generated several interesting *in vitro* results. Indeed, we showed that several anti-cancer therapies (photon and proton radiations as well as PARP inhibitors) induce the presence of senescent cells. As senescent cells have been associated with several negative effects in the context of cancer, we think that using senolytic might be a way to improve current treatments and to overcome resistance to anti-cancer treatments. Indeed, we added a senolytics to Oliparib used in combination with X-ray irradiation, a further decrease in cell survival curve was observed. These results have to be further explored preferably in an *in vivo* setting. The *in vivo* project would allow to characterize in depth the importance of the senescent-like phenotype induced by photons, protons and inhibitors of PARP. As more and more patients are being treated with particles, deciphering the differences between photons and protons is of the utmost importance. This PhD project opens the doors for several perspectives to hopefully answer the question regarding the impact of senescence in the context of therapy-induced senescence: when is senescence beneficial or detrimental to

cancer cells? The answer to this important question might bring new therapeutic venues for cancer patients.

F. References

1. Hajdu, S. I. A note from history: Landmarks in history of cancer, part 1. *Cancer* **117**, 1097–1102 (2011).
2. Weinberg, R. A. *The Biology of Cancer*.
3. Grünewald, T. G. *et al.* Sarcoma treatment in the era of molecular medicine. *EMBO Mol. Med.* **12**, (2020).
4. Tsolou, A. *et al.* Stemness and senescence related escape pathways are dose dependent in lung cancer cells surviving post irradiation. *Life Sci.* **242**, (2019).
5. Shain, A. H. & Bastian, B. C. From melanocytes to melanomas. *Nat. Rev. Cancer* **16**, 345–358 (2016).
6. Reiter, J. G. *et al.* An analysis of genetic heterogeneity in untreated cancers. *Nat. Rev. Cancer* **19**, 639–650 (2019).
7. Martínez-Jiménez, F. *et al.* A compendium of mutational cancer driver genes. *Nat. Rev. Cancer* **20**, 555–572 (2020).
8. Craene, B. D. & Berx, G. Regulatory networks defining EMT during cancer initiation and progression. *Nat. Rev. Cancer* **13**, 97–110 (2013).
9. Hanahan, D. & Weinberg, R. A. The Hallmarks of Cancer. *Cell* **100**, 57–70 (2000).
10. Hanahan, D. & Weinberg, R. A. Hallmarks of Cancer: The Next Generation. *Cell* **144**, 646–674 (2011).
11. Hanahan, D. Hallmarks of Cancer: New Dimensions. *Cancer Discov.* **12**, 31–46 (2022).
12. Sung, H. *et al.* Global Cancer Statistics 2020: GLOBOCAN Estimates of Incidence and Mortality Worldwide for 36 Cancers in 185 Countries. *CA. Cancer J. Clin.* **71**, 209–249 (2021).
13. Rahib, L. *et al.* Projecting Cancer Incidence and Deaths to 2030: The Unexpected Burden of Thyroid, Liver, and Pancreas Cancers in the United States. *Cancer Res.* **74**, 2913–2921 (2014).
14. Wu, S., Zhu, W., Thompson, P. & Hannun, Y. A. Evaluating intrinsic and non-intrinsic cancer risk factors. *Nat. Commun.* **9**, 3490 (2018).
15. Tomasetti, C. & Vogelstein, B. Variation in cancer risk among tissues can be explained by the number of stem cell divisions. *Science* **347**, 78–81 (2015).
16. Wu, S., Powers, S., Zhu, W. & Hannun, Y. A. Substantial contribution of extrinsic risk factors to cancer development. *Nature* **529**, 43–47 (2016).
17. Chabner, B. A. & Roberts, T. G. Chemotherapy and the war on cancer. *Nat. Rev. Cancer* **5**, 65–72 (2005).
18. DeVita, V. T. & Chu, E. A History of Cancer Chemotherapy. *Cancer Res.* **68**, 8643–8653 (2008).
19. Sherr, C. J. & Bartek, J. Cell Cycle–Targeted Cancer Therapies. *Annu. Rev. Cancer Biol.* **1**, 41–57 (2017).
20. Waldman, A. D., Fritz, J. M. & Lenardo, M. J. A guide to cancer immunotherapy: from T cell basic science to clinical practice. *Nat. Rev. Immunol.* **20**, 651–668 (2020).
21. Vaddepally, R. K., Kharel, P., Pandey, R., Garje, R. & Chandra, A. B. Review of Indications of FDA-Approved Immune Checkpoint Inhibitors per NCCN Guidelines with the Level of Evidence. *Cancers* **12**, 738 (2020).
22. Boutros, C. *et al.* Safety profiles of anti-CTLA-4 and anti-PD-1 antibodies alone and in combination. *Nat. Rev. Clin. Oncol.* **13**, 473–486 (2016).

23. Seidel, J. A., Otsuka, A. & Kabashima, K. Anti-PD-1 and Anti-CTLA-4 Therapies in Cancer: Mechanisms of Action, Efficacy, and Limitations. *Front. Oncol.* **8**, 86 (2018).
24. Ramos-Casals, M. *et al.* Immune-related adverse events of checkpoint inhibitors. *Nat. Rev. Dis. Primer* **6**, 38 (2020).
25. DeNardo, D. G. & Ruffell, B. Macrophages as regulators of tumour immunity and immunotherapy. *Nat. Rev. Immunol.* **19**, 369–382 (2019).
26. Durante, M. & Loeffler, J. S. Charged particles in radiation oncology. *Nat. Rev. Clin. Oncol.* **7**, 37–43 (2010).
27. Atun, R. *et al.* Expanding global access to radiotherapy. *Lancet Oncol.* **16**, 1153–1186 (2015).
28. Durante, M., Orecchia, R. & Loeffler, J. S. Charged-particle therapy in cancer: clinical uses and future perspectives. *Nat. Rev. Clin. Oncol.* **14**, 483–495 (2017).
29. Tinganelli, W. & Durante, M. Carbon Ion Radiobiology. *Cancers* **12**, 3022 (2020).
30. Huart, C., Chen, J.-W., Le Calvé, B., Michiels, C. & Wéra, A.-C. Could Protons and Carbon Ions Be the Silver Bullets Against Pancreatic Cancer? *Int. J. Mol. Sci.* **21**, 4767 (2020).
31. Mould, R. F. Invited review : Rontgen and the discovery of X-rays. *Br. J. Radiol.* **68**, 1145–76.
32. Alsharef, S., Alanazi, M., Alharthi, F., Qandil, D. & Qushawy, M. Review about radiopharmaceuticals: preparation, radioactivity and applications. *Int. J. Appl. Pharm.* 8–15 (2020).
33. Huh, H. D. & Kim, S. History of Radiation Therapy Technology. *Prog. Med. Phys.* **31**, 124–134 (2020).
34. *Medical Imaging Systems: An Introductory Guide*. vol. 11111 (Springer International Publishing, 2018).
35. Wéra, A.-C., Riquier, H., Heuskin, A.-C., Michiels, C. & Lucas, S. In vitro irradiation station for broad beam radiobiological experiments. *Nucl. Instrum. Methods Phys. Res. Sect. B Beam Interact. Mater. At.* **269**, 3120–3124 (2011).
36. *Basic clinical radiobiology*. (Hodder Arnold, 2009).
37. Murshed, H. Radiation Biology. in *Fundamentals of Radiation Oncology* 57–87 (Elsevier, 2019).
38. Loeffler, J. S. & Durante, M. Charged particle therapy—optimization, challenges and future directions. *Nat. Rev. Clin. Oncol.* **10**, 411–424 (2013).
39. Wéra, A.-C., Heuskin, A.-C., Riquier, H., Michiels, C. & Lucas, S. Low-LET Proton Irradiation of A549 Non-small Cell Lung Adenocarcinoma Cells: Dose Response and RBE Determination. *Radiat. Res.* **179**, 273–281 (2013).
40. Franken, N. A. P., Rodermond, H. M., Stap, J., Haveman, J. & van Bree, C. Clonogenic assay of cells in vitro. *Nat. Protoc.* **1**, 2315–2319 (2006).
41. Withers, H. R. The Four R's of Radiotherapy. in *Advances in Radiation Biology* vol. 5 241–271 (Elsevier, 1975).
42. Steel, G. G., McMillan, T. J. & Peacock, J. H. The 5Rs of Radiobiology. *Int. J. Radiat. Biol.* **56**, 1045–1048 (1989).
43. Boustani, Grapin, Laurent, Apetoh, & Mirjolet. The 6th R of Radiobiology: Reactivation of Anti-Tumor Immune Response. *Cancers* **11**, 860 (2019).
44. Galluzzi, L., Buqué, A., Kepp, O., Zitvogel, L. & Kroemer, G. Immunogenic cell death in cancer and infectious disease. *Nat. Rev. Immunol.* **17**, 97–111 (2017).

45. Vanpouille-Box, C. *et al.* DNA exonuclease Trex1 regulates radiotherapy-induced tumour immunogenicity. *Nat. Commun.* **8**, 15618 (2017).
46. Azad, A. *et al.* PD-L1 blockade enhances response of pancreatic ductal adenocarcinoma to radiotherapy. *EMBO Mol. Med.* **9**, 167–180 (2017).
47. Sato, H. *et al.* DNA double-strand break repair pathway regulates PD-L1 expression in cancer cells. *Nat. Commun.* **8**, 1751 (2017).
48. Demaria, S., Pilones, K. A., Vanpouille-Box, C., Golden, E. B. & Formenti, S. C. The Optimal Partnership of Radiation and Immunotherapy: from Preclinical Studies to Clinical Translation. *Radiat. Res.* **182**, 170–181 (2014).
49. Dewan, M. Z. *et al.* Fractionated but Not Single-Dose Radiotherapy Induces an Immune-Mediated Abscopal Effect when Combined with Anti–CTLA-4 Antibody. *Clin. Cancer Res.* **15**, 5379–5388 (2009).
50. Kong, Y. *et al.* Optimizing the Treatment Schedule of Radiotherapy Combined With Anti-PD-1/PD-L1 Immunotherapy in Metastatic Cancers. *Front. Oncol.* **11**, 638873 (2021).
51. Wang, H., Jiang, H., Van De Gucht, M. & De Ridder, M. Hypoxic Radioresistance: Can ROS Be the Key to Overcome It? *Cancers* **11**, 112 (2019).
52. Antonovic, L. *et al.* Clinical oxygen enhancement ratio of tumors in carbon ion radiotherapy: the influence of local oxygenation changes. *J. Radiat. Res. (Tokyo)* **55**, 902–911 (2014).
53. Robert Grimes, D. & Partridge, M. A mechanistic investigation of the oxygen fixation hypothesis and oxygen enhancement ratio. *Biomed. Phys. Eng. Express* **1**, 045209 (2015).
54. Bury, M., Le Calvé, B., Ferbeyre, G., Blank, V. & Lessard, F. New Insights into CDK Regulators: Novel Opportunities for Cancer Therapy. *Trends Cell Biol.* **31**, 331–344 (2021).
55. Otto, T. & Sicinski, P. Cell cycle proteins as promising targets in cancer therapy. *Nat. Rev. Cancer* **17**, 93–115 (2017).
56. Held, K. D. *et al.* Effects of Charged Particles on Human Tumor Cells. *Front. Oncol.* **6**, (2016).
57. Durante, M., Brenner, D. J. & Formenti, S. C. Does Heavy Ion Therapy Work Through the Immune System? *Int. J. Radiat. Oncol.* **96**, 934–936 (2016).
58. Gameiro, S. R. *et al.* Tumor Cells Surviving Exposure to Proton or Photon Radiation Share a Common Immunogenic Modulation Signature, Rendering Them More Sensitive to T Cell–Mediated Killing. *Int. J. Radiat. Oncol.* **95**, 120–130 (2016).
59. Chiblak, S. *et al.* Carbon irradiation overcomes glioma radioresistance by eradicating stem cells and forming an antiangiogenic and immunopermissive niche. *JCI Insight* **4**, e123837 (2019).
60. Langendijk, J. A. *et al.* National Protocol for Model-Based Selection for Proton Therapy in Head and Neck Cancer. *Int. J. Part. Ther.* **8**, 354–365 (2021).
61. Roos, W. P., Thomas, A. D. & Kaina, B. DNA damage and the balance between survival and death in cancer biology. *Nat. Rev. Cancer* **16**, 20–33 (2016).
62. Anne-Catherine Wera - PhD thesis (2012) - Development of an in vitro irradiation station for broad beam radiobiological experiment: study of A549 non-small cell lung cancer cell response after irradiation with charged particles of different LET.
63. Mah, L.-J., El-Osta, A. & Karagiannis, T. C. γH2AX: a sensitive molecular marker of DNA damage and repair. *Leukemia* **24**, 679–686 (2010).

64. Burma, S., Chen, B. P., Murphy, M., Kurimasa, A. & Chen, D. J. ATM Phosphorylates Histone H2AX in Response to DNA Double-strand Breaks. *J. Biol. Chem.* **276**, 42462–42467 (2001).
65. An, J. *et al.* DNA-PKcs plays a dominant role in the regulation of H2AX phosphorylation in response to DNA damage and cell cycle progression. *BMC Mol. Biol.* **11**, 18 (2010).
66. Sulli, G., Di Micco, R. & di Fagagna, F. d'Adda. Crosstalk between chromatin state and DNA damage response in cellular senescence and cancer. *Nat. Rev. Cancer* **12**, 709–720 (2012).
67. Chang, H. H. Y., Pannunzio, N. R., Adachi, N. & Lieber, M. R. Non-homologous DNA end joining and alternative pathways to double-strand break repair. *Nat. Rev. Mol. Cell Biol.* **18**, 495–506 (2017).
68. Scully, R., Panday, A., Elango, R. & Willis, N. A. DNA double-strand break repair-pathway choice in somatic mammalian cells. *Nat. Rev. Mol. Cell Biol.* **20**, 698–714 (2019).
69. Chatterjee, N. & Walker, G. C. Mechanisms of DNA damage, repair, and mutagenesis: DNA Damage and Repair. *Environ. Mol. Mutagen.* **58**, 235–263 (2017).
70. Kerr, J. F. R., Wyllie, A. H. & Currie, A. R. Apoptosis: A Basic Biological Phenomenon with Wideranging Implications in Tissue Kinetics. *Br. J. Cancer* **26**, 239–257 (1972).
71. Singh, R., Letai, A. & Sarosiek, K. Regulation of apoptosis in health and disease: the balancing act of BCL-2 family proteins. *Nat. Rev. Mol. Cell Biol.* **20**, 175–193 (2019).
72. Castedo, M. *et al.* Cell death by mitotic catastrophe: a molecular definition. *Oncogene* **23**, 2825–2837 (2004).
73. Kroemer, G., Galassi, C., Zitvogel, L. & Galluzzi, L. Immunogenic cell stress and death. *Nat. Immunol.* **23**, 487–500 (2022).
74. Fucikova, J. *et al.* Detection of immunogenic cell death and its relevance for cancer therapy. *Cell Death Dis.* **11**, 1013 (2020).
75. Galluzzi, L. *et al.* Consensus guidelines for the definition, detection and interpretation of immunogenic cell death. *J. Immunother. Cancer* **8**, e000337 (2020).
76. Lauber, K., Ernst, A., Orth, M., Herrmann, M. & Belka, C. Dying cell clearance and its impact on the outcome of tumor radiotherapy. *Front. Oncol.* **2**, (2012).
77. Hayflick, L. The Limited In Vitro Lifetime Of Human Diploid Cell Strains. *Exp. Cell Res.* **37**, 614–636 (1965).
78. Hayflick, L. & Moorhead, P. S. The serial cultivation of human diploid cell strains. *Exp. Cell Res.* **25**, 585–621 (1961).
79. Lee, S. & Schmitt, C. A. The dynamic nature of senescence in cancer. *Nat. Cell Biol.* **21**, 94–101 (2019).
80. Milanovic, M. *et al.* Senescence-associated reprogramming promotes cancer stemness. *Nature* **553**, 96–100 (2018).
81. Frey, N., Venturelli, S., Zender, L. & Bitzer, M. Cellular senescence in gastrointestinal diseases: from pathogenesis to therapeutics. *Nat. Rev. Gastroenterol. Hepatol.* **15**, 81–95 (2018).
82. d'Adda di Fagagna, F. Living on a break: cellular senescence as a DNA-damage response. *Nat. Rev. Cancer* **8**, 512–522 (2008).
83. Lujambio, A. To clear, or not to clear (senescent cells)? That is the question: Clearance of senescent cells. *BioEssays* **38**, S56–S64 (2016).

84. Gabai, Y., Assouline, B. & Ben-Porath, I. Senescent stromal cells: roles in the tumor microenvironment. *Trends Cancer* S2405803322001935 (2022) doi:10.1016/j.trecan.2022.09.002.
85. Krtolica, A., Parrinello, S., Lockett, S., Desprez, P.-Y. & Campisi, J. Senescent fibroblasts promote epithelial cell growth and tumorigenesis: A link between cancer and aging. *Proc. Natl. Acad. Sci.* **98**, 12072–12077 (2001).
86. Liu, X., Hoft, D. F. & Peng, G. Senescent T cells within suppressive tumor microenvironments: emerging target for tumor immunotherapy. *J. Clin. Invest.* **130**, 1073–1083 (2020).
87. Fagagna, F. d'Adda di *et al.* A DNA damage checkpoint response in telomere-initiated senescence. *Nature* **426**, 194–198 (2003).
88. Herbig, U., Jobling, W. A., Chen, B. P. C., Chen, D. J. & Sedivy, J. M. Telomere Shortening Triggers Senescence of Human Cells through a Pathway Involving ATM, p53, and p21CIP1, but Not p16INK4a. *Mol. Cell* **14**, 501–513 (2004).
89. Dobler, C., Jost, T., Hecht, M., Fietkau, R. & Distel, L. Senescence Induction by Combined Ionizing Radiation and DNA Damage Response Inhibitors in Head and Neck Squamous Cell Carcinoma Cells. *Cells* **9**, 2012 (2020).
90. Aasland, D. *et al.* Temozolomide Induces Senescence and Repression of DNA Repair Pathways in Glioblastoma Cells via Activation of ATR–CHK1, p21, and NF-κB. *Cancer Res.* **79**, 99–113 (2019).
91. Marcos, Malumbres. Cyclin dependent kinases. *Genome Biol.* (2014).
92. Campisi, J. & d'Adda di Fagagna, F. Cellular senescence: when bad things happen to good cells. *Nat. Rev. Mol. Cell Biol.* **8**, 729–740 (2007).
93. Brown, J. P., Wei, W. & Sedivy, J. M. Bypass of Senescence After Disruption of p21 $^{CIP1/WAF1}$ Gene in Normal Diploid Human Fibroblasts. *Science* **277**, 831–834 (1997).
94. Fang, L. *et al.* p21Waf1/Cip1/Sdi1 induces permanent growth arrest with markers of replicative senescence in human tumor cells lacking functional p53. *Oncogene* **18**, 2789–2797 (1999).
95. Hsu, C.-H., Altschuler, S. J. & Wu, L. F. Patterns of Early p21 Dynamics Determine Proliferation-Senescence Cell Fate after Chemotherapy. *Cell* **178**, 361-373.e12 (2019).
96. Wong, H. & Riabowol, K. Differential CDK-inhibitor gene expression in aging human diploid fibroblasts. *Exp. Gerontol.* **31**, 311–325 (1996).
97. Hara, E. *et al.* Regulation of p16CDKN2 expression and its implications for cell immortalization and senescence. *Mol. Cell. Biol.* **16**, 859–867 (1996).
98. Alcorta, D. A. *et al.* Involvement of the cyclin-dependent kinase inhibitor p16 (INK4a) in replicative senescence of normal human fibroblasts. *Proc. Natl. Acad. Sci.* **93**, 13742–13747 (1996).
99. Bracken, A. P., Ciro, M., Cocito, A. & Helin, K. E2F target genes: unraveling the biology. *Trends Biochem. Sci.* **29**, 409–417 (2004).
100. Hernandez-Segura, A., Nehme, J. & Demaria, M. Hallmarks of Cellular Senescence. *Trends Cell Biol.* **28**, 436–453 (2018).
101. Nishio, K., Inoue, A., Qiao, S., Kondo, H. & Mimura, A. Senescence and cytoskeleton: overproduction of vimentin induces senescent-like morphology in human fibroblasts. *Histochem. Cell Biol.* **116**, 321–327 (2001).
102. Druelle, C. *et al.* ATF6α regulates morphological changes associated with senescence in human fibroblasts. *Oncotarget* **7**, 67699–67715 (2016).

103. Volonte, D. & Galbiati, F. Caveolin-1, a master regulator of cellular senescence. *Cancer Metastasis Rev.* **39**, 397–414 (2020).
104. Freund, A., Laberge, R.-M., Demaria, M. & Campisi, J. Lamin B1 loss is a senescence-associated biomarker. *Mol. Biol. Cell* **23**, 2066–2075 (2012).
105. Motwani, M., Pesiridis, S. & Fitzgerald, K. A. DNA sensing by the cGAS–STING pathway in health and disease. *Nat. Rev. Genet.* **20**, 657–674 (2019).
106. Debacq-Chainiaux, F., Erusalimsky, J. D., Campisi, J. & Toussaint, O. Protocols to detect senescence-associated beta-galactosidase (SA-βgal) activity, a biomarker of senescent cells in culture and in vivo. *Nat. Protoc.* **4**, 1798–1806 (2009).
107. Lee, B. Y. Senescence-associated beta-galactosidase is lysosomal beta-galactosidase. *Aging Cell* **5**, 187–195 (2006).
108. Rodier, F. *et al.* DNA-SCARS: distinct nuclear structures that sustain damage-induced senescence growth arrest and inflammatory cytokine secretion. *J. Cell Sci.* **124**, 68–81 (2011).
109. Narita, M. *et al.* Rb-Mediated Heterochromatin Formation and Silencing of E2F Target Genes during Cellular Senescence. *Cell* **113**, 703–716 (2003).
110. Jochems, F. *et al.* The Cancer SENESCopedia: A delineation of cancer cell senescence. *Cell Rep.* **36**, 109441 (2021).
111. Wang, E. Senescent human fibroblasts resist programmed cell death, and failure to suppress bcl2 is involved. *Cancer Research* (1995).
112. Marcotte, R., Lacelle, C. & Wang, E. Senescent fibroblasts resist apoptosis by downregulating caspase-3. *Mech. Ageing Dev.* **125**, 777–783 (2004).
113. Sturmlechner, I. *et al.* Senescent cells limit p53 activity via multiple mechanisms to remain viable. *Nat. Commun.* **13**, 3722 (2022).
114. Fuhrmann-Stroissnigg, H. *et al.* Identification of HSP90 inhibitors as a novel class of senolytics. *Nat. Commun.* **8**, 422 (2017).
115. Al-Khalaf, H. H. & Aboussekhra, A. Survivin expression increases during aging and enhances the resistance of aged human fibroblasts to genotoxic stress. *AGE* **35**, 549–562 (2013).
116. Ma, K. *et al.* Nuclear accumulation of Yes-Associated Protein (YAP) maintains the survival of doxorubicin-induced senescent cells by promoting survivin expression. *Cancer Lett.* **375**, 84–91 (2016).
117. Hu, L. *et al.* Why Senescent Cells Are Resistant to Apoptosis: An Insight for Senolytic Development. *Front. Cell Dev. Biol.* **10**, 822816 (2022).
118. Gosselin, K. *et al.* Senescence-Associated Oxidative DNA Damage Promotes the Generation of Neoplastic Cells. *Cancer Res.* **69**, 7917–7925 (2009).
119. Fleury, H. *et al.* Exploiting interconnected synthetic lethal interactions between PARP inhibition and cancer cell reversible senescence. *Nat. Commun.* **10**, 2556 (2019).
120. Lee, S. & Schmitt, C. A. The dynamic nature of senescence in cancer. *Nat. Cell Biol.* **21**, 94–101 (2019).
121. Yu, X. *et al.* Radiation-promoted CDC6 protein stability contributes to radioresistance by regulating senescence and epithelial to mesenchymal transition. *Oncogene* **38**, 549–563 (2019).
122. Troiani, M. *et al.* Single-cell transcriptomics identifies Mcl-1 as a target for senolytic therapy in cancer. *Nat. Commun.* **13**, 2177 (2022).

123. Coppé, J.-P. *et al.* Senescence-Associated Secretory Phenotypes Reveal Cell-Nonautonomous Functions of Oncogenic RAS and the p53 Tumor Suppressor. *PLoS Biol.* **6**, e301 (2008).
124. Liu, D. & Hornsby, P. J. Senescent Human Fibroblasts Increase the Early Growth of Xenograft Tumors via Matrix Metalloproteinase Secretion. *Cancer Res.* **67**, 3117–3126 (2007).
125. Baker, D. J. *et al.* Naturally occurring p16Ink4a-positive cells shorten healthy lifespan. *Nature* **530**, 184–189 (2016).
126. Wang, L., Lankhorst, L. & Bernards, R. Exploiting senescence for the treatment of cancer. *Nat. Rev. Cancer* **22**, 340–355 (2022).
127. Krishnamurthy, J. *et al.* Ink4a/Arf expression is a biomarker of aging. *J. Clin. Invest.* **114**, 1299–1307 (2004).
128. Baker, D. J. *et al.* Clearance of p16Ink4a-positive senescent cells delays ageing-associated disorders. *Nature* **479**, 232–236 (2011).
129. Demaria, M. *et al.* Cellular Senescence Promotes Adverse Effects of Chemotherapy and Cancer Relapse. *Cancer Discov.* **7**, 165–176 (2017).
130. Baar, M. P. *et al.* Targeted Apoptosis of Senescent Cells Restores Tissue Homeostasis in Response to Chemotoxicity and Aging. *Cell* **169**, 132-147.e16 (2017).
131. Triana-Martínez, F. *et al.* Identification and characterization of Cardiac Glycosides as senolytic compounds. *Nat. Commun.* **10**, 4731 (2019).
132. Di Micco, R., Krizhanovsky, V., Baker, D. & d'Adda di Fagagna, F. Cellular senescence in ageing: from mechanisms to therapeutic opportunities. *Nat. Rev. Mol. Cell Biol.* **22**, 75–95 (2021).
133. Souers, A. J. *et al.* ABT-199, a potent and selective BCL-2 inhibitor, achieves antitumor activity while sparing platelets. *Nat. Med.* **19**, 202–208 (2013).
134. Hanzlikova, H., Gittens, W., Krejcikova, K., Zeng, Z. & Caldecott, K. W. Overlapping roles for PARP1 and PARP2 in the recruitment of endogenous XRCC1 and PNKP into oxidized chromatin. *Nucleic Acids Res.* (2016).
135. Schreiber, V., Dantzer, F., Ame, J.-C. & de Murcia, G. Poly(ADP-ribose): novel functions for an old molecule. *Nat. Rev. Mol. Cell Biol.* **7**, 517–528 (2006).
136. Todorova, T., Bock, F. J. & Chang, P. PARP13 regulates cellular mRNA post-transcriptionally and functions as a pro-apoptotic factor by destabilizing TRAILR4 transcript. *Nat. Commun.* **5**, 5362 (2014).
137. Liu, L. *et al.* The key players of parthanatos: opportunities for targeting multiple levels in the therapy of parthanatos-based pathogenesis. *Cell. Mol. Life Sci.* **79**, 60 (2022).
138. Ray Chaudhuri, A. & Nussenzweig, A. The multifaceted roles of PARP1 in DNA repair and chromatin remodelling. *Nat. Rev. Mol. Cell Biol.* **18**, 610–621 (2017).
139. Messner, S. *et al.* PARP1 ADP-ribosylates lysine residues of the core histone tails. *Nucleic Acids Res.* **38**, 6350–6362 (2010).
140. Poirier, G. G., de Murcia, G., Jongstra-Bilen, J., Niedergang, C. & Mandel, P. Poly(ADP-ribosyl)ation of polynucleosomes causes relaxation of chromatin structure. *Proc. Natl. Acad. Sci.* **79**, 3423–3427 (1982).
141. Ahel, D. *et al.* Poly(ADP-ribose)–Dependent Regulation of DNA Repair by the Chromatin Remodeling Enzyme ALC1. *Science* **325**, 1240–1243 (2009).
142. Luijsterburg, M. S. *et al.* PARP1 Links CHD2-Mediated Chromatin Expansion and H3.3 Deposition to DNA Repair by Non-homologous End-Joining. *Mol. Cell* **61**, 547–562 (2016).

143. Eleazer, R. & Fondufe-Mittendorf, Y. N. The multifaceted role of PARP1 in RNA biogenesis. *WIREs RNA* **12**, (2021).
144. Fatokun, A. A., Dawson, V. L. & Dawson, T. M. Parthanatos: mitochondrial-linked mechanisms and therapeutic opportunities: Players in parthanatos. *Br. J. Pharmacol.* **171**, 2000–2016 (2014).
145. Wang, Y., Luo, W. & Wang, Y. PARP-1 and its associated nucleases in DNA damage response. *DNA Repair* **81**, 102651 (2019).
146. Chen, Q., Kassab, M. A., Dantzer, F. & Yu, X. PARP2 mediates branched poly ADP-ribosylation in response to DNA damage. *Nat. Commun.* **9**, 3233 (2018).
147. Obaji, E., Maksimainen, M. M., Galera-Prat, A. & Lehtiö, L. Activation of PARP2/ARTD2 by DNA damage induces conformational changes relieving enzyme autoinhibition. *Nat. Commun.* **12**, 3479 (2021).
148. Sonnenblick, A., de Azambuja, E., Azim, H. A. & Piccart, M. An update on PARP inhibitors—moving to the adjuvant setting. *Nat. Rev. Clin. Oncol.* **12**, 27–41 (2015).
149. Rose, M., Burgess, J. T., O'Byrne, K., Richard, D. J. & Bolderson, E. PARP Inhibitors: Clinical Relevance, Mechanisms of Action and Tumor Resistance. *Front. Cell Dev. Biol.* **8**, 564601 (2020).
150. Sen, T. *et al.* Targeting DNA Damage Response Promotes Antitumor Immunity through STING-Mediated T-cell Activation in Small Cell Lung Cancer. *Cancer Discov.* **9**, 646–661 (2019).
151. Gelmon, K. A. *et al.* Olaparib in patients with recurrent high-grade serous or poorly differentiated ovarian carcinoma or triple-negative breast cancer: a phase 2, multicentre, open-label, non-randomised study. *Lancet Oncol.* **12**, 852–861 (2011).
152. Banerjee, S. *et al.* 811MO Maintenance olaparib for patients (pts) with newly diagnosed, advanced ovarian cancer (OC) and a BRCA mutation (BRCAm): 5-year (y) follow-up (f/u) from SOLO1. *Ann. Oncol.* **31**, S613 (2020).
153. Pujade-Lauraine, E. *et al.* Olaparib tablets as maintenance therapy in patients with platinum-sensitive, relapsed ovarian cancer and a BRCA1/2 mutation (SOLO2/ENGOT-Ov21): a double-blind, randomised, placebo-controlled, phase 3 trial. *Lancet Oncol.* **18**, 1274–1284 (2017).
154. Tutt, A. N. J. *et al.* Adjuvant Olaparib for Patients with *BRCA1* - or *BRCA2* -Mutated Breast Cancer. *N. Engl. J. Med.* **384**, 2394–2405 (2021).
155. Golan, T. *et al.* Maintenance Olaparib for Germline *BRCA* -Mutated Metastatic Pancreatic Cancer. *N. Engl. J. Med.* **381**, 317–327 (2019).
156. de Bono, J. *et al.* Olaparib for Metastatic Castration-Resistant Prostate Cancer. *N. Engl. J. Med.* **382**, 2091–2102 (2020).
157. Oza, A. M. *et al.* Antitumor activity and safety of the PARP inhibitor rucaparib in patients with high-grade ovarian carcinoma and a germline or somatic BRCA1 or BRCA2 mutation: Integrated analysis of data from Study 10 and ARIEL2. *Gynecol. Oncol.* **147**, 267–275 (2017).
158. Coleman, R. L. *et al.* Rucaparib maintenance treatment for recurrent ovarian carcinoma after response to platinum therapy (ARIEL3): a randomised, double-blind, placebo-controlled, phase 3 trial. *The Lancet* **390**, 1949–1961 (2017).
159. Abida, W. *et al.* Preliminary results from the TRITON2 study of rucaparib in patients (pts) with DNA damage repair (DDR)-deficient metastatic castration-resistant prostate cancer (mCRPC): Updated analyses. *Ann. Oncol.* **30**, v327–v328 (2019).

160. Mirza, M. R. *et al.* Niraparib Maintenance Therapy in Platinum-Sensitive, Recurrent Ovarian Cancer. *N. Engl. J. Med.* **375**, 2154–2164 (2016).
161. Moore, K. N. *et al.* Niraparib monotherapy for late-line treatment of ovarian cancer (QUADRA): a multicentre, open-label, single-arm, phase 2 trial. *Lancet Oncol.* **20**, 636–648 (2019).
162. Ettl, J. *et al.* Quality of life with talazoparib versus physician's choice of chemotherapy in patients with advanced breast cancer and germline BRCA1/2 mutation: patient-reported outcomes from the EMBRACA phase III trial. *Ann. Oncol.* **29**, 1939–1947 (2018).
163. Kim, C., Chen, C. & Yu, Y. Avoid the trap: Targeting PARP1 beyond human malignancy. *Cell Chem. Biol.* **28**, 456–462 (2021).
164. Huang, D. & Kraus, W. L. The expanding universe of PARP1-mediated molecular and therapeutic mechanisms. *Mol. Cell* (2022).
165. Shao, Z. *et al.* Clinical PARP inhibitors do not abrogate PARP1 exchange at DNA damage sites in vivo. *Nucleic Acids Res.* **48**, 9694–9709 (2020).
166. Shen, Y., Aoyagi-Scharber, M. & Wang, B. Trapping Poly(ADP-Ribose) Polymerase. *J. Pharmacol. Exp. Ther.* **353**, 446–457 (2015).
167. Donawho, C. K. *et al.* ABT-888, an Orally Active Poly(ADP-Ribose) Polymerase Inhibitor that Potentiates DNA-Damaging Agents in Preclinical Tumor Models. *Clin. Cancer Res.* **13**, 2728–2737 (2007).
168. Thomas, H. D. *et al.* Preclinical selection of a novel poly(ADP-ribose) polymerase inhibitor for clinical trial. *Mol. Cancer Ther.* **6**, 945–956 (2007).
169. Menear, K. A. *et al.* 4-[3-(4-Cyclopropanecarbonylpiperazine-1-carbonyl)-4-fluorobenzyl]-2 *H* -phthalazin-1-one: A Novel Bioavailable Inhibitor of Poly(ADP-ribose) Polymerase-1. *J. Med. Chem.* **51**, 6581–6591 (2008).
170. Wang, L. *et al.* MK-4827, a PARP-1/-2 inhibitor, strongly enhances response of human lung and breast cancer xenografts to radiation. *Invest. New Drugs* **30**, 2113–2120 (2012).
171. Shen, Y. *et al.* BMN 673, a Novel and Highly Potent PARP1/2 Inhibitor for the Treatment of Human Cancers with DNA Repair Deficiency. *Clin. Cancer Res.* **19**, 5003–5015 (2013).
172. Hopkins, T. A. *et al.* PARP1 Trapping by PARP Inhibitors Drives Cytotoxicity in Both Cancer Cells and Healthy Bone Marrow. *Mol. Cancer Res.* **17**, 409–419 (2019).
173. Wahlberg, E. *et al.* Family-wide chemical profiling and structural analysis of PARP and tankyrase inhibitors. *Nat. Biotechnol.* **30**, 283–288 (2012).
174. Murai, J. *et al.* Stereospecific PARP Trapping by BMN 673 and Comparison with Olaparib and Rucaparib. *Mol. Cancer Ther.* **13**, 433–443 (2014).
175. Lin, X. *et al.* PARP inhibitors trap PARP2 and alter the mode of recruitment of PARP2 at DNA damage sites. *Nucleic Acids Res.* **50**, 3958–3973 (2022).
176. Krastev, D. B. *et al.* The ubiquitin-dependent ATPase p97 removes cytotoxic trapped PARP1 from chromatin. *Nat. Cell Biol.* **24**, 62–73 (2022).
177. Maya-Mendoza, A. *et al.* High speed of fork progression induces DNA replication stress and genomic instability. *Nature* **559**, 279–284 (2018).
178. Lindström, M. S., Bartek, J. & Maya-Mendoza, A. p53 at the crossroad of DNA replication and ribosome biogenesis stress pathways. *Cell Death Differ.* **29**, 972–982 (2022).
179. Hoch, N. C. *et al.* XRCC1 mutation is associated with PARP1 hyperactivation and cerebellar ataxia. *Nature* **541**, 87–91 (2017).

180. Mandir, A. S. *et al.* Poly(ADP-ribose) polymerase activation mediates 1-methyl-4-phenyl-1,2,3,6-tetrahydropyridine (MPTP)-induced parkinsonism. *Proc. Natl. Acad. Sci.* **96**, 5774–5779 (1999).
181. Zheng, J., Devalaraja-Narashimha, K., Singaravelu, K. & Padanilam, B. J. Poly(ADP-ribose) polymerase-1 gene ablation protects mice from ischemic renal injury. *Am. J. Physiol.-Ren. Physiol.* **288**, F387–F398 (2005).
182. Schneider, M. *et al.* The PROTACtable genome. *Nat. Rev. Drug Discov.* **20**, 789–797 (2021).
183. Wang, S. *et al.* Uncoupling of PARP1 trapping and inhibition using selective PARP1 degradation. *Nat. Chem. Biol.* **15**, 1223–1231 (2019).
184. Cao, C. *et al.* Discovery of SK-575 as a Highly Potent and Efficacious Proteolysis-Targeting Chimera Degrader of PARP1 for Treating Cancers. *J. Med. Chem.* **63**, 11012–11033 (2020).
185. Zhao, Q., Lan, T., Su, S. & Rao, Y. Induction of apoptosis in MDA-MB-231 breast cancer cells by a PARP1-targeting PROTAC small molecule. *Chem. Commun.* **55**, 369–372 (2019).
186. Zheng, M. *et al.* Rational Design and Synthesis of Novel Dual PROTACs for Simultaneous Degradation of EGFR and PARP. *J. Med. Chem.* **64**, 7839–7852 (2021).
187. Kim, B. C. *et al.* Evaluation of premature senescence and senescence biomarkers in carcinoma cells and xenograft mice exposed to single or fractionated irradiation. *Oncol. Rep.* **31**, 2229–2235 (2014).
188. Gewirtz, D. A. Autophagy and senescence: A partnership in search of definition. *Autophagy* **9**, 808–812 (2013).
189. Toillon, R.-A. *et al.* Estrogens decrease γ-ray–induced senescence and maintain cell cycle progression in breast cancer cells independently of p53. *Int. J. Radiat. Oncol.* **67**, 1187–1200 (2007).
190. Efimova, E. V. *et al.* HMG-CoA Reductase Inhibition Delays DNA Repair and Promotes Senescence After Tumor Irradiation. *Mol. Cancer Ther.* **17**, 407–418 (2018).
191. Lafontaine, J. *et al.* Senolytic Targeting of Bcl-2 Anti-Apoptotic Family Increases Cell Death in Irradiated Sarcoma Cells. *Cancers* **13**, 386 (2021).
192. Russo, M. *et al.* Biochemical and Cellular Characterization of New Radio-Resistant Cell Lines Reveals a Role of Natural Flavonoids to Bypass Senescence. *Int. J. Mol. Sci.* **23**, 301 (2021).
193. Malaquin, N. *et al.* DNA Damage- But Not Enzalutamide-Induced Senescence in Prostate Cancer Promotes Senolytic Bcl-xL Inhibitor Sensitivity. *Cells* **9**, 1593 (2020).
194. Lee, J.-J. *et al.* PTEN status switches cell fate between premature senescence and apoptosis in glioma exposed to ionizing radiation. *Cell Death Differ.* **18**, 666–677 (2011).
195. Zanoni, M. *et al.* Irradiation causes senescence, ATP release, and P2X7 receptor isoform switch in glioblastoma. *Cell Death Dis.* **13**, 80 (2022).
196. Skinner, H. D. *et al. TP53* Disruptive Mutations Lead to Head and Neck Cancer Treatment Failure through Inhibition of Radiation-Induced Senescence. *Clin. Cancer Res.* **18**, 290–300 (2012).
197. Lehmann, B. D. *et al.* A Dominant Role for p53-Dependent Cellular Senescence in Radiosensitization of Human Prostate Cancer Cells. *Cell Cycle* **6**, 595–605 (2007).
198. Wang, M. *et al.* EGF Receptor Inhibition Radiosensitizes NSCLC Cells by Inducing Senescence in Cells Sustaining DNA Double-Strand Breaks. *Cancer Res.* **71**, 6261–6269 (2011).

199. Schoetz, U. *et al.* Early senescence and production of senescence-associated cytokines are major determinants of radioresistance in head-and-neck squamous cell carcinoma. *Cell Death Dis.* **12**, 1162 (2021).
200. Nyui, T., Yoshino, H., Nunota, T., Sato, Y. & Tsuruga, E. cGAS Regulates the Radioresistance of Human Head and Neck Squamous Cell Carcinoma Cells. *Cells* **11**, 1434 (2022).
201. Jung, H. *et al.* Human Papillomavirus E6/E7-Specific siRNA Potentiates the Effect of Radiotherapy for Cervical Cancer in Vitro and in Vivo. *Int. J. Mol. Sci.* **16**, 12243–12260 (2015).
202. Tesei, A. *et al.* TP53 drives abscopal effect by secretion of senescence-associated molecular signals in non-small cell lung cancer. *J. Exp. Clin. Cancer Res.* **40**, 89 (2021).
203. Walle, T. *et al.* Radiotherapy orchestrates natural killer cell dependent antitumor immune responses through CXCL8. *Sci. Adv.* **8**, eabh4050 (2022).
204. Wang, L. *et al.* Proton versus photon radiation-induced cell death in head and neck cancer cells. *Head Neck* **41**, 46–55 (2019).
205. Huart, C. *et al.* Taking Advantage of the Senescence-Promoting Effect of Olaparib after X-ray and Proton Irradiation Using the Senolytic Drug, ABT-263. *Cancers* **14**, 1460 (2022).
206. Wéra, A.-C., Lobbens, A., Stoyanov, M., Lucas, S. & Michiels, C. Radiation-induced synthetic lethality: combination of poly(ADP-ribose) polymerase and RAD51 inhibitors to sensitize cells to proton irradiation. *Cell Cycle* **18**, 1770–1783 (2019).
207. Schniewind, I. *et al.* Cellular plasticity upon proton irradiation determines tumor cell radiosensitivity. *Cell Rep.* **38**, 110422 (2022).
208. Kubo, N. *et al.* Radiosensitizing effect of carboplatin and paclitaxel to carbon-ion beam irradiation in the non-small-cell lung cancer cell line H460. *J. Radiat. Res. (Tokyo)* **56**, 229–238 (2015).
209. Jinno-Oue, A. *et al.* Irradiation With Carbon Ion Beams Induces Apoptosis, Autophagy, and Cellular Senescence in a Human Glioma-Derived Cell Line. *Int. J. Radiat. Oncol.* **76**, 229–241 (2010).
210. Benzina, S. *et al.* Cell death induced in a human glioblastoma cell line by p(65)+Be neutrons combined with cisplatin. *Life Sci.* **79**, 513–518 (2006).
211. Sunada Shigeaki, Kanai Hideki, & Lee Younghyun. Nontoxic concentration of DNA-PK inhibitor NU7441 radio-sensitizes lung tumor cells with little effect on double strand break repair. *Cancer Sci.* (2016).
212. Zhang, X. *et al.* Both Complexity and Location of DNA Damage Contribute to Cellular Senescence Induced by Ionizing Radiation. *PLOS ONE* **11**, e0155725 (2016).
213. Fitzgerald, A. L. *et al.* Reactive oxygen species and p21Waf1/Cip1 are both essential for p53-mediated senescence of head and neck cancer cells. *Cell Death Dis.* **6**, e1678–e1678 (2015).
214. Petragnano, F. *et al.* Modulating the dose-rate differently affects the responsiveness of human epithelial prostate- and mesenchymal rhabdomyosarcoma-cancer cell line to radiation. *Int. J. Radiat. Biol.* **96**, 823–835 (2020).
215. Potez, M. *et al.* Synchrotron Microbeam Radiation Therapy as a New Approach for the Treatment of Radioresistant Melanoma: Potential Underlying Mechanisms. *Int. J. Radiat. Oncol.* **105**, 1126–1136 (2019).
216. Zhang, H. *et al.* In Vitro Radiobiological Advantages of Hypofractionation Compared with Conventional Fractionation: Early-Passage NSCLC Cells are Less Aggressive after Hypofractionation. *Radiat. Res.* **190**, 584 (2018).

217. Lombard, A. P. *et al.* Olaparib-Induced Senescence Is Bypassed through G2–M Checkpoint Override in Olaparib-Resistant Prostate Cancer. *Mol. Cancer Ther.* **21**, 677–685 (2022).
218. Efimova, E. V. *et al.* Poly(ADP-Ribose) Polymerase Inhibitor Induces Accelerated Senescence in Irradiated Breast Cancer Cells and Tumors. *Cancer Res.* **70**, 6277–6282 (2010).
219. Alotaibi, M. *et al.* Radiosensitization by PARP Inhibition in DNA Repair Proficient and Deficient Tumor Cells: Proliferative Recovery in Senescent Cells. *Radiat. Res.* **185**, 229 (2016).
220. Yokoyama, T., Kohn, E. C., Brill, E. & Lee, J.-M. Apoptosis is augmented in high-grade serous ovarian cancer by the combined inhibition of Bcl-2/Bcl-xL and PARP. *Int. J. Oncol.* **50**, 1064–1074 (2017).
221. Sato, K., Iwasaki, S. & Yoshino, H. Effects and Related Mechanisms of the Senolytic Agent ABT-263 on the Survival of Irradiated A549 and Ca9-22 Cancer Cells. *Int. J. Mol. Sci.* **22**, 13233 (2021).
222. Liu, X. *et al.* Inhibition of survivin enhances radiosensitivity of esophageal cancer cells by switching radiation-induced senescence to apoptosis. *OncoTargets Ther.* **Volume 11**, 3087–3100 (2018).
223. Richard, I. A., Burgess, J. T., O'Byrne, K. J. & Bolderson, E. Beyond PARP1: The Potential of Other Members of the Poly (ADP-Ribose) Polymerase Family in DNA Repair and Cancer Therapeutics. *Front. Cell Dev. Biol.* **9**, 801200 (2022).
224. Rose, M., Burgess, J. T., O'Byrne, K., Richard, D. J. & Bolderson, E. PARP Inhibitors: Clinical Relevance, Mechanisms of Action and Tumor Resistance. *Front. Cell Dev. Biol.* **8**, 564601 (2020).
225. Murai, J. *et al.* Differential Trapping of PARP1 and PARP2 by Clinical PARP Inhibitors. *Cancer Res.* **72**, 5588–5599 (2012).
226. Kim, C., Wang, X.-D. & Yu, Y. PARP1 inhibitors trigger innate immunity via PARP1 trapping-induced DNA damage response. *eLife* **9**, e60637 (2020).
227. Fitsiou, E., Soto-Gamez, A. & Demaria, M. Biological functions of therapy-induced senescence in cancer. *Semin. Cancer Biol.* **81**, 5–13 (2022).
228. Fleury, H. *et al.* Exploiting interconnected synthetic lethal interactions between PARP inhibition and cancer cell reversible senescence. *Nat. Commun.* **10**, 2556 (2019).
229. Malaquin, N. *et al.* DNA Damage- But Not Enzalutamide-Induced Senescence in Prostate Cancer Promotes Senolytic Bcl-xL Inhibitor Sensitivity. *Cells* **9**, 1593 (2020).
230. Lombard, A. P. *et al.* Olaparib-Induced Senescence Is Bypassed through G2–M Checkpoint Override in Olaparib-Resistant Prostate Cancer. *Mol. Cancer Ther.* **21**, 677–685 (2022).
231. Malaquin, N., Martinez, A. & Rodier, F. Keeping the senescence secretome under control: Molecular reins on the senescence-associated secretory phenotype. *Exp. Gerontol.* **82**, 39–49 (2016).
232. Hernandez-Segura, A., Nehme, J. & Demaria, M. Hallmarks of Cellular Senescence. *Trends Cell Biol.* **28**, 436–453 (2018).
233. Coppé, J.-P., Desprez, P.-Y., Krtolica, A. & Campisi, J. The Senescence-Associated Secretory Phenotype: The Dark Side of Tumor Suppression. *Annu. Rev. Pathol. Mech. Dis.* **5**, 99–118 (2010).
234. Gonzalez, L. C., Ghadaouia, S., Martinez, A. & Rodier, F. Premature aging/senescence in cancer cells facing therapy: good or bad? *Biogerontology* **17**, 71–87 (2016).
235. Hanahan, D. Hallmarks of Cancer: New Dimensions. *Cancer Discov.* **12**, 31–46 (2022).

236. Baker, D. J. *et al.* Clearance of p16Ink4a-positive senescent cells delays ageing-associated disorders. *Nature* **479**, 232–236 (2011).
237. Jeon, O. H. *et al.* Local clearance of senescent cells attenuates the development of post-traumatic osteoarthritis and creates a pro-regenerative environment. *Nat. Med.* **23**, 775–781 (2017).
238. Baker, D. J. *et al.* Opposing roles for p16Ink4a and p19Arf in senescence and ageing caused by BubR1 insufficiency. *Nat. Cell Biol.* **10**, 825–836 (2008).
239. Childs, B. G. *et al.* Senescent intimal foam cells are deleterious at all stages of atherosclerosis. *Science* **354**, 472–477 (2016).
240. Yokoyama, T., Kohn, E. C., Brill, E. & Lee, J.-M. Apoptosis is augmented in high-grade serous ovarian cancer by the combined inhibition of Bcl-2/Bcl-xL and PARP. *Int. J. Oncol.* **50**, 1064–1074 (2017).
241. Debacq-Chainiaux, F., Erusalimsky, J. D., Campisi, J. & Toussaint, O. Protocols to detect senescence-associated beta-galactosidase (SA-βgal) activity, a biomarker of senescent cells in culture and in vivo. *Nat. Protoc.* **4**, 1798–1806 (2009).
242. Huart, C. *et al.* Taking Advantage of the Senescence-Promoting Effect of Olaparib after X-ray and Proton Irradiation Using the Senolytic Drug, ABT-263. 18 (2022).
243. Harper, J. W. *et al.* Inhibition of cyclin-dependent kinases by p21. *Mol. Biol. Cell* **6**, 387–400 (1995).
244. Gerdes, J., Schwab, U., Lemke, H. & Stein, H. Production of a mouse monoclonal antibody reactive with a human nuclear antigen associated with cell proliferation. *Int. J. Cancer* **31**, 13–20 (1983).
245. Kong, L. R. *et al.* Targeting codon 158 p53-mutant cancers via the induction of p53 acetylation. *Nat. Commun.* **11**, 2086 (2020).
246. Cohn, R. L., Gasek, N. S., Kuchel, G. A. & Xu, M. The heterogeneity of cellular senescence: insights at the single-cell level. *Trends Cell Biol.* (2022).
247. Mogilenko, D. A., Shchukina, I. & Artyomov, M. N. Immune ageing at single-cell resolution. *Nat. Rev. Immunol.* **22**, 484–498 (2022).
248. Batista, P. J. *et al.* m6A RNA Modification Controls Cell Fate Transition in Mammalian Embryonic Stem Cells. *Cell Stem Cell* **15**, 707–719 (2014).
249. Jochems, F. *et al.* The Cancer SENESCopedia: A delineation of cancer cell senescence. *Cell Rep.* **36**, 109441 (2021).
250. Fouillade, C. *et al.* FLASH Irradiation Spares Lung Progenitor Cells and Limits the Incidence of Radio-induced Senescence. *Clin. Cancer Res.* **26**, 1497–1506 (2020).
251. Davan-Wetton, C. S. A., Pessolano, E., Perretti, M. & Montero-Melendez, T. Senescence under appraisal: hopes and challenges revisited. *Cell. Mol. Life Sci.* **78**, 3333–3354 (2021).
252. Raffaele, M. & Vinciguerra, M. The costs and benefits of senotherapeutics for human health. *Lancet Healthy Longev.* **3**, e67–e77 (2022).
253. He, Y. *et al.* Using proteolysis-targeting chimera technology to reduce navitoclax platelet toxicity and improve its senolytic activity. *Nat. Commun.* **11**, 1996 (2020).
254. Wang, W. *et al.* A genome-wide CRISPR-based screen identifies *KAT7* as a driver of cellular senescence. *Sci. Transl. Med.* **13**, eabd2655 (2021).
255. Kohli, J. *et al.* Algorithmic assessment of cellular senescence in experimental and clinical specimens. *Nat. Protoc.* **16**, 2471–2498 (2021).

G. Annex

International Journal of
Molecular Sciences

MDPI

Review

Could Protons and Carbon Ions Be the Silver Bullets Against Pancreatic Cancer?

Camille Huart, Jia-Wei Chen, Benjamin Le Calvé, Carine Michiels and Anne-Catherine Wéra *

Unité de Recherche en Biologie Cellulaire (URBC), Namur Research Institute for Life Sciences (NARILIS), University of Namur, 5000 Namur, Belgium; camille.huart@unamur.be (C.H.); jia-wei.chen@unamur.be (J.-W.C.); benjamin.lecalve@unamur.be (B.L.C.); carine.michiels@unamur.be (C.M.)
* Correspondence: anne-catherine.wera@unamur.be; Tel.: +32-81725477

Received: 27 May 2020; Accepted: 1 July 2020; Published: 4 July 2020

Abstract: Pancreatic cancer is a very aggressive cancer type associated with one of the poorest prognostics. Despite several clinical trials to combine different types of therapies, none of them resulted in significant improvements for patient survival. Pancreatic cancers demonstrate a very broad panel of resistance mechanisms due to their biological properties but also their ability to remodel the tumour microenvironment. Radiotherapy is one of the most widely used treatments against cancer but, up to now, its impact remains limited in the context of pancreatic cancer. The modern era of radiotherapy proposes new approaches with increasing conformation but also more efficient effects on tumours in the case of charged particles. In this review, we highlight the interest in using charged particles in the context of pancreatic cancer therapy and the impact of this alternative to counteract resistance mechanisms.

Keywords: pancreatic cancer; protons; carbon ions; radioresistance; chemoresistance; targeted combination; immunotherapy

1. Introduction

Due to late diagnosis and resistance to treatment, pancreatic cancer represents the fourth cause of cancer related deaths worldwide [1]. If outcomes are not improved, the disease is predicted to be the second leading cause of cancer mortality within the next decade [2]. Pancreatic ductal adenocarcinoma (PDAC) is the most frequent type of pancreatic cancer (>85%) associated with the highest mortality rate; the five-year survival does not exceed 7% [2,3]. Median survival rates are going from 25 months for the earliest stage, between 10 to 15 months for locally advanced to less than 5 months for metastatic cancer. For early stages of unmetastasised PDAC, surgery is the only treatment with curative intention. However, the majority of patients are diagnosed at advanced stages since the disease often presents itself with non-specific symptoms such as diffuse abdominal discomfort and loss of appetite. At the time of diagnosis, only 15% to 20% of pancreatic cancers are said to be operable, as the tumour is usually in the border of, or even encloses, important vessels such as the celiac artery, portal vein, hepatic artery or superior mesenteric vein/artery [3]. Unmetastasised PDAC are thus said to be: (1) resectable (R-PDAC), no tumour contact with the mentioned vessels; (2) borderline resectable (BR-PDAC) in case of venous involvement, which can be reconstructed after resection; (3) locally advanced (LA-PDAC) if there is an extended involvement of the vessels or if the reconstruction is not possible after the resection. Other parameters than anatomical consideration, such as tumour biology or patient condition, might be taken into account for this classification and to determine the best treatment option.

As of now, the main chemotherapeutic agents involved in the management of PDAC are FOLFIRINOX and gemcitabine-based drugs [4,5]. On the one hand, FOLFIRINOX consists of: (1) 5-fluorouracil (5-FU), an antimetabolite drug inhibiting DNA synthesis and folinic acid (leuvocorin)

to potentiate the 5-FU anticancer activity; (2) irinotecan, a topoisomerase inhibitor inducing DNA strand breaks; (3) oxaliplatin, a platinum-based alkylating agent, which inhibits DNA repair and/or DNA synthesis. This combination, initially developed to treat metastatic colorectal cancer, was chosen in PDAC treatment for its synergism, differential mechanisms of action and non-overlapping toxicities of the drugs included in the combination [6]. On the other hand, gemcitabine exerts its anticancer properties by inhibiting DNA synthesis and thus blocking cell cycle progression. This drug is also used as chemotherapeutic agent in many cancers such as breast, ovarian and non-small cell lung cancers, especially paired with platinum-based drugs [7,8]. In PDAC, gemcitabine, associated with other chemotherapeutic agents, mostly 5-FU, capecitabine (an orally 5-FU prodrug) or nanoparticle-bound paclitaxel (nab-paclitaxel), is aimed to increase the response rate and survival benefits in patients [7,9]. Nab-paclitaxel is a novel albumin-bound, solvent-free and water-soluble formulation of paclitaxel, an anti-mitotic agent acting on the tubulins [10].

Radiation therapy can be combined to chemotherapy to increase local control. However, results of clinical trials failed to identify radiotherapy as an essential part of PDAC treatment [11]. In this review, we aim at putting forward the role that should be played by modern radiation therapy in the management of PDAC, especially when using charged particles (protons or carbon ions). We suggest an association of heavy charged particles with DNA repair targeted drugs as a very promising approach to act on local control and to enhance an immune response to trigger a systemic effect on pancreatic cancer.

2. Current Treatment for Unmetastasised PDAC

For R-PDAC and BR-PDAC, surgery is followed by adjuvant chemotherapy of gemcitabine plus capecitabine, a therapeutic approach generalised after the publication of the European Study Group for Pancreatic Cancer (ESPAC-4) trial in 2017. This study demonstrated the benefits of gemcitabine-capecitabine combination, with a five-year survival reaching 30%, compared with a gemcitabine monotherapy [5,9]. Currently, several studies for adjuvant therapy using nanoparticle nab-paclitaxel plus gemcitabine (APACT trial; NCT0196443) or modified FOLFIRINOX (mFOLFIRINOX) (PRODIGE trial; NCT01526135) are ongoing [5].

The place of radiation therapy (RT) combined to chemotherapy (chemoradiation, CRT) in adjuvant settings to surgery for the management of R-PDAC or BR-PDAC is still not settled due to conflicting results of clinical trials. Adjuvant CRT to surgery, namely a total of 40 Gy delivered in daily 2 Gy fractions associated with 5-FU, led to survival benefits in GISTG [12] and EORTC trials [13], while a decrease in the median survival was observed in ESPAC-1 [14]. The RTOG 9704 trial focused on comparing 5-FU and gemcitabine combined to RT [15]. In this trial, less than 30% local recurrences were observed, namely half compared to previous trials, but more than 70% presented distant relapse. Interestingly, RTOG 9704 included a quality assurance for radiation plan and delivery which allowed a secondary analysis highlighting that deviation from the specified RT protocol guidelines had deleterious impact on survival [16]. This is now corrected in the RTOG 0848 trial with a "real time, prospective, mandated review and correction of deviations prior to the start of radiotherapy" as stated in the aforementioned paper. This last study demonstrates the high constraint in dose conformation and RT regimen for the treatment of PDAC.

3. From Adjuvant to Neoadjuvant Treatment For Unmetastasised PDAC

After resection, margin analysis is of prime importance. In a retrospective study, Konstantinidis et al. showed that R1 resected patients, i.e., with at least one margin infiltrated with cancer cells, had only a slightly improved median survival compared to patients with LA-PDAC. Moreover, for a notable increase in the median survival, the resections without any trace of cancer cells, R0, had to be wider that 1 mm (35 vs. 16 months if margins stay within 1 mm) [17]. This shows that the reduction of margin positivity is required if one hopes to increase the overall survival of resected patients.

In their recent review, Hall and Goodman gathered data from different trials and studies and evidenced that neoadjuvant CRT is superior to adjuvant chemotherapy when considering: the rate of

positive margins (2–20% vs. 16–60%), the incidence of node positivity (17–40% vs. 62–80%) and the rate of local recurrence (5–15% vs. 19–53%) [11].

Recently, the PREOPANC trial compared preoperative CRT (36 Gy in 15 fractions + gemcitabine) to upfront surgery on R- and BR-PDAC. Among the assessed endpoints, the median survival was extended for BR-PDAC, the loco-regional and distant metastasis free interval were superior as well as the R0 rate (especially for BR-PDAC, 79% vs. 13%) [18]. According to multiple studies and analyses, FOLFORINOX seems to be the most effective regimen for neoadjuvant therapy in pancreatic cancer. However, not all patients benefit from this multi-drug regimen as it causes considerable toxicity [6,19,20]. The use of nab-paclitaxel paired with gemcitabine is also suggested to be a good strategy for neoadjuvant therapy [10,21].

Besides increasing local control for R-PDAC and BR-PDAC, neoadjuvant C(R)T can lead to secondary resectability of LA-PDAC thanks to the shrinkage, or even down-staging, of the tumour [22]. In their meta-analysis of responses to preoperative/neoadjuvant therapies, Gillen et al. conclude that one third of the patients that were initially considered non-resectable would benefit from surgery after neoadjuvant treatment at survival rate similar to initially resectable patients [23].

With the rise of more effective chemotherapies regarding systemic control, loco-regional control will become essential and RT is expected to play its part. With radiation therapy being a rapidly evolving field with new techniques in beam delivery, imaging capabilities and treatment planification algorithms, the next trials should associate modern techniques to take full advantage of RT and evaluate the benefit of CRT as (neo)adjuvant treatment of pancreatic cancer, and especially for LA-PDAC.

4. Pushing Forward Loco-Regional Control: Modern RT

Therapies aim to reach tumour control while minimising as much as possible normal tissue complications. This is the so-called therapeutic window. In the case of pancreatic cancer, the poor outcome achieved today shows that this window is quite small. While current treatments face resistance, dose escalation of CT or RT is limited by toxicities. New development in RT aims to reduce induced toxicities to allow dose escalation and hypofractionation. In addition, charged particles could avoid some of the resistance mechanisms present in PDAC.

4.1. Dose Conformation Towards Dose Escalation and Hypofractionation

The anatomical position of the pancreas implies a highly conformational dose deposition to reach a sufficient coverage of the tumour volume while sparing surrounding healthy tissues and organs at risk (OARs). Evolution in dose conformation of conventional photon beams goes from two-dimensional (2D) delivery for early trials such as GIST to 3DCRT (three-dimensional (3D) conformation radiotherapy) and IMRT (intensity modulated radiation therapy) for RTOG 0848. Studies show that IMRT should be favoured, as it leads to a significant reduction in toxicities [24]. Moreover, the sparing of OARs with a better dose conformation allows a hypofractionated regimen, associated with a higher radiobiological response (biological dose equivalent, BED) but also with a reduced overall time of treatment. Even ablative irradiation with BED superior to 100 Gy can be considered in the case of SBRT (stereotactic body radiotherapy) with image guidance.

SBRT is usually indicated in case of tumours with minimum motion uncertainty (brain, spinal cord) or for small tumours in organ with parallel functional subunits (lung, liver). This is not the case for pancreatic cancer as it is close to the gastrointestinal tract (serial functional subunits) but is also associated with uncertainties due to respiratory motion and luminal organ inter-fraction shape changes. For these reasons, SBRT treatments for pancreatic cancer need to be very carefully planned and delivered and associated with motion management. Krishnan et al. reported an improved overall survival (OS) (17.8 months vs. 15.0 months) for LA-PDAC patient receiving a BED higher than 70 Gy after chemotherapy treatment [25]. At the time of the publication, this was associated with expected survival rate of 36% and 31% at two and three years, respectively. Based on this study, two clinical trials for LA-PDAC, currently recruiting, will study hypofractionated ablative IMRT (NCT03523312) and the use of stereotactic magnetic resonance guided adaption radiation therapy (SMART, NCT03621644) based on very encouraging preliminary results [26].

In the seeking of dose conformation, charged particles, such as protons or carbon ions, present a clear advantage compare to photons thanks to their depth dose profile. Photons deposit most of their energy close to the surface entrance followed by a continuous decrease characteristic of their attenuation. This leads to dose deposition upstream and downstream the tumour. Charged particles, however, deposit a small fraction of their energy before what is called the Bragg peak, characterising the maximal energy released when the particles come at rest. The dose sharply decreases beyond this peak, allowing to spare downstream tissues. The position of the Bragg peak can be tuned to coincide with the tumour position and highly conformal dose deposition profiles can be obtained. Since the early 2000s, the introduction of beam scanning methods led to further improvement of conformation. As shown by Ling et al. in the frame of RTOG-0848, IMRT does slightly better than 3DCRT, but proton therapy (PT) outperforms both, with a clear reduction of deposited dose to OARs [27]. In their review, Rutenberg and Nichols concluded that PT is effective before or after surgical resection of PDAC. Moreover, as PT is well tolerated and reduced toxicities, it allows either further dose escalation or intensification of chemotherapy without delaying surgery [28]. Kim et al. demonstrated that adjuvant chemotherapy (capecitabine or 5-FU) could be safely administrated to PT and improve the OS [29]. In another study, Hiroshima et al. treated LA-PDAC patients with concurrent chemoradiotherapy with protons at dose of 50, 54–60 and 67.5 GyE [30]. They showed that OS was largely improved with increasing dose with 13.1 months at 50 GyE to 28.4 months at doses between 54–60 GyE and up to 42.5 months at 67.5 GyE. Moreover, the local recurrence time was higher than 36 months for doses from 54 GyE. Further developments in proton beam delivery are undertaken with, notably, continuous spot-scanning proton arc (SPArc), which can further decrease dose to OARs [31,32]. Shinoto et al. studied the concurrent gemcitabine with carbon ions for LA-PDAC patients [33]. They found that full dose of gemcitabine (1000 mg/m^2) was safely administrated with 55.2 GyE carbon therapy. At two years, the freedom from local progression rate was 83% and OS rates equal to 48%. More results of clinical trials based on SRBT, proton beams and carbon ions are summarised in [34]. Table 1 presents active and recruiting clinical trials for the treatment of pancreatic cancer with protons or carbon ions.

A last point worth noting is the development of FLASH irradiation, i.e., irradiation at ultrahigh dose-rate (>40–100 Gy/s compared to <0.1 Gy/s for conventional RT). Studies have observed that normal tissues irradiated at such a dose-rate display reduced toxicities compared to irradiation at the same dose with conventional RT, this is called the "FLASH effect" (reviewed in [35,36]). This effect was reproduced by different teams in a wide range of animal models or organs and even with different types of radiation (X-rays, electrons or protons). They reported an increased tolerance of normal tissues to FLASH RT with reduction in acute and delayed toxicities such as pneumonitis, lung fibrosis, cognitive impairment, skin necrosis etc. [35,36]. Moreover, as explained in these reviews, not only does FLASH RT reduce tissue toxicities, it maintains, and sometimes even increases, the response of tumour cells. On the one hand, FLASH RT can be used to reduce normal tissue complication at an equivalent tumour control; on the other hand, FLASH RT allows dose escalation to achieve tumour control at the same toxicity level. This is shown by Favaudon et al., who irradiated C57BL/6J murine whole lungs as well as xenografted human tumours and syngeneic orthotopic lung tumours with conventional and FLASH RT [37]. They demonstrated that FLASH RT protected the lungs from radiation-induced fibrosis as well as the blood vessels and bronchi from radiation-induced apoptosis but led to the same tumour control as the one obtained by conventional RT. Moreover, as FLASH RT allowed dose escalation, a better tumour control was achieved with FLASH at increased dose. This was also demonstrated with FLASH proton (FLASH PT) irradiation in C57BL/6J mice, presenting or not pancreatic flank tumour derived from KPC (LSL-Kras$^{G12D/+}$;LSL-Trp53$^{R172H/+}$;Pdx-1-Cre) [38]. Toxicities to normal tissue were reduced after FLASH PT compared to standard 15 Gy PT irradiation of the whole abdomen. Reduced intestinal fibrosis was also observed with FLASH regimen while maintaining the same tumour control as standard PT delivery. The first patient, who presented a multiresistant CD30+ T-cell cutaneous lymphoma, was treated with FLASH RT (electron beam) at the Lausanne University Hospital in 2019 with very encouraging complete tumour response with a short follow-up of five months [39].

Table 1. Ongoing clinical trials for pancreatic cancer patients treated with protons or carbon ions.

ID	Condition	Year	Status	*N*	Radiation	Dose	Concurrent Chemotherapy
NCT03885284	R-PDAC (adjuvant)	2019	Recruiting	12	Protons	25 Gy (RBE) in five fractions	mFOLFIRINOX
NCT01591733	R-PDAC (neoadjuvant)	2012	Active	48	Protons (Photons)	25 Gy (RBE) in five fractions (30 Gy in 10 fractions)	FOLFIRINOX + Capecitabine
NCT01494155	R-PDAC (neoadjvant)	2011	Active	50	Protons (Photons)	25 Gy (RBE) in five fractions (30 Gy in 10 fractions)	Capecitabine + Hydroxychloroquine
NCT03822936	R-PDAC (neoadjuvant)	2019	Recruiting	30	Carbon ions	38.4 Gy (RBE) in eight fractions	N/A
NCT02598349	Unresectable	2015	Recruiting	60	Protons	63 Gy (RBE) in 28 fractions	Capecitabine
NCT04194268	Unresectable	2019	Recruiting	25	Carbon ions	48 Gy (RBE) in 12 fractions	N/A
NCT03652428	LA-PDAC	2018	Recruiting	24	Protons	75 Gy (RBE) in 15 fractions	Gemcitabine
NCT03652428	LA-PDAC	2018	Recruiting	24	Protons	75 Gy (RBE)E in 15 fractions	Nab-paclitaxel + Gemcitabine
NCT04082455	LA-PDAC	2019	Recruiting	49	Carbon ions	60-67.5Gy (RBE) in 15 fractions	N/A
NCT01821729	LA-PDAC	2013	Active	50	Protons (Photons)	25 Gy (RBE) in five fractions (if persistent vascular involvement 50.4 Gy with vascular boost to 58.8 Gy)	FOLFIRIRINOX + Losartan
NCT03536182	LA-PDAC	2018	Active	110	Carbon ions (Photons)	55.2 or 57.6 Gy (RBE) in 12 fractions (50.4–56 Gy in 28 fractions)	• Gemcitabine • Gemcitabine + Nab-paclitaxel • FOLFIRINOX

4.2. Charged Particles to Increase Dose Response and Counteract PDAC Resistance to Treatment

Chemo- and radio-therapies are subjected to resistance mechanisms developed by tumour cells and PDAC is no exception. Some of these mechanisms could be counteracted by protons or carbon ions. Indeed, as explained below, the DNA damage distribution is not homogeneous but rather clustered after charged particles irradiation while this pattern is homogeneous with chemotherapeutic drugs and conventional RT. These more complex damages are less easily repaired, hence, leading to enhanced cell death.

4.2.1. Mechanisms of Resistance

Resistance can be intrinsic (de novo) and/or acquired in response to challenges during the treatment. Mechanisms of drug resistance in PDAC include the presence of highly resistant cancer cells, up- or down-regulated expression of specific microRNAs, aberrant gene expression, mutations and deregulation of key signalling pathways as well as features of the microenvironment and its components.

Intrinsic resistance is associated with proteins undergoing mutations during PDAC development, mostly; oncogenic with KRAS mutations (observed in more than 90% of patients) and tumour suppressor mutations such as p53, CDKN2A or SMAD4 mutated in more than 50% of patients [3,40].

Besides its role in sustained growth of PDAC, KRAS activation leads to a metabolic reprogramming that gives a selection advantage to the transformed cells, as PDAC tumours are subject to high metabolic stress due to severe hypoxia and limited nutriment availability [3]. Autophagy, glycolysis, glutamine uptake and NRF2 antioxidant program are particularly active in KRAS mutated PDAC [3]. Recently, it was shown that $KRAS^{G12C}$ could be targeted efficiently in pre-clinical and clinical settings. Indeed, treatment with ARS-1620, a $KRAS^{G12C}$ inhibitor, demonstrated significant tumour growth inhibition as well regression in a patient-derived xenograft (PDX) mouse model of PDAC [41]. The inhibition of $KRAS^{G12C}$ by AMG-510 was also found successful in a phase I trial in which patients presenting non-small cell lung cancers or colorectal cancers were enrolled. Out of the 22 patients enrolled, six patients achieved stable disease and one patient reached partial response [42]. Unfortunately, mutations in G12C only represent 1–4% of all KRAS mutations. Indeed, the predominant KRAS mutations in PDAC are $KRAS^{G12D}$ and $KRAS^{G12V}$, which are currently undruggable. Since directly targeting KRAS has proven difficult, therapies targeting the major downstream effector pathways are currently developed. These effectors include the RAS–RAF–MEK–ERK and PI3K–PDPK1–AKT signalling pathways. Several MEK inhibitors proceeded to clinical trials; however, they were shown to be inefficient in patients with PDAC as demonstrated in NCT01016483 and NCT01231581 trials. On the other hand, combining a MEK inhibitor to an autophagy inhibitor could display anti-proliferative effects as shown in cell lines and PDAC PDX tumours in mice [43].

Additionally to metabolism reprogramming, NRF2 has been shown to promote proliferation, angiogenesis, resistance to apoptosis and, through the epithelial to mesenchymal transition (EMT) activation, metastasis [44]. More details are awaited; however, Bailleul et al. did observe that NRF2 promotes radioresistance thanks to a powerful antioxidant response through metabolic reprogramming and pro-survival autophagy [45]. Autophagy is associated with either pro-survival or pro-death mechanisms depending on the circumstances [40,46]. Moreover, Wang et al. showed that SMAD4 deletion induces radioresistance through elevated reactive oxygen species (ROS) production along with autophagy induction [47]. These studies highlight that PDAC is able to manage ROS, with increased or decreased production, to promote resistance.

Mutations in cyclin-dependent kinase inhibitor 2A (CDKN2A) were shown to be often present in PDAC patients [48]. CDKN2A is known to code for two tumour suppressor proteins, p16INK4A (inhibitor of CDK4/6) and p14ARF (activator of p53). Thus, mutations in CDKN2A are associated with an increase in cellular proliferation. For this reason, two phase I clinical trials are currently investigating the use of CDK4/6 inhibitors in combination with mTOR inhibitors or nab-paclitaxel in patients with PDAC (NCT03065062 and NCT02501902, respectively). Furthermore, it was demonstrated that sequential administration of CDK4/6 inhibitors after taxane treatment resulted in a significant reduction

in the proliferation of PDAC cells in vitro and in vivo. CDK4/6 inhibitors prevented the cells treated with taxane to re-enter the cell cycle but also repressed homologous recombination [49]. Recently, encouraging pre-clinical results were obtained by combining a CDK4/6 inhibitor to MEK inhibitor [50]. Indeed, it was shown that combined treatment with a MEK inhibitor (trametinib) and a CDK4/6 inhibitor (palbociclib) induced a senescence-associated secretory phenotype (SASP), which led to a vascular remodelling in two mouse models of PDAC. This SASP-mediated vascular remodelling increased blood vessel density and permeability making the tumour more sensitive to the cytotoxic chemotherapy such as gemcitabine. These studies provide a strong proof of concept to combine CDK4/6 inhibitors to available chemotherapies in pancreatic cancer in order to amplify the effects of the latter.

Furthermore, pancreatic tumours are characterised by an abundant and dense collagenous stroma resulting from desmoplasia. The desmoplastic reaction observed in PDAC can be recognised through an excessive production of extra-cellular matrix with abundance of fibrillar proteins, glycoproteins, proliferating fibroblasts, inflammatory cytokines and immune cells [2,51]. The replacement of normal parenchyma with a desmoplastic environment increases pressure and causes vasculature constriction impairing drug delivery while creating a hypoxic environment for cancer cells [52].

Two types of hypoxia have been described: chronic hypoxia and cycling hypoxia. Chronic hypoxia corresponds to a deficit in oxygen for a continuous period of time, while cycling hypoxia consists of a back and forth between deep hypoxia and moderate hypoxia. Chronic and cycling hypoxia have different effects on resistance to treatment, tumour angiogenesis and tumour metastasis. Indeed, chronic hypoxia is going to severely influence the blood vessels while cycling hypoxia is known to affect cancer and stromal cells (for a review, see [53]). Tumour sensitivity to radiations depends on the degree of hypoxia at the time of irradiation and the duration of exposure to hypoxic conditions. However, studies have reported a higher radioresistance of cells exposed to cycling hypoxic conditions compared to the ones exposed to chronic hypoxia [54,55].

Hypoxia initiates the stabilisation of the Hypoxia Inducible Factor 1 (HIF-1α), which is one of the two subunits of the HIF-1 transcription factor. HIF-1 is key factor of many different signalling pathways implicated in tumour progression as well as in radio- and chemoresistance to cancer treatment [56,57]. In PDAC, Yokoi and Fidler demonstrated that hypoxia was able to mediate resistance to gemcitabine-induced apoptosis in the metastatic L3.6pl human pancreatic cancer cell line. This anti-apoptotic action was mainly exerted through the PI3K/Akt/NF-kB pathway, which is hyperactive under hypoxic conditions [58]. The hypoxia-induced chemoresistance also seems to act through the regulation of efflux pumps expression such as the ATP-binding cassette super-family G member 2 (ABCG2), which is a transmembrane protein responsible for the export of several chemotherapy drugs. In a study in the pancreatic cancer Capan-2 cell line, hypoxic conditions induced the overexpression of ABCG2 and resistance to gemcitabine [59]. This phenotype was suggested to be mediated by the phosphorylation of ERK1/2 which then activates HIF-1α in hypoxia. The activation of HIF-1α in turn regulates ABCG2 transcription by binding to its gene promoter. The inhibition of ERK1/2 and HIF-1α resulted in increased gemcitabine sensitivity in the Capan-2 cells [59]. Regarding radiotherapy, decreasing HIF-1 expression by HIF-1α inhibitor PX-478 was able to radiosensitise Panc-1 cells and BxPC-3 cells to X-ray irradiation in vitro [60]. In vivo, PX-478 markedly potentiated the anti-tumour activity of fractionated irradiation treatment, combined or not to 5-FU or gemcitabine chemotherapy, in Panc-1, CF-PAC-1 or SU.86.86 xenograft mice models [60]. Hypoxia also induces several changes in cancer cell metabolism that results in the physiochemical changes in the tumour microenvironment such as reduced pH and increased production of ROS [51]. Overall, there is strong evidence supporting the role of hypoxia and HIF-1 in treatment resistance in PDAC.

Radiotherapy used to be given at relatively small doses over several weeks, since the normal tissues present a slight survival advantage compared to the tumours. Importantly, this type of treatment regimen allows for the reoxygenation phenomenon to occur. Indeed, hypoxic tumour cells become oxygenated by the time of the next treatment [61]. As previously mentioned, recent advances in the field of radiotherapy have led to an increased usage of SBRT, which delivers high doses in fewer

fractions. In the case of PDAC, in which hypoxia can significantly vary, SBRT might not be optimal, depending on the extent to which reoxygenation can occur. However, as explained by Nahum in his work, for tumours associated with a lower alpha-beta ratio (parameters of the Linear-Quadratic model fitting survival fraction curves), a high number of fraction is not expected to increase tumour control for a given healthy tissue toxicity [62]. Pancreatic cancer is considered to have an alpha-beta ratio around 6 Gy, which is lower than the 10 Gy usually used for tumour cells [63]. This shows that PDAC could benefit from SBRT and the presence of hypoxia would then indicate that a higher overall dose should be used compared to oxic tumours. It also needs to be noted that, unexpectedly, high local controls have been observed following SBRT treatment [64]. The tumour response mechanisms behind high single dose efficacy are not fully understood and are still a work in progress, especially regarding the role of the tumour microenvironment [65,66].

Cancer stem cells (CSCs) and epithelial to mesenchymal transition (EMT) play a critical role in resistance to treatment [67–69]. CSCs are characterised by their capacity to self-renew and to generate multiple cell types along with cell division and tumour expansion. In PDAC, these cells expressing markers such as CD44, CD24, epithelial-specific antigen, CD133, CXCR4 or aldehyde dehydrogenase can also be used as potential CSCs markers [70–73]. EMT is a pro-invasive gene expression and signalling program enabling cancer cells to decrease cell-to-cell adhesion or cell-to-extracellular matrix and to acquire expression of mesenchymal proteins. During EMT, cancer cells undergo morphological changes and reorganise the cytoskeleton, resulting in increased motility and invasion abilities [74]. Besides its role in metastasis, a correlation between an EMT phenotype and chemo- or radioresistance has been established in cancer cells and notably in PDAC [69,75–77]. Several pathways, such as TGFβ, Wnt, Notch, EGFR, ERK or PI3K/AKT, are activated by RT or CT and promote the EMT phenotype. Subsequently, EMT can trigger transcription factors implicated in resistance (Snail, ZEB or Twist superfamily) [68,69,72,77–79]. Some of these pathways or regulators overlap with the ones activated by CSCs in PDAC such as TGFβ [80], Slug (Snail2) [81,82] or Notch1 [68].

CSC resistance to drug might also be explained by their relative quiescence state, i.e., a non-proliferative state. Quiescent cells are thought to be protected from chemotherapeutics agents as most of the drugs mediate their effects on one of the major characteristics that differentiate normal cells from cancer cells, which is their ability to indefinitely proliferate [83,84]. In PDAC, Cioffi et al. evidenced a quiescence-mediated chemoresistance in primary human pancreatic cancer cells obtained from patients and expanded in PDX [85]. The gemcitabine-resistant CSCs, isolated from PDX, were characterised by low expression of the miR-17-92 cluster members. Overexpression of miR-17-92 cluster in CSCs resulted in loss of the stemness phenotype, and a reduction of cells residing in G0 phase and G1 phase along with the abrogation of chemoresistance to gemcitabine. Inversely, the inhibition of the miR-17-92 cluster in non-CSCs PDAC cells induced a gain of stem-like features, abrogated cell proliferation and, subsequently, increased chemoresistance to gemcitabine [85].

Hypoxia-induced treatment resistance also seems to interplay with mechanisms implicating CSCs and EMT. For example, a link has been made between hypoxia-induced EMT and resistance to gemcitabine in PDAC cells [86]. Under hypoxic conditions, the PANC-1 and BxPC3 cell lines displayed an EMT-like phenotype, HIF-1α and NF-κB hyperactivity and reduced sensitivity to gemcitabine. The inhibition of the two transcription factors HIF-1α and NF-κB with siRNAs resulted in the reversal of EMT phenotype and an increased sensitivity of both cell lines to gemcitabine [86]. Furthermore, hypoxia was also shown to synergistically enhance gemcitabine-induced stemness and acquired resistance in Panc-1 and Patu8988 pancreatic cancer cell lines by activating the AKT/Notch1 signalling cascade, which evidenced that hypoxia plays an important role in maintaining and promoting CSC subpopulation in the tumour [87].

MicroRNAs (miRNAs) are non-coding small RNAs that are 17–25 nucleotides long. Some of them play an important role in drug sensitivity regulation in cancer cells. They act at a post-transcriptional level by binding mainly to 3′ untranslated region of target mRNA, which leads to repression or degradation of the mRNA [68]. MiRNAs can either act as oncogenes or tumour suppressors and

their expression level was also reported to be correlated to drug and radiation response during cancer treatment [88–90]. For example, high levels of miRNA-21, miRNA-1266 and miR-221 were reported to be linked with gemcitabine resistance in PDAC [91–94]. On the contrary, miRNA-101-3p seems to be lowly expressed in gemcitabine-resistant pancreatic cancer cells and of miRNA-101-3p mimic transfection restored cell sensitivity for the drug [95]. Much evidence also suggests the implication of miRNAs in chemosensitivity through the regulation of EMT process and stemness in cancer cells. For instance, the expression of some of miR-200 and let-7 miRNA family members is downregulated in gemcitabine-resistant cells with an EMT phenotype. The re-expression of miR-200 by transfection in gemcitabine-resistant cells resulted in a morphological reversal of the EMT phenotype and increased sensitivity to gemcitabine [96]. Compared to normal pancreatic ductal epithelial cells, miR-34 expression is reduced in pancreatic CSCs (CD44+/CD24+/ESA+) and pancreatic cancer tumour cells (MIA PaCa-2 and AsPC-1). The restoration of miR-34 expression inhibits growth and enhances sensitivity to gemcitabine [97]. Furthermore, miRNA-320a and miRNA-221-3p were found to be upregulated in 5-FU-resistant pancreatic cancer cells [98–100]. As demonstrated by deep sequencing, upregulated and downregulated miRNAs are implicated in radiation resistance of PDAC cell lines [101]. For example, miRNA-216a and miRNA-23b were also found to be downregulated in radioresistant PDAC cell lines [102,103]. Both studies pointed to a pro-survival role of autophagy after radiation as the re-expression of both miRNAs inhibited autophagy and increased cell death.

Growing evidence has brought the implication of extracellular microvesicles (EVs) as factors in chemo- and radioresistance of cancer cells [104–107]. EVs are microparticles with a lipid bilayer membrane, secreted from all cell types either in physiological and pathological conditions [81]. EVs are able to mediate drug resistance but also to confer resistance to drug-sensitive cancer cells through the transfer of cargoes including drug efflux pumps, pro-survival factors and inhibitors of apoptosis [104]. A part of EVs-mediated drug-resistance also relies on miRNAs transfer, as it was shown for miR-155 in gemcitabine-resistant pancreatic cancer cells [108]. Furthermore, these EVs containing miRNA can also be derived from immune cells such as tumour-associated macrophages (TAMs) or from cancer associated fibroblasts (CAFs), evidencing the existence of a complex collaboration between stromal or immune cells and cancer cells [104,109,110].

4.2.2. Charged Particles vs. Resistance

In addition to dose conformation, charged particles have a higher linear energy transfer (LET), i.e., an increased ionisation density, especially within the Bragg peak. The LET varies along the particles track, being small in the entrance region and increasing rapidly within the Bragg peak. The same profile is observed for the density of induced damages, i.e., smaller when passing through the body and much higher within the tumour. Increased ionisation leads to the formation of more complex DNA damages (clustered lesions) than photons and thus to a stronger cellular response [111,112]. Radiation-induced DNA damages are classified as direct damages (ionising radiation interacts directly with the DNA) and indirect damages (DNA damage is mediated through ROS). With increasing LET, and thus increasing ionisation density, direct damage proportion increases as well as the complexity of the DNA damage pattern and the release of DNA fragments [113–115]. This leads to an increased cell response, which is described by the relative biological effectiveness (RBE). The RBE is determined as the ratio of the doses required to obtain a given output for a reference radiation (photons) compared to the chosen radiation [111]. For a given particle, the RBE has been found to depend on several factors such as the dose and dose-rate or the intrinsic radiosensitivity of the tissue [112]. For protons that have an LET close to photons at high energies, a 1.1 RBE value is used in clinic, although within the Bragg peak this value increases. For carbon ions, an RBE of 3 is used, reflecting the higher complexity of the DNA damage pattern.

Thanks to this change in damage distribution, the use of charged particles such as protons or carbon ions might help to counteract some of the resistance mechanisms observed during cancer treatment [116,117].

For example, as high LET particles increase the production of direct DNA damages, their effect relies less on indirect damage mediated by ROS. As demonstrated by Georgakilas et al., with increasing LET, the number of induced cluster of DNA damage under normoxic and anoxic condition tends to be similar while it decreases for low LET photons [118]. This reduced addiction to ROS to induce DNA damages allows high LET particles to treat more efficiently hypoxic tumour [119–121]. Furthermore, photons and charged particles differ regarding the effect on signalling pathways: photons might upregulate one pathway while charged particles might induce the opposite effect, i.e., downregulate the very same pathway. For example, in glioblastoma, a differential effect of carbon ions versus photons was observed on orthotopic, syngeneic murine xenografts as well as glioma stem cell-enriched, PDX [122]. In their work, contrarily to photons, carbon ions downregulated Notch and Wnt pathways, angiogenesis, EMT and extracellular matrix remodelling. Works on CSCs response after charged particle irradiation, summarised in [116,123,124], showed that CSCs are more sensitive to protons and carbon ions than to photons. Moreover, inversely to conventional RT, HIF-1α has been found to be downregulated after proton or carbon ion irradiation [125,126]. The clustered DNA pattern and more particularly ROS distribution was hypothesised to be an explanation for the differences in gene upregulation or downregulation after conventional irradiation versus proton or carbon ion irradiation [126]. ROS distribution is homogeneous following photon exposure while it is concentrated around the ion track with charged particles [126].

Regarding PDAC, interesting results have been obtained in PDAC CSCs after carbon ion irradiation. Oonishis et al. analysed colony, spheroid and tumour formation as well as DNA double strand break (DSB) formation on PDAC CSCs treated with X-ray or carbon ions [127]. The proportion of CSCs was more enriched after X-rays compared to carbon ion irradiation. This was associated with an increased complexity of DSBs in the case of carbon ion irradiation. Similarly, Sai et al. showed that the proportion of CSCs was enriched after exposure to photons compared to carbon ions [128]. They evidenced that combination of carbon ions with gemcitabine synergistically enhanced CSCs death compared to carbon alone through an increase in complex DNA damage, in cell death (apoptosis and autophagy) and inhibition of cell proliferation.

Additionally, high LET radiation can induce apoptosis in a p53-independent manner thanks to the activation of caspase-9 instead of caspase-8 apoptotic pathway [129–131]. This feature is interesting knowing that TP53 is mutated in 60% to 70% of PDAC patients [3]. To target other mutations often found in PDAC, Ruscetti et al. used inhibitor of CDK4/6 and MEK, downstream actors of CDKN2A and KRAS. They have shown that the SASP induced by the inhibition of CDK6/4 and MEK led to vascular remodelling that increased blood vessel density and permeability, making the tumour more sensitive to the cytotoxic chemotherapy [50]. It is well accepted that conventional RT induces senescence, and thus, could also lead to a beneficial SASP [132,133]. Protons and carbon ions can also trigger senescence [134–136]. A study performed on glioma cell lines irradiated with carbon ions showed that cells did not die of apoptosis or of autophagy but became senescent regardless of the p53 status of the cell line [134]. The role of senescent cells and associated SASP in cancer treatment can lead to possible benefit (vascular remodelling, immune cell attraction) or liability (promotion of cell proliferation and invasion) for tumour progression [137,138]. In PDAC, the work of Ruscetti et al. indicates that inducing senescence could be a promising approach to improve response to treatment.

Several studies have shown the implication of miRNAs and EVs in pancreatic tumour progression and the influence of low LET photon radiation on the EVs cargoes. However, very few data were recorded regarding the effect of charged particle irradiation on these elements in pancreatic cancer. However, Yu et al. recently demonstrated the effect of carbon ion irradiation on miRNAs expression transported by EVs in prostate cancer [139]. They compared the miRNAs extracted from exosomes derived from prostate cancer patient blood samples before and after carbon ion radiotherapy. The analysis evidenced an altered expression of 57 miRNAs present in the exosomes. In view of these results, we can suggest that charged particle irradiation might influence the EVs cargoes in pancreatic cancer as well.

Finally, the ability of PDAC cells to manage ROS suggests that direct DNA damaging radiation such as heavy charged particles would be more efficient than photons. In addition, the characteristic distribution of ROS after charged particles might affect the capacity of PDAC to handle these radio-induced ROS [126].

The peculiar distribution of DNA damage (or damage to other cellular component) and ROS production intensify cell response to charged particles compared to conventional photon irradiation. The alteration of pathways usually involved in resistance to treatment opens a window for higher LET ions to counteract these mechanisms and to extend the tumour local control, as summarised in Figure 1.

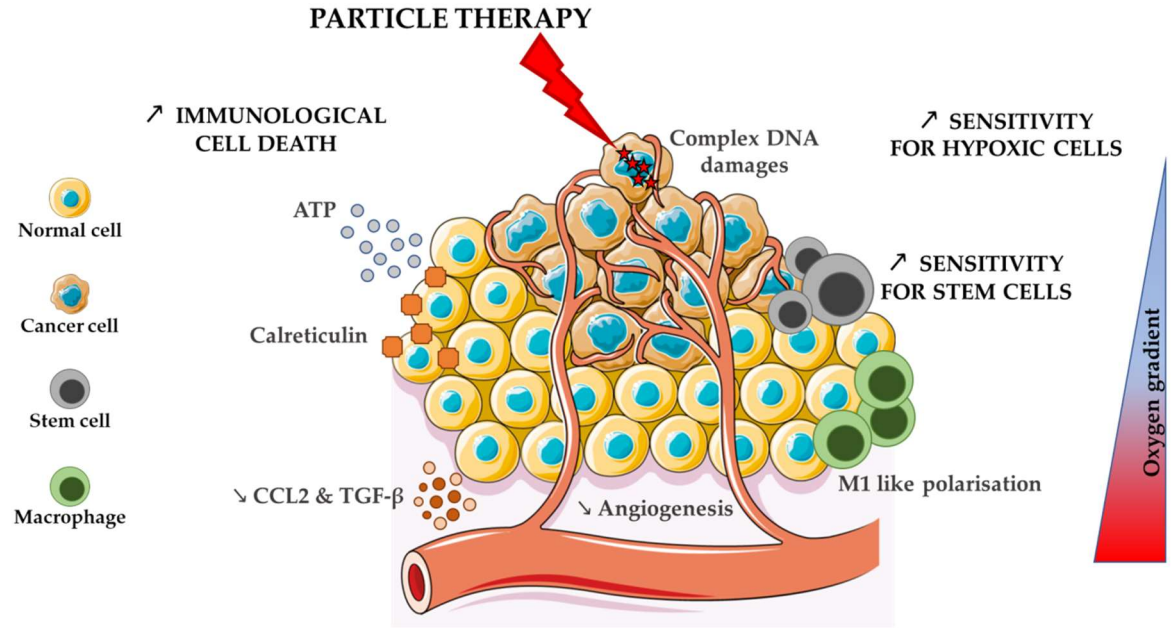

Figure 1. Attractive effects of charged particles in comparison to photons on the different tumour cell types.

4.3. Pushing Further PDAC Local Control: Charged Particles and Targeted Drug Combination

Enhanced DNA repair response to DNA damage is a cause of tumour resistance. Hence, we propose to further potentiate the effect of charged particles by targeting poly(ADP-ribose) polymerase (PARP) and homologous recombination (HR).

Indeed, about 10% of PDAC patients present mutations in BRAC2 and ATM. Patients with BRCA1/2 mutations have shown beneficial responses to PARP inhibitors [140]. Upon DNA damage, PARP binds to single-strand breaks (SSBs), which, in turn, activates its catalytic domain, provoking the recruitment of other DNA damage repair proteins. PARP inhibitors, like Olaparib, prevent DNA damage repair to occur by stabilising the SSBs. These SSBs are in turn translated into DSBs at the replication fork. These DSBs, produced during the S phase, are repaired through the HR pathway for which intact BRCA1 and BRCA2 are required. The results of the phase III Pancreas Cancer Olaparib Ongoing (POLO) trial, which showed great promise for enrolled patients with metastatic pancreatic cancer with mutation in BRCA1 or BRCA2, who were previously treated with platinum-based chemotherapy. The enrolled patients were randomised to receive either Olaparib or placebo as the maintenance therapy. The study met its primary endpoint with a progression free survival (PFS) in the Olaparib group significantly longer compared to placebo. Furthermore, significant responses were seen in 20 patients in the treated group compared to six in the placebo group. However, no overall survival benefit could be recorded after analysis of 46% of events [141]. As shown in both ovarian and breast cancer, the POLO trial demonstrated the potential for PARP inhibition in pancreatic cancer, likely setting a new standard of care in patients presenting pancreatic cancer with germline BRCA1 or BRCA2 mutation.

Recently, Szymonowicz et al. compared BRCA2-proficient BxPC3 and Capan-1 pancreatic cancer cells with BRCA2-deficiency, and showed that both cell lines were more sensitive to proton than to photon irradiation. The sensitising effect was even more noticeable in Capan-1 cells, leading the authors to suggest a predominant role of HR in the repair of clustered DNA damage induced by protons [142]. This was also demonstrated in lung cancer and glioblastoma cell lines where the impairment of HR led to a higher sensitisation after proton irradiation compared to photons for which the effect of NHEJ pathway inhibition was more pronounced [143].

In a previous work from our group, PARP and RAD51 inhibitors, Olaparib (AZD2281) and B02, respectively, were combined in order to sensitise cancer cells to proton irradiation [136]. Pancreatic cell lines, KP4 and PANC1, were radiosensitised to protons by each of the two inhibitors while the combination further increased cell death only for the fast cycling KP4 cell line. RAD51 is one of the key proteins of the HR pathway that is often overexpressed in cancer cells, notably in PDAC, and is thus now considered a clinically relevant target for combined therapies [144–146]. RAD51 inhibitors, such as B02, lead to HR inhibition, hence sensitising cells to DSBs [147–151]. This strategy could be used to counteract the resistance associated with PARP inhibitor but also to extend their use to patients without BRCA mutations. Furthermore, exposure to charged particles leads to the release of smaller DNA fragments compared to photons and notably fragments smaller than 40 base pairs [152]. Interestingly, Ku70/Ku80 heterodimer, a key player in non-homologous end joining (NHEJ) DSB repair pathway, is not able to bind these small fragments [152]. This means that the canonical NHEJ pathway is less efficient after irradiation with high LET particles. The repair of DSBs is thus in the hands of HR or alternative NHEJ pathways. This alternative NHEJ is dependent on PARP-1 [153]. Moreover, it has been shown that HR proteins such as RAD51 are downregulated under hypoxia [154,155]. These last observations show that combining PARP inhibitor with high LET particles such as carbon ions is very promising for improving local control. A combination of PARP inhibitor with a RAD51 inhibitor would push even further the local control obtained with charged particles irradiation [151,156].

5. PDAC Systemic management: Charged Particles to Trigger an Immune Response

In addition to the mechanisms cited above, immune evasion is also recognised to play a major role in tumour resistance. PDAC was originally considered as a 'non-immunogenic' neoplasm. However, it was recently demonstrated that PDAC immune microenvironment can play a considerable role in tumour evasion.

5.1. Immune Evasion in PDAC: T Cells and Tumour-Associated Macrophages

T cells are abundant in the stroma of PDAC, and patients with higher levels of CD4+ and/or CD8+ T cells have significantly prolonged survival. Unfortunately, a large number of PDAC tumours demonstrate increased infiltration of T regulatory cells, myeloid-derived suppressor cells (MDSCs) and M2-like macrophages, blocking the activities of CD4+ and CD8+ T cells. PDAC is also characterised by an abundant desmoplastic stromal reaction restricting the infiltration of T cells into the tumour. T cell activation is determined by a balance between the signals of both co-stimulatory or co-inhibitory ligands and receptors. CTLA-4 is a CD28 homolog with a high affinity for B7-1 and B7-2 ligands. The interaction between CD28:B7-1/2 serves as a co-stimulatory signal for T cells, while the interaction between CTLA-4:B7-1/2 acts as a co-inhibitory signal to terminate the immune response. Thus, an effective way to promote lymphocyte activation is by reducing their inhibition. The checkpoint inhibitor Ipilimumab (anti-CTLA-4) has been administered as a single agent to patients with locally advanced or metastatic pancreatic cancer with disappointing results, as it was unable to demonstrate efficacy or prolong patient survival [157]. Another way to target T cell responses is through the PD-1/PD-L1 pathway. PD-1 is also a receptor of the CD28 family. This receptor can recognise two ligands: programmed death ligand 1 (PD-L1) and programmed death ligand 2 (PD-L2). The engagement of PD-1 by its ligands induces T cell inactivation. Anti-PD-1/PD-L1 have demonstrated clinical efficacy in several cancer types such as melanoma, non-small cell lung cancer and classical Hodgkin lymphoma. However, the same therapy

showed no therapeutic benefits in patients with pancreatic cancer [158]. In their work, Ruscetti et al. combined a CDK4/6 inhibitor (palbociclib) to a MEK inhibitor (trametinib) in two mouse models of PDAC [50]. The SASP induced by this combination led to vascular remodelling with an increased permeability. They showed that exhausted CD8+ T cells easily infiltrated the tumour, as demonstrated by the presence of several exhaustion markers, PD-1, 2B4, CTLA-4 and LAG3, at the surface of the isolated cytotoxic T cells. CD8+ T cells isolated from tumours treated with senescence-inducing agents and anti-PD-1 combined therapy, displayed reduced expression of exhaustion markers as well as increased expression of several activation markers when compared to CD8+ T cells isolated from tumours treated with the senescence-inducing agents only [50].

Tumour-associated macrophages (TAMs) represent major actors in the tumour microenvironment. The presence of macrophages has been associated with poor prognosis in several cancer types and PDAC [159–161]. In the context of PDAC, TAMs were thought to originate only from circulating monocytes. However, it was recently shown that TAMs in pancreatic cancer can originate from circulating monocytes as well as from embryonic precursors [162]. Regardless of developmental origin, macrophages can adopt several functions, and are classified using the M1-M2 scale, similarly to the Th1-Th2 classification used for T cells. M1 macrophages, also known as classically activated, have pro-inflammatory and anti-tumour properties, whereas M2 macrophages, also known as alternative activated macrophages, exhibit anti-inflammatory and pro-tumour capabilities. In the tumour microenvironment, macrophages tend to adapt a M2-like phenotype, making them attractive targets for anti-tumour interventions. Strategies to target TAMs focus on their depletion, on blocking their recruitment into the tumour or on rewiring their phenotype towards the anti-tumour M1 phenotype.

Trabectedin (ET-743), a molecule derived from sea squirt, *Ecteinascidia turbinate*, is approved for the treatment of advanced soft tissue sarcoma and ovarian cancers that relapsed. In addition to its anti-proliferating abilities, this drug is able to induce the depletion of myelomonocytic cells through the activation of caspase-8 via TNF-related apoptosis-inducing ligand (TRAIL) receptors [163]. A recent study, focused on the epigenetic profile of T cells after treatment with trabectedin, revealed that the depletion of TAMs can switch the phenotype of T cells from pro-tumour to anti-tumour in PDAC. Indeed, tumour-infiltrating lymphocytes (TILs) showed a reactivation both at the epigenetic and functional levels, with a switch from IL10-secreting T cells towards an effector/memory phenotype [164]. Combining trabectedin with checkpoint inhibitors might be efficient in PDAC patients, as it was successful in a murine model of ovarian cancer [165].

Circulating monocytes can be recruited into the tumour by the CCL2-CCR2 axis and the blockade of CCR2 decreases monocyte recruitment, tumour growth and metastasis in an orthotropic model of PDAC [166]. This pre-clinical study was followed by a phase Ib clinical trial testing CCR2 blockade in combination with chemotherapy in patients with advanced PDAC, which demonstrated that more patients achieved partial response when treated with CCR2 inhibitor and FOLFIRINOX [167]. Circulating monocytes are also recruited through the colony-stimulating factor 1 (CSF1)/CSF1 receptor (CSF1R) axis. It was shown that targeting macrophages with an inhibitor of CSF1R was able to increase mouse survival in the genetic KPC PDAC mouse model [168]. The inhibition of CSF1R can also improve the response of chemotherapy in an orthotopic mouse model [169]. A similar conclusion was drawn after treatment of PDAC bearing mice with RT and anti-CSF1 antibody [170]. Furthermore, the inhibition of CSF1/CSF1R is also capable of modulating the phenotype of macrophages in order to boost T cells [171]. A pilot study, NCT03153410, will be looking at the efficiency of cyclophosphamide, pembrolizumab, GVAX (pancreatic cancer vaccine) and IMC-CS4 (CSF1R monoclonal antibody) combinations in patients with BR-PDAC.

Several approaches have been developed to switch the phenotype of M2 macrophages with pro-tumour abilities towards M1 macrophages with anti-tumour properties. CD40 is a member of the tumour necrosis factor (TNF) receptor superfamily and is expressed by immune cells such as B cells, dendritic cells (DC) and monocytes. In combination with gemcitabine therapy, CD40 agonists are capable of re-educating macrophages. When mice were treated with CD40 agonist, macrophages in

the KPC tumours upregulated the expression of MHC class II and CD86, which is consistent with a M1 phenotype, when compared to untreated controls [172]. Nab-paclitaxel has also been demonstrated to induce anti-tumour immunity through the reprogramming of tumour-associated macrophages via TLR4 in vitro and in vivo. Indeed, treatment of RAW 264.7 cells with nab-paclitaxel induced an increased expression of IL-1alpha, IL-1beta, IL-6, IL-12p40 and TNF-alpha. The drug was also shown to induce M1 polarisation in an orthotopic murine model. Indeed, flow cytometry analysis revealed that nab-paclitaxel is able to increase the MHC II+ CD80+ CD86+ macrophage population [173,174]. In a similar fashion, lipopolysaccharide (LPS), known as an TLR4 agonist, can be used alone or in combination with IFN-γ to switch the polarisation of macrophages towards a M1 phenotype in order to induce anti-tumour response [175].

5.2. Conventional RT and Immune Response in PDAC

It is well known that RT induces an immune response. Whether this response is in favour of immune stimulation or of immune repression is not trivial, as both types of responses are observed [176–178].

A combination of checkpoint inhibitors for RT should be efficient as RT upregulates PD-L1 expression in PDAC. Indeed, RT upregulates the expression of PD-L1 in KPC and Pan02 cell lines when compared to unirradiated control cells [179]. Anti-PD-L1 treatment significantly enhanced the tumour growth delay observed in vivo after giving high doses (12 Gy or 5 × 3 Gy) to Pan02 tumour model in mice. Several inflammatory cytokines were analysed in the sera of treated mice, stromal derived factor 1 (SDF-1) was significantly downregulated after receiving anti-PD-L1 and radiotherapy. Knowing that SDF-1 is implicated in the creation of an immunosuppressive microenvironment, the authors concluded that combining radiotherapy to checkpoint blockade is able to influence the tumour microenvironment and give favourable results [179]. This pre-clinical study demonstrated the efficacy of combining checkpoint blockers to RT, since checkpoint blockers on their own had failed to show benefits in PDAC patients. However, a recent study demonstrated that inhibiting autophagy might be able to sensitise PDAC tumours to dual immune checkpoint blockade (anti-PD-1 and anti-CTLA-4 antibodies) [180]. By screening a panel of human PDAC cell lines, the authors showed that MHC I was predominantly localised within the autophagosomes and lysosomes when compared to non-transformed human pancreatic ductal epithelial cells. Furthermore, the reduced expression of MHC I in the plasma membrane was shown to facilitate the evasion of cancer cells from cytotoxic T cells, which are capable of recognising tumour antigens when presented by MHC I. Inhibiting autophagy by the use of chloroquine increased MHC I expression levels in the plasma membrane in vitro as well as in vivo. However, as previously demonstrated, the use of chloroquine as a mono-therapy is unable to reduce the tumour burden [181], whereas combining chloroquine to dual immune checkpoint blockade significantly decreased tumour weight on treated mice bearing orthotopic tumours (HY15549), underlying the important role of autophagy to mount an immunological response [180]. The role of autophagy during pancreatic cancer development and progression is not as straightforward as mentioned above [46,182]. For example, autophagy has also been shown to play a major role in triggering immunological cell death (ICD) since it leads to ATP release which is one requirement for an efficient immune response.

In order for conventional RT to activate an immune response, it has been demonstrated that the activation of cyclic GMP-AMP synthase (cGAS)/stimulator of interferon genes (STING) pathway is required. Indeed, the activation of the cGAS-STING pathway upregulates the expression of type I interferon, which plays an important role in the recruitment of DCs. However, it was shown that RT can upregulate the expression of Trex1, an exonuclease capable of degrading cytosolic dsDNA, thus preventing the activation of the cGAS-STING pathway. RT seems to upregulate the expression of Trex1 at doses around 12 to 18 Gy in different mouse and human carcinoma cell lines [183].

Regarding TAMs recruitment, the blockade of CCL2-CCR2 could also be used in combination with radiotherapy since CCL2 is responsible for radioresistance in a syngeneic mouse model of PDAC [184]. RT increased the expression of PDAC derived CCL2 leading to an increase in

inflammatory monocytes/macrophages. In a surprising manner, the phenotype of these inflammatory monocytes/macrophages isolated from tumours after radiotherapy did not reveal differences in gene expression when compared to sham irradiated control. However, mice treated with a combination of RT and anti-CCL2 antibody showed prolonged survival probably due to impairment in inflammatory monocyte recruitment [184].

Finally, RT has the potential to switch TAMs phenotype from M1 to M2. For example, low-dose RT (2 Gy) has also been shown to be capable of inducing the reprogramming of tumour-associated macrophages in a genetic mouse model of insulinomas. Indeed, the expression of the M1 marker, iNOS as well as several M2 markers, namely, HIF-1, Ym-1, Fizz-1 and Arg1, was investigated in CD11b+ peritoneal macrophages from RT5 mice after receiving whole-body irradiation. Radiation led to an increase in iNOS expression, while reducing the expression of M2 markers in peritoneal macrophages. However, the authors observed that local irradiation alone is unable to swift the phenotype of TAMs toward a M1-like phenotype [185]. Furthermore, the same group also demonstrated that macrophages could be re-tuned towards an anti-tumour phenotype after whole body irradiation in RT5 mice [186]. These studies demonstrated the potential of RT to elicit anti-tumour immunity. However, it has to be noted that the effect of conventional RT is highly is dependent on the dose and the regimen schedule used [187].

5.3. Charged Particles to Improve Immune Response in PDAC

Charged particles feature an attracting dose deposition profile associated with a better dose conformation. This allows sparing circulating T cells and other immune cells during treatment. As explained in the review of Durante and Formenti, although the damages induced by charged particles to lymphocytes are more complex, it was shown in vivo that the size of the irradiated field is more relevant than DNA damage complexity to induce lymphopenia [188].

As evidenced in the previous section, charged particles also present an increased density of ionisation leading to an enhanced biological response due to the higher complexity of DNA damage. This enhanced response of tumour cells could help trigger T cells and TAMs response.

For example, it was recently demonstrated that RT induces ICD in a dose-dependent manner and that particles could increase the immunogenic response [189,190]. Indeed, translocation of calreticulin to the cell membrane of irradiated cells was observed, as well as the release of high mobility group box 1 (HMGB-1) and ATP release. The release of these damage-associated molecular patterns (DAMPs) can trigger a cascade leading to the activation of DCs, which will prime CD8+ T cells. In vitro study has suggested that higher LET radiation may lead to a broader immunogenic response. Indeed, protons mediate calreticulin translocation to cell surface at higher levels than photons, leading to increased cross priming and higher sensitivity to cytotoxic T cells [190]. Furthermore, proton therapy did not increase the expression of PD-L1 on cancer cells, meaning that the activity of T cells would not be inhibited as it is the case for conventional RT. High-LET radiation was also shown to increase autophagy via the unfolded protein response (UPR), suggesting that high-LET radiation might effectively induce ICD and subsequent immune response in the context of pancreatic cancer [191,192]. A phase II clinical trial (NCT01494155) is currently underway to test the efficacy of capecitabine and hydroxychloroquine combined to photon or proton irradiation to control the growth of tumours in 50 patients with pancreatic cancer.

Particle therapy could help in the rewiring of TAMs phenotype. Indeed, protons were shown to partially reprogram, in vitro, M2-polarised macrophages towards an anti-tumour M1 phenotype [193]. Moreover, as opposed to photons, carbon ions were able to increase M1 and reduce M2 populations associated with increased abundance of cytotoxic CD8+ T cells in vivo in a mouse model of glioblastoma [122].

The role of FLASH PT to modulate the immune response is also worth investigating. Indeed, TGFβ1 level 24 h and 1 month after irradiation was significantly reduced normal human diploid lung fibroblasts with ultrahigh dose-rate irradiation compared to standard regimen [194]. Two other

works mentioned the potential of FLASH PT and both evidenced the involvement of an immune response. Firstly, the effect of FLASH PT was evaluated on C57BL/6 mice 8 to 36 weeks after whole thorax irradiation and compared to standard dose-rate PT [195]. The authors reported a reduction in lung fibrosis and skin dermatitis. A genome wide microarray analysis revealed an elevation of DCs maturation, protein kinase C signalling in lymphocytes, TH1 pathway modulation and calcium-induced T lymphocyte apoptosis after standard regimen while they were decreased after FLASH dose-rate indicating the involvement of an immune response in the reduction of toxicities. The other study compared the efficacy of 18 Gy FLASH PT to standard dose-rate on the eradication of Lewis Cell Carcinoma syngeneic, orthotopic mouse model [196]. Mice irradiated with FLASH PT presented smaller tumours with an increased recruitment of CD4+ and CD8+ T cells in the tumour core than standard dose-rate irradiation. In their review, Dutt et al. assembled evidence on immunomodulation from novel dose-rate regimen such as FLASH RT [197]. For example, they presented that conventional irradiation led to an increased release of CCL2, which in turn attracted monocytes at tumour sites and promoted their differentiation into TAMs. Furthermore, HIF-1α, upregulated after RT, increased the expression of CSF1, which polarised these TAMs towards an M2 phenotype. M2 TAMs secretes TGFβ, which is known to convert CD4+ T cells into T regulatory cells [197]. In short, they showed that conventional RT can lead to an immunosuppressive response. However, this is not as simple as conventional RT is able to trigger both immunosuppressive and immunostimulatory responses [198].

The advantages of charged particles over photons on the immune response are summarised in Figure 1.

Protons and carbon ions downregulate the expression of genes associated with an immunosuppressive response such as HIF-1α, VEGF, CCL2 or even TGFβ at ultrahigh dose-rate, but also lead to a stable expression of PD-L1. We can then expect charged particles to trigger an immunostimulatory response. Combining PARP and RAD51 inhibitor with charged particles could further enhance this response. Indeed, PARP inhibitors display an immunomodulatory effect by promoting the cGAS/STING pathway, thanks to the accumulation of cytosolic DNA, and by stimulating the expression of type I IFN, as explained in [199]. A combination with RAD51 inhibition would further push the STING pathway mediating an innate immune response by accumulation of cytosolic DNA [200].

Such a combination of charged particles with PARP and RAD51 inhibitor seems a promising approach to loco-regional control of PDAC with an increased level of clustered DNA whose repair relies mostly on HR and alt-NHEJ pathways. This combination could also lead to a systemic response by favouring an immune response.

6. Conclusions

Current treatment modalities used for pancreatic cancer have not been able to dramatically change the course of this deadly disease. A variety of resistance mechanisms and induced toxicities of the current treatment have hampered their curative potential. Fortunately, the recent developments made in the field of radiotherapy allow highly conformal technique such as SBRT and charged particle therapy aiming at dose escalation and improved local control with limited toxicities to OARs. Several differences in tumour response to charged particles compared to photons have been highlighted in this review. These differences evidence that charged particles could help to counteract some of the resistance mechanisms found in PDAC. We suggest that charged particles also hold great promises when combined with DNA repair inhibitors such as PARP and RAD51 to improve local control. Moreover, this combination could be able to mount an efficient immune response thanks to the release of several DAMPs enabling the activation of T cells and downregulation of immunosuppressive genes. Pre-clinical studies also demonstrate that unlike conventional radiotherapy, proton and carbon ions are able to reprogram macrophages towards an anti-tumour phenotype. Additionally, senescence-associated therapies, such as radiotherapy, can create several vulnerabilities in pancreatic cancer leading to drug delivery enhancement and T cell infiltration. Therefore, combining particle therapy to complementary

DNA repair inhibitor could be beneficiary in the context of pancreatic cancer in order to increase local and distant control of the tumour.

The availability as well as the cost of this technique have, up to now, limited its use in clinical practise over conventional photon radiotherapy. Coming clinical trials have to evidence the balance between efficiency and cost to help address which patients would benefit from particle therapy. Currently, the clinical data regarding the advantages of particle therapy over conventional radiotherapy are limited, but the results presented above are encouraging. With several clinical trials underway, the effects of particle therapy in the context of pancreatic cancer should bring forward this promising form of treatment.

Author Contributions: C.H., J.-W.C. and A.-C.W. wrote the manuscript. B.L.C. and C.M. reviewed the manuscript. All authors read and agreed to the published version of the manuscript.

Funding: C.H. and A.C.W. are supported by the Belgian Funds for Scientific Research (FRS-FNRS, Belgium). J.W.C. is a recipient of a Région Wallonne Grant (ProtherWal project).

Conflicts of Interest: The authors declare no conflict of interest.

Abbreviations

3DCRT	three-dimensional conformation radiation therapy
5-FU	5-fluorouracil
ABCG2	ATP-binding cassette super-family G member 2
AKT	protein kinase B
Arg	arginase
ATM	ataxia telangiectasia mutated
ATP	adenosine triphosphate
BED	biological equivalent dose
BRCA2	breast cancer type 2 susceptibility protein
BR-PDAC	borderline resectable PDAC
CAF	cancer associated fibroblast
CCL2	chemokine ligand 2
CCR2	C-C chemokine receptor type 2
CDK4/6	cyclin-dependent kinase 4 and 6
CDKN2A	cyclin-dependent kinase inhibitor 2A
cGAS	cyclic GMP-AMP synthase
CRT	chemoradiotherapy
CSC	cancer stem cell
CSF1	colony-stimulating factor
CSF1R	colony-stimulating factor 1 receptor
CT	chemotherapy
CTLA4	cytotoxic T-lymphocyte associated protein 4
CXCR4	C-X-C motif chemokine receptor 4
DAMPs	damage associated molecular patterns
DC	denditric cell
EGFR	epidermal growth factor receptor
EMT	epithelial to mesenchymal transition
EORTC	European organisation for research and treatment of cancer
ERK	mitogen-activated protein kinase 1
ESPAC	European study group for pancreatic cancer
EV	extracellular vesicle
FLASH RT	ultrahigh dose-rate radiation therapy
GIST	gastrointestinal study group
HIF-1α	hypoxia inducible factor 1
HMGB-1	high mobility group box 1
HR	homologous recombination

ICD	immunogenic cell death
IFN-γ	interferon-γ
IMRT	intensity modulated radiation therapy
iNOS	inducible nitric oxide synthase
KRAS	kirsten rat sarcoma
LA-PDAC	locally advanced PDAC
LET	linear energy transfer
LPS	lipopolysaccharide
MDSC	myeloid-derived suppressor cells
MEK	mitogen-activated protein kinase kinase
MHC 1	major histocompatibility complex class 1
mTOR	mammalian target of rapamycin
nab-paclitaxel	nanoparticle-bound paclitaxel
NF-κB	nuclear factor kappa B
NHEJ	non homologous end joining
NRF2	nuclear factor erythroid 2-related factor 2
OAR	organ at risk
OS	overall survival
PARP	poly(ADP-ribose) polymerase
PDAC	pancreatic ductal adenocarcinoma
PD1	programmed cell death 1
PDK1	pyruvate dehydrogenase kinase 1
PD-L1	programmed cell death ligand 1
PDX	patient-derived xenograft
PI3K	phosphatidylinositol 3-kinase
POLO	pancreas cancer olaparib ongoing
PREOPANC	preoperative chemoradiotherapy versus immediate surgery for resectable and borderline resectable pancreatic cancer
PRODIGE	trial comparing adjuvant chemotherapy with gemcitabine versus mfolfirinox to treat resected pancreatic adenocarcinoma
PT	proton therapy
RAF	rapidly accelerated fibrosarcoma
RAS	rat sarcoma
RBE	relative biological effectiveness
ROS	reactive oxygen species
R-PDAC	resectable PDAC
RT	radiotherapy
RTOG	radiation therapy oncology group
SBRT	stereotactic body radiation therapy
SDF-1	stromal derived factor 1
SMAD4	mothers against decapentaplegic homolog 4
SMART	stereotactic magnetic resonance guide adaption radiation therapy
SPArc	continuous spot-scanning protons arc
STING	stimulator of interferon genes
TAM	tumour-associated macrophages
TGFβ	transforming growth factor beta
TIL	tumour infiltrating lymphocytes
TNF	tumour necrosis factor
TRAIL	TNF-related apoptosis-inducing ligand
Trex1	three prime repair exonuclease 1
UPR	unfolded protein response
VEGF	vascular endothelial growth factor
Wnt	wingless-integration-1
ZEB	zinc finger E-box binding homeobox

References

1. Ferlay, J.; Colombet, M.; Soerjomataram, I.; Dyba, T.; Randi, G.; Bettio, M.; Gavin, A.; Visser, O.; Bray, F. Cancer incidence and mortality patterns in europe: Estimates for 40 countries and 25 major cancers in 2018. *Eur. J. Cancer* **2018**, *103*, 356–387. [CrossRef]
2. Kleeff, J.; Korc, M.; Apte, M.; La Vecchia, C.; Johnson, C.D.; Biankin, A.V.; Neale, R.E.; Tempero, M.; Tuveson, D.A.; Hruban, R.H.; et al. Pancreatic cancer. *Nat. Rev. Dis. Primers* **2016**, *2*, 16022. [CrossRef]
3. Ryan, D.P.; Hong, T.S.; Bardeesy, N. Pancreatic adenocarcinoma. *N. Engl. J. Med.* **2014**, *371*, 2140–2141. [CrossRef]
4. Ducreux, M.; Seufferlein, T.; Van Laethem, J.L.; Laurent-Puig, P.; Smolenschi, C.; Malka, D.; Boige, V.; Hollebecque, A.; Conroy, T. Systemic treatment of pancreatic cancer revisited. *Semin. Oncol.* **2019**, *46*, 28–38. [CrossRef] [PubMed]
5. Neoptolemos, J.P.; Kleeff, J.; Michl, P.; Costello, E.; Greenhalf, W.; Palmer, D.H. Therapeutic developments in pancreatic cancer: Current and future perspectives. *Nat. Rev. Gastroenterol. Hepatol.* **2018**, *15*, 333–348. [CrossRef] [PubMed]
6. Conroy, T.; Gavoille, C.; Samalin, E.; Ychou, M.; Ducreux, M. The role of the FOLFIRINOX regimen for advanced pancreatic cancer. *Curr. Oncol. Rep.* **2013**, *15*, 182–189. [CrossRef] [PubMed]
7. Amrutkar, M.; Gladhaug, I.P. Pancreatic Cancer Chemoresistance to Gemcitabine. *Cancers* **2017**, *9*. [CrossRef] [PubMed]
8. de Sousa Cavalcante, L.; Monteiro, G. Gemcitabine: Metabolism and molecular mechanisms of action, sensitivity and chemoresistance in pancreatic cancer. *Eur. J. Pharmacol.* **2014**, *741*, 8–16. [CrossRef] [PubMed]
9. Neoptolemos, J.P.; Palmer, D.H.; Ghaneh, P.; Psarelli, E.E.; Valle, J.W.; Halloran, C.M.; Faluyi, O.; O'Reilly, D.A.; Cunningham, D.; Wadsley, J.; et al. Comparison of adjuvant gemcitabine and capecitabine with gemcitabine monotherapy in patients with resected pancreatic cancer (ESPAC-4): A multicentre, open-label, randomised, phase 3 trial. *Lancet* **2017**, *389*, 1011–1024. [CrossRef]
10. Springfeld, C.; Jager, D.; Buchler, M.W.; Strobel, O.; Hackert, T.; Palmer, D.H.; Neoptolemos, J.P. Chemotherapy for pancreatic cancer. *Presse Med.* **2019**, *48*, e159–e174. [CrossRef]
11. Hall, W.A.; Goodman, K.A. Radiation therapy for pancreatic adenocarcinoma, a treatment option that must be considered in the management of a devastating malignancy. *Radiat. Oncol.* **2019**, *14*, 114. [CrossRef] [PubMed]
12. GIST. Further evidence of effective adjuvant combined radiation and chemotherapy following curative resection of pancreatic cancer. *Cancer* **1987**, *59*, 2006–2010. [CrossRef]
13. Klinkenbijl, J.H.; Jeekel, J.; Sahmoud, T.; van Pel, R.; Couvreur, M.L.; Veenhof, C.H.; Arnaud, J.P.; Gonzalez, D.G.; de Wit, L.T.; Hennipman, A.; et al. Adjuvant radiotherapy and 5-fluorouracil after curative resection of cancer of the pancreas and periampullary region: Phase III trial of the EORTC gastrointestinal tract cancer cooperative group. *Ann. Surg.* **1999**, *230*, 776–782, discussion 782–774. [CrossRef] [PubMed]
14. Neoptolemos, J.P.; Stocken, D.D.; Friess, H.; Bassi, C.; Dunn, J.A.; Hickey, H.; Beger, H.; Fernandez-Cruz, L.; Dervenis, C.; Lacaine, F.; et al. A randomized trial of chemoradiotherapy and chemotherapy after resection of pancreatic cancer. *N. Engl. J. Med.* **2004**, *350*, 1200–1210. [CrossRef] [PubMed]
15. Regine, W.F.; Winter, K.A.; Abrams, R.; Safran, H.; Hoffman, J.P.; Konski, A.; Benson, A.B.; Macdonald, J.S.; Rich, T.A.; Willett, C.G. Fluorouracil-based chemoradiation with either gemcitabine or fluorouracil chemotherapy after resection of pancreatic adenocarcinoma: 5-year analysis of the U.S. Intergroup/RTOG 9704 phase III trial. *Ann. Surg. Oncol.* **2011**, *18*, 1319–1326. [CrossRef]
16. Abrams, R.A.; Winter, K.A.; Regine, W.F.; Safran, H.; Hoffman, J.P.; Lustig, R.; Konski, A.A.; Benson, A.B.; Macdonald, J.S.; Rich, T.A.; et al. Failure to adhere to protocol specified radiation therapy guidelines was associated with decreased survival in RTOG 9704—A phase III trial of adjuvant chemotherapy and chemoradiotherapy for patients with resected adenocarcinoma of the pancreas. *Int. J. Radiat. Oncol. Biol. Phys.* **2012**, *82*, 809–816. [CrossRef]
17. Konstantinidis, I.T.; Warshaw, A.L.; Allen, J.N.; Blaszkowsky, L.S.; Castillo, C.F.; Deshpande, V.; Hong, T.S.; Kwak, E.L.; Lauwers, G.Y.; Ryan, D.P.; et al. Pancreatic ductal adenocarcinoma: Is there a survival difference for R1 resections versus locally advanced unresectable tumors? What is a "true" R0 resection? *Ann. Surg.* **2013**, *257*, 731–736. [CrossRef]

18. Versteijne, E.; Suker, M.; Groothuis, K.; Akkermans-Vogelaar, J.M.; Besselink, M.G.; Bonsing, B.A.; Buijsen, J.; Busch, O.R.; Creemers, G.M.; van Dam, R.M.; et al. Preoperative Chemoradiotherapy Versus Immediate Surgery for Resectable and Borderline Resectable Pancreatic Cancer: Results of the Dutch Randomized Phase III PREOPANC Trial. *J. Clin. Oncol.* **2020**, *38*, 1763–1773. [CrossRef]
19. Janssen, Q.P.; Buettner, S.; Suker, M.; Beumer, B.R.; Addeo, P.; Bachellier, P.; Bahary, N.; Bekaii-Saab, T.; Bali, M.A.; Besselink, M.G.; et al. Neoadjuvant FOLFIRINOX in Patients With Borderline Resectable Pancreatic Cancer: A Systematic Review and Patient-Level Meta-Analysis. *J. Natl. Cancer Inst.* **2019**, *111*, 782–794. [CrossRef]
20. Janssen, Q.P.; O'Reilly, E.M.; van Eijck, C.H.J.; Groot Koerkamp, B. Neoadjuvant Treatment in Patients With Resectable and Borderline Resectable Pancreatic Cancer. *Front. Oncol.* **2020**, *10*, 41. [CrossRef]
21. Dhir, M.; Zenati, M.S.; Hamad, A.; Singhi, A.D.; Bahary, N.; Hogg, M.E.; Zeh, H.J., 3rd; Zureikat, A.H. FOLFIRINOX Versus Gemcitabine/Nab-Paclitaxel for Neoadjuvant Treatment of Resectable and Borderline Resectable Pancreatic Head Adenocarcinoma. *Ann. Surg. Oncol.* **2018**, *25*, 1896–1903. [CrossRef] [PubMed]
22. Klaiber, U.; Hackert, T. Conversion Surgery for Pancreatic Cancer-The Impact of Neoadjuvant Treatment. *Front. Oncol.* **2019**, *9*, 1501. [CrossRef]
23. Gillen, S.; Schuster, T.; Meyer Zum Buschenfelde, C.; Friess, H.; Kleeff, J. Preoperative/neoadjuvant therapy in pancreatic cancer: A systematic review and meta-analysis of response and resection percentages. *PLoS Med.* **2010**, *7*, e1000267. [CrossRef]
24. Bittner, M.I.; Grosu, A.L.; Brunner, T.B. Comparison of toxicity after IMRT and 3D-conformal radiotherapy for patients with pancreatic cancer—A systematic review. *Radiother. Oncol.* **2015**, *114*, 117–121. [CrossRef]
25. Krishnan, S.; Chadha, A.S.; Suh, Y.; Chen, H.C.; Rao, A.; Das, P.; Minsky, B.D.; Mahmood, U.; Delclos, M.E.; Sawakuchi, G.O.; et al. Focal Radiation Therapy Dose Escalation Improves Overall Survival in Locally Advanced Pancreatic Cancer Patients Receiving Induction Chemotherapy and Consolidative Chemoradiation. *Int. J. Radiat. Oncol. Biol. Phys.* **2016**, *94*, 755–765. [CrossRef]
26. Reyngold, M.; Parikh, P.; Crane, C.H. Ablative radiation therapy for locally advanced pancreatic cancer: Techniques and results. *Radiat. Oncol.* **2019**, *14*, 95. [CrossRef] [PubMed]
27. Ling, T.C.; Slater, J.M.; Mifflin, R.; Nookala, P.; Grove, R.; Ly, A.M.; Patyal, B.; Slater, J.D.; Yang, G.Y. Evaluation of normal tissue exposure in patients receiving radiotherapy for pancreatic cancer based on RTOG 0848. *J. Gastrointest. Oncol.* **2015**, *6*, 108–114. [CrossRef] [PubMed]
28. Rutenberg, M.S.; Nichols, R.C. Proton beam radiotherapy for pancreas cancer. *J. Gastrointest. Oncol.* **2020**, *11*, 166–175. [CrossRef] [PubMed]
29. Kim, T.H.; Lee, W.J.; Woo, S.M.; Kim, H.; Oh, E.S.; Lee, J.H.; Han, S.S.; Park, S.J.; Suh, Y.G.; Moon, S.H.; et al. Effectiveness and Safety of Simultaneous Integrated Boost-Proton Beam Therapy for Localized Pancreatic Cancer. *Technol. Cancer Res. Treat.* **2018**, *17*, 1533033818783879. [CrossRef]
30. Hiroshima, Y.; Fukumitsu, N.; Saito, T.; Numajiri, H.; Murofushi, K.N.; Ohnishi, K.; Nonaka, T.; Ishikawa, H.; Okumura, T.; Sakurai, H. Concurrent chemoradiotherapy using proton beams for unresectable locally advanced pancreatic cancer. *Radiother. Oncol.* **2019**, *136*, 37–43. [CrossRef]
31. Ding, X.; Li, X.; Qin, A.; Zhou, J.; Yan, D.; Stevens, C.; Krauss, D.; Kabolizdeh, P. Have we reached proton beam therapy dosimetric limitations?-A novel robust, delivery-efficient and continuous spot-scanning proton arc (SPArc) therapy is to improve the dosimetric outcome in treating prostate cancer. *Acta Oncol.* **2018**, *57*, 435–437. [CrossRef] [PubMed]
32. Schreuder, A.N.; Shamblin, J. Proton therapy delivery: What is needed in the next ten years? *Br. J. Radiol.* **2020**, *93*, 20190359. [CrossRef] [PubMed]
33. Shinoto, M.; Yamada, S.; Terashima, K.; Yasuda, S.; Shioyama, Y.; Honda, H.; Kamada, T.; Tsujii, H.; Saisho, H. Carbon Ion Radiation Therapy With Concurrent Gemcitabine for Patients With Locally Advanced Pancreatic Cancer. *Int. J. Radiat. Oncol. Biol. Phys.* **2016**, *95*, 498–504. [CrossRef] [PubMed]
34. Dell'Oro, M.; Short, M.; Wilson, P.; Bezak, E. Clinical Limitations of Photon, Proton and Carbon Ion Therapy for Pancreatic Cancer. *Cancers* **2020**, *12*, 163. [CrossRef] [PubMed]
35. Vozenin, M.C.; Hendry, J.H.; Limoli, C.L. Biological Benefits of Ultra-high Dose Rate FLASH Radiotherapy: Sleeping Beauty Awoken. *Clin. Oncol.* **2019**, *31*, 407–415. [CrossRef] [PubMed]
36. Wilson, J.D.; Hammond, E.M.; Higgins, G.S.; Petersson, K. Ultra-High Dose Rate (FLASH) Radiotherapy: Silver Bullet or Fool's Gold? *Front. Oncol.* **2019**, *9*, 1563. [CrossRef] [PubMed]

37. Favaudon, V.; Caplier, L.; Monceau, V.; Pouzoulet, F.; Sayarath, M.; Fouillade, C.; Poupon, M.F.; Brito, I.; Hupe, P.; Bourhis, J.; et al. Ultrahigh dose-rate FLASH irradiation increases the differential response between normal and tumor tissue in mice. *Sci. Transl. Med.* **2014**, *6*, 245ra293. [CrossRef]
38. Diffenderfer, E.S.; Verginadis, I.I.; Kim, M.M.; Shoniyozov, K.; Velalopoulou, A.; Goia, D.; Putt, M.; Hagan, S.; Avery, S.; Teo, K.; et al. Design, Implementation, and in Vivo Validation of a Novel Proton FLASH Radiation Therapy System. *Int. J. Radiat. Oncol. Biol. Phys.* **2020**, *106*, 440–448. [CrossRef]
39. Bourhis, J.; Sozzi, W.J.; Jorge, P.G.; Gaide, O.; Bailat, C.; Duclos, F.; Patin, D.; Ozsahin, M.; Bochud, F.; Germond, J.F.; et al. Treatment of a first patient with FLASH-radiotherapy. *Radiother. Oncol.* **2019**, *139*, 18–22. [CrossRef]
40. Seshacharyulu, P.; Baine, M.J.; Souchek, J.J.; Menning, M.; Kaur, S.; Yan, Y.; Ouellette, M.M.; Jain, M.; Lin, C.; Batra, S.K. Biological determinants of radioresistance and their remediation in pancreatic cancer. *Biochim. Biophys. Acta Rev. Cancer* **2017**, *1868*, 69–92. [CrossRef]
41. Janes, M.R.; Zhang, J.; Li, L.S.; Hansen, R.; Peters, U.; Guo, X.; Chen, Y.; Babbar, A.; Firdaus, S.J.; Darjania, L.; et al. Targeting KRAS Mutant Cancers with a Covalent G12C-Specific Inhibitor. *Cell* **2018**, *172*, 578–589. [CrossRef] [PubMed]
42. Fakih, M.; O'Neil, B.; Price, T.J.; Falchook, G.S.; Desai, J.; Kuo, J.; Govindan, R.; Rasmussen, E.; Morrow, P.K.H.; Ngang, J.; et al. Phase 1 study evaluating the safety, tolerability, pharmacokinetics (PK), and efficacy of AMG 510, a novel small molecule KRASG12C inhibitor, in advanced solid tumors. *J. Clin. Oncol.* **2019**, *37*, 3003. [CrossRef]
43. Kinsey, C.G.; Camolotto, S.A.; Boespflug, A.M.; Guillen, K.P.; Foth, M.; Truong, A.; Schuman, S.S.; Shea, J.E.; Seipp, M.T.; Yap, J.T.; et al. Protective autophagy elicited by RAF–>MEK–>ERK inhibition suggests a treatment strategy for RAS-driven cancers. *Nat. Med.* **2019**, *25*, 620–627. [CrossRef] [PubMed]
44. Panieri, E.; Buha, A.; Telkoparan-Akillilar, P.; Cevik, D.; Kouretas, D.; Veskoukis, A.; Skaperda, Z.; Tsatsakis, A.; Wallace, D.; Suzen, S.; et al. Potential Applications of NRF2 Modulators in Cancer Therapy. *Antioxidants* **2020**, *9*, 193. [CrossRef]
45. Bailleul, J.; Yazal, T.; Sung, D.; Palomera, D.; Sehgal, A.; Dao, A.; Vlashi, E. Abstract C59: NRF2 drives metabolic reprogramming in irradiated pancreatic cancer cells and promotes radioresistance. *Cancer Res.* **2019**, *79*, C59. [CrossRef]
46. Gorgulu, K.; Diakopoulos, K.N.; Kaya-Aksoy, E.; Ciecielski, K.J.; Ai, J.; Lesina, M.; Algul, H. The Role of Autophagy in Pancreatic Cancer: From Bench to the Dark Bedside. *Cells* **2020**, *9*, 1063. [CrossRef]
47. Wang, F.; Xia, X.; Yang, C.; Shen, J.; Mai, J.; Kim, H.C.; Kirui, D.; Kang, Y.; Fleming, J.B.; Koay, E.J.; et al. SMAD4 Gene Mutation Renders Pancreatic Cancer Resistance to Radiotherapy through Promotion of Autophagy. *Clin. Cancer Res.* **2018**, *24*, 3176–3185. [CrossRef]
48. Bailey, P.; Chang, D.K.; Nones, K.; Johns, A.L.; Patch, A.M.; Gingras, M.C.; Miller, D.K.; Christ, A.N.; Bruxner, T.J.; Quinn, M.C.; et al. Genomic analyses identify molecular subtypes of pancreatic cancer. *Nature* **2016**, *531*, 47–52. [CrossRef]
49. Salvador-Barbero, B.; Alvarez-Fernandez, M.; Zapatero-Solana, E.; El Bakkali, A.; Menendez, M.D.C.; Lopez-Casas, P.P.; Di Domenico, T.; Xie, T.; VanArsdale, T.; Shields, D.J.; et al. CDK4/6 Inhibitors Impair Recovery from Cytotoxic Chemotherapy in Pancreatic Adenocarcinoma. *Cancer Cell* **2020**, *37*, 340–353. [CrossRef]
50. Ruscetti, M.; Morris, J.P.t.; Mezzadra, R.; Russell, J.; Leibold, J.; Romesser, P.B.; Simon, J.; Kulick, A.; Ho, Y.J.; Fennell, M.; et al. Senescence-Induced Vascular Remodeling Creates Therapeutic Vulnerabilities in Pancreas Cancer. *Cell* **2020**, *181*, 424–441. [CrossRef]
51. Thomas, D.; Radhakrishnan, P. Tumor-stromal crosstalk in pancreatic cancer and tissue fibrosis. *Mol. Cancer* **2019**, *18*, 14. [CrossRef] [PubMed]
52. Grasso, C.; Jansen, G.; Giovannetti, E. Drug resistance in pancreatic cancer: Impact of altered energy metabolism. *Crit. Rev. Oncol. Hematol.* **2017**, *114*, 139–152. [CrossRef] [PubMed]
53. Michiels, C.; Tellier, C.; Feron, O. Cycling hypoxia: A key feature of the tumor microenvironment. *Biochim. Biophys. Acta* **2016**, *1866*, 76–86. [CrossRef] [PubMed]
54. Ma, N.Y.; Tinganelli, W.; Maier, A.; Durante, M.; Kraft-Weyrather, W. Influence of chronic hypoxia and radiation quality on cell survival. *J. Radiat. Res.* **2013**, *54* (Suppl. 1), i13–i22. [CrossRef]
55. Zolzer, F.; Streffer, C. Increased radiosensitivity with chronic hypoxia in four human tumor cell lines. *Int. J. Radiat. Oncol. Biol. Phys.* **2002**, *54*, 910–920. [CrossRef]

56. Rebucci, M.; Michiels, C. Molecular aspects of cancer cell resistance to chemotherapy. *Biochem. Pharmacol.* **2013**, *85*, 1219–1226. [CrossRef]
57. Huang, R.; Zhou, P.-K. HIF-1 signaling: A key orchestrator of cancer radioresistance. *Radiat. Med. Prot.* **2020**, *1*, 7–14. [CrossRef]
58. Yokoi, K.; Fidler, I.J. Hypoxia increases resistance of human pancreatic cancer cells to apoptosis induced by gemcitabine. *Clin. Cancer Res.* **2004**, *10*, 2299–2306. [CrossRef]
59. He, X.; Wang, J.; Wei, W.; Shi, M.; Xin, B.; Zhang, T.; Shen, X. Hypoxia regulates ABCG2 activity through the activivation of ERK1/2/HIF-1alpha and contributes to chemoresistance in pancreatic cancer cells. *Cancer Biol. Ther.* **2016**, *17*, 188–198. [CrossRef]
60. Schwartz, D.L.; Bankson, J.A.; Lemos, R., Jr.; Lai, S.Y.; Thittai, A.K.; He, Y.; Hostetter, G.; Demeure, M.J.; Von Hoff, D.D.; Powis, G. Radiosensitization and stromal imaging response correlates for the HIF-1 inhibitor PX-478 given with or without chemotherapy in pancreatic cancer. *Mol. Cancer Ther.* **2010**, *9*, 2057–2067. [CrossRef]
61. Connell, P.P.; Hellman, S. Advances in radiotherapy and implications for the next century: A historical perspective. *Cancer Res.* **2009**, *69*, 383–392. [CrossRef]
62. Nahum, A.E. The radiobiology of hypofractionation. *Clin. Oncol.* **2015**, *27*, 260–269. [CrossRef] [PubMed]
63. Chapman, J.D. Can the two mechanisms of tumor cell killing by radiation be exploited for therapeutic gain? *J. Radiat. Res.* **2014**, *55*, 2–9. [CrossRef] [PubMed]
64. Sia, J.; Szmyd, R.; Hau, E.; Gee, H.E. Molecular Mechanisms of Radiation-Induced Cancer Cell Death: A Primer. *Front. Cell Dev. Biol.* **2020**, *8*, 41. [CrossRef] [PubMed]
65. Karam, S.D.; Bhatia, S. The radiobiological targets of SBRT: Tumor cells or endothelial cells? *Ann. Transl. Med.* **2015**, *3*, 290. [CrossRef] [PubMed]
66. Moding, E.J.; Mowery, Y.M.; Kirsch, D.G. Opportunities for Radiosensitization in the Stereotactic Body Radiation Therapy (SBRT) Era. *Cancer J.* **2016**, *22*, 267–273. [CrossRef]
67. Atashzar, M.R.; Baharlou, R.; Karami, J.; Abdollahi, H.; Rezaei, R.; Pourramezan, F.; Zoljalali Moghaddam, S.H. Cancer stem cells: A review from origin to therapeutic implications. *J. Cell. Physiol.* **2020**, *235*, 790–803. [CrossRef]
68. Wang, Z.; Li, Y.; Ahmad, A.; Banerjee, S.; Azmi, A.S.; Kong, D.; Sarkar, F.H. Pancreatic cancer: Understanding and overcoming chemoresistance. *Nat. Rev. Gastroenterol. Hepatol.* **2011**, *8*, 27–33. [CrossRef]
69. Zhou, S.; Zhang, M.; Zhou, C.; Wang, W.; Yang, H.; Ye, W. The role of epithelial-mesenchymal transition in regulating radioresistance. *Crit. Rev. Oncol. Hematol.* **2020**, *150*, 102961. [CrossRef]
70. Duong, H.Q.; Hwang, J.S.; Kim, H.J.; Kang, H.J.; Seong, Y.S.; Bae, I. Aldehyde dehydrogenase 1A1 confers intrinsic and acquired resistance to gemcitabine in human pancreatic adenocarcinoma MIA PaCa-2 cells. *Int. J. Oncol.* **2012**, *41*, 855–861. [CrossRef]
71. Hong, S.P.; Wen, J.; Bang, S.; Park, S.; Song, S.Y. CD44-positive cells are responsible for gemcitabine resistance in pancreatic cancer cells. *Int. J. Cancer J. Int. Du Cancer* **2009**, *125*, 2323–2331. [CrossRef] [PubMed]
72. Shah, A.N.; Summy, J.M.; Zhang, J.; Park, S.I.; Parikh, N.U.; Gallick, G.E. Development and characterization of gemcitabine-resistant pancreatic tumor cells. *Ann. Surg. Oncol.* **2007**, *14*, 3629–3637. [CrossRef] [PubMed]
73. Hermann, P.C.; Huber, S.L.; Herrler, T.; Aicher, A.; Ellwart, J.W.; Guba, M.; Bruns, C.J.; Heeschen, C. Distinct populations of cancer stem cells determine tumor growth and metastatic activity in human pancreatic cancer. *Cell Stem Cell* **2007**, *1*, 313–323. [CrossRef] [PubMed]
74. Hanahan, D.; Weinberg, R.A. Hallmarks of Cancer: The Next Generation. *Cell* **2011**, *144*, 646–674. [CrossRef]
75. Wang, J.; Wei, Q.; Wang, X.; Tang, S.; Liu, H.; Zhang, F.; Mohammed, M.K.; Huang, J.; Guo, D.; Lu, M.; et al. Transition to resistance: An unexpected role of the EMT in cancer chemoresistance. *Genes Dis.* **2016**, *3*, 3–6. [CrossRef]
76. Zheng, X.; Carstens, J.L.; Kim, J.; Scheible, M.; Kaye, J.; Sugimoto, H.; Wu, C.C.; LeBleu, V.S.; Kalluri, R. Epithelial-to-mesenchymal transition is dispensable for metastasis but induces chemoresistance in pancreatic cancer. *Nature* **2015**, *527*, 525–530. [CrossRef]
77. Elaskalani, O.; Razak, N.B.; Falasca, M.; Metharom, P. Epithelial-mesenchymal transition as a therapeutic target for overcoming chemoresistance in pancreatic cancer. *World J. Gastrointest. Oncol.* **2017**, *9*, 37–41. [CrossRef]

78. Arumugam, T.; Ramachandran, V.; Fournier, K.F.; Wang, H.; Marquis, L.; Abbruzzese, J.L.; Gallick, G.E.; Logsdon, C.D.; McConkey, D.J.; Choi, W. Epithelial to mesenchymal transition contributes to drug resistance in pancreatic cancer. *Cancer Res.* **2009**, *69*, 5820–5828. [CrossRef]
79. Lambies, G.; Miceli, M.; Martinez-Guillamon, C.; Olivera-Salguero, R.; Pena, R.; Frias, C.P.; Calderon, I.; Atanassov, B.S.; Dent, S.Y.R.; Arribas, J.; et al. TGFbeta-Activated USP27X Deubiquitinase Regulates Cell Migration and Chemoresistance via Stabilization of Snail1. *Cancer Res.* **2019**, *79*, 33–46. [CrossRef]
80. Lonardo, E.; Hermann, P.C.; Mueller, M.T.; Huber, S.; Balic, A.; Miranda-Lorenzo, I.; Zagorac, S.; Alcala, S.; Rodriguez-Arabaolaza, I.; Ramirez, J.C.; et al. Nodal/Activin signaling drives self-renewal and tumorigenicity of pancreatic cancer stem cells and provides a target for combined drug therapy. *Cell Stem Cell* **2011**, *9*, 433–446. [CrossRef]
81. Adamska, A.; Elaskalani, O.; Emmanouilidi, A.; Kim, M.; Abdol Razak, N.B.; Metharom, P.; Falasca, M. Molecular and cellular mechanisms of chemoresistance in pancreatic cancer. *Adv. Biol. Regul.* **2018**, *68*, 77–87. [CrossRef]
82. Tsukasa, K.; Ding, Q.; Yoshimitsu, M.; Miyazaki, Y.; Matsubara, S.; Takao, S. Slug contributes to gemcitabine resistance through epithelial-mesenchymal transition in CD133(+) pancreatic cancer cells. *Hum. Cell* **2015**, *28*, 167–174. [CrossRef] [PubMed]
83. Perusina Lanfranca, M.; Thompson, J.K.; Bednar, F.; Halbrook, C.; Lyssiotis, C.; Levi, B.; Frankel, T.L. Metabolism and epigenetics of pancreatic cancer stem cells. *Semin. Cancer Biol.* **2019**, *57*, 19–26. [CrossRef] [PubMed]
84. Yang, L.; Shi, P.; Zhao, G.; Xu, J.; Peng, W.; Zhang, J.; Zhang, G.; Wang, X.; Dong, Z.; Chen, F.; et al. Targeting cancer stem cell pathways for cancer therapy. *Signal Transduct. Target. Ther.* **2020**, *5*, 8. [CrossRef] [PubMed]
85. Cioffi, M.; Trabulo, S.M.; Sanchez-Ripoll, Y.; Miranda-Lorenzo, I.; Lonardo, E.; Dorado, J.; Reis Vieira, C.; Ramirez, J.C.; Hidalgo, M.; Aicher, A.; et al. The miR-17-92 cluster counteracts quiescence and chemoresistance in a distinct subpopulation of pancreatic cancer stem cells. *Gut* **2015**, *64*, 1936–1948. [CrossRef]
86. Cheng, Z.X.; Wang, D.W.; Liu, T.; Liu, W.X.; Xia, W.B.; Xu, J.; Zhang, Y.H.; Qu, Y.K.; Guo, L.Q.; Ding, L.; et al. Effects of the HIF-1alpha and NF-kappaB loop on epithelial-mesenchymal transition and chemoresistance induced by hypoxia in pancreatic cancer cells. *Oncol. Rep.* **2014**, *31*, 1891–1898. [CrossRef]
87. Zhang, Z.; Han, H.; Rong, Y.; Zhu, K.; Zhu, Z.; Tang, Z.; Xiong, C.; Tao, J. Hypoxia potentiates gemcitabine-induced stemness in pancreatic cancer cells through AKT/Notch1 signaling. *J. Exp. Clin. Cancer Res.* **2018**, *37*, 291. [CrossRef]
88. Khan, M.A.; Zubair, H.; Srivastava, S.K.; Singh, S.; Singh, A.P. Insights into the Role of microRNAs in Pancreatic Cancer Pathogenesis: Potential for Diagnosis, Prognosis, and Therapy. *Adv. Exp. Med. Biol.* **2015**, *889*, 71–87. [CrossRef]
89. Ren, L.; Yu, Y. The role of miRNAs in the diagnosis, chemoresistance, and prognosis of pancreatic ductal adenocarcinoma. *Ther. Clin. Risk Manag.* **2018**, *14*, 179–187. [CrossRef]
90. Gandellini, P.; Rancati, T.; Valdagni, R.; Zaffaroni, N. miRNAs in tumor radiation response: Bystanders or participants? *Trends Mol. Med.* **2014**, *20*, 529–539. [CrossRef]
91. Liu, B.; Wu, S.; Ma, J.; Yan, S.; Xiao, Z.; Wan, L.; Zhang, F.; Shang, M.; Mao, A. lncRNA GAS5 Reverses EMT and Tumor Stem Cell-Mediated Gemcitabine Resistance and Metastasis by Targeting miR-221/SOCS3 in Pancreatic Cancer. *Mol. Ther. Nucleic Acids* **2018**, *13*, 472–482. [CrossRef] [PubMed]
92. Hwang, J.H.; Voortman, J.; Giovannetti, E.; Steinberg, S.M.; Leon, L.G.; Kim, Y.T.; Funel, N.; Park, J.K.; Kim, M.A.; Kang, G.H.; et al. Identification of microRNA-21 as a biomarker for chemoresistance and clinical outcome following adjuvant therapy in resectable pancreatic cancer. *PLoS ONE* **2010**, *5*, e10630. [CrossRef]
93. Moriyama, T.; Ohuchida, K.; Mizumoto, K.; Yu, J.; Sato, N.; Nabae, T.; Takahata, S.; Toma, H.; Nagai, E.; Tanaka, M. MicroRNA-21 modulates biological functions of pancreatic cancer cells including their proliferation, invasion, and chemoresistance. *Mol. Cancer Ther.* **2009**, *8*, 1067–1074. [CrossRef]
94. Zhang, X.; Ren, D.; Wu, X.; Lin, X.; Ye, L.; Lin, C.; Wu, S.; Zhu, J.; Peng, X.; Song, L. miR-1266 Contributes to Pancreatic Cancer Progression and Chemoresistance by the STAT3 and NF-kappaB Signaling Pathways. *Mol. Ther. Nucleic Acids* **2018**, *11*, 142–158. [CrossRef] [PubMed]
95. Fan, P.; Liu, L.; Yin, Y.; Zhao, Z.; Zhang, Y.; Amponsah, P.S.; Xiao, X.; Bauer, N.; Abukiwan, A.; Nwaeburu, C.C.; et al. MicroRNA-101-3p reverses gemcitabine resistance by inhibition of ribonucleotide reductase M1 in pancreatic cancer. *Cancer Lett.* **2016**, *373*, 130–137. [CrossRef] [PubMed]

96. Li, Y.; VandenBoom, T.G., 2nd; Kong, D.; Wang, Z.; Ali, S.; Philip, P.A.; Sarkar, F.H. Up-regulation of miR-200 and let-7 by natural agents leads to the reversal of epithelial-to-mesenchymal transition in gemcitabine-resistant pancreatic cancer cells. *Cancer Res.* **2009**, *69*, 6704–6712. [CrossRef]
97. Nalls, D.; Tang, S.N.; Rodova, M.; Srivastava, R.K.; Shankar, S. Targeting epigenetic regulation of miR-34a for treatment of pancreatic cancer by inhibition of pancreatic cancer stem cells. *PLoS ONE* **2011**, *6*, e24099. [CrossRef]
98. Fesler, A.; Ju, J. Development of microRNA-based therapy for pancreatic cancer. *J. Pancreatol.* **2019**, *2*, 147–151. [CrossRef]
99. Wang, W.; Zhao, L.; Wei, X.; Wang, L.; Liu, S.; Yang, Y.; Wang, F.; Sun, G.; Zhang, J.; Ma, Y.; et al. MicroRNA-320a promotes 5-FU resistance in human pancreatic cancer cells. *Sci. Rep.* **2016**, *6*, 27641. [CrossRef]
100. Zhao, L.; Zou, D.; Wei, X.; Wang, L.; Zhang, Y.; Liu, S.; Si, Y.; Zhao, H.; Wang, F.; Yu, J.; et al. MiRNA-221-3p desensitizes pancreatic cancer cells to 5-fluorouracil by targeting RB1. *Tumour Biol. J. Int. Soc. Oncodevelopmental Biol. Med.* **2016**. [CrossRef]
101. Wang, S.-L.; Wang, Y.-J.; Wu, S.-M.; Yuan, Z.; Du, H.-M.; Liu, X.; Zhu, X.-K. Identification of unique microRNAs associated with pancreatic cancer radioresistance using deep sequencing. *Transl. Cancer Res.* **2018**, *7*, 828–838. [CrossRef]
102. Zhang, X.; Shi, H.; Lin, S.; Ba, M.; Cui, S. MicroRNA-216a enhances the radiosensitivity of pancreatic cancer cells by inhibiting beclin-1-mediated autophagy. *Oncol. Rep.* **2015**, *34*, 1557–1564. [CrossRef] [PubMed]
103. Wang, P.; Zhang, J.; Zhang, L.; Zhu, Z.; Fan, J.; Chen, L.; Zhuang, L.; Luo, J.; Chen, H.; Liu, L.; et al. MicroRNA 23b regulates autophagy associated with radioresistance of pancreatic cancer cells. *Gastroenterology* **2013**, *145*, 1133–1143. [CrossRef] [PubMed]
104. Maacha, S.; Bhat, A.A.; Jimenez, L.; Raza, A.; Haris, M.; Uddin, S.; Grivel, J.C. Extracellular vesicles-mediated intercellular communication: Roles in the tumor microenvironment and anti-cancer drug resistance. *Mol. Cancer* **2019**, *18*, 55. [CrossRef]
105. Ni, J.; Bucci, J.; Malouf, D.; Knox, M.; Graham, P.; Li, Y. Exosomes in Cancer Radioresistance. *Front. Oncol.* **2019**, *9*, 869. [CrossRef]
106. Lucchetti, D.; Ricciardi Tenore, C.; Colella, F.; Sgambato, A. Extracellular Vesicles and Cancer: A Focus on Metabolism, Cytokines, and Immunity. *Cancers* **2020**, *12*, 171. [CrossRef]
107. O'Neill, C.P.; Gilligan, K.E.; Dwyer, R.M. Role of Extracellular Vesicles (EVs) in Cell Stress Response and Resistance to Cancer Therapy. *Cancers* **2019**, *11*, 136. [CrossRef]
108. Mikamori, M.; Yamada, D.; Eguchi, H.; Hasegawa, S.; Kishimoto, T.; Tomimaru, Y.; Asaoka, T.; Noda, T.; Wada, H.; Kawamoto, K.; et al. MicroRNA-155 Controls Exosome Synthesis and Promotes Gemcitabine Resistance in Pancreatic Ductal Adenocarcinoma. *Sci. Rep.* **2017**, *7*, 42339. [CrossRef]
109. Binenbaum, Y.; Fridman, E.; Yaari, Z.; Milman, N.; Schroeder, A.; Ben David, G.; Shlomi, T.; Gil, Z. Transfer of miRNA in Macrophage-Derived Exosomes Induces Drug Resistance in Pancreatic Adenocarcinoma. *Cancer Res.* **2018**, *78*, 5287–5299. [CrossRef]
110. Richards, K.E.; Zeleniak, A.E.; Fishel, M.L.; Wu, J.; Littlepage, L.E.; Hill, R. Cancer-associated fibroblast exosomes regulate survival and proliferation of pancreatic cancer cells. *Oncogene* **2017**, *36*, 1770–1778. [CrossRef]
111. Karger, C.P.; Peschke, P. RBE and related modeling in carbon-ion therapy. *Phys. Med. Biol.* **2017**, *63*, 01TR02. [CrossRef] [PubMed]
112. Durante, M. New challenges in high-energy particle radiobiology. *Br. J. Radiol.* **2014**, *87*, 20130626. [CrossRef] [PubMed]
113. Rydberg, B. Clusters of DNA damage induced by ionizing radiation: Formation of short DNA fragments. II. Experimental detection. *Radiat. Res.* **1996**, *145*, 200–209. [CrossRef] [PubMed]
114. Hoglund, E.; Blomquist, E.; Carlsson, J.; Stenerlow, B. DNA damage induced by radiation of different linear energy transfer: Initial fragmentation. *Int. J. Radiat. Biol.* **2000**, *76*, 539–547. [CrossRef] [PubMed]
115. Pang, D.; Chasovskikh, S.; Rodgers, J.E.; Dritschilo, A. Short DNA Fragments Are a Hallmark of Heavy Charged-Particle Irradiation and May Underlie Their Greater Therapeutic Efficacy. *Front. Oncol.* **2016**, *6*, 130. [CrossRef]
116. Konings, K.; Vandevoorde, C.; Baselet, B.; Baatout, S.; Moreels, M. Combination Therapy With Charged Particles and Molecular Targeting: A Promising Avenue to Overcome Radioresistance. *Front. Oncol.* **2020**, *10*, 128. [CrossRef]

117. Held, K.D.; Kawamura, H.; Kaminuma, T.; Paz, A.E.; Yoshida, Y.; Liu, Q.; Willers, H.; Takahashi, A. Effects of Charged Particles on Human Tumor Cells. *Front. Oncol.* **2016**, *6*, 23. [CrossRef]
118. Georgakilas, A.G.; O'Neill, P.; Stewart, R.D. Induction and repair of clustered DNA lesions: What do we know so far? *Radiat. Res.* **2013**, *180*, 100–109. [CrossRef]
119. Durante, M.; Debus, J. Heavy Charged Particles: Does Improved Precision and Higher Biological Effectiveness Translate to Better Outcome in Patients? *Semin. Radiat. Oncol.* **2018**, *28*, 160–167. [CrossRef]
120. Durante, M.; Flanz, J. Charged particle beams to cure cancer: Strengths and challenges. *Semin. Oncol.* **2019**, *46*, 219–225. [CrossRef]
121. Durante, M.; Loeffler, J.S. Charged particles in radiation oncology. *Nat. Rev. Clin. Oncol.* **2010**, *7*, 37–43. [CrossRef] [PubMed]
122. Chiblak, S.; Tang, Z.; Lemke, D.; Knoll, M.; Dokic, I.; Warta, R.; Moustafa, M.; Mier, W.; Brons, S.; Rapp, C.; et al. Carbon irradiation overcomes glioma radioresistance by eradicating stem cells and forming an antiangiogenic and immunopermissive niche. *JCI Insight* **2019**, 4. [CrossRef] [PubMed]
123. Dini, V.; Belli, M.; Tabocchini, M.A. Targeting cancer stem cells: Protons versus photons. *Br. J. Radiol.* **2020**, *93*, 20190225. [CrossRef] [PubMed]
124. Arnold, C.R.; Mangesius, J.; Skvortsova, I.I.; Ganswindt, U. The Role of Cancer Stem Cells in Radiation Resistance. *Front. Oncol.* **2020**, *10*, 164. [CrossRef]
125. Girdhani, S.; Lamont, C.; Hahnfeldt, P.; Abdollahi, A.; Hlatky, L. Proton irradiation suppresses angiogenic genes and impairs cell invasion and tumor growth. *Radiat. Res.* **2012**, *178*, 33–45. [CrossRef]
126. Wozny, A.S.; Vares, G.; Alphonse, G.; Lauret, A.; Monini, C.; Magne, N.; Cuerq, C.; Fujimori, A.; Monboisse, J.C.; Beuve, M.; et al. ROS Production and Distribution: A New Paradigm to Explain the Differential Effects of X-ray and Carbon Ion Irradiation on Cancer Stem Cell Migration and Invasion. *Cancers* **2019**, *11*. [CrossRef]
127. Oonishi, K.; Cui, X.; Hirakawa, H.; Fujimori, A.; Kamijo, T.; Yamada, S.; Yokosuka, O.; Kamada, T. Different effects of carbon ion beams and X-rays on clonogenic survival and DNA repair in human pancreatic cancer stem-like cells. *Radiother. Oncol.* **2012**, *105*, 258–265. [CrossRef]
128. Sai, S.; Wakai, T.; Vares, G.; Yamada, S.; Kamijo, T.; Kamada, T.; Shirai, T. Combination of carbon ion beam and gemcitabine causes irreparable DNA damage and death of radioresistant pancreatic cancer stem-like cells in vitro and in vivo. *Oncotarget* **2015**, *6*, 5517–5535. [CrossRef]
129. Takahashi, A.; Matsumoto, H.; Yuki, K.; Yasumoto, J.; Kajiwara, A.; Aoki, M.; Furusawa, Y.; Ohnishi, K.; Ohnishi, T. High-LET radiation enhanced apoptosis but not necrosis regardless of p53 status. *Int. J. Radiat. Oncol. Biol. Phys.* **2004**, *60*, 591–597. [CrossRef]
130. Yamakawa, N.; Takahashi, A.; Mori, E.; Imai, Y.; Furusawa, Y.; Ohnishi, K.; Kirita, T.; Ohnishi, T. High LET radiation enhances apoptosis in mutated p53 cancer cells through Caspase-9 activation. *Cancer Sci.* **2008**, *99*, 1455–1460. [CrossRef]
131. Mori, E.; Takahashi, A.; Yamakawa, N.; Kirita, T.; Ohnishi, T. High LET heavy ion radiation induces p53-independent apoptosis. *J. Radiat. Res.* **2009**, *50*, 37–42. [CrossRef] [PubMed]
132. Ewald, J.A.; Desotelle, J.A.; Wilding, G.; Jarrard, D.F. Therapy-induced senescence in cancer. *J. Natl. Cancer Inst.* **2010**, *102*, 1536–1546. [CrossRef] [PubMed]
133. Roninson, I.B.; Broude, E.V.; Chang, B.D. If not apoptosis, then what? Treatment-induced senescence and mitotic catastrophe in tumor cells. *Drug Resist. Updat.* **2001**, *4*, 303–313. [CrossRef] [PubMed]
134. Jinno-Oue, A.; Shimizu, N.; Hamada, N.; Wada, S.; Tanaka, A.; Shinagawa, M.; Ohtsuki, T.; Mori, T.; Saha, M.N.; Hoque, A.S.; et al. Irradiation with carbon ion beams induces apoptosis, autophagy, and cellular senescence in a human glioma-derived cell line. *Int. J. Radiat. Oncol. Biol. Phys.* **2010**, *76*, 229–241. [CrossRef] [PubMed]
135. Zhang, X.; Ye, C.; Sun, F.; Wei, W.; Hu, B.; Wang, J. Both Complexity and Location of DNA Damage Contribute to Cellular Senescence Induced by Ionizing Radiation. *PLoS ONE* **2016**, *11*, e0155725. [CrossRef] [PubMed]
136. Wera, A.C.; Lobbens, A.; Stoyanov, M.; Lucas, S.; Michiels, C. Radiation-induced synthetic lethality: Combination of poly(ADP-ribose) polymerase and RAD51 inhibitors to sensitize cells to proton irradiation. *Cell Cycle Georget. Tex.* **2019**, *18*, 1770–1783. [CrossRef] [PubMed]
137. Lecot, P.; Alimirah, F.; Desprez, P.Y.; Campisi, J.; Wiley, C. Context-dependent effects of cellular senescence in cancer development. *Br. J. Cancer* **2016**, *114*, 1180–1184. [CrossRef]
138. Perez-Mancera, P.A.; Young, A.R.; Narita, M. Inside and out: The activities of senescence in cancer. *Nat. Rev.* **2014**, *14*, 547–558. [CrossRef]

139. Yu, Q.; Li, P.; Weng, M.; Wu, S.; Zhang, Y.; Chen, X.; Zhang, Q.; Shen, G.; Ding, X.; Fu, S. Nano-Vesicles are a Potential Tool to Monitor Therapeutic Efficacy of Carbon Ion Radiotherapy in Prostate Cancer. *J. Biomed. Nanotechnol.* **2018**, *14*, 168–178. [CrossRef]
140. Fong, P.C.; Boss, D.S.; Yap, T.A.; Tutt, A.; Wu, P.; Mergui-Roelvink, M.; Mortimer, P.; Swaisland, H.; Lau, A.; O'Connor, M.J.; et al. Inhibition of poly(ADP-ribose) polymerase in tumors from BRCA mutation carriers. *N. Engl. J. Med.* **2009**, *361*, 123–134. [CrossRef]
141. Golan, T.; Hammel, P.; Reni, M.; Van Cutsem, E.; Macarulla, T.; Hall, M.J.; Park, J.O.; Hochhauser, D.; Arnold, D.; Oh, D.Y.; et al. Maintenance Olaparib for Germline BRCA-Mutated Metastatic Pancreatic Cancer. *N. Engl. J. Med.* **2019**, *381*, 317–327. [CrossRef] [PubMed]
142. Szymonowicz, K.; Krysztofiak, A.; Linden, J.V.; Kern, A.; Deycmar, S.; Oeck, S.; Squire, A.; Koska, B.; Hlouschek, J.; Vullings, M.; et al. Proton Irradiation Increases the Necessity for Homologous Recombination Repair Along with the Indispensability of Non-Homologous End Joining. *Cells* **2020**, *9*. [CrossRef] [PubMed]
143. Fontana, A.O.; Augsburger, M.A.; Grosse, N.; Guckenberger, M.; Lomax, A.J.; Sartori, A.A.; Pruschy, M.N. Differential DNA repair pathway choice in cancer cells after proton- and photon-irradiation. *Radiother. Oncol.* **2015**, *116*, 374–380. [CrossRef] [PubMed]
144. Ward, A.; Khanna, K.K.; Wiegmans, A.P. Targeting homologous recombination, new pre-clinical and clinical therapeutic combinations inhibiting RAD51. *Cancer Treat. Rev.* **2015**, *41*, 35–45. [CrossRef]
145. Maacke, H.; Jost, K.; Opitz, S.; Miska, S.; Yuan, Y.; Hasselbach, L.; Lüttges, J.; Kalthoff, H.; Stürzbecher, H.W. DNA repair and recombination factor Rad51 is over-expressed in human pancreatic adenocarcinoma. *Oncogene* **2000**, *19*, 2791–2795. [CrossRef]
146. Han, H.; Bearss, D.J.; Browne, L.W.; Calaluce, R.; Nagle, R.B.; Von Hoff, D.D. Identification of Differentially Expressed Genes in Pancreatic Cancer Cells Using cDNA Microarray. *Cancer Res.* **2002**, *62*, 2890–2896.
147. Alagpulinsa, D.A.; Ayyadevara, S.; Shmookler Reis, R.J. A Small-Molecule Inhibitor of RAD51 Reduces Homologous Recombination and Sensitizes Multiple Myeloma Cells to Doxorubicin. *Front. Oncol.* **2014**, *4*, 289. [CrossRef]
148. Huang, F.; Mazina, O.M.; Zentner, I.J.; Cocklin, S.; Mazin, A.V. Inhibition of homologous recombination in human cells by targeting RAD51 recombinase. *J. Med. Chem.* **2012**, *55*, 3011–3020. [CrossRef]
149. Ma, H.; Takahashi, A.; Yoshida, Y.; Adachi, A.; Kanai, T.; Ohno, T.; Nakano, T. Combining carbon ion irradiation and non-homologous end-joining repair inhibitor NU7026 efficiently kills cancer cells. *Radiat. Oncol.* **2015**, *10*, 225. [CrossRef]
150. Huang, F.; Mazin, A.V. A small molecule inhibitor of human RAD51 potentiates breast cancer cell killing by therapeutic agents in mouse xenografts. *PLoS ONE* **2014**, *9*, e100993. [CrossRef]
151. Huang, F.; Motlekar, N.A.; Burgwin, C.M.; Napper, A.D.; Diamond, S.L.; Mazin, A.V. Identification of specific inhibitors of human RAD51 recombinase using high-throughput screening. *ACS Chem. Biol.* **2011**, *6*, 628–635. [CrossRef] [PubMed]
152. Wang, H.; Wang, X.; Zhang, P.; Wang, Y. The Ku-dependent non-homologous end-joining but not other repair pathway is inhibited by high linear energy transfer ionizing radiation. *DNA Repair* **2008**, *7*, 725–733. [CrossRef] [PubMed]
153. Iliakis, G.; Murmann, T.; Soni, A. Alternative end-joining repair pathways are the ultimate backup for abrogated classical non-homologous end-joining and homologous recombination repair: Implications for the formation of chromosome translocations. *Mutat. Res. Genet. Toxicol. Environ. Mutagenesis* **2015**, *793*, 166–175. [CrossRef] [PubMed]
154. Chan, N.; Pires, I.M.; Bencokova, Z.; Coackley, C.; Luoto, K.R.; Bhogal, N.; Lakshman, M.; Gottipati, P.; Oliver, F.J.; Helleday, T.; et al. Contextual synthetic lethality of cancer cell kill based on the tumor microenvironment. *Cancer Res.* **2010**, *70*, 8045–8054. [CrossRef] [PubMed]
155. Chan, N.; Koritzinsky, M.; Zhao, H.; Bindra, R.; Glazer, P.M.; Powell, S.; Belmaaza, A.; Wouters, B.; Bristow, R.G. Chronic hypoxia decreases synthesis of homologous recombination proteins to offset chemoresistance and radioresistance. *Cancer Res.* **2008**, *68*, 605–614. [CrossRef] [PubMed]
156. Bagnolini, G.; Milano, D.; Manerba, M.; Schipani, F.; Ortega, J.A.; Gioia, D.; Falchi, F.; Balboni, A.; Farabegoli, F.; De Franco, F.; et al. Synthetic Lethality in Pancreatic Cancer: Discovery of a New RAD51-BRCA2 Small Molecule Disruptor That Inhibits Homologous Recombination and Synergizes with Olaparib. *J. Med. Chem.* **2020**, *63*, 2588–2619. [CrossRef]

157. Royal, R.E.; Levy, C.; Turner, K.; Mathur, A.; Hughes, M.; Kammula, U.S.; Sherry, R.M.; Topalian, S.L.; Yang, J.C.; Lowy, I.; et al. Phase 2 trial of single agent Ipilimumab (anti-CTLA-4) for locally advanced or metastatic pancreatic adenocarcinoma. *J. Immunother.* **2010**, *33*, 828–833. [CrossRef]
158. Henriksen, A.; Dyhl-Polk, A.; Chen, I.; Nielsen, D. Checkpoint inhibitors in pancreatic cancer. *Cancer Treat. Rev.* **2019**, *78*, 17–30. [CrossRef]
159. Fridman, W.H.; Zitvogel, L.; Sautes-Fridman, C.; Kroemer, G. The immune contexture in cancer prognosis and treatment. *Nat. Rev. Clin. Oncol.* **2017**, *14*, 717–734. [CrossRef]
160. Lankadasari, M.B.; Mukhopadhyay, P.; Mohammed, S.; Harikumar, K.B. TAMing pancreatic cancer: Combat with a double edged sword. *Mol. Cancer* **2019**, *18*, 48. [CrossRef]
161. Hu, H.; Hang, J.J.; Han, T.; Zhuo, M.; Jiao, F.; Wang, L.W. The M2 phenotype of tumor-associated macrophages in the stroma confers a poor prognosis in pancreatic cancer. *Tumour Biol. J. Int. Soc. Oncodevelopmental Biol. Med.* **2016**, *37*, 8657–8664. [CrossRef] [PubMed]
162. Zhu, Y.; Herndon, J.M.; Sojka, D.K.; Kim, K.W.; Knolhoff, B.L.; Zuo, C.; Cullinan, D.R.; Luo, J.; Bearden, A.R.; Lavine, K.J.; et al. Tissue-Resident Macrophages in Pancreatic Ductal Adenocarcinoma Originate from Embryonic Hematopoiesis and Promote Tumor Progression. *Immunity* **2017**, *47*, 323–338.e6. [CrossRef]
163. Germano, G.; Frapolli, R.; Belgiovine, C.; Anselmo, A.; Pesce, S.; Liguori, M.; Erba, E.; Uboldi, S.; Zucchetti, M.; Pasqualini, F.; et al. Role of macrophage targeting in the antitumor activity of trabectedin. *Cancer Cell* **2013**, *23*, 249–262. [CrossRef] [PubMed]
164. Borgoni, S.; Iannello, A.; Cutrupi, S.; Allavena, P.; D'Incalci, M.; Novelli, F.; Cappello, P. Depletion of tumor-associated macrophages switches the epigenetic profile of pancreatic cancer infiltrating T cells and restores their anti-tumor phenotype. *Oncoimmunology* **2018**, *7*, e1393596. [CrossRef] [PubMed]
165. Guo, Z.; Wang, H.; Meng, F.; Li, J.; Zhang, S. Combined Trabectedin and anti-PD1 antibody produces a synergistic antitumor effect in a murine model of ovarian cancer. *J. Transl. Med.* **2015**, *13*, 247. [CrossRef] [PubMed]
166. Sanford, D.E.; Belt, B.A.; Panni, R.Z.; Mayer, A.; Deshpande, A.D.; Carpenter, D.; Mitchem, J.B.; Plambeck-Suess, S.M.; Worley, L.A.; Goetz, B.D.; et al. Inflammatory monocyte mobilization decreases patient survival in pancreatic cancer: A role for targeting the CCL2/CCR2 axis. *Clin. Cancer Res.* **2013**, *19*, 3404–3415. [CrossRef] [PubMed]
167. Nywening, T.M.; Wang-Gillam, A.; Sanford, D.E.; Belt, B.A.; Panni, R.Z.; Cusworth, B.M.; Toriola, A.T.; Nieman, R.K.; Worley, L.A.; Yano, M.; et al. Targeting tumour-associated macrophages with CCR2 inhibition in combination with FOLFIRINOX in patients with borderline resectable and locally advanced pancreatic cancer: A single-centre, open-label, dose-finding, non-randomised, phase 1b trial. *Lancet Oncol.* **2016**, *17*, 651–662. [CrossRef]
168. Candido, J.B.; Morton, J.P.; Bailey, P.; Campbell, A.D.; Karim, S.A.; Jamieson, T.; Lapienyte, L.; Gopinathan, A.; Clark, W.; McGhee, E.J.; et al. CSF1R(+) Macrophages Sustain Pancreatic Tumor Growth through T Cell Suppression and Maintenance of Key Gene Programs that Define the Squamous Subtype. *Cell Rep.* **2018**, *23*, 1448–1460. [CrossRef]
169. Mitchem, J.B.; Brennan, D.J.; Knolhoff, B.L.; Belt, B.A.; Zhu, Y.; Sanford, D.E.; Belaygorod, L.; Carpenter, D.; Collins, L.; Piwnica-Worms, D.; et al. Targeting tumor-infiltrating macrophages decreases tumor-initiating cells, relieves immunosuppression, and improves chemotherapeutic responses. *Cancer Res.* **2013**, *73*, 1128–1141. [CrossRef]
170. Seifert, L.; Werba, G.; Tiwari, S.; Giao Ly, N.N.; Nguy, S.; Alothman, S.; Alqunaibit, D.; Avanzi, A.; Daley, D.; Barilla, R.; et al. Radiation Therapy Induces Macrophages to Suppress T-Cell Responses Against Pancreatic Tumors in Mice. *Gastroenterology* **2016**, *150*, 1659–1672. [CrossRef]
171. Zhu, Y.; Knolhoff, B.L.; Meyer, M.A.; Nywening, T.M.; West, B.L.; Luo, J.; Wang-Gillam, A.; Goedegebuure, S.P.; Linehan, D.C.; DeNardo, D.G. CSF1/CSF1R blockade reprograms tumor-infiltrating macrophages and improves response to T-cell checkpoint immunotherapy in pancreatic cancer models. *Cancer Res.* **2014**, *74*, 5057–5069. [CrossRef]
172. Beatty, G.L.; Chiorean, E.G.; Fishman, M.P.; Saboury, B.; Teitelbaum, U.R.; Sun, W.; Huhn, R.D.; Song, W.; Li, D.; Sharp, L.L.; et al. CD40 agonists alter tumor stroma and show efficacy against pancreatic carcinoma in mice and humans. *Science* **2011**, *331*, 1612–1616. [CrossRef] [PubMed]
173. Cullis, J.; Siolas, D.; Avanzi, A.; Barui, S.; Maitra, A.; Bar-Sagi, D. Macropinocytosis of Nab-paclitaxel Drives Macrophage Activation in Pancreatic Cancer. *Cancer Immunol. Res.* **2017**, *5*, 182–190. [CrossRef] [PubMed]

174. Wanderley, C.W.; Colon, D.F.; Luiz, J.P.M.; Oliveira, F.F.; Viacava, P.R.; Leite, C.A.; Pereira, J.A.; Silva, C.M.; Silva, C.R.; Silva, R.L.; et al. Paclitaxel Reduces Tumor Growth by Reprogramming Tumor-Associated Macrophages to an M1 Profile in a TLR4-Dependent Manner. *Cancer Res.* **2018**, *78*, 5891–5900. [CrossRef]
175. Prakash, H.; Nadella, V.; Singh, S.; Schmitz-Winnenthal, H. CD14/TLR4 priming potentially recalibrates and exerts anti-tumor efficacy in tumor associated macrophages in a mouse model of pancreatic carcinoma. *Sci. Rep.* **2016**, *6*, 31490. [CrossRef] [PubMed]
176. Carvalho, H.A.; Villar, R.C. Radiotherapy and immune response: The systemic effects of a local treatment. *Clinics* **2018**, *73*, e557s. [CrossRef]
177. Arina, A.; Gutiontov, S.I.; Weichselbaum, R.R. Radiotherapy and Immunotherapy for Cancer: From "Systemic" to "Multisite". *Clin. Cancer Res.* **2020**. [CrossRef]
178. Burnette, B.; Weichselbaum, R.R. Radiation as an immune modulator. *Semin. Radiat. Oncol.* **2013**, *23*, 273–280. [CrossRef]
179. Azad, A.; Yin Lim, S.; D'Costa, Z.; Jones, K.; Diana, A.; Sansom, O.J.; Kruger, P.; Liu, S.; McKenna, W.G.; Dushek, O.; et al. PD-L1 blockade enhances response of pancreatic ductal adenocarcinoma to radiotherapy. *EMBO Mol. Med.* **2017**, *9*, 167–180. [CrossRef]
180. Yamamoto, K.; Venida, A.; Yano, J.; Biancur, D.E.; Kakiuchi, M.; Gupta, S.; Sohn, A.S.W.; Mukhopadhyay, S.; Lin, E.Y.; Parker, S.J.; et al. Autophagy promotes immune evasion of pancreatic cancer by degrading MHC-I. *Nature* **2020**. [CrossRef]
181. Wolpin, B.M.; Rubinson, D.A.; Wang, X.; Chan, J.A.; Cleary, J.M.; Enzinger, P.C.; Fuchs, C.S.; McCleary, N.J.; Meyerhardt, J.A.; Ng, K.; et al. Phase II and pharmacodynamic study of autophagy inhibition using hydroxychloroquine in patients with metastatic pancreatic adenocarcinoma. *Oncology* **2014**, *19*, 637–638. [CrossRef] [PubMed]
182. New, M.; Tooze, S. The Role of Autophagy in Pancreatic Cancer-Recent Advances. *Biology* **2019**, *9*, 7. [CrossRef] [PubMed]
183. Vanpouille-Box, C.; Alard, A.; Aryankalayil, M.J.; Sarfraz, Y.; Diamond, J.M.; Schneider, R.J.; Inghirami, G.; Coleman, C.N.; Formenti, S.C.; Demaria, S. DNA exonuclease Trex1 regulates radiotherapy-induced tumour immunogenicity. *Nat. Commun.* **2017**, *8*, 15618. [CrossRef] [PubMed]
184. Kalbasi, A.; Komar, C.; Tooker, G.M.; Liu, M.; Lee, J.W.; Gladney, W.L.; Ben-Josef, E.; Beatty, G.L. Tumor-Derived CCL2 Mediates Resistance to Radiotherapy in Pancreatic Ductal Adenocarcinoma. *Clin. Cancer Res.* **2017**, *23*, 137–148. [CrossRef]
185. Klug, F.; Prakash, H.; Huber, P.E.; Seibel, T.; Bender, N.; Halama, N.; Pfirschke, C.; Voss, R.H.; Timke, C.; Umansky, L.; et al. Low-dose irradiation programs macrophage differentiation to an iNOS(+)/M1 phenotype that orchestrates effective T cell immunotherapy. *Cancer Cell* **2013**, *24*, 589–602. [CrossRef] [PubMed]
186. Prakash, H.; Klug, F.; Nadella, V.; Mazumdar, V.; Schmitz-Winnenthal, H.; Umansky, L. Low doses of gamma irradiation potentially modifies immunosuppressive tumor microenvironment by retuning tumor-associated macrophages: Lesson from insulinoma. *Carcinogenesis* **2016**, *37*, 301–313. [CrossRef] [PubMed]
187. Genard, G.; Lucas, S.; Michiels, C. Reprogramming of Tumor-Associated Macrophages with Anticancer Therapies: Radiotherapy versus Chemo- and Immunotherapies. *Front. Immunol.* **2017**, *8*, 828. [CrossRef]
188. Durante, M.; Formenti, S. Harnessing radiation to improve immunotherapy: Better with particles? *Br. J. Radiol.* **2020**, *93*, 20190224. [CrossRef]
189. Gameiro, S.R.; Jammeh, M.L.; Wattenberg, M.M.; Tsang, K.Y.; Ferrone, S.; Hodge, J.W. Radiation-induced immunogenic modulation of tumor enhances antigen processing and calreticulin exposure, resulting in enhanced T-cell killing. *Oncotarget* **2014**, *5*, 403–416. [CrossRef]
190. Gameiro, S.R.; Malamas, A.S.; Bernstein, M.B.; Tsang, K.Y.; Vassantachart, A.; Sahoo, N.; Tailor, R.; Pidikiti, R.; Guha, C.P.; Hahn, S.M.; et al. Tumor Cells Surviving Exposure to Proton or Photon Radiation Share a Common Immunogenic Modulation Signature, Rendering Them More Sensitive to T Cell-Mediated Killing. *Int. J. Radiat. Oncol. Biol. Phys.* **2016**, *95*, 120–130. [CrossRef]
191. Jin, X.; Li, F.; Zheng, X.; Liu, Y.; Hirayama, R.; Liu, X.; Li, P.; Zhao, T.; Dai, Z.; Li, Q. Carbon ions induce autophagy effectively through stimulating the unfolded protein response and subsequent inhibiting Akt phosphorylation in tumor cells. *Sci. Rep.* **2015**, *5*, 13815. [CrossRef] [PubMed]
192. Jin, X.; Liu, Y.; Ye, F.; Liu, X.; Furusawa, Y.; Wu, Q.; Li, F.; Zheng, X.; Dai, Z.; Li, Q. Role of autophagy in high linear energy transfer radiation-induced cytotoxicity to tumor cells. *Cancer Sci.* **2014**, *105*, 770–778. [CrossRef] [PubMed]

193. Genard, G.; Wera, A.C.; Huart, C.; Le Calve, B.; Penninckx, S.; Fattaccioli, A.; Tabarrant, T.; Demazy, C.; Ninane, N.; Heuskin, A.C.; et al. Proton irradiation orchestrates macrophage reprogramming through NFkappaB signaling. *Cell Death Dis.* **2018**, *9*, 728. [CrossRef] [PubMed]
194. Buonanno, M.; Grilj, V.; Brenner, D.J. Biological effects in normal cells exposed to FLASH dose rate protons. *Radiother. Oncol.* **2019**, *139*, 51–55. [CrossRef] [PubMed]
195. Girdhani, S.; Abel, E.; Katsis, A.; Rodriquez, A.; Senapati, S.; KuVillanueva, A.; Jackson, I.L.; Eley, J.; Vujaskovic, Z.; Parry, R. Abstract LB-280: FLASH: A novel paradigm changing tumor irradiation platform that enhances therapeutic ratio by reducing normal tissue toxicity and activating immune pathways. *Cancer Res.* **2019**, *79*, LB-280. [CrossRef]
196. Rama, N.; Saha, T.; Shukla, S.; Goda, C.; Milewski, D.; Mascia, A.E.; Vatner, R.E.; Sengupta, D.; Katsis, A.; Abel, E.; et al. Improved Tumor Control Through T-cell Infiltration Modulated by Ultra-High Dose Rate Proton FLASH Using a Clinical Pencil Beam Scanning Proton System. *Int. J. Radiat. Oncol. Biol. Phys.* **2019**, *105*, S164–S165. [CrossRef]
197. Dutt, S.; Ahmed, M.M.; Loo, B.W., Jr.; Strober, S. Novel Radiation Therapy Paradigms and Immunomodulation: Heresies and Hope. *Semin. Radiat. Oncol.* **2020**, *30*, 194–200. [CrossRef]
198. Sato, H.; Okonogi, N.; Nakano, T. Rationale of combination of anti-PD-1/PD-L1 antibody therapy and radiotherapy for cancer treatment. *Int. J. Clin. Oncol.* **2020**, *25*, 801–809. [CrossRef]
199. Yelamos, J.; Moreno-Lama, L.; Jimeno, J.; Ali, S.O. Immunomodulatory Roles of PARP-1 and PARP-2: Impact on PARP-Centered Cancer Therapies. *Cancers* **2020**, *12*, 392. [CrossRef]
200. Bhattacharya, S.; Srinivasan, K.; Abdisalaam, S.; Su, F.; Raj, P.; Dozmorov, I.; Mishra, R.; Wakeland, E.K.; Ghose, S.; Mukherjee, S.; et al. RAD51 interconnects between DNA replication, DNA repair and immunity. *Nucleic Acids Res.* **2017**, *45*, 4590–4605. [CrossRef]